UNIVERSITY OF LONDON THESIS

Degree PhD Year 2007 Name of Author GRAHAM PALMER

SPECIES RELEASE FROM GLASS IONOMER CEMENT

Thesis submitted by

Graham Palmer

in partial fulfilment of the requirements for the degree of

DOCTOR OF PHILOSOPHY

In the

University of London

◇ 2007 ◇

Division of Biomaterials and Tissue Engineering

Eastman Dental Institute

UCL

256, Gray's Inn Road

London

WC1X 8LD

UK

ProQuest LLC
789 East Eisenhower Parkway
P.O. Box 1346
Ann Arbor, MI 48106-1346

"Everything is both simpler than we can imagine,

and more complicated that we can conceive."

Johann Wolfgang von Goethe

Acknowledgements

I would like to thank my supervisors Professor Gavin Pearson and Dr Frances Jones for their constant advice, support and badgering during this PhD project. I would also like to thank Dr Frances Jones for the XPS work that she did for me.

I would also like to thank Dr Mary Anstice and Mrs Jill Williams who have previously supervised me throughout this long project.

Special thanks go to my HOD, Professor Jonathan Knowles for giving me ample time to write this thesis.

I would like to thank Dr Anne Young for her help with interpreting the FTIR spectra, Nicky Mordan for her help with the use and interpretation of the elemental analysis system on the SEM and Amy Sherpa and Sandra Parker for their help with the Malvern particle sizer. Thanks go also to Dave Pickup from The University of Kent for running the XRF specimens for me.

Thanks also go to both Richard Billington and Professor Mike Braden for their input with the understanding of the mechanisms involved in this thesis.

I would also like to thank my colleagues at the Eastman Dental Institute, especially Ifty Ahmed, Roopa Prabhakar, Sam Ho and Anita Patel for their support, encouragement, advice and especially their friendship.

In addition I would also like to thank my friends outside the Eastman especially Matthew Pigott for his continually egging me on to get finished.

I would also like to thank my colleague Dr George Georgiou for taking on the greater share of our joint responsibilities while I have been trying to get this PhD finished.

Finally, special thanks go to my partner Richard Willson for enduring this solitary and singular obsession of mine at the expense of our social life.

Abstract

Glass-ionomer-cements (GIC) have been shown to act as matrices for the slow release of fluoride ions. The aim of the current research is to assess whether the incorporation of differing species leads to a similar release pattern. In this study, the objective is to attempt to clarify the release mechanism within the cement. GICs evaluated had differing glass compositions; all glasses having Si Al Ca and O present. AH2 has additionally Na, F and P, MP4 had additionally Na, LG26 had additionally F and P and LG30 P only. The influence of different ions on the binding and release characteristics of the cement were evaluated. This study investigated the use of four different experimental GICs as carriers for the release of chlorhexidine acetate (CHA) and amprolium hydrochloride (AHCl) at included concentrations ranging from 0.5% to 13.0% of added species by weight. Release into water at 37 °C was examined using high-performance liquid chromatography (HPLC). Physical properties evaluated included compressive strengths, and working times and setting times. In general, the more added species that was included, the greater the amount released. More amprolium hydrochloride was released and at a faster rate than chlorhexidine acetate. For most GICs, compressive strengths were found to be decreased by the presence of an additional species, while working and setting times increased. Amprolium hydrochloride had a more marked effect than chlorhexidine acetate. The effects of included species on the surfaces of the GICs were observed by Scanning Electron Microscopy. The influences of the additional species on the chemical setting of the GICs were measured by spectroscopic methods including FTIR.

List of Abbreviations

AHCl.... Amprolium hydrochloride

AMM.... Average molecular mass

ATR .... Attenuated total reflectance

BE..... Binding energy

CHA ... Chlorhexidine acetate (di-acetate)

CHG .... Chlorhexidine gluconate

DTA .... Differential thermal analysis

EDX..... Energy dispersive X-ray analysis

EVA..... Ethylene vinyl acetate copolymer

FTIR.... Fourier transform infrared spectroscopy

GI ..... Gastro-intestinal

GIC ..... Glass-ionomer-cement

HPLC... High-performance liquid chromatography

HSS..... Hydrocortisone sodium succinate

HV..... Vickers hardness

IR ..... Infrared

LALLS.. Low angle laser light scattering

NMR.... Nuclear magnetic resonance spectroscopy

OR ..... Oscillating rheometer

PAA..... Poly(acrylic acid)

P/L..... Powder / liquid

PMMA.. Poly(methyl methacrylate)

RMM.... Relative molecular mass

SATW.. Super atmosphere supporting thin window

SEM .... Scanning electron microscopy

..... or scanning electron micrograph

SDS..... Sodium dodecyl sulphate

UV..... Ultraviolet

w/v ..... Weight per volume

XRF..... X-ray fluorescence

XRMA.. X-ray microanalysis

Contents

List of Figures

List of tables

1 Introduction

By the mid 1960s the dental silicate cement had been unchanged for 50 years. It was flawed in that it dissolved in oral fluids irritated pulp and had no adhesion to tooth material (Hill and Wilson, 1988b). In the late 1960s it was generally recognised that these physical properties were inadequate and new materials were sought. The first outcome was smith's polycarboxylate cement that utilised the adhesive properties of poly(acrylic acid) (Smith, 1968).

The glass ionomer cement also resulted from this response to the inadequate materials produced so far. It was produced as a dental restorative material in 1969 and resulted from studies in dental silicate cements where the phosphoric acid was replaced by organic chelating acids (Wilson, 1968). It has favourable properties in that it can release fluoride for up to 18 months. Although the GIC is a restorative material that has been used for over 30 years, the setting mechanism is still not completely clear though many studies have been performed to determine this mechanism. It is composed of both inorganic and organic parts, these being a fluoro alumino silicate glass and poly(acrylic acid). It is therefore a composite material with the exception from traditional dental composites in that the filler participates in the setting reaction.

In the original work on GICs (Wilson and Kent, 1972) an acid-base reaction was proposed in which a hydrating cementing salt was formed. In this mechanism hydrated protons penetrate the surface of the powder displacing Al^{3+} and Ca^{2+} cations and degrade the aluminosilicate network to a hydrated siliceous gel. These workers found that strength was shown to increase with increasing

concentration of PAA in the liquid, the practical limit being the viscosity of the liquid. This problem of gelation at high concentrations has been investigated by replacing PAA with a number of co-polymers such as those of acrylamide, methacrylic acid, itaconic acid and maleic acid (Crisp *et al.*, 1980; Krishnan and Sreekumar, 1996).

Water is an essential part of a GIC as it hydrates the reaction product. Too little was found to produce a weak cement and too much produced a weak, slow setting cement (Prosser *et al.*, 1986a). Therefore protection of the cement against hydration/desiccation during the early stages of the setting reaction is essential (McLean and Wilson, 1977; Saito, 1978; Andersson and Dahl, 1994. Many additives have been evaluated to increase working time and sharpen set but only the positive enantiomorph of tartaric acid produces this effect ([crisp and Wilson 1976 V tartaric acid]).

Aluminium phosphate is often added to improve translucency and increase working and setting times (Wilson *et al.*, 1980; Griffin and Hill, 2000a). In small amounts it also increases compressive strength, Young' modulus and fracture toughness.

In the firing of a GIC glass, cryolite ($Na_3Al_2F_6$) is added to reduce the temperature at which the glass fuses and increase translucency of the set cement. It has long been known that fluoride prevents caries in enamel and that GICs release fluoride into their surroundings. Other incorporated species may do the same. This has been done in a random way without consideration of the mechanisms involved. Novel acid-base cements have been developed for use as formulations for the release of copper, cobalt and selenium (Prosser *et al.*, 1986b) though the authors were only interested in the ability of the

ingredients to form a cement and its ability to release copper, cobalt and selenium. They were not concerned with the chemistry of the cements and whether the cobalt, copper and selenium salts were involved in matrix formation or acted as inert fillers.

It is possible that we could introduce materials with specific chemical structures which have similarity to that which is present already. Wasson and Nicholson in 1993 made a weak cement from an experimental glass (G338) and acetic acid. Introducing another material in the form of an acetate may also participate in the GIC reaction and may also itself release from the cement. Introducing another material in the form of a halide may, like fluoride, not take part in the reaction but may also exhibit diffusion related release like fluoride.

2 Literature review

2.1 History of the Glass ionomer cement

By the early to mid 1960s the science and technology of dental silicate cements had remained unchanged for about 60 years. The dental silicate cement, although flawed, was still the principle anterior cement and it had remained unchanged for 50 years despite the fact that it dissolved in oral fluids, irritated pulp possibly through the leaching of phosphoric acid and had no adhesion to tooth material (Hill and Wilson, 1988b). The setting and structure were imperfectly understood. In the late 1960s and early 1970s there was a general recognition that these physical properties were inadequate, that restorative materials should be more than inert obturating materials and that biocompatibility and adhesion were important. New materials were therefore sought. The first outcome was Smith's zinc polycarboxylate cement in 1968 that utilised the adhesive properties of poly(acrylic acid) (PAA).

2.1.1 Invention

The glass-ionomer cement (GIC) also resulted from this response to the inadequate materials thus far used. The GIC is a hybrid of both inorganic and organic material and is a composite material where the filler participates in the setting reaction.

It was produced as a dental restorative material in 1969 by Wilson & Kent and resulted from studies in dental silicate cements where the phosphoric acid was replaced by organic chelating acids (Wilson, 1968). A commercial dental cement of this type was launched in 1975. It consisted of 45% aqueous PAA

and calcium fluoroaluminosilicate glass (Nicholson, 1998). It was called ASPA, short for alumino silicate poly(alkenoic acid) and also became known as polyalkenoate cement. The glasses used were of the same general type as had been used in dental silicate cements but were modified to be of greater basicity to compensate for the reduced acidity of PAA as compared to phosphoric acid (Wilson and Kent, 1972).

2.2 Properties

GIC consists of an ion-leachable calcium aluminosilicate glass powder which when mixed with a poly(alkenoic acid) sets in a few minutes. It can be regarded as a glass filled polymer composite. It is quite aesthetically pleasing as it has a ceramic-like translucency due to the glass and has the advantage over the older dental silicate cements as it is adhesive to dentine due to its polyelectrolyte character (Lacefield *et al.*, 1985). It has favourable bioactive properties in that it can release fluoride for at least 18 months (Wilson *et al.*, 1985).

2.3 Uses

GIC is also used in splint bandaging material as an alternative to plaster of Paris. It has a compressive strength of 200 MPa at 24 hours and 350 MPa at 1 year (Crisp *et al.*, 1976a). It has also found use as a bone cement (Otsuka *et al.*, 1995) and has also been successfully used in the restoration of the middle ear by reconstruction of the ossicular chain (Muller *et al.*, 1994).

2.4 Components

2.4.1 Glass

The composition of the glasses can be varied greatly but those based on ion-leachable calcium aluminosilicates ($SiO_2 - Al_2O_3 - CaO$ or $SiO_2 - Al_2O_3 - CaF_2$) are the only ones to date found to have practical application. All glasses used commercially are of the aluminosilicate type containing additionally Ca and F (Hill and Wilson, 1988b). The simplest glass would consist of SiO_4 tetrahedra and would be impervious to acid attack. The substitution of Si^{4+} by Al^{3+} in the glass happens only up to a ratio of 1:1 as above this the Al is no longer forced to adopt the tetrahedral structure of the SiO_4 units. A number of people, however, are working in the area of replacing aluminium with alternative trivalent materials such as iron (Kamitakahara *et al.*, 2000; Hurrell-Gillingham *et al.*, 2003). The composition of the original ionomer glass, G-200, is given in Table 1 based on the general formula SiO_2 - Al_2O_3 - CaF_2 - CaO. The three essential constituents of ionomer glasses are silica (SiO_2), alumina (Al_2O_3) and calcium fluoride (CaF_2). Phosphate is thought to aid glass degradation by providing additional phosphorous-oxygen bonds for hydrolysis (Griffin and Hill, 2000a). The setting rate is largely controlled by the Al_2O_3/SiO_2 ratio (Wilson and McLean, 1988). On heating the constituents of the glass, aluminium enters the silica network, replacing silicon, and the network therefore becomes negatively charged and susceptible to acid attack. The melt is shock cooled by either pouring onto a metal plate or into water. This forms of a coarse frit that is ground to a powder using a ball mill.

Species	Composition (%)
SiO_2	30.1
Al_2O_3	19.9
AlF_3	2.6
CaF_2	34.5
NaF	3.7
$AlPO_4$	10.0

Table 1 Chemical composition of the original G-200 glass / weight %

The powder is then passed through a sieve of diameter 45 μm for restorative materials and 15 μm for luting agents (Kent *et al.*, 1979; Wilson *et al.*, 1980). Modern glasses have even smaller size particles. If enough Al ions are present in the network, then the silica network is disturbed, and the glass completely decomposes. The Al_2O_3/SiO_2 ratio is therefore important.

Three main systems have been described by Hill and Wilson having different firing temperatures (Hill and Wilson, 1988b):

Type I SiO_2 - Al_2O_3 – CaO (1350 - 1500 °C)

Type II SiO_2 - Al_2O_3 - CaF_2 (1150 - 1300 °C)

Type III SiO_2 - Al_2O_3 - CaO -CaF_2 (1250 - 1500 °C)

Silica, alumina and CaO/CaF_2 are the major constituents but the glasses employed are frequently more complex in that they often contain materials to provide radiopacity. Dental cements are broadly of type (II) to which cryolite ($Na_3Al_2F_6$) is added. This flux reduces the temperature at which the glass fuses and increases translucency of the set cement. Aluminium phosphate is also

often added; it improves translucency and increases working and setting times (Wilson *et al.*, 1980; Griffin and Hill, 2000a). In small amounts, it increases compressive strength, Young's modulus and fracture toughness but in higher amounts phosphate excessively disrupts the crosslinking process in the cement matrix by competing with carboxylate groups for the cations and results in the reduction of compressive strength and Young's moduli (Griffin and Hill, 2000a). Type II cements are usually shock cooled but may also be annealed.

2.4.1.1 SiO_2 - Al_2O_3 - CaO glasses (Figure 1)

Only glasses containing less than 61% silica can form a cement (Hill and Wilson, 1988b). In powdered form, the majority yield fast setting cements that set between 2 and 10 minutes. The compositional region for more slowly setting glasses is very restricted (Figure 1). Glasses in the anorthite region have compressive strengths that are weaker than those in the gehlenite region. Broadly speaking, strength is inversely proportional to silica content. There is an approximate relationship between strength and setting time. The optimum strength is achieved with setting times between 2 minutes 45 seconds and 3 minutes and drops off either side (Hill and Wilson, 1988b).

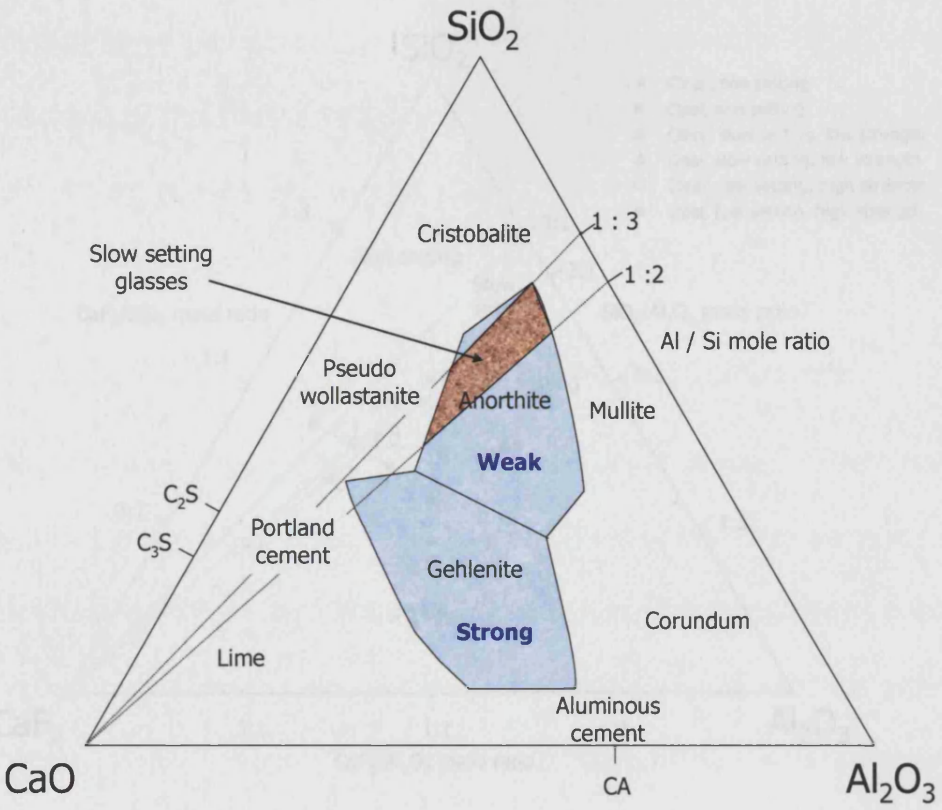

Figure 1 A triangular compositional diagram for SiO_2-Al_2O_3-CaO indicating the relative strengths of their cements (adapted from Hill and Wilson, 1988b)

2.4.1.2 SiO_2 - Al_2O_3 - CaF_2 glasses (Figure 2)

These are the basic type from which glass-ionomer cements are derived. Some glasses are transparent e.g. if alumina and CaF_2 are approximately equal by mass and there is ≥ 35% silica. These are shock-cooled and if re-heated they phase-separate. The SiO_2/Al_2O_3 mass ratio is considered to be critical (Hill and Wilson, 1988b). If it is greater than 2.0 then the glass does not form a cement. A ratio below 2.0 yields a fast setting cement (2.5 to 5.0 minutes). If the ratio equals 2.0 then a medium setting cement is formed (6 to 15 minutes).

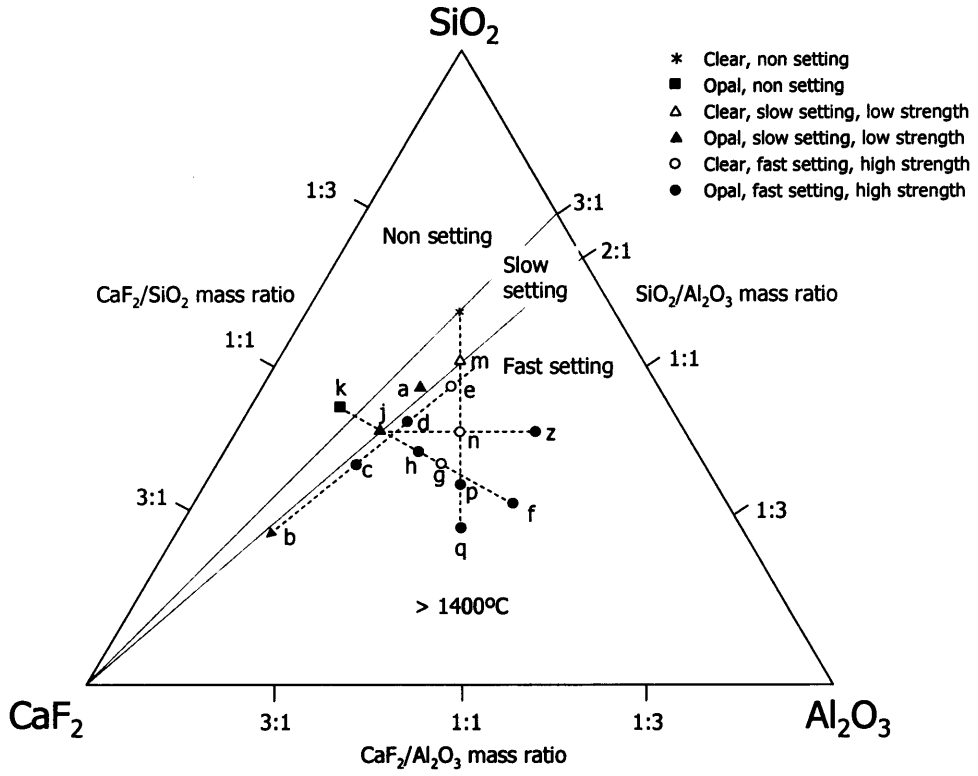

Figure 2 A triangular compositional diagram showing the appearance of the glasses and the setting characteristics and properties of their cements (adapted from Hill and Wilson, 1988)

SiO_2 is an acidic and Al_2O_3 an amphoteric oxide. Their ratio controls the acid-base balance of the glass. If the SiO_2/ Al_2O_3 ratio is less than 1.33 then phase separation of fluorite and corrundum crystallites takes place and the glasses become translucent (Hill and Wilson, 1988b). As the ratio drops below 1.33 the setting time increases slightly.

Increasing the SiO_2/Al_2O_3 ratio decreases compressive strength until it reaches zero. Increasing the ratio above 1.3 leads to the setting time being increased rapidly until at 3.0 the glasses cease to form cements (Hill and Wilson, 1988b).

The replacement of CaO with CaF_2 would be expected to make the glass less basic and less reactive (Hill and Wilson, 1988b). The change in the glass structure may well affect the basicity of the glass for the following reason.

Fluoride has a similar ionic radius to O^{2-}. Replacement of O^{2-} by F^- reduces the screening of the central cation therefore strengthening the cation-oxygen bond. This is less susceptible to acid attack. The F^- is non-bridging and therefore breaks the structure.

2.4.1.3 SiO_2 - Al_2O_3 - CaO - CaF_2 (not shown)

These glasses are hybrids of the two previous glasses. They have unusual features and various discontinuities. All glasses are clear except for the high fluoride glass at the end of the range, which contains crystals of fluorite. There are two discontinuities encountered when the CaF_2/CaO ratio is altered. There is little change in the working and setting times of the cement when the ratio is changed from 0 to 1:5. At a ratio of 1:3, the glass becomes extremely reactive and mixing it with a polyacid solution generates considerable heat and a solid mass is formed before mixing is complete. Further increases in the ratio to 3:1 yield glasses with similar behaviour. A further increase to 9:1 yields a glass which when mixed with polyacid, produces a cement that sets slowest of all in the series.

2.4.1.4 Phase separated glasses

Most GICs are thought to be phase separated (Rafferty *et al.*, 2000). Currently, whether this is the case or not is a matter of some conjecture (Griffin and Hill, 1999). Phase separated glasses yield stronger cements both in flexure and compression compared to clear glasses. The release of Ca^{2+} and Al^{3+} ions from phase separated glasses proceeds at different rates. When the reaction between the glass and polyacid has proceeded for 15 s, 76% of the total calcium extracted during the reaction and 45% of the aluminium has been

released. After 3 min these figures are 95% and 81% respectively. This can only be explained by assuming there are two phases of differing composition and that one is leached selectively (Barry *et al.*, 1979). High temperature Dynamical-mechanical thermal analysis (DMTA) (Rafferty *et al.*, 2000) has been used to measure the glass transition temperatures of the original composition of a fluoro-alumino-silicate glass and to follow amorphous phase separation within the glass. Two maxima in tan delta were observed corresponding to two glass transition temperatures. This demonstrated amorphous phase separation of the parent glass into two glass phases.

As with all glasses, working time can be extended by washing the glass with dilute acetic acid (Schmitt W *et al.*, 1983). In the case of phase separated glasses, this procedure removes Ca^{2+} from the surface of the phase separated droplets and hence reduces the calcium extracted at the start of the reaction. The consequences of washing the glasses removes the surface cations that are extracted at the start of the reaction thus slowing the rate of set. The release of Ca^{2+} and Al^{3+} ions from phase separated glasses have been observed to proceed at different rates (Hill and Wilson, 1988b). This would indicate that the two phases have different compositions and that one phase is leached selectively.

All glasses, once having been fired are normally acid washed to reduce their reactivity. This preferentially depletes ions used in setting. The original work was carried out by the company ESPE (Seefelt Uberbey, Germany).

2.4.2 The poly(alkenoic acid)

In some of the original work on GIC (Wilson and Kent, 1972) the strengths of cements were shown to increase with increasing concentration of PAA in the liquid. The practical limit was the viscosity of the liquids that increased with increasing average molecular mass (AMM). When the liquids became too viscous they became impossible to mix. It was therefore more advantageous to use lower molecular weight PAA of low viscosity at higher concentrations, preventing gelation, than vice versa. Lower molecular weight PAA also reduced 'cobwebbing' due to the formation of transient elastomers during setting (Wilson and Crisp, 1980).

PAA is preferable in powder form as when in solution at high concentration, it slowly forms hydrogen bonds and cross links to form a gel. These materials, however, have lower fatigue resistance (Nakajima *et al.*, 1996). Limitations of viscosity increase may be partially overcome by incorporating the dried PAA with glass. To get around the problem of gelation at high concentrations, a number of co-polymers have been used such as those of acrylamide, methacrylic acid, itaconic acid and maleic acid (Crisp *et al.*, 1980; Krishnan and Sreekumar, 1996). These produce similar sorts of cements.

2.4.3 Water

Water is an essential part of a glass ionomer cement as it hydrates the reaction products. Too little water will result in a weak cement and too much will result in a weak, slow setting cement (Prosser *et al.*, 1986a). Control of the hydrated state is critical in maintaining cement quality, and protection of the cement

against hydration/desiccation during the early stages of the setting reaction is essential (McLean and Wilson, 1977; Saito, 1978; Andersson and Dahl, 1994).

2.4.4 Tartaric acid

Many additives have been evaluated to increase working time and sharpen set but only the positive enantiomorph of tartaric acid produces this effect (Crisp and Wilson, 1976). The release of ions from the glass into the matrix is facilitated by tartaric acid which reacts preferentially with the glass readily forming complexes with these ions and preventing the early binding of cations to the polyacid chains (Crisp and Wilson, 1974; Barry *et al.*, 1979; Prosser *et al.*, 1982). ^{13}C NMR spectroscopy (Prosser *et al.*, 1982) showed suppression of the polysalt formation in the presence of D-tartaric acid which reacted preferentially with the glass and prevented early binding of the cations in the polysalt matrix. Information on the pH of the cement was obtained from the position of the peak in the NMR spectra. The freshly mixed cement mix had an initial pH of 1.25 and tartaric acid was found to be fully complexed at pH 3 at which point complexing of the poly(acrylic acid) occurred resulting in a pH of 5 for the final set cement.

FTIR analysis (Nicholson *et al.*, 1988) concurred with the NMR study above by showing that tartaric acid inhibited the initial set by reacting preferentially with the glass powder thus inhibiting the formation of calcium polyacrylate. When tartaric acid is present, calcium tartrate is the first salt to form. The presence of tartaric acid also accelerated the rate of formation of aluminium polyacrylate although the exact reason for this was unclear. Aluminium can under certain conditions complex and decomplex as it takes on 3 or 4 coordination, which

may contribute to this effect. Aluminium does not form discrete Al^{3+} ions in an aqueous environment (Nicholson and Wilson, 1987) and in the presence of fluoride ions a variety of species of the form AlF^{2+} and AlF_2^+ can form (Wilson, 1978). Therefore it is probable that aluminium polyacrylate is a complex molecule that incorporated fluoride ions and bound water. Rheological studies have shown that tartaric acid delays the onset of viscosity and hence increases working time but also decreases setting time (Hill and Wilson, 1988a). It has been suggested (Cook, 1983a) that the primary function of tartaric acid appears to be as a chelating agent that prevents premature gelation is in the vicinity of the glass particle.

2.4.5 Modifications

There have been many attempts to improve GICs, some of which are listed below:

- The use of dried polymer powders mixed with glass, activated by water (Prosser *et al.*, 1984).
- Cermet - containing cements (ceramic metal hybrid) calcium aluminosilicate glass fused with silver (McLean and Gasser, 1985).
- The use of alternative polymers such as poly(vinyl phosphonic acid) (Ellis *et al.*, 1991).
- Metal reinforced cements when a metal such as silver-tin alloy (Williams *et al.*, 1992a) or stainless steel (Kerby and Bleiholder, 1991) is added to

an otherwise conventional glass ionomer cement in an attempt to reinforce a set cement.

Silver or alloy addition is an example of an inclusion in an attempt to increase strength (Williams *et al.*, 1992a) and is of particular relevance to this study as it is concerned with the inclusion of species and their possible influence on the GIC.

2.5 The setting reaction

2.5.1 Acid attack and formation of metal polyacrylates

The setting chemistry of GIC has been studied with a variety of techniques. These include FTIR (Nicholson *et al.*, 1988), ^{13}C nuclear magnetic resonance spectroscopy (NMR) (Prosser *et al.*, 1982), electron probe microanalysis (Hatton and Brook, 1992) and pH change (Wasson and Nicholson, 1991a). These all show that the setting of these cements involved neutralisation of the polyacid by the basic glass with the formation of metal polyacrylates.

When GIC was invented, an initial mechanism was suggested for the setting reaction which has been modified over the last 30 years. Originally, an acid base reaction was proposed (Wilson and Kent, 1972) in which a hydrating cementing salt was formed. According to this mechanism hydrated protons penetrate the surface of the powder displacing Al^{3+} and Ca^{2+} cations and degrade the aluminosilicate network to a hydrated siliceous gel (Figure 3). Modern thinking suggests that although this surface zone is postulated to be silica gel (Wasson and Nicholson, 1993b), it is more correct to call it an 'ion depleted zone' (Billington *et al.*, 2004). Cations migrate into the aqueous phase

of the cement paste where metallic salt bridges form between the chains of charged polycarboxylate ions. Al^{3+} was expected to be more effective for ion binding than Ca^{2+} as the fluoride ions tend to bind calcium as calcium fluoride.

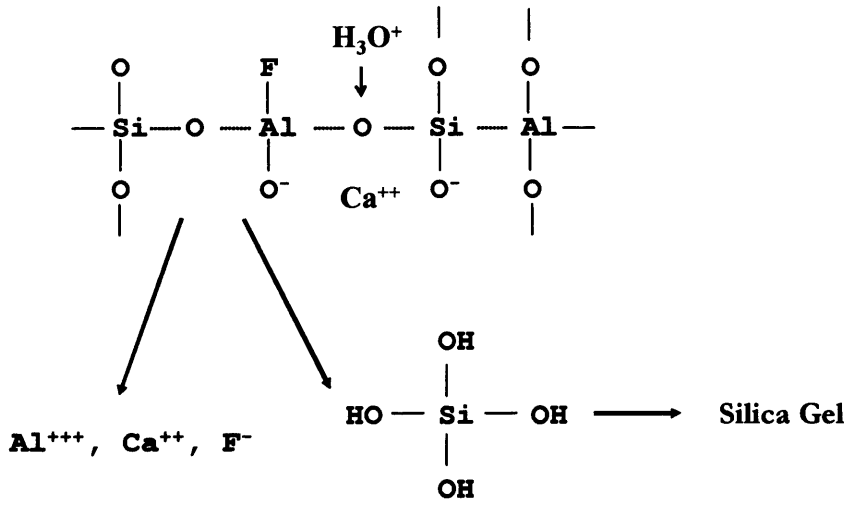

Figure 3 Initial attack of acid on cement (Culbertson, 2001)

These migrating ions then coordinate with the negatively charged oxygen ions (Figure 4), coordinating four CO_2^- groups leading to the formation of metal poylsalts. Infrared analysis (Crisp *et al.*, 1974) showed that the aluminosilicate network of the powder was degraded to a siliceous gel and that calcium and aluminium salts were formed. Initially, only calcium salts (polyalkenoate) were formed and these were responsible for the initial set. The aluminium salt was formed later and was responsible for the final hardening and strength. In the fully hardened cement, both salts were present in approximately equal amounts. Some of the carboxylate groups remained unreacted and it was suggested that this was partly for steric reasons and because the highly ionized polyacrylate chain firmly bound the remaining hydrogen by electrostatic forces.

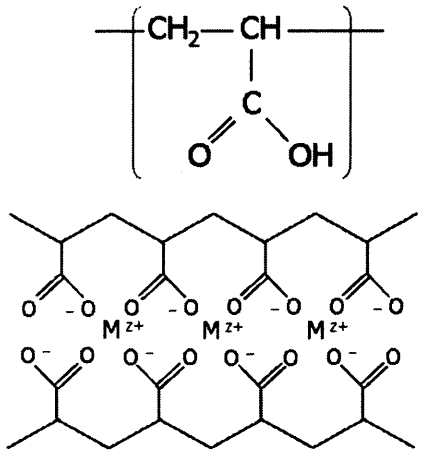

Figure 4 Formation of metal polysalts (modified from Kent and Wilson, 1973)

Further evidence for the preferential release of Ca in the initial reaction has been found by TEM of freshly made G-200 glass (Barry *et al.*, 1979). The glass was fired between 1150 °C and 1300 °C. As it cooled, droplets were formed between 1100 °C and 1000 °C. Quenching stopped much of this formation resulting in little crystallinity of the melt and formation of small droplets. The outer non-crystalline zone of these droplets was rich in Ca and was preferentially attacked by acids. This study explained why Ca is preferentially released and Ca polyacrylate is preferentially formed in the early stages of the cement-forming reaction. Aluminium is derived from the main continuous phase of the glass which is less reactive than Ca-rich glassy zone surrounding the droplets. It is likely that Al will be less accessible under these circumstances due to the greater resistance to acid attack of the continuous phase. The sequential appearance of Ca and Al carboxylate was confirmed by FTIR (Nicholson *et al.*, 1988).

Quantitative X-ray microanalysis (Barry *et al.*, 1979) has shown calcium, silicon and aluminium present in the unreacted glass and the polymer matrix

containing calcium and aluminium with very little silicon. The outer surface of glass grains were shown to be depleted in aluminium indicating that the poly(acrylic acid) had leached aluminium from the alumina-silicate glass leaving a silica gel containing particles of fluorite. This process of dissolution did not affect the glass core which remained intact with the original higher Al content.

As part of a detailed investigation of the setting mechanisms of dental polyelectrolyte cements, the Al^{3+}, Ca^{2+} and Na^{+} concentrations in the matrix phase of glass ionomer cements were measured as a function of the cement's age by the use of a selective degradation technique. This involved immersion of the set GIC at various time intervals into concentrated alkaline solution, to remove ions from the matrix only (Cook, 1983a). In the early stages of cement formation, all three cations were rapidly released from the glass, and it was inferred that both Ca^{2+} and Al^{3+} were responsible for gelation. Even after 5×10^4 min (35 days), the reaction was incomplete and still continuing. Although these ions were released from the glass, to contribute to the matrix, there was no indication that they would all be used up in matrix formation. The final set structure was found to consist of original glass particles sheathed by a siliceous hydrogel bonded together by a matrix phase consisting of hydrated fluoridated calcium and aluminium polyacrylates (Figure 5).

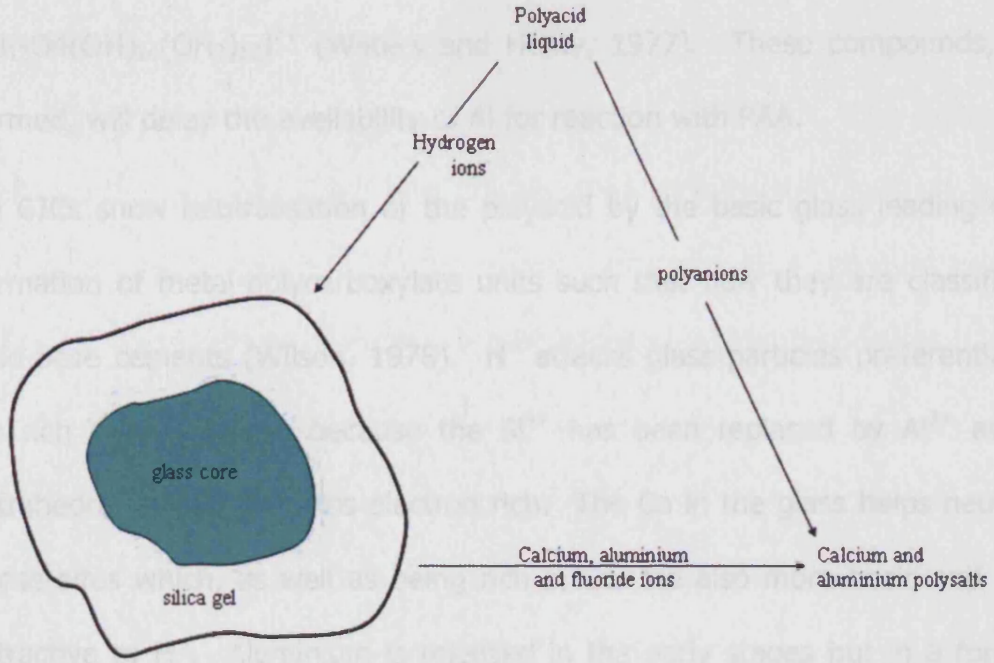

Figure 5 A diagrammatic representation of the setting reaction (modified from Hill and Wilson, 1988b)

Further evidence that acid attacks calcium sites preferentially has been published (Wasson and Nicholson, 1990) though there was no evidence of the initial release of calcium from the glass as opposed to aluminium. Large amounts of Si and Na were also released raising questions about their role in the setting and structure of the cement. Over the first 24 h maturation there was progressive cross-linking of the polyacrylate structure. Infrared studies, however, have shown that aluminium polyacrylate is formed much later than calcium polyacrylate. This apparent discrepancy is explained by the nature of the aluminium species that is released into solution. Due to its high charge and small ionic radius it forms very strong bonds with marked covalent character. Al forms many compounds when in contact with water, some of them being:

$[Al(H_2O)_6]^{3+}$, $[Al(H_2O)_5(OH)]^{2+}$ (Hill and Holman, 1989) and $[Al_{13}O4(OH)_{24}(OH_2)_{12}]^{7+}$ (Waters and Henty, 1977). These compounds, once formed, will delay the availability of Al for reaction with PAA.

All GICs show neutralisation of the polyacid by the basic glass leading to the formation of metal-polycarboxylate units such that now they are classified as acid-base cements (Wilson, 1978). H^+ attacks glass particles preferentially at Ca rich sites. This is because the Si^{4+} has been replaced by Al^{3+} as MO_4 tetrahedra making the sites electron rich. The Ca in the glass helps neutralise those sites which, as well as being rich in Ca, are also more basic and hence attractive to H^+. Aluminium is released in the early stages but in a form not available for reaction. Phosphorous was also found distributed throughout the matrix (Hatton and Brook, 1992).

The reaction occurs at the glass surface and it is thought that only about 10% of the glass dissolves (Hatton and Brook, 1992; Kaplan *et al.*, 2004), the rest remaining as a reinforcing filler and potentially for further reaction during the cement life. The initial setting is now regarded to be due to chain entanglement as well as weak ionic cross-linking (Smith, 1998).

2.5.2 Formation of silicate matrix

When ionomer glasses were treated with aqueous acetic acid, all the species in the glass were found to be released (Wasson and Nicholson, 1990). This is primarily a dissolution process in which ions are preferentially leached from the glass surface leaving a residue of silica behind which is more resistant to acid attack. To investigate this hypothesis, cements were prepared with a number of acids whose simple salts were insoluble in water (Wasson and Nicholson,

1991a). These cements were water-stable 6 h after mixing but studies of pH showed that the initial neutralisation was rapid. It therefore seemed that there was a secondary reaction that stabilised these cements. This theory was supported by a study using quantitative X-ray microanalysis (XRMA) (Hatton and Brook, 1992) in which two GICs were sectioned with a diamond knife and subjected to X-ray microanalysis in a transmission electron microscope.

It showed a glass core rich in aluminium and calcium with the outer layer depleted of these metal ions and proportionately rich in silicon. A low concentration of silicon was seen in the matrix along with calcium and aluminium. The original model did not account for the presence of silicon in the matrix and it was suggested that this also takes part in the setting reaction of a GIC (Hatton and Brook, 1992). Other workers have also found Si present in the matrix phase as well as Al and Ca (Andersson and Dahl, 1994).

IR studies (Matsuya *et al.*, 1996) have shown that cross-linking of the PAA by Ca^{2+} and Al^{3+} ions was completed in 24 h. ^{29}Si and ^{27}Al NMR studies from the same paper indicated that further strengthening was caused by silicate network formation.

The glass-ionomer cement is closely related to the zinc polycarboxylate cement which is formed by the reaction of ZnO:MgO and poly(acrylic acid). In this case, the setting is only due to the formation of zinc polyacrylate as there is no silica phase. In contrast to GICs, these do not increase in strength after 24 h (Nicholson *et al.*, 1992).

Further work (Wasson and Nicholson, 1993b) has examined the compressive strength change with age of a cement made from an experimental glass (G338)

and acetic acid. This glass formulation, however, is different from the majority of those used in GICs. An increase in strength over 3 months was observed. As there was no polymer in the cement, the hardening was deemed to be due to another source namely the silica which formed the basis of a solid phase and that formed slowly and contributed towards the strength of the cement. More recently however, Wasson and Nicholson's has been repeated using MP4 cement, a fluoride and phosphate-free glass (Shahid *et al.*, 2007). MP4 glass failed to produce a hydrolytically stable cement indicating that factors other than silica control the secondary setting mechanism.

2.6 Factors affecting the setting reaction

In the initial investigation of the reaction in GIC (Crisp *et al.*, 1977), three factors were thought to govern the rate of reaction:

- Polyacid concentration. The higher the concentration, the faster the rate of reaction.
- Viscosity of liquid. The reaction was retarded by increase in viscosity.
- Powder / liquid (P/L) ratio of mix. As the P/L ratio is increased so the rate of reaction is accelerated because of the greater surface area per volume of liquid.

All these properties will affect the rate of set and in turn the maturation rate of the cement. This will have a longer term effect on cement properties with

respect to time. The working time, i.e. the time available for manipulation, only depends on the P/L ratio whilst the other two factors affect the reaction rate at a later stage in the reaction. The effect of polyacid concentration was significant at low viscosities but as the viscosity of the liquid increased this became the predominant influence.

The effect of increasing the powder/liquid ratio is to increase the viscosity of the mix. The kinetics of the reaction do not change (Cook, 1983b) but differential thermal analysis (DTA) has shown that a high P/L ratio also produced a lower exotherm (Walls *et al.*, 1988) although it is low in all of these cases and is unlikely to affect the rate of reaction to any extent.

Other factors have also been found to affect the setting reaction:

- Moisture
- Polyacid RMM
- Glass particle size
- Glass composition
- Form in which PAA is presented

2.6.1 Moisture

GICs are susceptible to change in moisture composition during the early stages of the setting reaction, with a deleterious effect upon their physical properties and appearance (Causton, 1981). However, the strength of the set cement was only reduced if exposure to water occurred during the first hour after mixing. A

comparative lactic acid erosion study between GIC, silicate cement, zinc phosphate and zinc polycarboxylate cement (Williams *et al.*, 1992b) found that materials containing phosphoric acid do not show erosion rates which change significantly with time whereas those containing polymeric acid do show a reduction. For polycarboxylates this was small but for GIC the reduction in erosion rate was highly significant with increasing maturation time. The explanation was that cements made with polymeric acid have the ability to form new cross-links as others are broken and also that calcium and aluminium ions form a stronger matrix than zinc and phosphate. Early moisture exposure has also been shown to result in considerable aluminium ion release from GIC resulting in extensive loss of polymer matrix (Andersson and Dahl, 1994). The water is converted from an initial unbound form to a more tightly bound form as the structure of the cement forms. A later study of luting cements has shown increased dissolution of the cement surface as measured by reduction in mass caused by early water exposure (Gemalmaz *et al.*, 1998). Desiccation will also affect the cement in its early maturation producing some changes in physical properties.

2.6.2 Polyacid RMM

An increase in molecular weight of PAA produced a decrease in working and setting times and an increase in compressive and tensile strengths. High molecular weight acids therefore produce stronger cements. This may only be achieved above molecular weights of 20,000 by vacuum drying the acid and using water as the means of cement formation. In this case, only the outer surface of the PAA particles dissolve initially (Pearson, 2005).

2.6.3 Glass particle size

The particle size of the glass affects the setting reaction and is adjusted to modify the setting time of the cement (Guggenberger *et al.*, 1998). Kaplan *et al.* have indicated that small particle sizes will give an increased surface area that is likely to accelerate the setting of the material and lead in turn to a faster maturation rate such that the mechanical properties will increase more rapidly (Kaplan *et al.*, 2004). There was, however, no significant change in the flexural strength between cements made from glasses with differing particle sizes. The flexural strength was measured after 24 h when the specimens were matured. The particle size may have affected the initial setting phase; smaller particle sizes being expected to accelerate the setting. The authors, however, did not examine this. The reason given was that smaller particles are more likely to be completely dissolved with the result of a matrix with no glassy core and hence a cement with weaker mechanical properties. It would seem that under the conditions of the experiment, the effects were antagonistic.

2.6.4 Glass composition

Finally, the composition of the glass will have an effect on the setting reaction. As the substitution of Si^{4+} by Al^{3+} leaves a net negative charge on the structure (Nicholson, 1998), the greater the Al to Si ratio, the more reactive the glass (Wilson and McLean, 1988; Hill and Wilson, 1988b). The addition of CaO, replacing the bridging SiO_2 units, leads to the development of non-bridging O atoms in the glass which are more free to give up electrons. This will lead to a more basic and, hence, a more reactive cement. As mentioned above, the addition of $AlPO_4$ increases working and setting time (Wilson *et al.*, 1980; Griffin

and Hill, 2000a). In higher amounts it disrupts the crosslinking process resulting in reduced compressive strength (Griffin and Hill, 2000a).

2.7 Release of ions from polyalkenoate cements

It has been long known that fluoride is effective in reducing caries in enamel. Further, it has also been demonstrated that GICs release fluoride ions into their surroundings (Forsten, 1976; Kuhn *et al.*, 1982; Meryon and Smith, 1984). In 1985, Wilson and co-workers found that fluoride was released from the cement into distilled water for at least 600 days at which point the experiment was terminated. Although the amount of sodium present in the original cement was a much smaller than that of fluoride, 1.3% compared to 13.65%, the amount of sodium eluted was twice that of the amount of both fluoride and silica. The actual proportions released from the cement were 47% of the Na, 2.3% of the F^- and 2.2% of the SiO_2. It seemed that the release of fluoride was determined by the release of sodium to preserve electroneutrality and that for future improvement in fluoride release the sodium content of the glass should be increased. This original theory that there was a counter ion released has been demonstrated to be inconclusive. It is now thought to be through an ion-exchange mechanism where fluoride ions are exchanged for hydroxyl ions in the water (Hill *et al.*, 1995).

Later Davies *et al.* found that rate of release of fluoride is primarily dependent of the maturity of the cement at immersion and becomes less dependent on cement type with age (Davies *et al.*, 1993). The research strongly suggested that the condition of the matrix determines the rate of release of fluoride and

not the original F^- content of the glass. It was also found that a decrease in the P/L ratio always resulted in an increase in fluoride release. This was explained in terms of weakening of the cement. It is surprising that the authors did not mention that this is also dependent on the amount of fluoride released from the matrix during the cement forming process.

Andersson and Dahl in 1994 examined aluminium release from both conventional and resin-modified GICs (RMGIC) into physiological saline solution (0.9% NaCl) during early water exposure (4 minutes). Considerable amounts of aluminium were released resulting in considerable loss of polymer matrix. In the light of previous comments (section 2.6), this is most likely associated with breakdown of the cement. This study would suggest that early water exposure is inadvisable.

Ion release from Miracle mix (GC Corporation, Japan), ChelonSilver (ESPE, Seefeld, Germany), KetacSilver (ESPE, Seefeld, Germany), OpusSilver (Schottlander, Letchworth, UK) and OpusFil W (Schottlander, Letchworth, UK) into artificial saliva and water showed that metal-reinforced glass-ionomers have only a limited capacity to release metal ions (Williams *et al.*, 1997). They could however, release fluoride. It would appear that different mechanisms govern the release of different ions and that several opposing forces may operate. After immersion in a solution of 2 mg/l of silver solution, the silver ion concentration was reduced though aluminium, sodium and silica ion concentrations increased. Silver was not re-released subsequently into water.

The release of calcium, aluminium, strontium and fluoride from four glass ionomer cements has been studied and was found to be pH dependent (Ngo *et al.*, 1998). Lower pH produced more release of all species. The GICs all

exhibited an initial burst of release for the first three days that tapered off with time.

The release of Al, F, Na and K from a range of ionomeric cements containing sodium or potassium oxide has been studied (Devlin *et al.*, 1998). For these alkali metal ICs, the amount of sodium released was directly related to the sodium content of the constituent glass. Similarly, the amount of potassium released was directly related to the potassium content. The release of Al, however, was not found to be dependent on the Al content of the glass unlike the other species. Fluoride release was affected by alkali metal cation concentration. The cement with the highest monovalent cation concentration released the most fluoride and the material with no monovalent cations released the least fluoride. This gives support to the counter ion theory.

2.8 Controlled release of incorporated elements

Literature on the slow dissolution of solids is to be found in the fields of time-release of drugs from capsules (Wise, 2000; Saltzman, 2001), the weathering of rocks (White *et al.*, 1999), and the leaching of radioisotopes sealed into glassy matrices (Sinha and Krishnasamy, 1996). This work suggests that there are at least three mechanisms of release to be considered:

- a time independent wash-off of species adhering to the surface
- the diffusion of species through the bulk of the cement represented by a $t^{1/2}$ term

- erosion of material from the surface fissures as the cement network breaks down, represented by a time term

This gives an overall expression:

$$M_t = C + at^{\frac{1}{2}} + bt \quad \textbf{Equation 1}$$

(Kuhn and Wilson, 1985)

where M_t represents the total amount leached at time t and 'C', 'a' and 'b' are constants for the wash-off, diffusion and erosion respectively. Other workers (Demoor *et al.*, 1996) have produced similar values and have shown that fluoride release from restorative glass ionomer cement can be expressed by a time term and root time term indicating two kinetic processes.

Novel acid-base reaction cements have been developed for use as formulations for the controlled release of copper, cobalt and selenium (Prosser *et al.*, 1986b). They consisted of a liquid component in the form of a Bronsted or Lewis acid and a solid component in the form of a metal salt. The release of copper, cobalt and selenium were linear after the initial wash-out. The release of Cu I and Cu II from a copper phosphate cement was linear with respect to time indicating the release mechanism was one of erosion. The release from a Cu/Co/Se cement bolus placed in the rumen of a sheep was also linear with respect to time but did not go through the origin. This was due to initial wash-off as represented by the first term of the equation. The authors concluded from the field trials that this method of incorporation of cobalt and selenium compounds into a copper cement matrix produced a controlled release formulation which is capable of delivering adequate amounts of these trace elements to sheep and cattle for 4 months. This paper was only concerned

with the ability of the ingredients to form cement and the ability of the cement to release copper, cobalt and selenium. It was not concerned with the chemistry of the cements formed and it is not clear if in the case of the copper phosphate cement, the added copper, cobalt and selenium salts were involved in matrix formation or acted as inert fillers.

Potassium ions have been added in the form of KCl (Williams *et al.*, 2001) and their release studied. KCl is similar to NaF in that the ionic species are of the same respective groups. At the higher inclusion of potassium (0.1% w/v per liquid component of the mix equivalent to 0.0125% w/v per specimen) release took 1½ years after which no significant quantities were released between 1.5 and 2.4 years. It tended towards the pattern exhibited by naturally occurring fluoride from glass ionomer cements, it being proportional to $t^{1/2}$. Not all of the added potassium was released and this varied according to specimen dimensions; the thicker specimens retaining more potassium. The range of release was 79% from the 2mm x 2mm x 24 mm bar to 14% for the 20mm diameter disc of thickness 1.5mm. The immersion water was changed at regular intervals to avoid saturation by potassium ions. It differed, however, from the release of sodium which is not proportional to t or $t^{1/2}$ (Hadley *et al.*, 1999). This shows that adding similar species does not necessarily result in the same pattern of release.

GIC has been found capable of releasing dyes or high RMM proteins incorporated into their matrix during the setting of the cement (Wittwer *et al.*, 1994). Set GICs were capable of absorbing then desorbing high RMM proteins but not very efficient at releasing dyes. The authors conclude that GICs may

be suitable as release matrices for certain drugs and growth factors and that further study was warranted.

Known amounts of fluoride compounds were added to a fluoride and sodium free glass (LG30) (Williams *et al.*, 2003). Approximately 1.5% of each of sodium, calcium and aluminium fluorides was added to three portions of control blend. The sodium and fluoride release into deionised water from discs of each cement blend was measured for 8 months. At this point this was complete release for sodium but not for fluoride. The addition of calcium fluoride had no significant effect on sodium or fluoride release and aluminium fluoride had minimal effects. Adding sodium fluoride significantly enhanced release of both ions although fluoride release was less than from a glass containing 5% fluoride. Only a small proportion of the additions, 2-5% of the fluoride and 13% of sodium, were released. This may have been related to the solubility of sodium fluoride, it being 4.0 g / 100 ml at 20 C. Sodium and fluoride appeared to be released independently. For this specific glass, one of which is being used in the current study, it was found that additives were poor at supplying extra ions.

Work was done in 1996 on enhancing the fluoride release from a conventional glass ionomer cement by mixing the cement powder with varying NaF solutions (Thevadass *et al.*, 1996). At the highest fluoride concentration (4%) there was no significant difference in compressive strength as compared with a standard mix GIC. The working time was affected significantly for only the 4% solution but setting times were affected significantly for both the 2% and 4% solutions. There was significantly more fluoride released from the 4% NaF specimens at most time points. As the fluoride was introduced as a solution, it was much

more readily available for reaction. The disadvantage of using a solution, especially of a material with low solubility, is that when it is mixed with the powder of a P/L ratio of 7:1, the actual concentration of the material in the cement is reduced eight-fold, making the highest added fluoride concentration in this study 0.5% (w/w).

2.9 Controlled release

2.9.1 Introduction

The term "drug delivery" covers a broad range of techniques used to get therapeutic agents into the body. There are limitations in the traditional techniques such as ingested tablets and intravenous/subcutaneous/ intramuscular. The first method has low bioavailability and many drugs can cause possible liver damage. The second has the disadvantage of being invasive and painful, and of limited duration. To overcome these limitations other modes of delivery have been investigated since the 1970s. These are Transdermal, transmucosal, transocular, transalveolar, implantable and injectable. They have had varying degrees of success over the last 25 years. Transdermal, transmucosal, specifically intestinal, transocular and subcutaneous implants have found varying degrees of commercial acceptance. Inhalation appears promising for a limited class of agents and three companies have products in advanced state of clinical trials. Two other modes are receiving increased attention:

- nanoparticles for delivering DNA or genes to cells for transfection

- needleless injectables

A common theme underlying these delivery modes is increased therapeutic efficiency as well as increased patient compliance. The common key ingredient of all these technologies is a polymeric material.

2.10Channel and crack theory

2.10.1 Introduction

Three mechanisms have been identified for controlled release (Langer *et al.*, 1986):

- Non-erodible polymers
- Bioerodible polymers
- Magnetic

2.10.1.1 Non-erodible polymers

In the 1970's a number of polypeptide and other macromolecules were released from biocompatible polymers such as ethyl-vinyl-acetate (EVA) over a time period of 30 $h^{1/2}$ (37 days). At low loading, not all the BSA was released. The reason given for this was that during casting, particles were situated at random within the polymer matrix and the chance of particles touching each other is

small when the BSA loading is small thus most BSA particles are completely surrounded by EVA. At higher loadings, particles are more apt to touch to leave connected pore space on particle dissolution. Increase in particle size gave increased release because larger particles are more likely to touch the surface of the matrix.

2.10.1.2 Bioerodible polymers

Controlled release matrices composed of hydrophilic biodegradable polymers such as poly (lactic acid) and poly (glycolic acid) generally erode in a homogeneous manner. This leads to a loosening of the matrix permeability and reduced mechanical strength. Heterogeneous erosion is preferable in which the surface is eroded first giving zero-order release. For this to happen, diffusional release must be minimal and the device must maintain its overall shape.

2.10.1.3 Magnetic

Small magnetic spheres have been embedded within polymer matrices impregnated with BSA (Langer, 1983). The rate of release increased by applying an oscillating magnetic field. Ultrasound can also trigger release.

The release rate from magnetic devices decrease or stay constant over time. Further studies (Edelman *et al.*, 1985) have found that the critical parameters were position, orientation, magnetic strength of the embedded objects and the amplitude and frequency of the applied magnetic field. SEM of surfaces revealed a gap of c.100 microns between the embedded objects and adjacent polymer material after repeated exposure to an oscillating magnetic field. This was found around all beads subjected to an oscillating magnetic field but around none of those samples that were not.

2.10.2 Release of large molecules

It has been suggested (Rhine *et al.*, 1980) that macromolecules are too large to diffuse through polymer films but it is possible that sustained release can occur via diffusion through channels in the matrix. It has also been suggested that incorporation of macromolecules during casting may introduce such channels through which the drug can diffuse. In this case, observed differences in release rates for different proteins would be attributable to differences in protein properties (solubility and diffusivity) and matrix characteristics (porosity and tortuosity.) Investigating polymers for sustained macromolecular release, Rhine *et al.* in 1980 incorporated three macromolecules: bovine serum albumin (BSA), beta-lactoglobulin and lysozyme, into an ethylene vinyl acetate copolymer (EVA). Three ranges of particle size and four loadings were used. In general, it was found that as the loading got greater, the greater was the percentage released and as the particle size increased, so did the percentage release.

It was suggested that release rate increase caused by increase in particle size may have resulted from the formation of larger channels or pores in the polymer matrix. It was also suggested that increased loading may have provided simpler pathways – (lower tortuosity) and greater porosity for diffusion.

Langer *et al.* in 1981 studied the release of BSA from a ethylene-vinyl acetate (EVA) copolymer into a release media of physiological saline. It was also found that greater particle size and greater loading lead to more release. After all proteins were released channels large enough to permit macromolecular

diffusion were observed. It was speculated that channels were interconnecting and that because of the large size of macromolecules, release occurred solely through the channels and not via diffusion through the polymer. Therefore observed differences in release rates for different macromolecules were attributed to differences in solubility, diffusivity, and matrix properties (porosity and tortuosity). It was also suggested that increase in particle size resulted in the formation of larger channels or pores and that increase in loading provided simpler pathways (lower tortuosity) and greater porosity for diffusion.

Further evidence was provided (Langer, 1982) when release through a polymer film was compared to release of a material incorporated in a polymer matrix. EVA allowed release of substances as large as 2×10^6 RMM from a polymer matrix but the polymer film would not allow molecules greater than 300 RMM to pass through.

Gurny *et al.* in 1982 modelled the release of water-soluble drugs from porous hydrophilic polymers. KCl was incorporated in ethyl cellulose (80,000 Mw) at a concentration of 0.565 g cm^{-3}. The initial drug loading was well above the solubility of KCl in water and the prevailing mechanism was dissolution of solid drug particles into water-filled pores. As the drug became depleted its concentration became low enough so that it could dissolve in the water-filled pores below its saturation concentration. At this point and beyond, drug release was diffusion controlled and could be described by Fickian diffusion. Finally as the drug was almost totally depleted, it was suggested that major changes of the void fraction and porosity might lead to considerable increase in the release rate. KCl is a relatively small molecule and although it was useful in

helping with the understanding of the theoretical models proposed, it cannot be assumed that much larger molecules would behave in the same way.

Brook and van-Noort in 1985 explored the release of hydrocortisone via channels and cracks from acrylic polymers. They sought to address the problem of poor diffusion of high molecular weight drugs through a polymer matrix. These drugs are effectively trapped in the polymer and only a small amount of surface release occurs. Hydrated polymers have been shown to be more permeable to water soluble diffusants. Cowsar *et al.* in 1976 looked at the fluoride release from hydrogels consisting of poly(methyl methacrylate (PMMA) and poly(hydroxylethyl methacrylate) (HEMA). The rate of release was determined by the relative proportions of these hydrophobic and hydrophilic polymers. Hydrocortisone sodium succinate (HSS) in powder form was added to (PMMA) containing benzoyl peroxide. Samples were made by the addition of monomer liquid and dimethyl-p-toluidine. Varying ratios of MMA to HEMA were added. As well as normal discs, trilaminate discs were produced by polymerizing a 1 mm thick outer coating of drug-free acrylic around HEMA-free samples loaded with 11.1% drug. The release study showed that the higher the drug loading, the more rapid the release of the drug and the greater the percentage of drug eluted. Increasing the porosity by bench curing rather than under pressure at 55 °C also caused the rate of drug release to increase and the total percentage of drug eluted to be increased. The channel/crack mechanism was used as an explanation for the drug release observed whereas diffusion did not. At high loadings, when there was greater chance of particles being in contact, with each other, rapid release of most of the HSS occurred. At lower loadings, initial surface release occurred after which the rate of drug

release was greatly reduced and a large part of the drug remained trapped in the polymer. The trilaminated discs, however, showed no drug release even after 1400 h. This strengthened the theory that diffusion through intact acrylic resin did not take place.

The theoretical diffusion through a porous polymer has been discussed (Balazs *et al.*, 1985) in which a random walk simulation was used. The authors found that the specific interactions among the diffusing particles have little influence on the overall release rate. Diffusion through more complicated structures was investigated by simulating diffusion through two pores connected by a single channel. By varying the length and width of this channel, it was found that release rates could be decreased and consequently release times increased by two orders of magnitude by decreasing the width and expanding the length of the interconnecting channel.

2.11 Release of chlorhexidine and amprolium from GIC

2.11.1 Chlorhexidine

Since GICs can potentially be used as matrices for the slow release of therapeutic agents, and chlorhexidine acetate has been of interest as an antibacterial agent added to GICs (Hoszek and Ericson, 1990), it is therefore quite feasible that GICs can be used as a carrier for the release of chlorhexidine acetate (CHA). Much work has been carried out on the addition of chlorhexidine for antimicrobial purposes. Little if any work, has attempted to

determine the mode of action of CHA on the cement and the consequent changes which can occur in the cement.

Chlorhexidine in various forms has been known to have antibacterial properties, was first discovered in the 1950s and the first published use was in 1956 (Beeuwkes and Devries, 1956). It was first combined with a GIC in 1983 (Jedrychowski *et al.*, 1983) where chlorhexidine gluconate and chlorhexidine dihydrochloride were added to Fuji II. They both affected the mechanical properties of the cement in different ways. The addition of 10% dihydrochloride did not significantly affect tensile strength whereas 5% gluconate significantly reduced tensile strength. Compressive strength was affected differently in that there were significant increases when 1% dihydrochloride and 5% gluconate were added. Overall, the dihydrochloride had less effect.

Later, Ribiero added chlorhexidine acetate (CHA) and chlorhexidine gluconate to two commercial glass ionomers Aqua Cem and Chem Fil II (Ribeiro and Ericson, 1991). Only a maximum of 5% CHA was released and partial dissolution of the cement resulted. A significant antimicrobial effect was observed which lasted longer with increasing concentrations of chlorhexidine. There were two reasons given as to why the chlorhexidine release was low:

1. The small surface area of the tablets and binding of chlorhexidine acetate within may explain the low percentage released.
2. The chlorhexidine in the test tubes inhibited release from the tablets.

It was suggested that as the chlorhexidine acetate was incorporated into the GIC as a powder, it did not dissolve before the cement set, its slow release being due to exposure of CHA particles during deterioration of the material.

Chlorhexidine has also been added to a RMGIC (Sanders *et al.*, 1997). Diametral tests showed no significant difference at 24 h and 6 weeks between RMGICs with/without chlorhexidine though erosion of the chlorhexidine containing RMGIC was significantly more at 6 weeks. A later, more detailed report (Sanders *et al.*, 2002) also looked at the surface hardness of RMGICs with and without 5% CHA and found that there was no significant difference between the two groups at 24 h but that at 6 weeks the standard RMGIC group was significantly harder than the CHA group. The diametral tensile strength test indicated no difference between the control and CHA groups at 24 h or at 6 weeks. Chemical assay gave peak elution at 1 week with residual elution at weeks 2 and 3. The markedly different formation of an RMGIC with a water soluble polymer HEMA included makes comparison with a conventional material rather complex.

2.11.2 Amprolium

Amprolium hydrochloride (AHCl) was first discovered in the 1950s and has been used solely in the veterinary industry. It's first published use was in 1960 where it was used as a coccidiostat in chickens (Cuckler *et al.*, 1960). Its structure is known and is similar to that of thiamine (Shin and Oh, 1993) but has not yet been incorporated in GICs. Amprolium has approval for the treatment and prevention of E. bovis and E. zurnii in cattle and calves. Amprolium has been used in dogs, swine, sheep, and goats for the control of

coccidiosis. By mimicking its structure, amprolium competitively inhibits thiamine utilization by the parasite. Prolonged high dosages can cause thiamine deficiency in the host and excessive thiamine in the diet can reduce or reverse the anticoccidial activity of the drug. In 1972 amprolium was used to induce thiamine inadequacy and polioencaphalomalacia in sheep (Loew and Dunlop, 1972) and in 1998, it was used to induce cerebrocortical necrosis in dromedary racing camels when administered in large amounts (Wernery *et al.*, 1998).

In 2004 Athanassopoulou *et al.* tested the efficacy and toxicity of orally administrated anti-coccidial drugs for the treatment of Myxobolus sp. infection in Puntazzo puntazzo (sheepshead bream) (Athanassopoulou *et al.*, 2004). Puntazzo puntazzo infected with the parasite were treated with a combination of salinomycin and amprolium, origanum essential oil, fumagillin or toltrazuril. The salinomycin and amprolium treatment proved the most effective for Myxobolus sp. infection of Puntazzo puntazzo.

Later Karagouni *et al.* studied the antiparasitic and immunomodulatory effect of salinomycin and amprolium, origanum essential oil or fumagillin against myxosporean parasites on the innate immune system of sharpsnout sea bream (Diplodus puntazzo) (Karagouni *et al.*, 2005). The fish were again treated by oral administration. After one month post treatment, all drugs caused a significant decrease in prevalence and intensity of infection in comparison to untreated infected fish. The effect was most prominent in salinomycin with amprolium treated fish that exhibited nearly total elimination of parasites. The conclusion was that this may be a promising treatment for myxosporean infections in intensely-cultured warm-water fish.

2.12 Methods of analysis

2.12.1 Working and setting time

2.12.1.1 Gillmore needle

The latest standard including the Gillmore needle requires a large specimen BS EN 196-3, 2005. This is a major disadvantage for these types of GIC with short working and setting times as mixing in bulk is very difficult. Working time is defined in this case as the time at which the needle does not penetrate through the specimen. It is slightly subjective in that the needle is flat ended and therefore will not go right through the specimen due to material being trapped between the flat end and the bottom of the mould. In practice, however, it was fairly easy to judge this point.

Standards have changed for the measurement of setting with the Gillmore needle. In 1991 the international standard for water-based cements suggested using a 400g weight and 1 mm diameter needle (ISO 9917, 1991). A more recent standard (BS EN 196-3, 2005) suggested using a 'Vicat' vertical loading apparatus with a 300 g weight. The needle was 1 mm diameter for the measurement of initial set and 5 mm diameter needle for final set with differing depths of penetration being the point of set.

In the construction industry, different degrees of setting are observed. In a patent for Gypsum set accelerator (US patent 4019920, 1977), it was observed that calcined gypsum, mixed with a proper amount of water, will normally set in about 25 minutes to a hardness such that a one-fourth lb (113 g) Gillmore needle will no longer make any substantial indentation; this is referred to as 'initial set'. It was also observed that in about 35 minutes it will set to a

hardness such that a 1 lb (453 g) Gillmore needle will no longer make any substantial indentation; this is referred to as 'final set'. This highlights the problem of using the Gillmore needle for GIC when adoption of a setting time measurement clearly used for long sets is adapted for dental use.

As the work in this study was of a comparative nature, the load used was of less significance as long as it was consistent for all tests. In both techniques for measuring working and setting times, an in-house designed vertical loading apparatus and 300 g weight were used.

2.12.1.2 Oscillating rheometer

Although the Gillmore needle is a simple piece of equipment, the results are dependent on operator skill and attentiveness. Other attempts at measuring setting times have been explored such as the measurement of peak temperature during the setting reaction (Wolcott *et al.*, 1951) and decrease in residual monomer content of restorative resins (Scheerer *et al.*, 1964). Both these methods are not suitable for routine tests. The advantages of using the oscillating rheometer to investigate the setting characteristics of impression material has been discussed (Wilson, 1964). This method was not suitable for use with restorative materials for two reasons: the platen was large, requiring a large amount of material which was impractical for the same reason as mentioned above regarding the Gillmore needle standard, and the movement was too great for a material that sets to a rigid solid. Based on this previous work, the oscillating rheometer was redesigned with a smaller platen (10 mm) and smaller angle of movement (1.2°) and found to suitable for the measurement of working and setting time (Bovis *et al.*, 1971). Reservations

were expressed as to the clinical usefulness of the information obtained by the oscillating rheometer (Jacobsen, 1976) and as a result, the theory and mechanics of this technique were critically analysed (Cook and Brockhurst, 1980). They found that the oscillating rheometer measured a complex mixture of the dynamic viscosity and storage modulus of the material and a spring constant. They found that the working time approximated the time of gelation of the material. They also found that the setting time had less theoretical significance due to the instrument's poor sensitivity in this region due to the tension in the springs. They concluded, however, that the storage modulus of the material at the measured setting time attained a value characteristic of a material passing through a glass transition. They concluded from this, that it is appropriate to call this stage in the reaction the setting time.

2.12.2 HPLC

Prior to the 1970s, there were few chromatographic methods available to the laboratory scientist. During the 1970s, most chemical separations were carried out using open-column chromatography, paper chromatography and thin-layer chromatography. During this time, pressure liquid chromatography came into use to decrease flow-through time thus reducing purification times of compounds being isolated by column chromatography. Flow rates were however, inconsistent and there was debate as to whether constant flow rate or constant pressure was desirable (Deininger and Halasz, 1971; Hamilton and Sewell, 1982).

High pressure liquid chromatography (HPLC) was developed in the mid-1970s and rapidly improved with the development of column packing materials and in-

line detectors. In the late 1970s, reverse phase liquid chromatography, in which the stationary phase is less polar than the mobile phase, allowed for improved separation between similar compounds (Meyer, 1988).

By the 1980s HPLC was commonly used for the separation of chemical compounds due to improved separation, identification and quantification. Automation and the use of computers added to the convenience of this technique, and improvements in types of columns and reproducibility were made as micro-columns and Fast HPLC emerged.

2.12.2.1 Mobile phase

The mobile phase is the solvent that is continuously applied to the column, which acts as a carrier for the sample. A sample solution is injected into the mobile phase either manually or automatically by an autosampler. As the sample flows through the column, the components migrate according to the ionic interactions of the compounds with the column. Those components which have greater interactions with the mobile phase than with the stationary phase elute from the column faster and thus have shorter retention times and vice-versa. The mobile phase can be altered to manipulate the interactions of the sample and stationary phase.

There are two main types of mobile phase:

1. Isocratic elution in which the mobile phase has a constant composition. All compounds begin migration through the column at onset, however, each migrate at a different rate resulting in faster or slower elution rates and therefore shorter or longer

retention times. This is both simple and inexpensive but resolution of some compounds is questionable.

2. Gradient elution in which different compounds are eluted by increasing the strength of the organic solvent. Initially the mobile phase has a high aqueous component and the strength of the organic part is increased resulting in the elution of initially retained components. Compared with isocratic elution, resolution and separation are improved and bandwidths are nearly equal Snyder *et al.*, 1983.

2.12.2.2 Stationary phase

The stationary phase refers to the solid support within the column over which the mobile phase flows. There are many types of stationary phase, the two most common being Normal Phase and Reverse Phase:

- In normal phase HPLC the stationary phase is polar and the mobile phase is less polar. Hydrophobic compounds elute more quickly than hydrophilic compounds.
- In reverse phase HPLC the stationary phase is generally made up of hydrophobic alkyl chains that interact with the analyte. There are three common chain lengths, C_4, C_8 and C_{18}. Chains of length C_4 are generally used for larger molecules such as proteins and C_{18} used for smaller molecules such as peptides. The idea being that the larger protein molecules will have more hydrophobic moieties to interact with the column thus making a shorter chain length more appropriate. Peptides

are smaller and need the more hydrophobic longer chain lengths to be captured.

2.12.2.3 Column

The stationary phase sits in a tubular column typically 4.6 mm internal diameter and length between 10 and 25 cm. The most common columns are packed with silica beads which are characterised by particle and pore size. Particle sizes vary between 3 and 50 microns and the pore size varies between 10 and 100 nm (Majors, 1980). Each silica particle acts as a base for the stationary phase. As it is impossible to coat all of the silica particles completely with the stationary phase, it is important not to expose the column to high pH.

2.12.2.4 Detection

A common method of detection for organic species is via the absorption of ultraviolet (UV) light (Skoog and Leary, 1992). When a beam of parallel radiation passes through a solution of thickness *b* cm and a concentration *c* of absorbing species, the interactions between the photons and the absorbing particles cause the power of the beam to be attenuated from P_0 to P. The *transmittance* T of the solution is the fraction of incident radiation transmitted, and is expressed as a percentage such that

$$\%T = \frac{P}{P_0} \times 100 \qquad \textbf{Equation 2}$$

and the absorbance A of a solution is defined as

$$A = -\log_{10} T \qquad \textbf{Equation 3}$$

Absorbance is proportional to the path length *b* through the solution and concentration of species *c*, such that

$A = abc$ **Equation 4**

where *a* is the proportionality constant called the *absorptivity*.

The equation above is a statement of *Beer's Law*.

Beer's Law is successful in describing the absorption behaviour of dilute solutions only. At high concentrations, the distance between species responsible for absorption is diminished to the point where each one effects the charge distribution of its neighbours such that the species' ability to absorb a given wavelength is altered.

The practical outcome of the above theory is a technique that that can separate components in time and measure their concentrations as they elute from the HPLC column. It is important that the concentration of the component being detected by UV does not go above the point at which Beer's law no longer operates. The output is either a trace on a chart or more commonly an output on a PC screen.

3 Aims and Objectives

Aim

The aim of the study was to determine the effect of adding active species to glass ionomer cement both on the release of those species and also on the glass ionomer cement produced.

The objectives of the study were:-

1. To produce four glass ionomer cements contain different glass formulations with similar particle sizes.
2. To incorporate various concentrations of two active species within these cements and measure the release into water from the cements formed.
3. To determine the effect of inclusion of the species on the working and setting times of the cements.
4. To measure the mechanical properties of the cements with and without inclusion to determine the effect of the inclusion on the cement. No effect of CHA on the diametral tensile strength of RMGIC has been found (Sanders *et al.*, 2002). It is therefore possible that CHA will have no effect on the mechanical properties of a conventional GIC.
5. To examine the samples microscopically to determine surface change which may occur with time, after immersion in water.
6. To determine the chemical reactions which were proceeding in the cement using suitable techniques such as FTIR and XPS.

4 Materials and Methods

4.1 Raw materials

4.1.1 Materials used

Four glass formulations were investigated (AH2, MP4, LG30 and LG26). The initial batch came from Advanced Health Care, Tonbridge, UK and the final batch from Cera Dynamics, Stoke on Trent, Staffordshire. All glasses contained Si, Al, Ca and P. MP4 had added Na, LG30 added P, LG26 added F and P, AH2 added Na, F and P.

The glasses were fired using the compositions in Table 2 and a summary of the ions present are set out in Table 3.

	AH2	MP4	LG30	LG26
SiO_2	40.0	28	25.3	24.3
Al_2O_3	22.9	35	28.6	27.5
$AlPO_4$	6.2	-	-	-
Na_3AlF_6	18.5	-	-	-
CaF_2	12.4	-	-	14.0
CaO	-	26	26.2	15.1
Na_2O	-	11	-	-
P_2O_5	-	-	19.9	19.1

Table 2 Original components of the four glasses / weight %

Glasses	Na	F	P	Al, Si, Ca, O
AH2	X	X	X	X
MP4	X	-	-	X
LG30	-	-	X	X
LG26	-	X	X	X

Table 3 Ions present in the four glasses. X = present, – = absent

4.1.2 Firing

Initially glasses were prepared commercially by firing the various constituents in a covered crucible heated to c. 1400 °C. The melt was then poured onto a metal plate and then into cold water leading to the formation of a fine frit. This was then ground and sieved. A later batch of glasses was prepared using the cold top production method in which the ingredients were put in an electrically heated tank. When the constituents had melted, the bottom 50% of the glass was drained off. This latter method reduced the risk of fluoride loss from the surface of the melt.

All glass frits were then ball milled in a ceramic drum with ceramic balls as the charge. The glass particles were then characterised for particle size to ensure that the particle size distributions of all glasses were of a similar order in the range < 45 microns.

4.1.3 Acid treatment of glass

All glasses were then treated with acetic acid to reduce the reactivity of the originally fired glass. Each glass was mixed with a 5% solution of acetic acid and agitated for 1 h at 230 °C in a flask. The slurry was then left to stand for 23 h before filtering off the solution and washing the glass thoroughly with deionised water. The glass was then dried in an oven at 370 °C for 24 h. The cake which was formed was then broken up by shaking in a ball mill.

4.1.4 Characterisation of the glasses – XRF

4.1.4.1 Aim

The aim of this part of the study was to ascertain the compositions of the four glasses after firing. The compositions, as supplied by the manufacturer, were as known before firing. They did not have any information on the compositions after firing. Fluorine and sodium are the lowest molecular weight components and the two most volatile in the pre – glass mix. As firing is likely to have an effect on the more volatile components of the glass more than on the other components, and as there is uncertainty about the homogeneity of the melt (see section 4.1.2 above), a selection of glasses were submitted to XRF analysis.

4.1.4.2 Experimental details

An XRF consists of an X-ray source (Figure 6) that is directed from a side window onto the sample. Electrons from the inner shells of atoms in the sample are ejected from the atom and the energies released by the outer electrons that drop into the vacancies left in the inner shells are emitted from the sample. These X-rays sample pass through a primary collimator, and towards a diffraction crystal. They are then diffracted towards a secondary collimator, from which they pass into a scintillation detector. This consists of a gas chamber in which the X-ray photons impart their kinetic energy to atoms in the gas creating a series of electron-cation pairs which are detected by the scintillation counter; the current being proportional to the intensity of the incident photon.

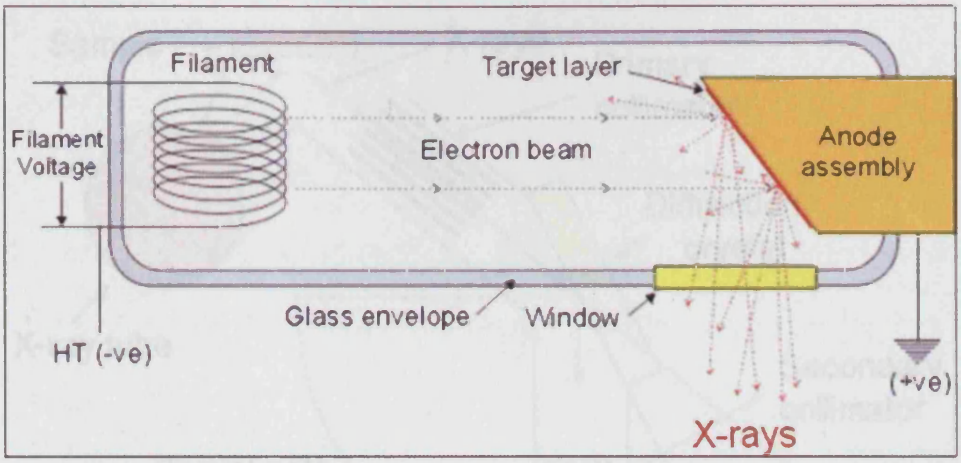

Figure 6 X-ray source for an XRF

The energy levels in atoms are element specific. Therefore, from the position of the emission lines and from the quantification of their area it is possible to obtain a quantitative elemental analysis. The XRF analysis can be performed using a calibration method (obtained measuring standards of known composition) or standardless method (rely on algorithms that describe the detector's response to pure elements).

In this study the experiment was carried out using the standardless technique on a Bruker S4 with powdered samples held in nylon holders with 3 micron mylar windows in a helium atmosphere.

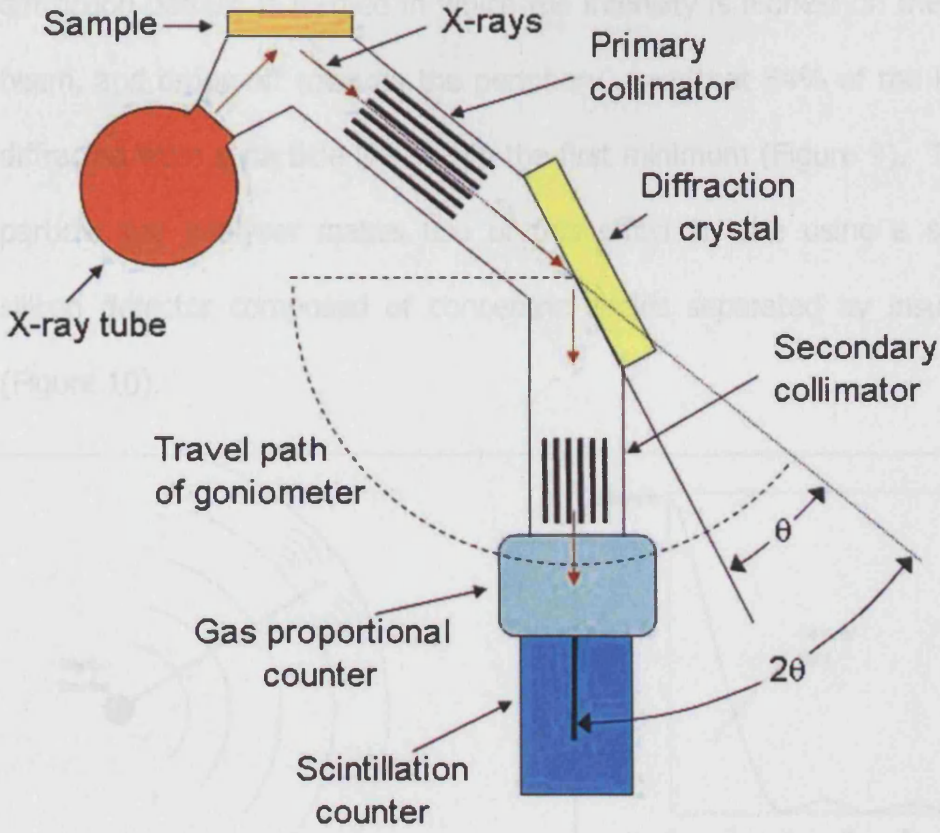

Figure 7 Schematic of an XRF

4.1.5 Characterisation of the glasses - particle size

4.1.5.1 Aim

The objective of this part of the study was to measure the particle size and distribution of the four glasses and determine that they were relatively similar.

4.1.5.2 Experimental details

The glass particle sizes were determined using a Malvern Mastersizer E (Malvern Instruments Ltd (UK), Malvern, Worcestershire) which uses 'Low angle laser light scattering' (LALLS). This makes use of the diffraction of light by particles. The fringe patterns formed by diffraction effects can be analyzed using Huygens' principle (Figure 8). When a beam of light hits a particle, a

diffraction pattern is formed in which the intensity is highest on the axis of the beam, and drops off towards the periphery, such that 84% of the light energy diffracted from a particle lies within the first minimum (Figure 9). The Malvern particle size analyser makes use of this effect by the using a semi-circular silicon detector composed of concentric circles separated by insulating gaps (Figure 10).

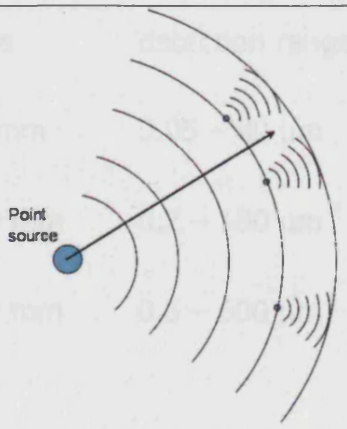

Figure 8 Huygen's Principle

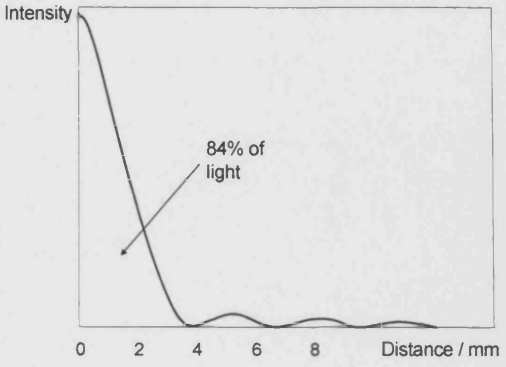

Figure 9 Fraunhofer Diffraction Pattern

(Above diagrams are from the instruction manual for the Malvern Mastersizer E)

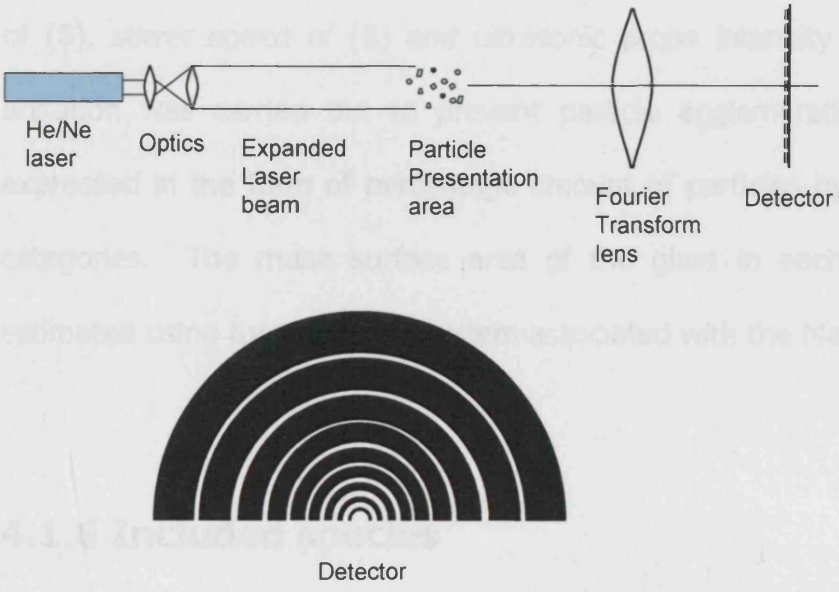

Figure 10 Particle sizer schematic with Si detector (ibid.)

The analyser can measure particle sizes between 0.1 and 600 μm. The lower limit is determined by the wavelength of the He-Ne laser (632.8 nm). The system has both a small cell and a pumped recirculation particle suspension system that can take 1 l of solution for suspension of the powder. Three lenses of differing focal length are available for measuring different ranges of particle sizes. The lenses and their ranges were as follows:

Lens	detection range
45 mm	0.05 – 80 μm
100 mm	0.2 – 180 μm
300 mm	0.5 – 600 μm

The middle range lens was used initially and the others were used depending on particle size distribution observed. All glass specimens were suspended in distilled water in the stainless steel bath and stirred at a constant pump speed of (8), stirrer speed of (8) and ultrasonic probe intensity of (5). Ultrasonic agitation was carried out to prevent particle agglomeration. Results were expressed in the form of percentage amount of particles by volume in 32 size categories. The mean surface area of the glass in each cement was also estimated using the computer system associated with the Malvern analyser.

4.1.6 Included species

A pilot study was performed on four included species. These were selected according to their differing molecular size, shape, and atomic structure.

Ovalbumin was the largest species considered being made up of 385 amino acids and having a RMM of 45 kD. Chlorhexidine acetate was composed of two benzene rings, had a RMM of 626, had a linear formation of N and C bonds terminated at both ends by a benzene ring and its functional group was acetate. Chlorhexidine gluconate was again composed of two benzene rings, had a RMM of 696 and its functional group was gluconate, a ring structure. Amprolium hydrochloride was also composed of two benzene rings, had a RMM 315, was composed of two benzene rings in close proximity to one another and its functional groups were HCl and Cl^-.

4.1.6.1 Solubility of included species

Known weights of the two species selected for inclusion were added incrementally to one beaker containing a known volume of water at 23 °C. After each addition, the solution was observed until the added species dissolved then further amounts were added until a saturated solution was obtained. The solution was then heated to 37 °C and the above procedure repeated until a saturated solution was again obtained. The solution was stirred using a magnetic stirrer throughout the experiment.

4.2 Setting cement

4.2.1 Cement formulation

Under normal conditions, at this stage a standard cement formulation would be produced by mixing the glass with 2% tartaric acid (w/w) and then blending with vacuum dried poly(acrylic acid). In the present study, however, tartaric

acid was excluded from the mix. This acid component was vacuum dried poly(acrylic acid) (PAA), (MW viscosity average = 50 kD), (Advanced Health Care, Tonbridge, UK). The mixing ratios used for AH2, LG30, MP4 and LG26 (2^{nd} melt) were 1 part PAA : 4 parts glass by weight. The powders were mixed together in a universal tube by rotating end-over-end on a lathe at the slowest speed of 38 rpm for five minutes (190 revolutions). The ends of the tube were occasionally tapped to stop agglomeration of the powders. The powder was then mixed with water at a powder to liquid (P/L) ratio of 7:1 by weight. The PAA / water ratio of the mixes was 1.4:1. The initial batch of LG26 was treated differently since the set was too rapid and even when powder and liquid components and mixing pad were refrigerated, at the normal ratio used for the other three glasses the mix set within a few seconds. This rapid setting prevented specimen preparation. The proportions of the components for LG26 cement were therefore altered to a glass : PAA ratio of 2 : 0.67, and a powder : water ratio of 5.733 : 1. This resulted in a PAA : water ratio of 1.44 : 1.

4.2.1.1 Active species for inclusion

As a result of the pilot study, two species were selected as inclusions, namely chlorhexidine di-acetate (CHA) (Beckpharm Ltd. product No. 14109 purity > 98%) and amprolium hydrochloride (AHCl) (Sigma, Lot 46F0514 purity > 99%). They were incorporated into the mix of the four types of GIC. Details of the two included specie are described in Table 4. Chlorhexidine is a widely used anti-microbial and the acetate form was chosen over the alternative gluconate as this was only available as a 20% aqueous solution giving only a maximum inclusion of 2.9% in the made cement. Amprolium hydrochloride is used in the

veterinary industry and was chosen because of its differing functional group, more compact molecular structure and its smaller molecular weight. The release of a molecular species from a GIC may be related to a purely physical entrapment or may be affected by chemical bonding between the species in its ionic form and components of the GIC.

4.2.1.2 Characterisation of the included species

CHA had low solubility and during incorporation into the GIC mix, did not appear to dissolve completely before the cement was set. An analysis of the particle size was therefore carried out on the Malvern Mastersizer E to give an indication of the size of particles left in the cement. As chlorhexidine is soluble in water, its particle size was measured in hexane using a small cell which is sealed against the atmosphere and requires a small amount of solvent. The stirring speed was set to the same rate as for the glasses but the ultrasonic probe was not available for this cell. The particle size of AHCl was not measured as it dissolved readily on contact with water and would not have been present in the cement in particulate form.

	Chlorhexidine di-acetate	**Amprolium hydrochloride**
Structure	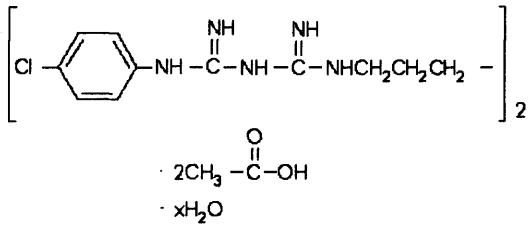	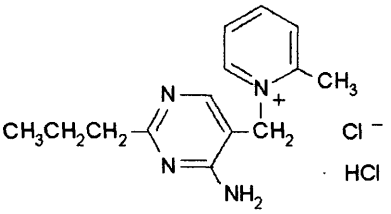
3D form	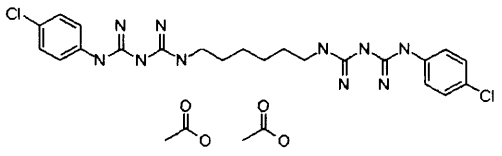	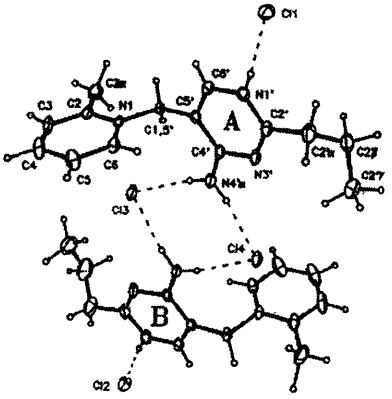 (from Shin and Oh, 1993)
Synonyms	1,6-bis(N5-[p-Chlorophenyl]-N1-biguanido)hexane 1,1'-Hexamethylenebis(5-[p-chlorophenyl]biguanide)	1-(4-Amino-2-propyl-5-pyrimidinyl methyl)-2-methylpyridinium chloride hydrochloride
Formula	$C_{22}H_{30}Cl_2N_{10}.2C_2H_4O_2$	$C_{14}H_{19}N_4Cl.HCl$
RMM	625.558	315.246
Solubility	1.9% (w/v) (British Pharmacopoeia, 2007)	33% (w/w) (Clarke's analysis of drugs and poisons, 2004)

Table 4 Physical data for the active species selected

4.2.1.3 Cement formation with species inclusion

All cement formulations were based on the general formula described above. Added species were blended into the glass and PAA mix reducing the P/L ratio slightly.

% glass	% PAA	% water	% added species	P/L in absence of added species (equivalent ratio)
70.0	17.5	12.5	0.00	7.00
69.6	17.4	12.5	0.46	6.96
69.4	17.4	12.5	0.70	6.94
69.2	17.3	12.5	0.96	6.92
68.8	17.2	12.5	1.5	6.88
68.5	17.2	12.5	1.8	6.85
68.4	17.1	12.5	2.0	6.84
67.1	16.8	12.5	3.6	6.71
66.5	16.6	12.5	4.4	6.65
64.3	16.1	12.5	7.1	6.43
64.2	16.1	12.5	7.2	6.42
63.0	15.7	12.5	8.8	6.30
62.9	15.7	12.5	8.9	6.29
62.0	15.5	12.5	10.0	6.20
61.0	15.2	12.5	11.3	6.10

Table 5 Compositions of specimens made from AH2, MP4, LG30 and second batch of LG26 used in study / % (w/w)

% glass	% PAA	% water	% added species	P/L in absence of added species (equivalent ratio)
63.80	21.34	14.85	0.00	5.73
62.38	20.92	14.85	1.85	5.61
60.43	20.23	14.85	4.49	5.43
56.43	18.88	14.85	9.83	5.07

Table 6 Compositions of LG26 specimens used in study / % (w/w) (first LG26 batch only)

The powder and liquid were then weighed on to a 3M mixing pad and mixed for the requisite mixing time.

4.2.2 Wallace hardness measurements

4.2.2.1 Aim

During the initial incorporation of CHA and AHCl it was noticed that there were variations in viscosity related to the amount of incorporated material. Large amounts of CHA produced a more viscous mix than cement with no inclusion and large amounts of AHCl produced a less viscous mix. The hardness of a material is related to its degree of set; the harder a material, the more it is set. Other workers have measured the hardness of setting cements with time (De Moor and Verbeeck, 1998a; Forss *et al.*, 1991). Hardness tests were therefore performed on a selection of cements to get an indication of the relative sets of the two species-containing cements.

4.2.2.2 Experimental detail

Figure 11 shows the Wallace micro indentation tester, model H5B (H. W. Wallace and Co. Ltd., Croydon, England). The instrument measures the depth of penetration of an indenter into material under a known static load.

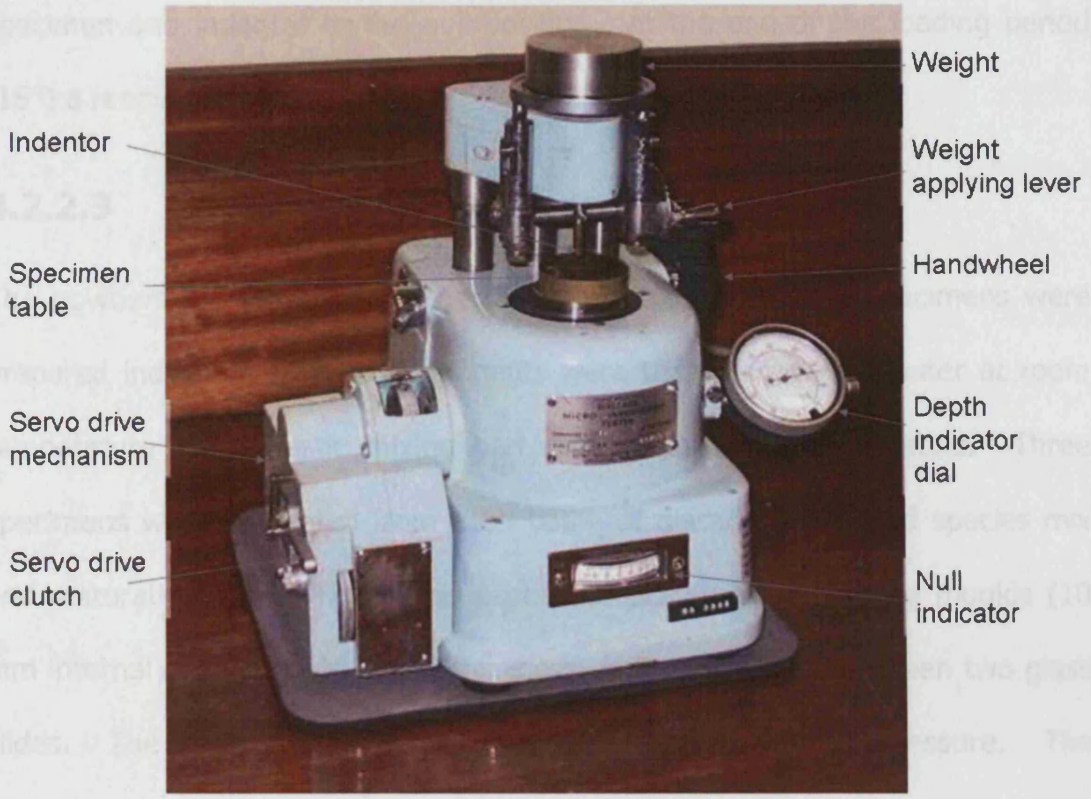

Figure 11 Photograph of the Wallace micro-indentation tester

The instrument consists of an indenter and a means of applying a primary load followed by a secondary load to the indenter. The specimen is mounted on the table and indentation measured by raising the table until the indenter is returned to the vertical position it occupied before the secondary load was applied, the movement of the table being equal to the depth of indentation. The position of the indenter before and after the secondary load is applied is called the "null position" and this coincides with the balance condition of a capacity comparator. As a load is applied to the indenter, the null position is lost. The capacity comparator is then unbalanced causing it to provide a potential to an electric motor which is geared to move the specimen table up or down depending on the direction of unbalance. The motor returns the table,

specimen and indenter to the null position. At the end of the loading period (15") a reading is taken.

4.2.2.3 Specimen preparation

The powders were mixed together as described previously. Specimens were prepared individually. The components were then mixed with water at room temperature on a plastic mixing pad with a stainless steel spatula. Three specimens were fabricated from each batch of glass/PAA/included species mix and maturation time. The mixed paste was placed into split ring moulds (10 mm internal diameter and 1 mm thickness) and sandwiched between two glass slides. The excess material was expelled using firm hand pressure. The assembly was placed in an incubator at 37°C for either 1 h or 24 h. Ten indentation measurements were taken per specimen at different points on the specimen surface using a 0.856 g primary load and 300 g secondary load. The median Vickers Hardness Number (VHN) (g μm^{-2}) was calculated for each specimen.

4.2.3 The setting reaction - working and setting times

4.2.3.1 Aim

The aim of this part of the study was to determine the effect of added species on the working and setting time of the cement using an oscillating rheometer (OR) (Bovis *et al.*, 1971) and Gillmore needle (GM) (ASTM Annual Book of Standards, 1999). The working time is defined as the time from the start of mix that the operator has available to manipulate the material after which

further manipulation will cause disruption of the newly-formed bonds. The setting time is defined as the time at which the reaction is complete and the material appears solid. In reality, GICs set rapidly at first, are often considered set by 1 hour and continue setting at an increasingly slower rate for up to 4 months (Pearson and Atkinson, 1991). This has been corroborated by Williams and Billington who also found that over the period 24 hours to 4 months, those materials containing PAA, maintained or even showed slight increase in strength (Williams and Billington, 1991).

4.2.3.2 Experimental setup – Oscillating rheometer

The oscillating rheometer consists of two circular platens, the upper of which may be temperature regulated. One of the plates is fixed and the other oscillates eccentrically via a pair of equally tensioned springs. The platen oscillation was detected by a mirror/ photoresistor setup (Figure 12). As the mirror oscillates, so more or less light hits the photoresistor. As the light increases to the photoresistor, so the resistance drops thus allowing more current to flow. The light source and mirror position are adjusted to eliminate clipping. This occurs if the light reaches an intensity that matches the minimum resistance in the photoresistor. Any further increases in light will therefore produce no further reduction in resistance.

The eccentric movement of the upper plate exerts a shear strain on the material. As the material sets, its stiffness increases, thus reducing the movement of the oscillating plate. The reduction in movement can be equated to the material's rate of set.

The OR test could give a variable reading due to excessive applied shear forces affecting the bonds in the material. To reduce these shear forces, the angular movement is minimised.

The oscillating rheometer used a serrated plate of diameter 9 mm and an inter-platen distance of 1 mm (Khouw-Liu *et al.*, 1999). The chart recorder trace had a cycle time of 6.3 s (9.5 rpm) at both experimental temperatures (23 and 37 ^{0}C). The total circular oscillation of the platen was 0.19 degrees.

The top platen was temperature controlled by means of a water bath and circulating pump at either 23 °C or 37 °C. Ideally, the working time would be measured at 23 °C (room temperature) and setting time at 37 °C (mouth temperature). The extra data, working time at 37 °C and setting time at 23 °C was supplemental. The powder and liquid were weighed out onto a mixing slab at the correct P/L ratio. The chart recorder was started at the point at which mixing was commenced. On completion of the mix the paste was placed on the lower platen, the upper platen was swung into place and lowered to a point which gave an inter-platen distance of 1 mm. The initial amplitude of the trace was regarded as representing the material in its unset state. Once the trace had been completed the working time was determined by noting the time at which the trace width was 95% of full trace. The setting time was that where the trace was 5% of the initial trace width. Six traces were obtained for each temperature/glass/added species concentration and the median value obtained.

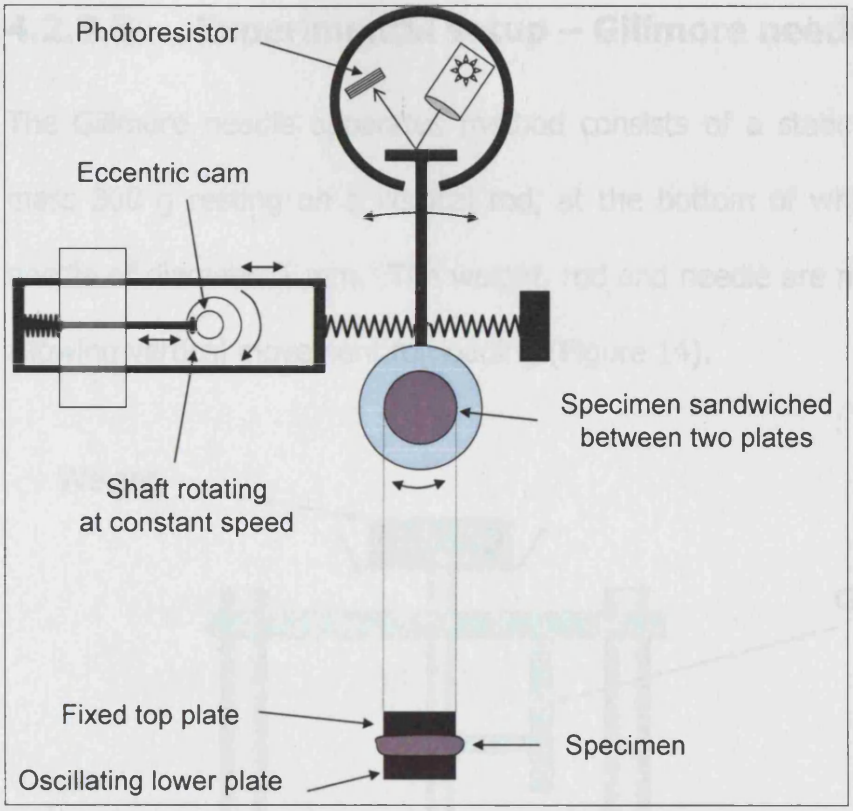

Figure 12 Oscillating rheometer in diagrammatic form (plan view)
Movement of the eccentric cam causes movement of the extended arm attached to the specimen. This results in the mirror reflecting light on the photoresistor, changing the EMF produced which is then displayed as a trace on a chart recorder.

A typical trace is shown in Figure 13.

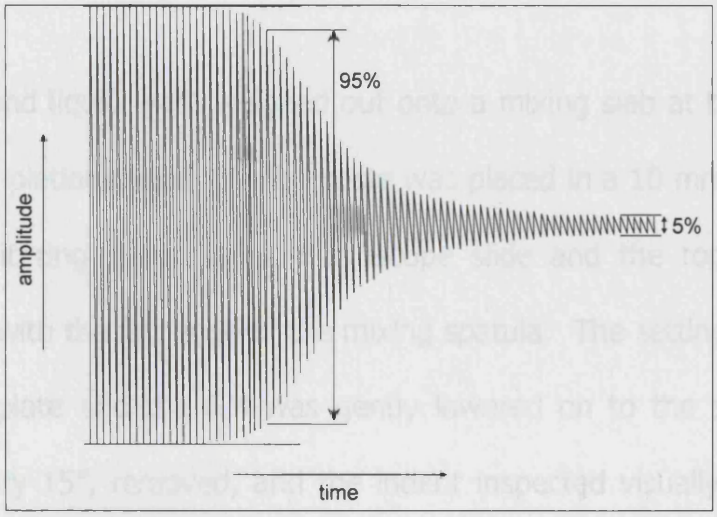

Figure 13 Typical oscillating rheometer trace showing the working time (95% amplitude) and setting time (5% amplitude)

4.2.3.3 Experimental setup – Gillmore needle

The Gillmore needle apparatus method consists of a static loading device of mass 300 g resting on a vertical rod, at the bottom of which is a flat-ended needle of diameter 1 mm. The weight, rod and needle are mounted in a frame allowing vertical movement for loading (Figure 14).

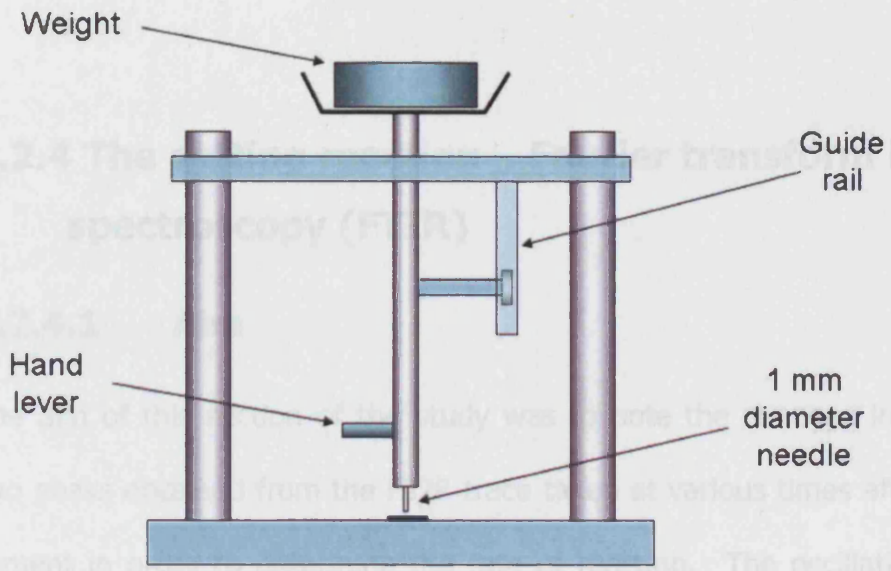

Figure 14 Vertical loading Gillmore needle apparatus

The powder and liquid were weighed out onto a mixing slab at the correct P/L ratio. On completion of the mix the paste was placed in a 10 mm diameter × 1 mm thick split ring placed on a microscope slide and the top surface was skimmed flat with the flat edge of the mixing spatula. The setting material was placed on a plate and the GM was gently lowered on to the surface of the specimen every 15", removed, and the indent inspected visually. Initially the needle penetrates through the specimen completely. As the cement sets it becomes more viscous until, on lowering of the indenter, the indent does not

penetrate the specimen completely. This is called the 'working time'. Further indents were made at the same time interval, with the indenter making progressively smaller indents as the material's setting reaction progressed. The setting time of the material is the point at which the circular depression of the indenter on the surface of the specimen does not form a complete circle. Three specimens were produced for each cement / inclusion mix.

4.2.4 The setting reaction – Fourier transform infrared spectroscopy (FTIR)

4.2.4.1 Aim

The aim of this section of the study was to note the changes in amplitude of two peaks obtained from the FTIR trace taken at various times after mixing the cement in order to determine the rate of reaction. The oscillating rheometer mentioned previously measures the viscosity of the material and FTIR spectroscopy measures changes in the chemical structure. The results from these two techniques could then be related to one another.

4.2.4.2 The FTIR spectrometer

In an FTIR there are four main components: Source, Interferometer, Sample and Detector.

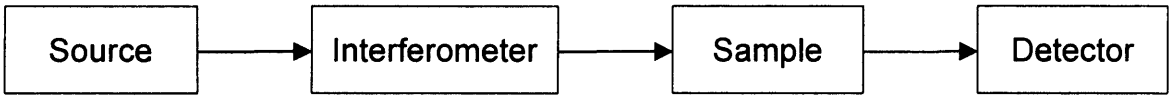

Figure 15 Block diagram of an FTIR spectrometer

The source is an inert ceramic that is heated to a temperature of between 1500 and 2200 K by an electric current. The maximum intensity occurs at about 2 μm. At longer wavelengths, the intensity falls off smoothly until at 15 μm, it is about 1% of the maximum. At the shorter wavelength side its falloff is much more rapid. The interferometer is a 'Michelson' type that uses a KBr beam splitter and moveable mirror to produce an interferogram. This passes through the sample via a 21.2 mm aperture to the mid IR deuterated triglycerine sulphate photo resistor detector. This detector has a very high resistance in the dark which falls off under light. The time domain frequency spectrum generated is converted by a Fourier transform process into the frequency domain which is displayed on the PC.

4.2.4.3 Experimental setup

The setting reactions were monitored using a Perkin Elmer FTIR spectrometer model number 2000 with a diamond attenuated total reflectance (ATR) unit and Spectrum 'Timebase' software. Initially a background scan was taken of the diamond ATR unit alone and this was automatically subtracted from the subsequent spectra.

The 'Golden Gate' single reflection diamond ATR unit (Figure 16) consists of a type IIa industrial grade single diamond crystal that has been high temperature bonded into a tungsten carbide support disc at 1000 °C. Samples are forced into contact with the diamond using a sapphire anvil clamping assembly that ensures continuity with the diamond face.

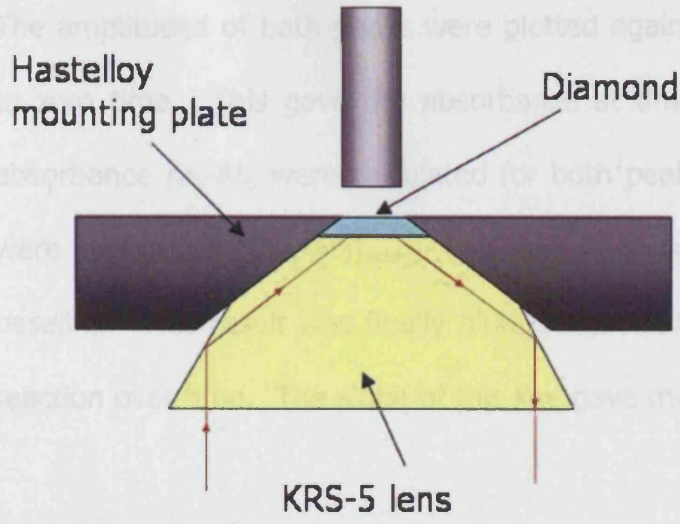

Figure 16 The Golden Gate ATR unit (Coombs, 1998)

4.2.4.4 Procedure

Preliminary investigations indicated that the relevant peaks which showed changes during the setting reaction were at 1702 cm^{-1} for the acid group (COOH) and 1537-1550 cm^{-1} for the salt (COOM), where 'M' is the cation. The scans were therefore taken between 1800 cm^{-1} and 800 cm^{-1}. This permitted an increased sampling frequency and reduced file sizes to aid storage. Spectra were formed every 30 seconds and were made from an average of four scans to improve the signal to noise ratio.

The individual components of the GIC were weighed to 0.0001g then mixed together on a mixing pad with a stainless steel spatula as described previously. The mix was then immediately placed on the diamond of the ATR unit and spectra were taken between the wavelengths and at the frequency mentioned above for 500 minutes from the start of mix.

The amplitudes of both peaks were plotted against time and extrapolated back to zero time. This gave the absorbance at time 0 $A(t_0)$. The differences in absorbance At_x-At_0 were calculated for both peaks and then their absorbances were subtracted $((At_x\text{-}At_0)_{acid} - (At_x\text{-}At_0)_{salt})$ to compensate for changes in the baseline. This result was finally plotted against time to give the completion of reaction over time. The slope of this line gave the rate of reaction.

4.3 Release behaviour in fluids

4.3.1 Release studies

4.3.1.1 Aim

The aim of these experiments was to determine if the incorporated species were released from the GIC and to measure the amount released as a function of time. The rate, pattern and duration of release were evaluated. Release measurement was carried out by high performance liquid chromatography (HPLC) and ultraviolet (UV) detector.

4.3.1.2 Experimental detail

Figure 17 shows a schematic of the setup of the HPLC [Thermo-Separation Products (formerly Spectral Physics)] used for detection of CHA and AHCl released from GICs. It consisted of a degasser with holder for four 1 litre solvent reservoirs, a microprocessor-controlled two-stage pump system, 120 vial auto-sampler, silica base column (coated with C_8 for CHA or C_{18} for AHCl), UV 100 detector and a PC for data acquisition with 'Spectrum' software.

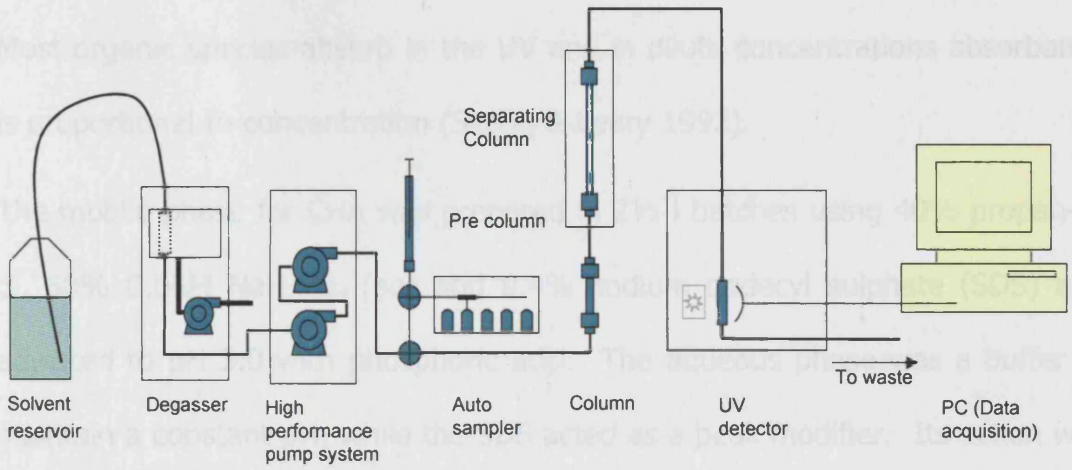

Figure 17 Schematic of the HPLC system

The mobile phase was the solvent continuously applied to the column, which acted as a carrier for the sample. A sample solution was injected into the mobile phase either manually or automatically by an automated sampler. As the sample flowed through the column, the components migrated according to the ionic interactions of the compounds with the column. Those components which had greater interactions with the mobile phase than with the stationary phase elute from the column faster and thus had shorter retention times and vice-versa. The mobile phase could be altered to manipulate the interactions between the sample and stationary phase. In the current study, isocratic elution was used as only one eluted component was of interest. The mobile phase in this case had a constant composition. Each compound in the solution therefore migrated at a different rate resulting in faster or slower elution from the column and therefore shorter or longer retention times. The analyte, having been eluted from the column, passed to the detector. The method of detection of choice for organic species is the absorption of ultraviolet (UV) light.

Most organic species absorb in the UV and in dilute concentrations absorbance is proportional to concentration (Skoog & Leary 1992).

The mobile phase for CHA was prepared in 2½ l batches using 40% propan-2-ol, 60% 0.05M NaH_2PO_4 (aq) and 0.4% sodium dodecyl sulphate (SDS) and adjusted to pH 3.0 with phosphoric acid. The aqueous phase was a buffer to maintain a constant pH, while the SDS acted as a peak modifier. Its action was designed to sharpen the tail of the peak and also to separate the components by extending the retention times. After mixing, the mobile phase was filtered through a 0.2 μm pore filter (Anodisc 47, Whatman Ltd, Maidstone Kent) to remove particulates that could foul the column.

The flow rate was constant throughout each run and was varied between 1.3 $cm^3\ min^{-1}$ and 2.0 $cm^3\ min^{-1}$. This was selected to enable separation from interfering peaks whilst allowing short retention times. The UV detector was set to a detection wavelength of 270 nm. The injection volume was 20 μl and the stationary phase was a 10 cm C_8 column of pore size 5 μm (Jones Chromatography) (method modified from Izumoto *et al.*, 1997). The chromatograph was calibrated using CHA solutions of known concentration. A linear relationship was observed between detector response and CHA concentration.

The mobile phase for amprolium hydrochloride was prepared in 2½ l batches using 40% methanol, 60% water, 0.5% acetic acid, 0.5% triethylamine and 4.6 mM octane sulphonic acid. The flow rate was constant throughout each run and was varied between 1.7 $cm^3\ min^{-1}$ and 2.0 $cm^3\ min^{-1}$. The injection volume

was 20 μl and the stationary phase was a 15 cm C_{18} column of pore size 10 μm (Jones Chromatography) (Tan *et al.*, 1996).

4.3.1.3 Specimen preparation

The powders were mixed as described previously[1] in section 4.2.1. It was possible to prepare two specimens from one batch for the slower setting mixes and one specimen for the faster setting mixes. The components were then mixed with water at room temperature on a plastic mixing pad with a stainless steel spatula. Six specimens were fabricated from each batch of glass/PAA/included species mix. The mixed paste was placed into split ring moulds (10 mm internal diameter and 1 mm thickness) and sandwiched between two glass slides. The excess material was expelled through the split by firm hand pressure. The assembly was placed in an incubator at 37°C for 1 h. After removal from the moulds the specimens were weighed (±0.0001 g) prior to immersion in sample tubes containing 20 ml of water. This volume of water was chosen so as to be small enough to give a measurable concentration of included specie and large enough so as to reduce the possibility of eluted species' concentration affecting the release profile. The sample tubes were chosen to allow minimum contact between the specimen and tube walls and therefore permit diffusion of CHA or AHCl from all surfaces of the specimen into the surrounding aqueous medium. The sealed tubes were placed in an incubator at 37 °C and agitated daily.

To determine the quantity of CHA and AHCl released from each of the cement formulations, 20 μl aliquots were taken at intervals so as to produce evenly

---

1 N.b. Note different composition for first batch of LG26

spaced points on an x-axis of time$^{1/2}$, and injected into the HPLC. These time points were typically 1 h, 2 h, 4 h, 6 h, 24 h, 2d, 6d, 9d, 15d, 22d, 36d, 44d, 51d, 63d, 78d, 93d, 107d, 132, 146d, 162d after immersion. The reduction in volume after each aliquot was taken was accounted for in the release calculations at the point where the measured concentration was converted to mg of species in the sample tube. From the known amount of CHA and AHCl added to the cements, the proportion released was calculated and the median values obtained from the six specimens. Median values were used as this does not require an assumption of normality of results. In the case of an even number of readings, there are two median values, 3rd and 4th ranking and therefore the median is taken to be the mean of these two values. Typical traces for CHA and AHCl are shown in the two figures below.

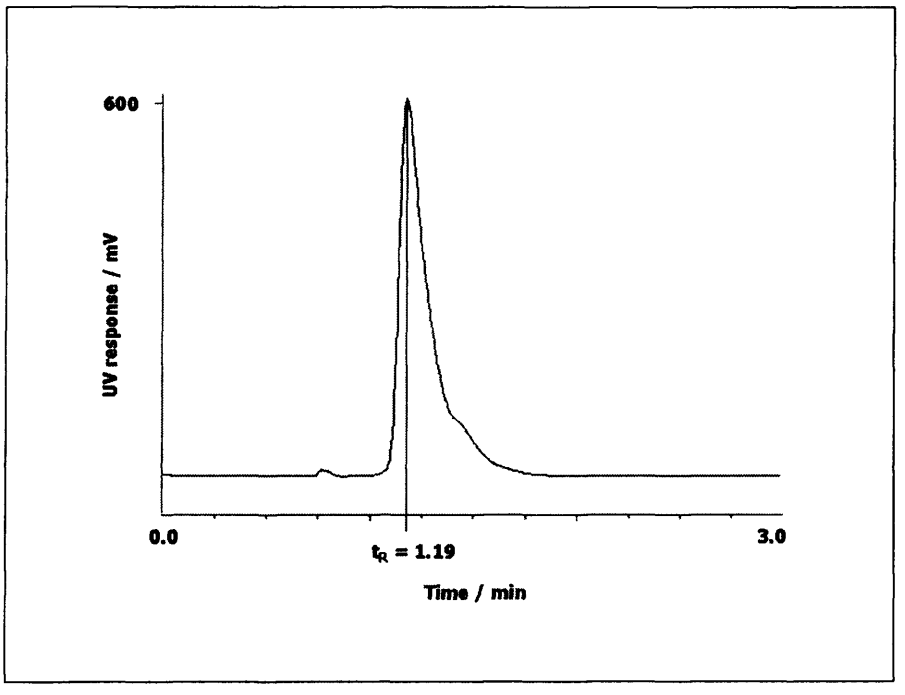

Figure 18 Typical HPLC trace for CHA showing CHA response with a retention time of 1.19 minutes

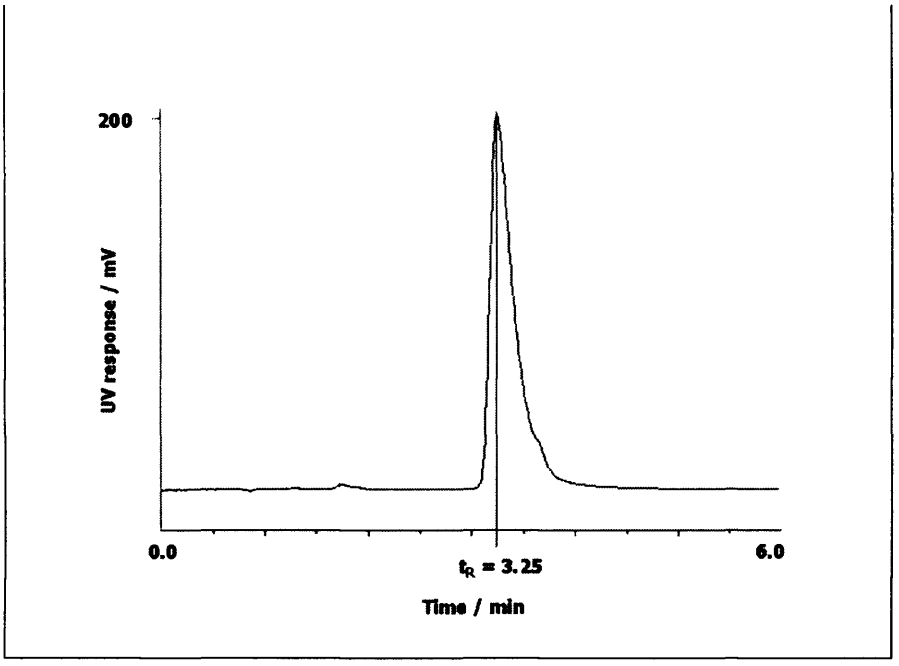

Figure 19 Typical HPLC trace for AHCl showing AHCl response with a retention time of 3.25 minutes

4.3.2 Effect of storage volume

This study was concerned with release into a fixed volume of liquid. Additional experiments were performed to determine the effect of reservoir volume on the release of CHA from MP4 cement containing 8.8% CHA and the release of AHCl from AH2 cement containing 8.8% AHCl.

The specimens containing both CHA and AHCl were split into four groups with initially six specimens in each group. The first group were immersed in 20 ml distilled water which was replaced with fresh water after sampling every 24 hours. The second, third and fourth groups were immersed in 20, 40 and 60 ml distilled water respectively and the water was not changed. CHA and AHCl release were calculated and on observing the large scatter of values for CHA release, a further six specimens were made for each of the four groups and the data added to that for the previous four groups.

Further experiments were performed to determine the effect of reservoir volume on the release of AHCl for two included concentrations.

Samples containing 6.8% AHCl were split into two groups: one group was immersed in 10 ml distilled water and the other group immersed in 20 ml distilled water.

A similar experiment was then extended for samples containing 9.0% AHCl. These samples were split into three groups of 20, 40 and 60 ml respectively.

4.3.3 Effect of maturation time

It was shown by Causton in 1981 that GICs are susceptible to moisture contamination during the early stages of the setting reaction so additional experiments were performed to determine the effect of maturation time on the release of AHCl. Comparisons were made between 24 h maturation and 7 day maturation for AH2 cement with two concentrations of included AHCl, namely 2.5% and 1.0%. This was especially important for AHCl as, noted earlier, it had a marked effect on the compressive strength and working and setting times of the GIC cements.

4.3.4 Ion-release studies

4.3.4.1 Aim

Poor blending of cement ingredients at the mixing stage can lead to uneven distribution of the included species, thus affecting the amount of release. If the

specimens exhibiting higher release did so because of uneven distribution, it was possible that these same specimens would exhibit high Ca^{2+} and Na^{+} release. The aim of these experiments was to compare Ca^{2+} and Na^{+} release with CHA release from the same specimens to test this theory.

4.3.4.2 Experimental setup

Figure 20 shows a schematic of the setup for the ion chromatography system (Dionex ICS-1000) used for detection of cations. It consisted of a liquid eluent, high pressure pump, automatic sampler, sample injector, a separation column, chemical suppressor, conductivity cell and a PC for data acquisition.

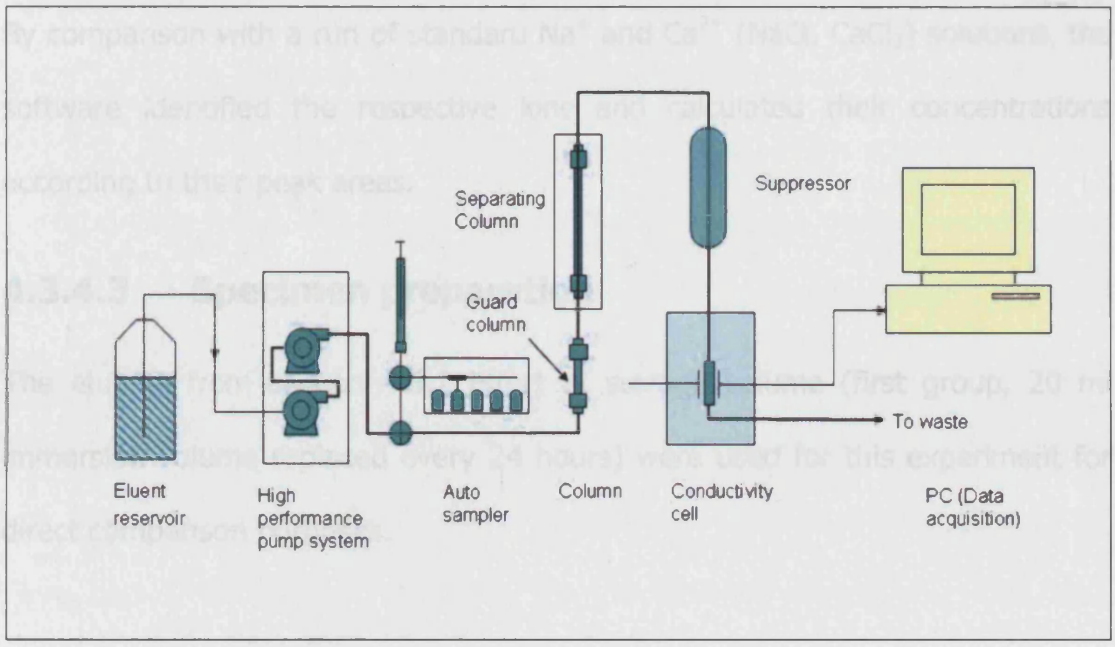

Figure 20 Schematic of the Ion chromatography system

The eluent was continuously applied to the column and acted as a carrier for the sample. A sample solution was injected into the eluent stream either manually by a hand-operated syringe or automatically by an automated

sampler. As the sample flowed through the column, a chemically inert tube filled with polymeric resin, the sample ions were separated. The mode of separation is ion exchange in which different ions migrate through the column at different rates, depending on the interactions with the ion exchange sites.

After the eluent containing the unknown sample ions had left the column, they flowed through a suppressor that suppressed the conductivity of the eluent and enhanced that of the sample ions. The conductivities of the separated components were measured as they flowed through the cell. This produced a voltage that was sent to a PC running Chromeleon software version 6.50 (Dionex corporation, Camberley, Surrey, UK). As each ion separately passed through the detector, a voltage was produced above the background voltage. By comparison with a run of standard Na^+ and Ca^{2+} (NaCl, $CaCl_2$) solutions, the software identified the respective ions and calculated their concentrations according to their peak areas.

4.3.4.3 Specimen preparation

The eluents from section 4.3.2 Effect of storage volume (first group, 20 ml immersion volume replaced every 24 hours) were used for this experiment for direct comparison purposes.

4.4 Degradation studies

4.4.1 Compressive strength

4.4.1.1 Aim

The aim of these experiments was to determine the effect on species addition on the compressive strength of samples. This provides some indication of the disruption caused by the species addition.

4.4.1.2 Experimental setup

The powder and cement were prepared as previously described for the release studies. The mixed paste was packed into steel split moulds (4 mm internal diameter and 6 mm thickness). Two glass slides were placed on top and bottom and the assembly clamped. The samples were allowed to mature at 37 °C for 1 h. After this, the clamps and glass plates were removed and the exposed ends were finished with 1000 grit silicon carbide paper to ensure even contact with the loading platens. The samples were then removed from their moulds and immersed in sample tubes containing distilled water. The sealed tubes were placed in an incubator at 37 °C and left for 48 h prior to testing. The influence of early loss of added species was not accounted for and may have had a detrimental effect on the compressive strengths. This test, therefore, was measuring the effect, on compressive strength, of inclusion of an added species and its subsequent release over 48 h. All specimens including the controls, however, were treated the same way.

The diameter of each specimen was measured in three places using a digital caliper (Mitutoyo) and the mean calculated. The specimens were then placed

between the platens of a universal load testing machine (4505 Universal Testing Machine, Instron High Wycombe, UK), fitted with a 50 kN load cell. Pieces of damp filter paper (Whatman No. 1) were placed on the specimen ends. The moistened filter paper acted as a buffer to compensate for small imperfections in the surface and ensure even load distribution during the test as well as to reduce the risk of desiccation of the specimens. Specimens were then loaded to failure at a cross-head speed of 1 mm min^{-1}. The plot of applied load vs. extension was displayed via computer software (Instron series IX) and the load at specimen failure obtained. Six specimens were made for each glass/added species concentration and the median value for load at failure obtained. The compressive strength was calculated using the formula S=P/area*1000 where S is the compressive strength in MPa, P is the load at specimen failure in kN and area is the cross-sectional area of the specimen in mm^2.

4.4.2 Weight loss studies

4.4.2.1 Aim

The aim of these experiments was to determine the effect on species addition on the degradation of the samples during their immersion in water. This provides some indication of the disruption caused by the species addition.

4.4.2.2 Experimental setup

The specimens used in the release studies were also used for these experiments. The final mass of the specimen after immersion in water for over

two years was subtracted from the original specimen mass before immersion to give the mass loss. These specimens were then dried in a desiccator at 37 °C to constant mass and a third mass recorded. This third mass reading gave an indication of the amount of free water in the GIC as opposed to water that was bound in the cement.

4.4.3 Scanning electron microscopy and elemental analysis

4.4.3.1 Replication efficacy

4.4.3.1.1 Aim

A well-known disadvantage of SEM is that specimens have to be dry to be viewed under vacuum. On drying and vacuuming, crack artefacts are produced on a cement surface obscuring some of the original topographical detail. In order to observe cracks that have occurred during the leaching of included species from the cement, replicas were made of the cement surface.

The technique of replicating, however, can also lead to artefacts. If the impression material is not fluid enough for a time long enough for it to flow into all the topographical features of the surface to be replicated, detail can be lost. If the replicating material is too viscous and sets too quickly detail can also be lost (Palmer *et al.*, 1999). With a two-stage replicating procedure dust contamination becomes of concern. In normal specimen preparation, dust has to be avoided as this can settle on the surface to be examined thus showing up as 'charging' during viewing with an electron beam. In a two-stage replication procedure there are three stages at which dust contamination may be of

concern: Initial exposure of specimen before the impression is taken, exposure of impression to air before the replica is poured onto the surface and exposure of the replica to air before and after being coated with gold. There was also a possibility that an impression material might not remove cleanly from the original surface but retain loose parts of the surface, especially at undercuts.

4.4.3.1.2 Experimental procedure

In order to test the accuracy of the chosen replication procedure, an identifiable are on a fractured surface of cement (AH2) was replicated. The original surface was viewed, followed by the impression, a second impression and the replica made from the second impression. The second impression was taken to check if the first impression resulted in material removal from a delicate surface.

4.4.3.2 Scanning electron microscopy of surfaces

4.4.3.2.1 Aim

Theories have been postulated as to species release through cracks and channels (Rhine *et al.*, 1980). To examine the possibility of cracks and channels in these specimens a study was carried out in which a selection of specimens were examined in an SEM at various stages of elution.

4.4.3.2.2 Experimental detail

The time periods chosen were time 0 when the specimen was released from the mould, 48 hours when approximately half of the total release had occurred and 35 days where most release had stopped (plateau region on the cumulative release graphs).

4.4.3.2.3 Specimen preparation

Specimens were prepared in split rings in the same manner as for the release experiments. For each of the four glasses two specimens were made for each of the following concentrations.

CHA	AHCl
0%	*
4.4%	4.4%
8.8%	8.8%

Table 7 Concentrations of species for SEM study
*** this is the same as 0% CHA**

For each species / concentration combination both specimens were matured for 24 hours. After this each specimen was placed over a thin metal rod and fractured by finger pressure either side of the rod. Part A was replicated and the original stored at 37 deg C over saturated KBr (aq) to give 80% humidity. Part B was stored in water at 37 deg C for 48 hours and then fractured as above. Part B1 was replicated and the original stored in 80% humidity and part B2 was stored in water at 37 deg C for 35 days and then fractured as above. Part B2A was replicated and the original stored in 80% humidity. Part B2B was stored in water for possible use later. This is illustrated in Figure 21.

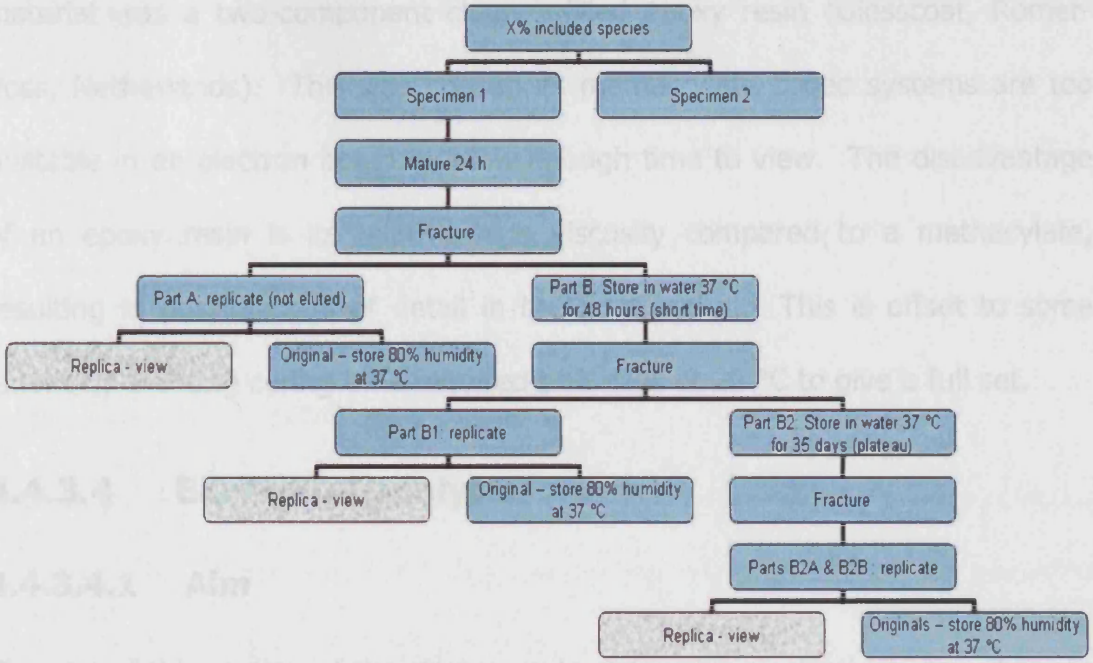

Figure 21 Block diagram of SEM study plan

Please note: plan shown only for specimen 1 of 2 duplicates.

4.4.3.3 Replication

Doric light, an addition-cured dental impression material (Davis, Schottlander and Davis Ltd., Letchworth, England) was mixed using the supplied syringe and automatic mixing tip and a small amount was placed on the edge of the specimen. This was then blown with a Dust-off compressed air duster (Falcon Safety Products, New Jersey, USA) across the surface of the specimen thus reducing air bubble entrapment. More impression material was poured on top to add bulk and a cover-slip placed on top of this level to the workbench. This was done so that once set, the impression had a flat base allowing it to sit levelly on the bench allowing ease of pouring of the replicating material.

After the impression material had set, it was carefully peeled off the original specimen that was immediately placed in 80% humidity. The replicating

material was a two-component clear unfilled epoxy resin (Glosscoat, Romer-Voss, Netherlands). This was chosen as methacrylate based systems are too unstable in an electron beam to allow enough time to view. The disadvantage of an epoxy resin is its relative high viscosity compared to a methacylate, resulting in possibly loss of detail in the final replica. This is offset to some extent by the long curing time required of 8 days at 20 °C to give a full set.

4.4.3.4 Elemental analysis

4.4.3.4.1 Aim

The aim of this section of the study was to determine qualitatively any changes to the surface topography of the samples as a result of the inclusion of the added species with respect to time after immersion. Some simple quantitative evaluations were also carried out to determine the site of the included species.

4.4.3.4.2 Experimental details

The principle of scanning electron microscopy is that the surface of the sample is swept by a finely focussed electron beam in a raster pattern. Various signals are produced, including secondary, back-scattered and Auger electrons, X-ray fluorescence and other photons. The most commonly used signals are back-scattered and secondary electrons, which are the basis of SEM, and X-ray fluorescence, the basis of electron probe microanalysis. In the current work, the electron source was a tungsten filament which was heated by an electric current. The electrons were accelerated towards the specimen at an accelerating voltage of 25 kV. The X-rays were detected by a Pentafel Plus® detector (Oxford Instruments) which was liquid nitrogen cooled. The silicon (lithium drifted) detector had a window known as a SATW (super atmosphere

supporting thin window) which allows transmission of elements from beryllium onwards. The energies of the X-rays were detected by energy dispersive X-ray analysis (EDX). The secondary electron signal was used to assess the GIC surface visually, while the X-ray fluorescence signal was used to examine chemical composition by EDX.

4.4.3.4.3 Procedure

Various leached samples of AH2 + CHA and AH2 + AHCl cements were selected and placed in a desiccator until they were dehydrated. Other freshly prepared specimens with the same concentrations of the two added species were made for comparison purposes. These are listed in Table 8.

Concentration of added species	Leached	Newly prepared
8.9% AHCl	AM74	A1
	AM76	A3
11.3% CHA	CHA073	D1
	CHA078	D3

Table 8 Specimens selected for elemental analysis

These were dehydrated in the same way. Each specimen was sectioned with a razor blade and each section put into one of two groups. Samples from group A were laid flat on the stub and fixed with carbon paint to provide a conducting pathway between the specimen surface and the aluminium stub. Samples from group B were carefully polished on the sectioned edge with 4000 grit silicon carbide paper and placed polished edge up on the stub, for viewing in cross-

section, and again fixed in position with carbon paint. They were then coated under vacuum with carbon in an Polaron CC7650 carbon coater. Carbon coating was preferred to the normal gold or gold/palladium as the peaks for gold /palladium would have interfered with the spectra from the elements in the EDX analysis. The specimens were then examined using a Cambridge Stereoscan S90B (Cambridge Instrument Company, Cambridge, UK) scanning electron microscope with EDX probe from Oxford Instruments (Witney, Ofordshire) at an accelerating voltage of 25 kV. The secondary electron images were captured using Oxford Instruments INCA software with a resolution of 2000 lines and saved in jpeg format. These were acquired at various standardised magnifications of up to × 4000.

4.4.4 X-ray photoelectron spectroscopy (XPS)

4.4.4.1 Aim

The aim of XPS was to determine changes in surface chemistry of unleached specimens doped with CHA or AHCl compared to leached specimens. A schematic of a typical XPS system is shown in Figure 22.

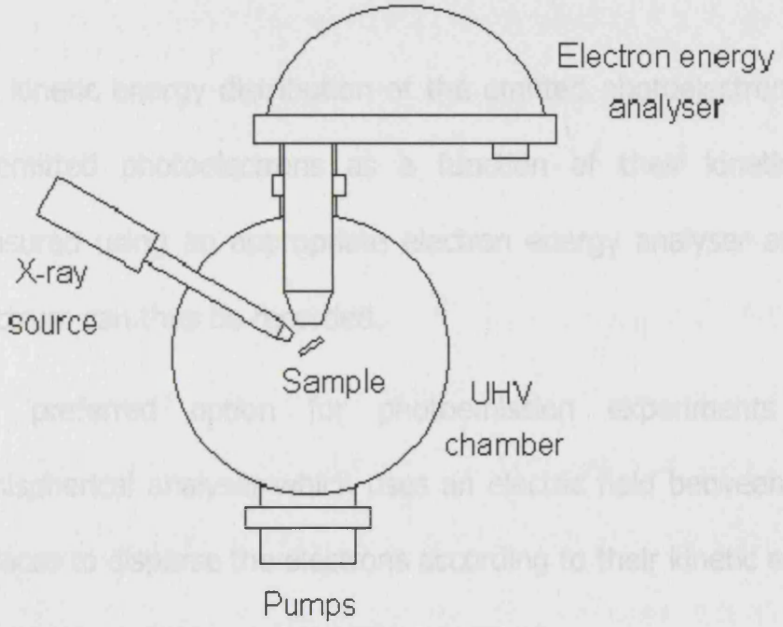

Figure 22 Schematic of a typical XPS system

4.4.4.2 Principle of operation

XPS is a surface analysis technique that looks at the elemental composition of the outermost atomic layers of a solid. It involves irradiation of a sample under high vacuum by X-rays of known energy which causes photo-ejection of electrons from atoms near the surface (5-10 nm depth). The high vacuum is necessary to avoid collisions between the emitted photoelectrons and gas molecules. The electron emission process is shown in Figure 23.

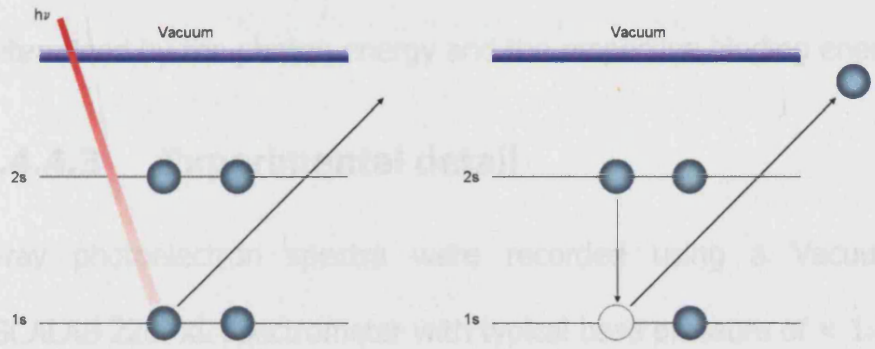

Figure 23 XPS - Electron emission process

The kinetic energy distribution of the emitted photoelectrons (i.e. the number of emitted photoelectrons as a function of their kinetic energy) can be measured using an appropriate electron energy analyser and a photoelectron spectrum can thus be recorded.

The preferred option for photoemission experiments is a concentric hemispherical analyser which uses an electric field between two hemispherical surfaces to disperse the electrons according to their kinetic energy.

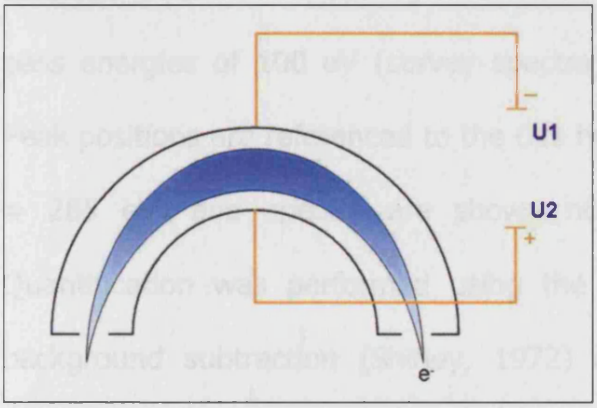

Figure 24 XPS - Hemispherical analyser

For each element, there will be a characteristic binding energy associated with each core atomic orbital and therefore each element will give rise to a characteristic set of peaks in the photoelectron spectrum at kinetic energies determined by the photon energy and the respective binding energies.

4.4.4.3 Experimental detail

X-ray photoelectron spectra were recorded using a Vacuum Generators ESCALAB 220i-XL spectrometer with typical base pressure of $< 1\times10^{-9}$ mbar.

Spectra were excited using a monochromated Al Kα X-ray source (hν=1486.6 eV) at a 1 mm spot size. Photoelectrons were detected using a magnetic objective lens system and 300 mm diameter 180° hemispherical electron energy analyser. Charge compensation was achieved *via* a Ta mask placed in good electrical contact, coupled with low energy (4 eV) electron flooding of the sample. No *in situ* surface preparation was carried out prior to analysis, although samples were allowed to dehydrate *in vacuo* for several hours (overnight where necessary) to avoid excessive outgassing. Spectra were recorded at normal emission, in constant analyser energy (CAE) mode using pass energies of 100 eV (survey spectra) and 20 eV (narrow scan spectra). Peak positions are referenced to the C1s hydrocarbon peak (arbitrarily set at BE = 285 eV) and spectra are shown normalised to the C1s peak height. Quantification was performed using the VG Eclipse software, using Shirley background subtraction (Shirley, 1972) and atomic sensitivity factors from Wagner *et al.* (Wagner *et al.*, 1981).

GIC samples for XPS analysis were in the form of discs (10 mm diameter × 1 mm thick). After mixing, discs were clamped between cellulose acetate sheets in split-ring moulds and cured in a 37°C high humidity oven for 1 hour. They were then washed, dried and stored in a desiccator until analysis. The control disc was mixed with deionised water. "Doped" discs were mixed at a ratio of 7:1 with amprolium hydrochloride (overall concentration 8.8 %) or chlorhexidine acetate (overall concentration 11.0 %). Leached discs were made up in the same way (8.8 % AHCl and 11.3% CHA) and then immersed in water for 490 days (108 $h^{1/2}$). For comparison, XPS spectra were also recorded from GIC discs immersed in 1.9 % CHA solution or 20 % AHCl solution for 48 h.

5 Results

5.1 Raw materials

5.1.1 Characterisation of the glasses – XRF

The technique of XRF oxidises the components and gives the proportions of sample components as their oxide form. The original pre-firing composition data from the manufacturer are shown in Table 9 for purpose of comparison and the post-firing XRF data are shown in Table 10.

	AH2	MP4	LG30	LG26
SiO_2	40.0	28	25.3	24.3
Al_2O_3	22.9	35	28.6	27.5
CaO	-	26	26.2	15.1
Na_2O	-	11	-	-
P_2O_5	-	-	19.9	19.1
$AlPO_4$	6.2	-	-	-
Na_3AlF_6	18.5	-	-	-
CaF_2	12.4	-	-	14.0

Table 9 Original glass components / weight % (manufacturer's data)

	AH2	MP4	LG30	LG26
SiO_2	44.22	26.1	30.35	23.21
Al_2O_3	31.93	35.4	34.17	28.74
CaO	12.49	29.4	21.41	29.64
Na_2O	7.45	9.2	1.01	0.61
P_2O_5	3.90	-	13.07	17.38
SrO	-	-	-	0.41

Table 10 XRF glass composition / weight %

The data, as presented, does not allow direct comparison. The data was therefore separated into the constituent elements and converted into mole percent. These are shown in the two tables below. As there was no XRF data for F, the original glass components were recalculated without F and as there was no original data for Sr in the original glass components, the post-firing data was recalculated without Sr. These recalculated data are shown in the right hand parts of Table 11 and Table 12.

	All components					Without F			
	AH2	MP4	LG30	LG26		AH2	MP4	LG30	LG26
Si	18.7	13.1	11.8	11.4		22.3	13.1	11.8	12.2
Al	15.9	18.5	15.1	14.6		18.9	18.5	15.1	15.6
O	35.3	41.6	45.6	41.0		42.0	41.6	45.6	43.9
P	1.6	0.0	8.7	8.3		1.9	0.0	8.7	8.9
Na	6.1	8.2	0.0	0.0		7.3	8.2	0.0	0.0
Ca	6.4	18.6	18.7	18.0		7.6	18.6	18.7	19.3
F	16.1	0.0	0.0	6.8					
Totals	100.0	100.0	100.0	100.0		100.0	100.0	100.0	100.0

Table 11 Original glass components (pre-firing) / mol %

	All components					Without Sr			
	AH2	MP4	LG30	LG26		AH2	MP4	LG30	LG26
Si	20.7	12.2	14.2	10.8		20.7	12.2	14.2	10.8
Al	16.9	18.7	18.1	15.2		16.9	18.7	18.1	15.2
O	46.3	41.3	46.0	44.4		46.3	41.3	46.0	44.5
P	1.7	0.0	5.7	7.6		1.7	0.0	5.7	7.6
Na	5.5	6.8	0.7	0.5		5.5	6.8	0.7	0.5
Ca	8.9	21.0	15.3	21.2		8.9	21.0	15.3	21.3
Sr	0.0	0.0	0.0	0.3					
totals	100.0	100.0	100.0	100.0		100.0	100.0	100.0	100.0

Table 12 Final glass components (post-firing) / mol % (red – higher than expected, blue – lower than expected allowing for XRD accuracy of ± 10%)

As the XRF technique used was only accurate to ± 10%, the data was interpreted with that in mind. In general the pre and post-firing compositions are very similar. Both LG30 and LG26 had no Na in the original mixture but small amounts, 0.7 mol % and 0.5 mol % respectively were detected in the final glass composition. The XRF system used could not detect elements lighter than Na and therefore there is no data for F. The P content, before and after firing, was almost identical for AH2 glass but lower for LG30 and LG26; no P was detected in the final glass composition of MP4. There was a small amount of Sr in LG26. This may have been present as a contaminant in CaF^2 or CaO, it belonging to the same chemical group as Ca.

The data for AH2, MP4 and LG26 cements showed the same trend between original and final glass components. LG30 showed the opposite trend for Ca and Al. The pre-firing composition shows 15.1 mol % Al and 18.7 mol % Ca. Post firing, this data is almost reversed with 18.1 mol % Al and 15.4 mol % Ca.

5.1.2 Characterisation of the glasses – particle size

The data output from the 'Malvern' were in the form of a table and bar chart listing the upper and lower limits for each range and the volume percentage of particles within each range. An example of particle size distribution plot is shown in Figure 25. For most samples, the distribution was too wide for one lens and the distributions for two lenses had to be combined into one composite graph as in Figure 26.

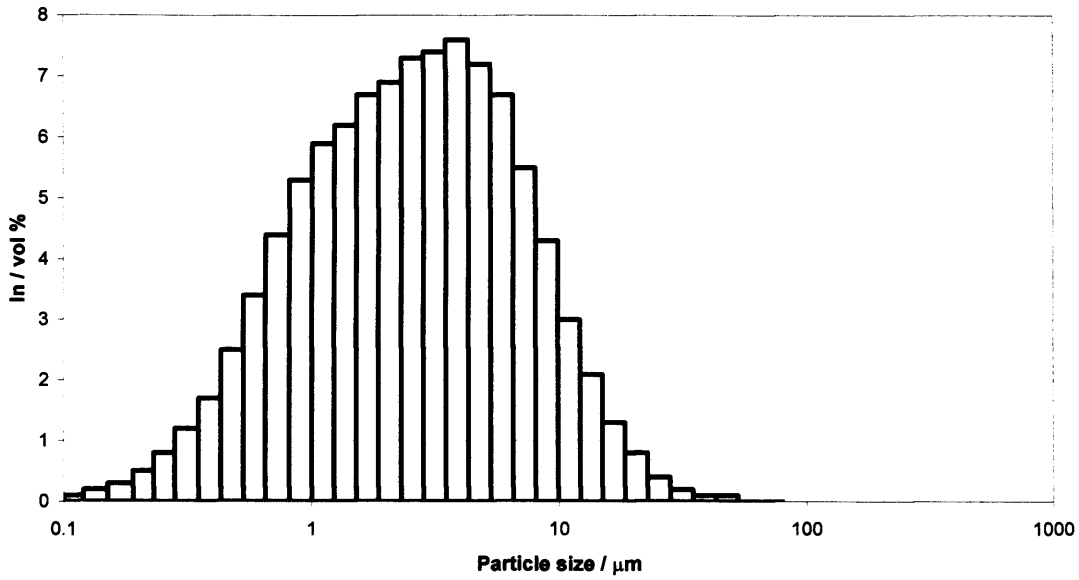

Figure 25 Particle size distribution for LG26 (initial)

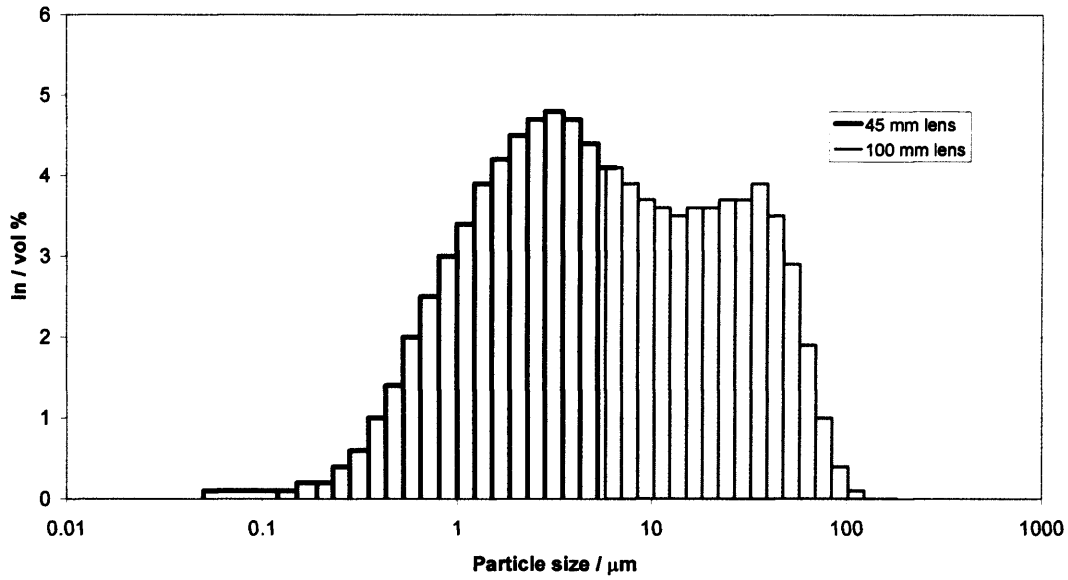

Figure 26 Particle size distribution for LG30 (later)

The distributions are more easily represented by the 'D' values for 0.1, 0.5 and 0.9 which are the particle sizes below which 10%, 50% and 90% of the particles lie (by volume). These are referred to as D[V,0.1], D[V,0.5] and D[V,0.9] and are shown in Table 13. The values are plotted in Figure 27.

Glass	Focal length	D[V, 0.1]	D[V, 0.5]	D[V, 0.9]
AH2	45	4.15	6.47	(40.95)
AH2	100	(1.39)	6.71	41.15
MP4 OLD	100	(2.30)	13.89	46.45
MP4 NEW	45	0.42	6.67	(44.45)
MP4 NEW	100	(0.79)	5.97	21.34
LG30 OLD	45	0.99	7.17	(28.00)
LG30 OLD	100	(0.84)	7.08	29.30
LG30 NEW	45	0.91	6.49	(50.37)
LG30 NEW	100	(0.8)	5.12	38.75
LG26 OLD	45	0.63	2.59	(9.04)
LG26 NEW	45	1.10	7.81	(39.49)
LG26 NEW	100	(0.77)	6.11	29.73
CHA	300	2.31	14.03	71.90

Table 13 D values for the various glasses used

Comparing the initial and later batches of MP4, for all three D values, the initial glass had a higher proportion of larger particles making the initial glass less reactive than the newer one. In production, however, if the glass is too reactive, it is acid washed to remove ions from the surface of the glass particles thus making it less reactive. Comparing the initial and later batches of LG30, the difference between batches was less clear. The later batch had a slightly higher proportion of larger particles but the older batch had a slightly higher proportion of medium and smaller particles. The overall effect of this was not clear.

Despite these differences, the CHA release data, which showed a generally greater release from cements made from the later batches of MP4 and LG30 as compared to the initial batches. As the acid washing in production of the glass was not controlled, it is not possible to find a clear relationship between glass size and rate and amount of release of added species.

The LG26 initial batch had the largest proportion of small particles of all the glasses which gave it a high reactivity. This is supported by the early attempts at mixing LG26 cement in which the setting reaction was too fast to allow adequate mixing and presentation of the cement to the mould, which resulted in an alteration of the ratio of components to produce a cement that set in a reasonable time.

The D values for CHA are also shown in the table and figure below. The D50% reading of 14.03 confirms the results from the SEM (Figure 105) which gave an average particle size of between 10 and 20 μm. This was included in an attempt to explain the gritty feel of cement mixes with high proportions of added CHA. The high D90 and D50 values would explain that this was due to a greater proportion of higher particle sizes.

In conclusion, particle size analysis has shown that most glasses have similar particle size distributions with the exception of LG26 initial which had a generally smaller particle size distribution and MP4 initial which had a generally larger particle size distribution.

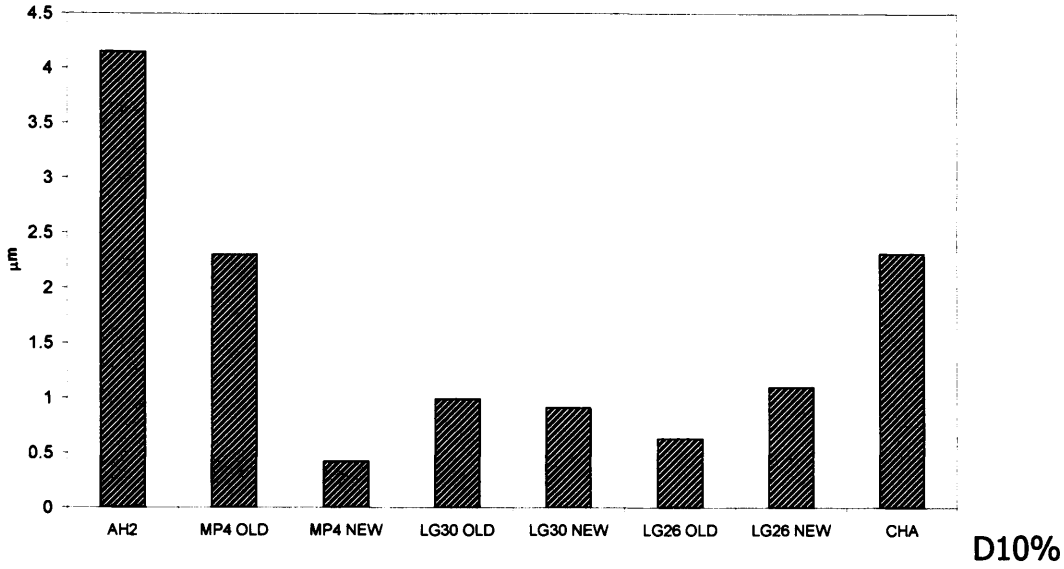

D10%

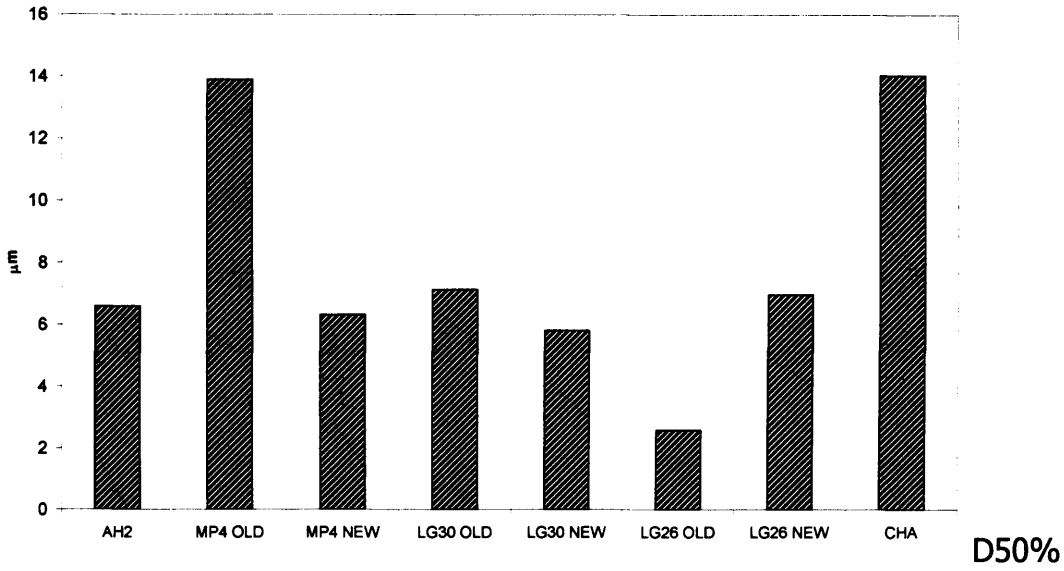

D50%

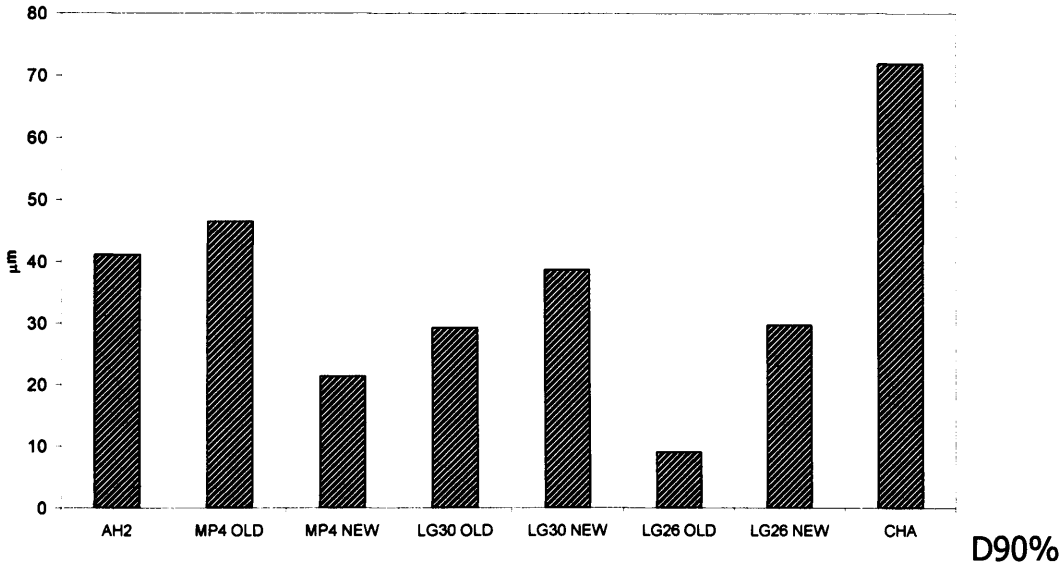

D90%

Figure 27 D values for the various glasses used (e.g. D90 for AH2 = 42 means that 90% of AH2 particles are less than 42 µm)

5.1.3 Selection of included species

We selected four include species according to size, shape, chemical structure and functional group. A pilot study was carried out on each of the four specie to check their viability for inclusion in the cements.

5.1.3.1 Chlorhexidine gluconate

This release study was performed on AH2 glass. The complete release profiles expressed as milligrams CHGlu release per g of cement with respect to time up to 14 $h^{½}$ are set out in Figure 28.

CHGlu was available commercially as a 20% solution only and in this experiment the maximum amount of CHGlu that was possible was incorporated

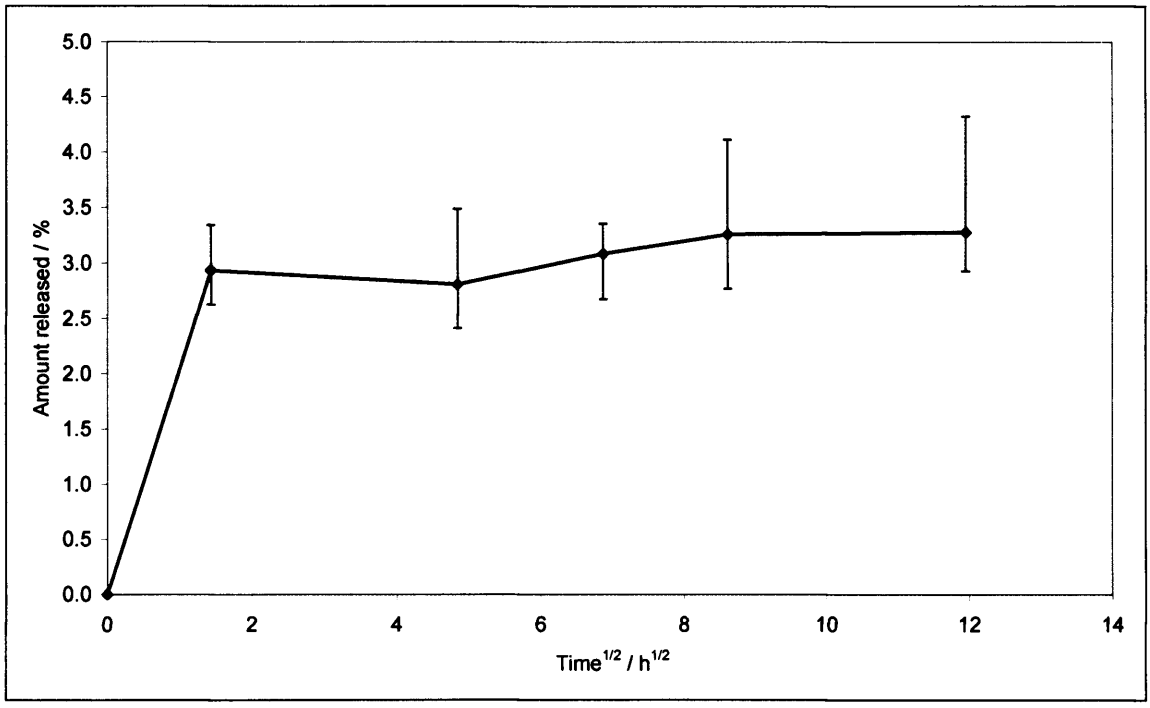

Figure 28 Cumulative CHGlu release / % to t½ = 14 h½ (8 days) n=6

into the GIC. The very small release (maximum of 3.3% (0.8 mg g^{-1})) lead to the conclusion that CHGlu solution was not suitable for this study and the experiment was therefore aborted.

5.1.3.2 Ovalbumin

This release study was performed on AH2 glass. The 3 day results for 8.8% included ovalbumin using the Folin-Lowry method showed 0.67% release. These readings were at the low end of the detection capability of the UV spectrometer giving potentially inaccurate results. The mix was very stiff and it was not possible to incorporate all the water into the material before the material started to set. This part of the study was abandoned at this point.

5.1.3.3 Chlorhexidine acetate

This release study was performed on AH2 glass. The release profiles for 8.8% included CHA expressed as percentage release of total incorporated with respect to time up to 48 $h^{½}$ (96 days) are set out in Figure 29. This release profile expressed as a percentage (2.9%) was similar to that for the release of CHGlu but when expressed as amount release per mass of cement was 2.6 mg g^{-1}.

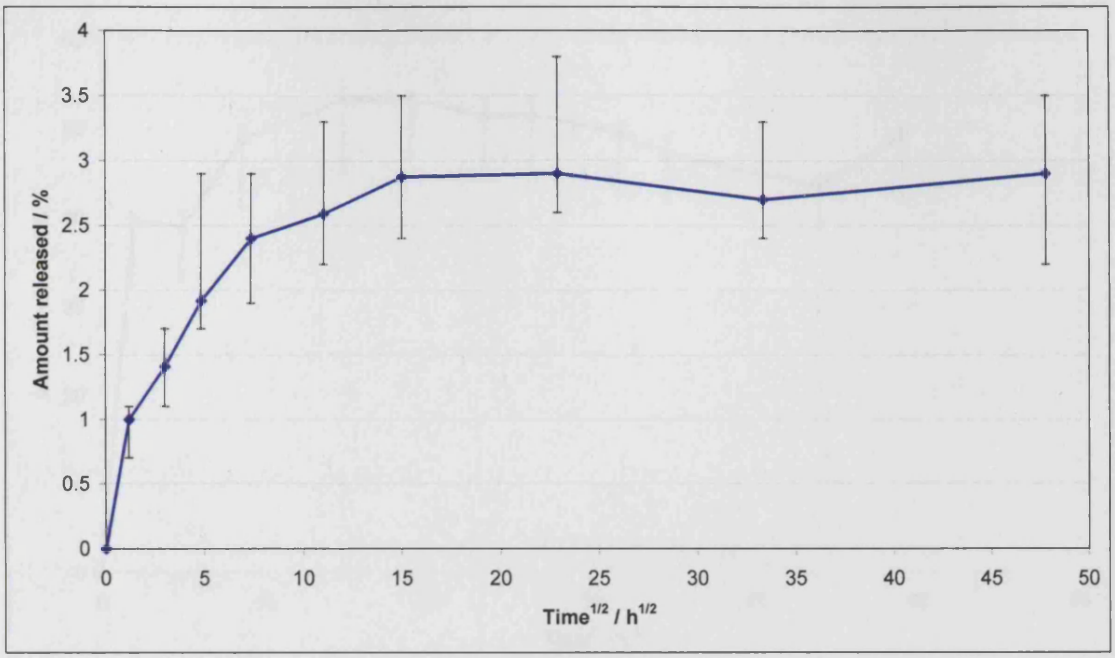

Figure 29 Cumulative CHA release / % to t½ = 48 h½ (96 days),

A further experiment was carried out using 11.3% included CHA. This resulted in a maximum release figure of 5.5% (6.2 mg g^{-1}). This was considered acceptable and CHA was selected for further experimentation.

5.1.3.4 Amprolium hydrochloride

This release study was performed on AH2 glass. The release profiles expressed as percentage release of total incorporated with respect to time up to 49 $h^{½}$ (100 days) are set out in Figure 30. The 9 day (14.7 $h^{½}$) results for 8.8% included amprolium hydrochloride showed 53% (47 mg g^{-1}) release.

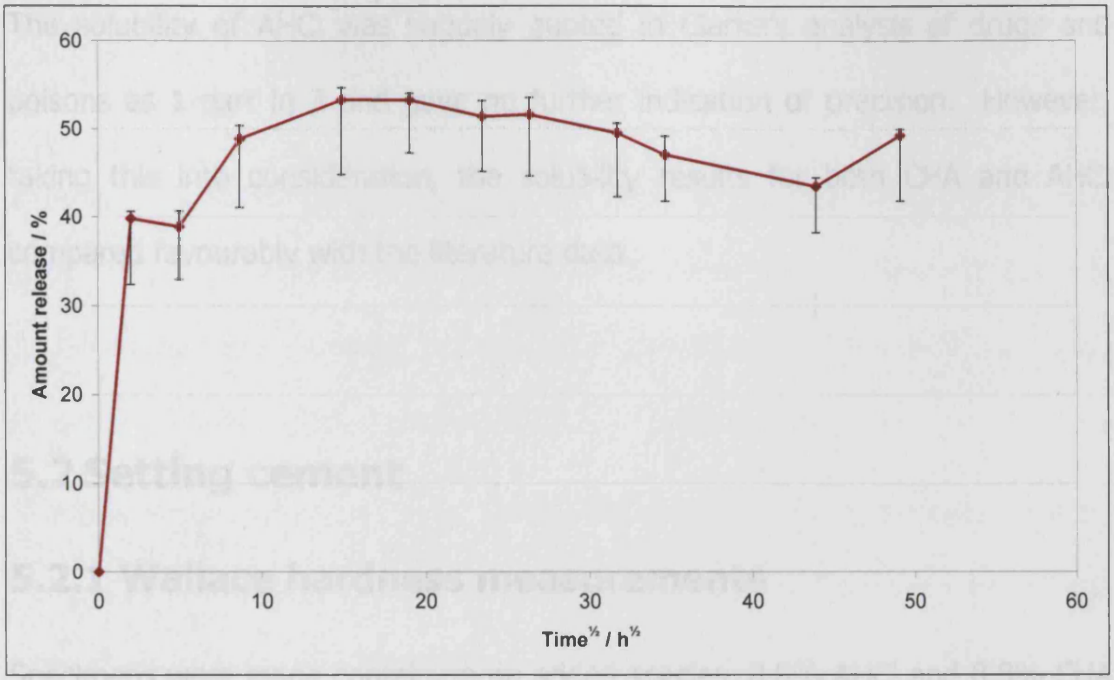

Figure 30 Cumulative AHCl release / % to t½ = 48 h½ (96 days),

This was considered acceptable and AHCl was selected for further experimentation.

5.1.3.5 Solubility of included species

The solubility of two species selected from the results of the pilot study are shown in Table 14.

Species	Experimental data (23 °C)	Experimental data (37 °C)	Literature data (23 °C)	Source of Literature data
AHCl	40% (w/v)	56% (w/v)	33% (w/v)	Clarke's analysis of drugs and poisons, 2004
CHA	2.0% (w/v)	2.0% (w/v)	1.9% (w/v)	British Pharmacopoeia, 2007

Table 14 Measured and literature solubilites of AHCl and CHA in water

The solubility of AHCl was vaguely quoted in Clarke's analysis of drugs and poisons as 1 part in 3 and gave no further indication of precision. However, taking this into consideration, the solubility results for both CHA and AHCl compared favourably with the literature data.

5.2 Setting cement

5.2.1 Wallace hardness measurements

Specimens were made containing no added species, 8.8% AHCl and 8.8% CHA and were matured for both 1 hour and 24 hours. The Wallace hardness indenter gives a depth of penetration reading in "Wallace units" which are equivalent to 0.00001 inches or 0.254 μm. Results were expressed in terms of Vickers hardness (HV) which is defined as:

$$HV = \frac{1854.4 \times load\ (g)}{indent\ diagonal\ (\mu m)^2}$$

Equation 5 Vickers hardness

The diagonal of a Vickers pyramid indent is related to the penetration depth as follows:

$$diagonal = \frac{2 \times depth}{\tan(22°)}$$

Equation 6

These Vickers Hardness Numbers (VHNs) (g μm^{-2}) and are set out in the three following figures below.

Figure 31 shows VHN of the three cement mixes for the four glass cements at 1 hour maturation, Figure 32 shows VHN of the three cement mixes for the four glass cements at 24 hour maturation and Figure 33 shows VHN of CHA included cement and AHCl included cement at both maturation times.

The hardness results for 1 hour maturation show no significant difference for both LG30 cement and LG26 cement between CHA containing cement and unmodified cement. In both the case of MP4 and AH2, the unmodified cement was significantly harder than that containing 8.8% CHA (p=0.00 in Mann-Whitney U test).

The hardness values after 24 hour maturation show no significant difference between the unmodified cements and those containing 8.8% CHA for all four cements.

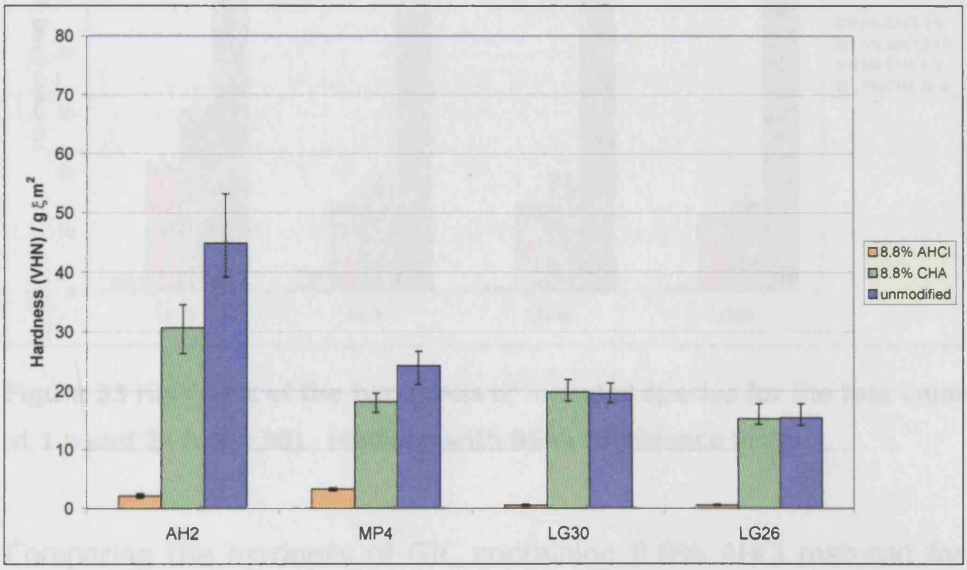

Figure 31 Hardness of the two levels of included species and of the unmodified cement for the four cement mixes at 1 h (n=30). Medians with 95% confidence limits

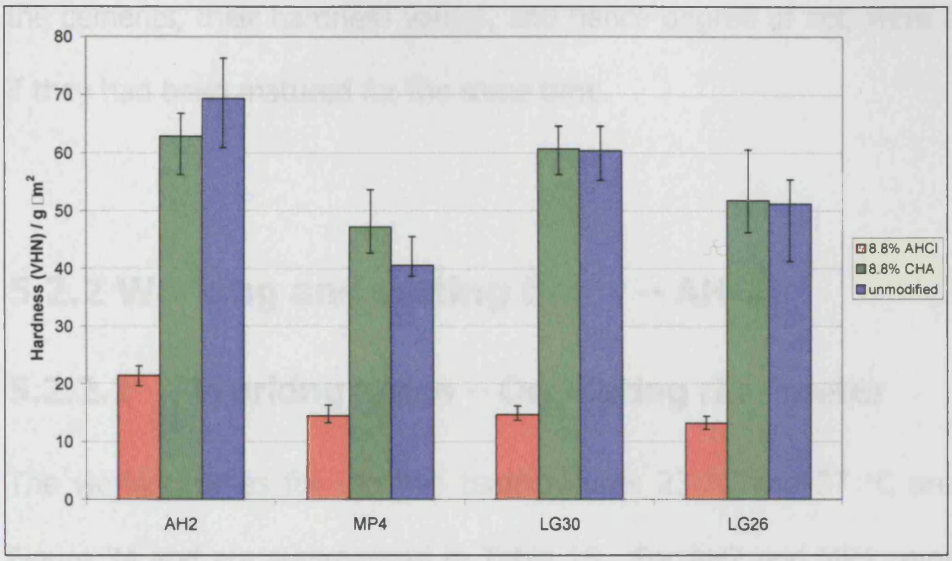

Figure 32 Hardness of the two levels of included species and of the unmodified cement for the four cement mixes at 24 h (n=30). Medians with 95% confidence limits

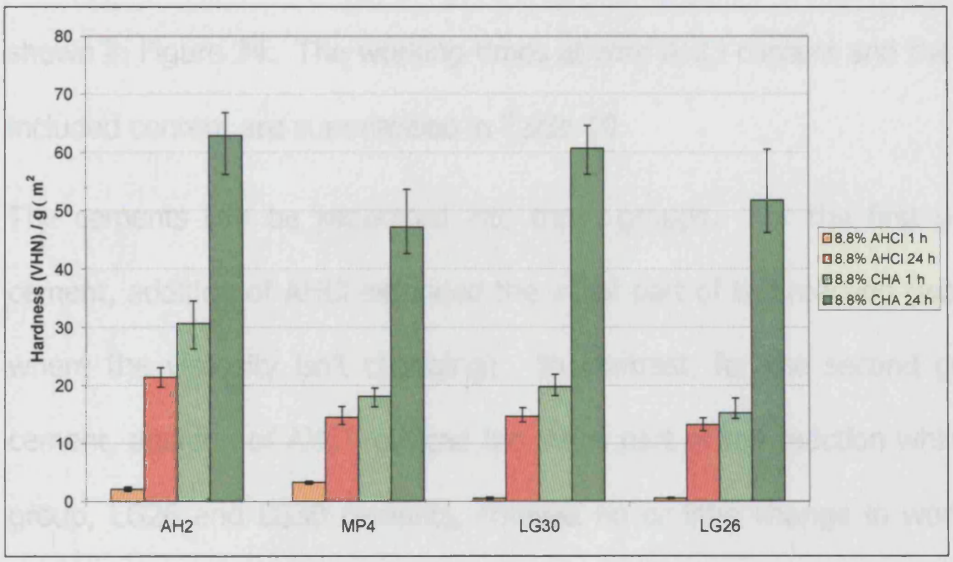

Figure 33 Hardness of the two levels of included species for the four cement mixes at 1 h and 24 h (n=30). Medians with 95% confidence limits

Comparing the hardness of GIC containing 8.8% AHCl matured for 24 h and those containing 8.8% CHA matured for 1 h in Figure 33 yielded the following results: AH2 and LG30, highly significant,($p<0.00$); MP4, significant, ($p<0.01$);

LG26 not significant. Although there was a significant difference for three of the cements, their hardness values, and hence degree of set, were closer than if they had been matured for the same time.

5.2.2 Working and setting times – AHCl

5.2.2.1 Working times – Oscillating rheometer

The working times for the two temperatures 23 °C and 37 °C are shown in Figure 34 and are summarised in Table 15. For AH2 and MP4 cements it was possible to fit an exponential curve to the data. The correlation coefficient values were low in all cases however, and it was decided to use general trends to analyse the data. These curves with their equations and R^2 values are also shown in Figure 34. The working times at zero AHCl content and the maximum included content are summarised in Table 10.

The cements can be separated into three groups. For the first group, AH2 cement, addition of AHCl extended the initial part of the reaction (working time where the viscosity isn't changing). In contrast, for the second group, MP4 cement, addition of AHCl reduced the initial part of the reaction while the third group, LG26 and LG30 cements, showed no or little change in working times with the addition of AHCl. This is summarised in Table 16.

	Working times 23 °C		Working times 37 °C	
	0 %	6.7%	0 %	6.7%
AH2	2.9	7.1	1.9	6.2
MP4	2.5	0.9 (4.4%)	1.8	0.8
LG30	2.0	2.2	1.4	6.7
LG26	2.5	2.9	2.0	2.0

Table 15 Selected working times / minutes of cements containing 0% and 6.7% AHCl concentration (OR)

	23 °C	37 °C
AH2	++	++
MP4	– –	–
LG30	0	0
LG26	0	0

Table 16 Effect of AHCl on working times of the four cements (OR)

+ extends, - reduces, -- reduces to a greater degree

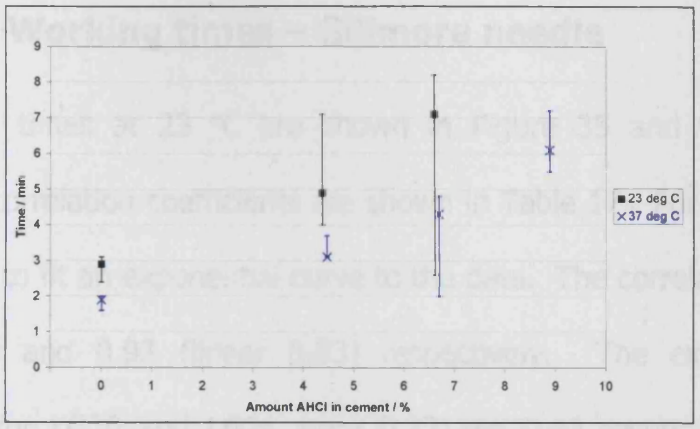

AH2

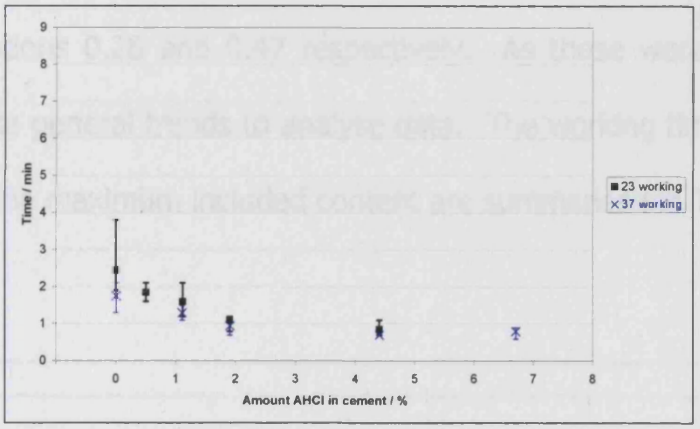

MP4

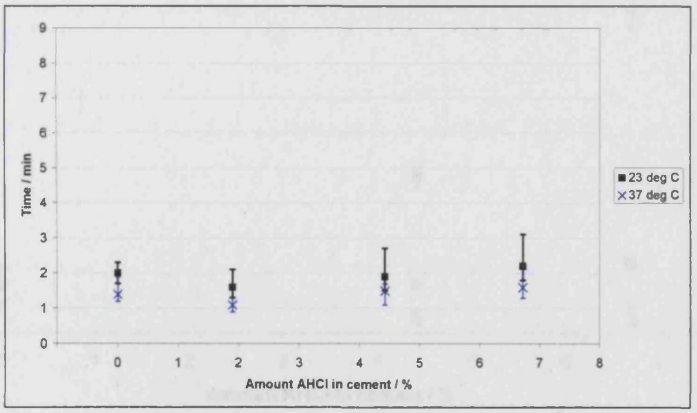

LG30

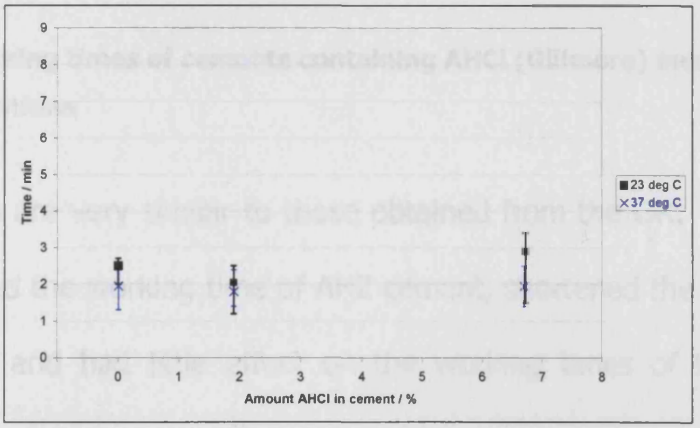

LG26

Figure 34 Working times of cements containing AHCl (OR). Medians (n=6), with 95% confidence limits

5.2.2.2 Working times – Gillmore needle

The working times at 23 °C are shown in Figure 35 and their linear and exponential correlation coefficients are shown in Table 17. For AH2 and MP4 it was possible to fit an exponential curve to the data. The correlations were 0.98 (linear 0.90) and 0.93 (linear 0.83) respectively. The exponential curve correlations for LG30 and LG26 were 0.27 and 0.42 respectively and linear curve correlations 0.28 and 0.47 respectively. As these were so low, it was decided to use general trends to analyse data. The working times at zero AHCl content and the maximum included content are summarised in Table 18.

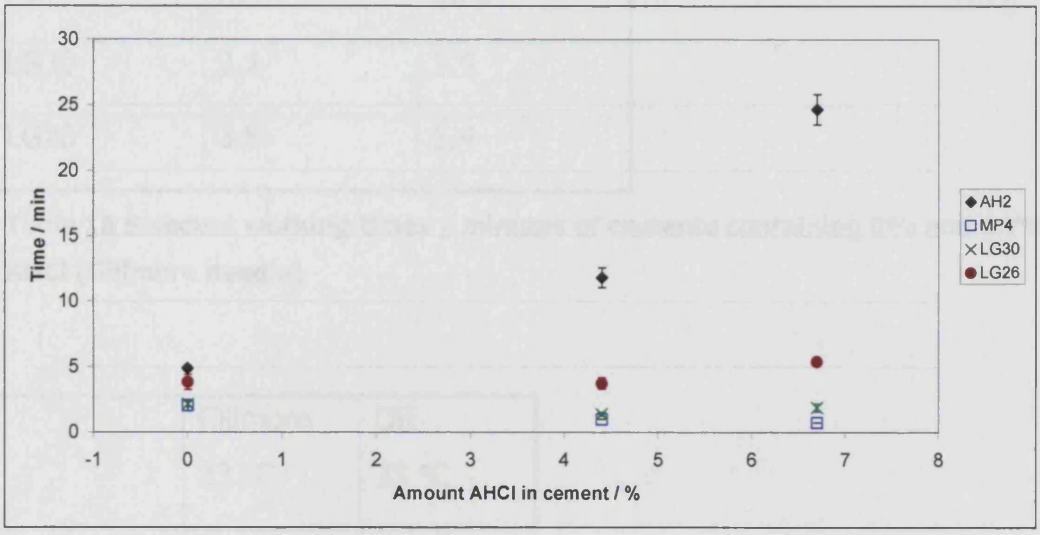

Figure 35 Working times of cements containing AHCl (Gillmore) means (n=3) with standard deviations

These results are very similar to those obtained from the OR. The addition of AHCl extended the working time of AH2 cement, shortened the working time of MP4 cement and had little effect on the working times of LG30 and LG26 cements.

	Linear	Exponential
AH2	0.90	0.98
MP4	0.83	0.93
LG30	0.28	0.27
LG26	0.47	0.42

Table 17 R^2 values for linear and exponential regression lines for working times of cements containing AHCl (Gillmore)

	WORKING TIMES (23 °C)	
	0 %	6.7 %
AH2	4.9	24.7
MP4	2.1	0.75
LG30	2.2	1.9
LG26	3.8	5.4

Table 18 Selected working times / minutes of cements containing 0% and 6.7% AHCl (Gillmore needle)

	Gillmore 23 °C	OR 23 °C
AH2	++	++
MP4	–	– –
LG30	0	0
LG26	+	0

Table 19 Effect of AHCl on working times of the four cements (Gillmore with OR at 23 °C for comparison purposes)

+ extends, ++ extends to a greater degree, – reduces, – – reduces to a greater degree

5.2.2.3 Setting times – Oscillating rheometer

The setting times for the two temperatures 23 °C and 37 °C are shown in Figure 36. Table 20 gives the setting times for the cements for the control (0% included AHCl) and for the cements with the maximum AHCl content studied.

The cements fall into two groups. The first group of AH2, LG30 and LG26 cements showed an increase in setting times at both temperatures with an increase in AHCl content. This indicates strong involvement of the AHCl in retarding the setting reaction especially in the case of AH2 and LG30 and lesser involvement in LG26. The second group consisted of just MP4 cement, which showed a marked decrease in setting time at 23 °C and a slight decrease at 37 °C. This is summarised in Table 21.

	Setting times at 23 °C		Setting times at 37 °C	
	0 %	6.7%	0 %	6.7%
AH2	13.4	85.0	8.5	104.0
MP4	43.0	7.7 (4.4%)	17.7	13.7
LG30	19.0	101.0	13.3	60.0
LG26	27.5	70.3	18.7	53.15

Table 20 Selected setting times of cements containing 0% and 6.7% AHCl (OR)

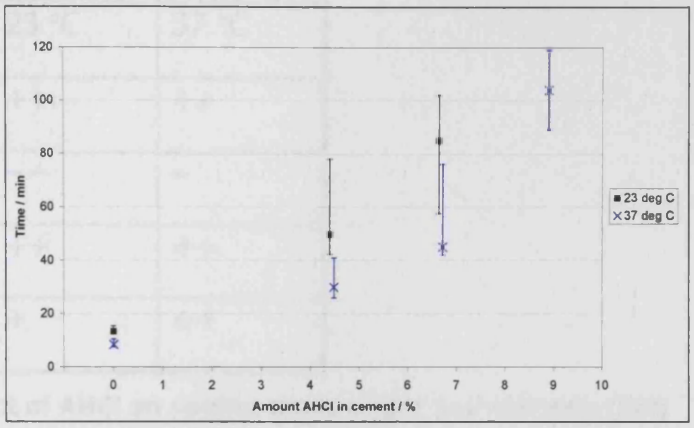

AH2

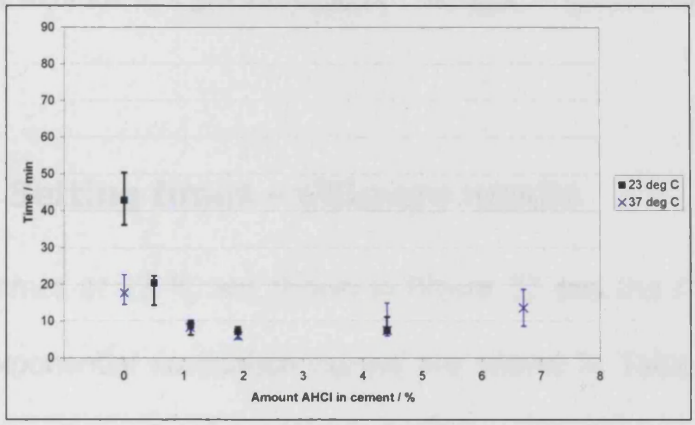

MP4

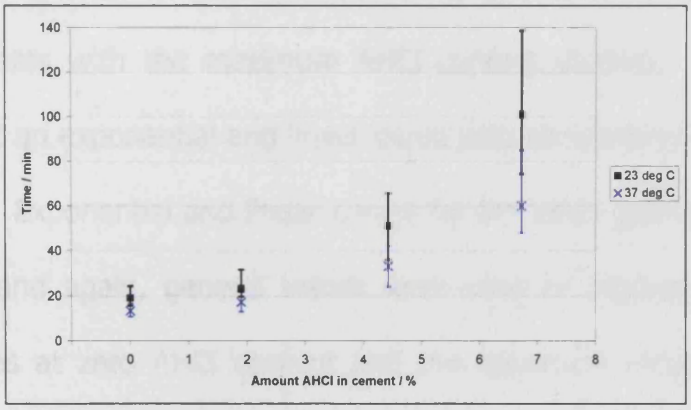

LG30

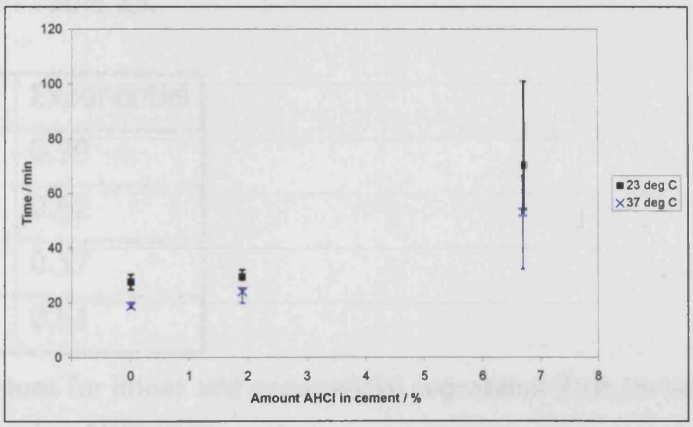

LG26

Figure 36 Setting times of cements containing AHCl at 23°C and 37°C (OR) . Medians (n=6), with 95% confidence limits (note different y scales)

	23 °C	37 °C
AH2	++	++
MP4	– –	–
LG30	++	++
LG26	+	++

Table 21 Effect of AHCl on setting times of the four cements (OR)
+ extends, ++ extends to a greater degree, - reduces, -- reduces to a greater degree

5.2.2.4 Setting times – Gillmore needle

The setting times at 23 °C are shown in Figure 37 and the r^2 values for their linear and exponential correlation curves are shown in Table 22. Table 23 gives the setting times for the cements for the control (0% included AHCl) and for the cements with the maximum AHCl content studied. For AH2 it was possible to fit an exponential and linear curve with correlations of 0.99 and 0.91 respectively. Exponential and linear curves for the other glasses both gave low correlations and again, general trends were used to analyse the data. The working times at zero AHCl content and the maximum included content are summarised in Table 23.

	Linear	Exponential
AH2	0.91	0.99
MP4	0.79	0.62
LG30	0.55	0.57
LG26	0.58	0.61

Table 22 R^2 values for linear and exponential regression lines for setting times of cements containing AHCl (Gillmore)

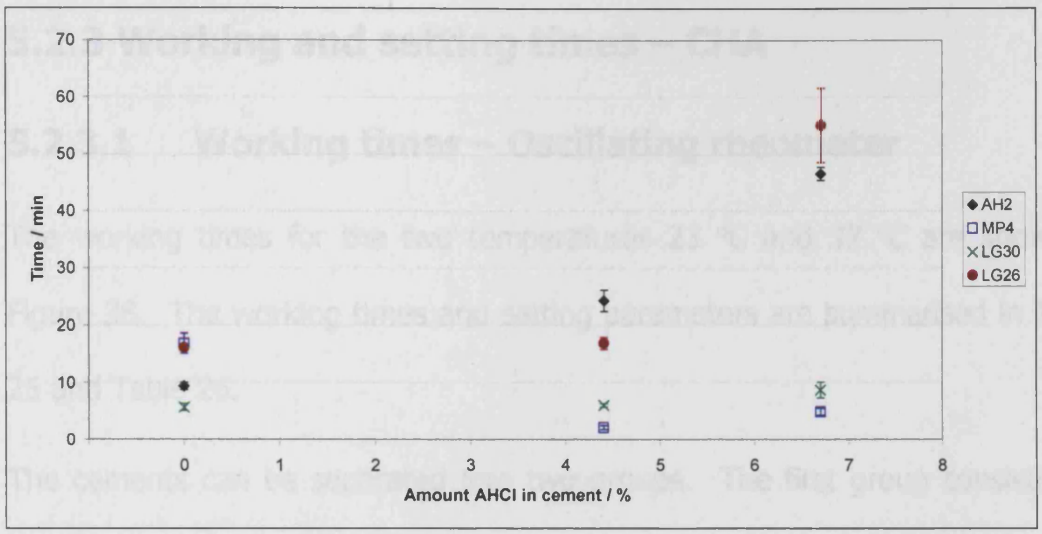

Figure 37 Setting times of cements containing AHCl (Gillmore) means (n=3) with standard deviations

	Setting times 23 deg C	
	0 %	6.7 %
AH2	9.4	46.5
MP4	16.9	4.9
LG30	5.8	8.8
LG26	16.8	55.0

Table 23 Selected setting times / minutes of cements containing 0% and 6.7% AHCl (Gillmore)

	Gillmore 23 °C	OR 23 °C
AH2	++	++
MP4	– –	– –
LG30	0	++
LG26	++	+

Table 24 Effect of AHCl on setting times of the four cements (Gillmore with OR at 23 °C for comparison purposes)

+ extends, ++ extends to a greater degree, – reduces, – – reduces to a greater degree, 0 no effect

The trend in setting times as measured by Gillmore needle are nearly identical for AH2, MP4 and LG26 cements compared with OR. LG30 cement, however, showed no change in setting time with the addition of AHCl.

5.2.3 Working and setting times – CHA

5.2.3.1 Working times – Oscillating rheometer

The working times for the two temperatures 23 °C and 37 °C are shown in Figure 38. The working times and setting parameters are summarised in Table 25 and Table 26.

The cements can be separated into two groups. The first group consisted of AH2 and MP4 cement where the addition of CHA had either a slight retarding effect or no effect on the setting reaction of the glass ionomer cement. The second group consisted of LG30 and LG26 cement where the addition of CHA accelerated the initial setting reaction with the exception of LG30 at 23 °C. Linear regression lines were drawn for all data but goodness of fit was poor.

	Working times at 23 °C / min		Working times at 37 °C / min	
	0 %	10.1 %	0 %	10.1 %
AH2 (initial)	2.75	3.6 (11.3 %)	1.90	2.50 (11.3 %)
MP4 (all new)	2.5	2.6	1.8	1.85
LG30	3.8(initial)	1.8 (initial)	1.35 (later)	1.60 (later)
LG26(all new)	2.5	2.15 (4.5 %)	2.0	1.9 (4.5 %)

Table 25 Selected working times / minutes of cements containing CHA

	23 °C	37 °C
AH2	0	0
MP4	0	0
LG30	–	0
LG26	–	–

Table 26 Effect of CHA on working times of the four cements

0 no effect, – reduces

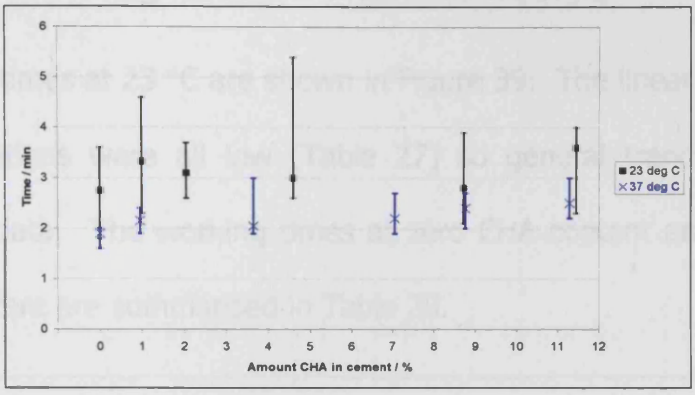

AH2

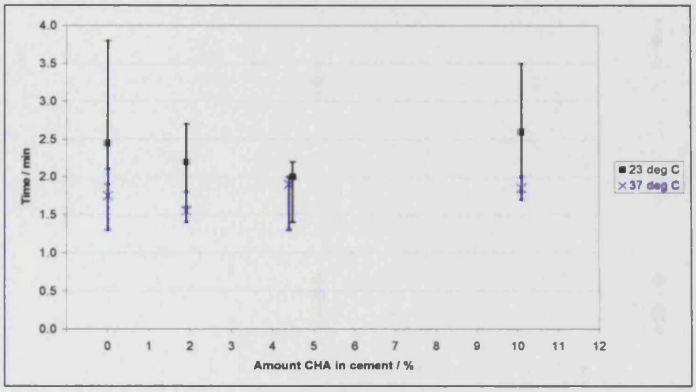

MP4

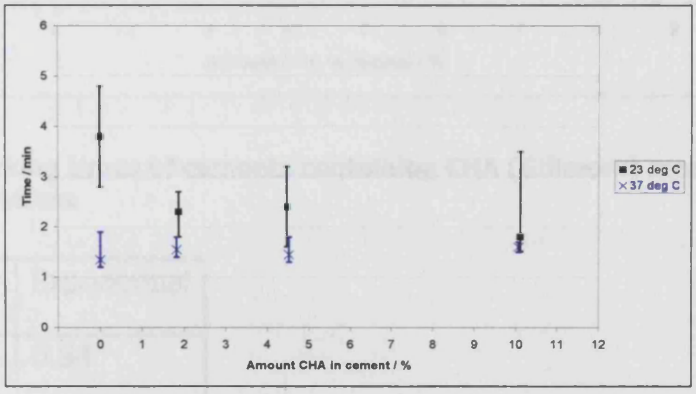

LG30

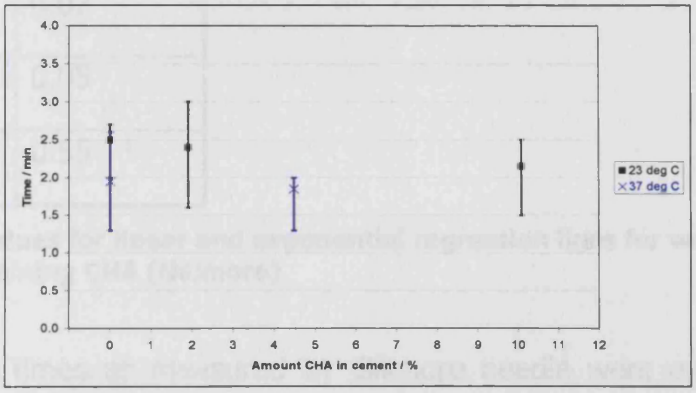

LG26

Figure 38 Working times of cements containing CHA (OR) . Medians (n=6), with 95% confidence limits (please note different y axes)

5.2.3.2 Working times – Gillmore needle

The working times at 23 °C are shown in Figure 39. The linear and exponential curve correlations were all low (Table 27) so general trends were used to analyse the data. The working times at zero CHA content and the maximum included content are summarised in Table 28.

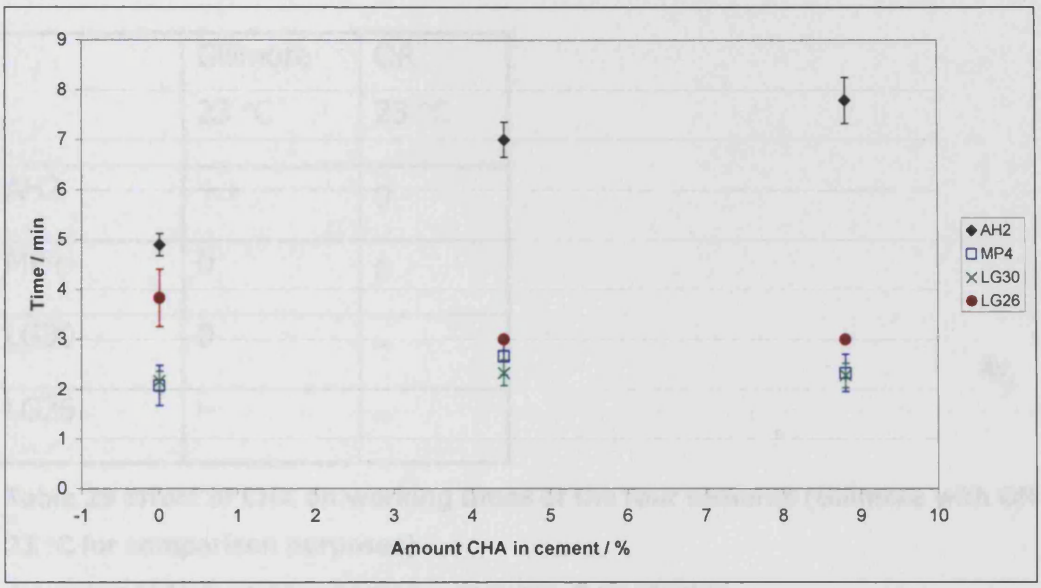

Figure 39 Working times of cements containing CHA (Gillmore) means (n=3) with standard deviations

	Linear	Exponential
AH2	0.86	0.84
MP4	0.06	0.07
LG30	0.05	0.05
LG26	0.51	0.55

Table 27 R^2 values for linear and exponential regression lines for working times of cements containing CHA (Gillmore)

The working times as measured by Gillmore needle were extended for AH2 cement, shortened for LG26 cement and the other two cements showed little change with addition of AHCl.

	Working times at 23 °C / min	
	0 %	8.8 %
AH2	4.9	7.8
MP4	2.1	2.3
LG30	2.2	2.3
LG26	3.8	3.0

Table 28 Working times / minutes at 0% and 8.8% CHA concentration (Gillmore)

	Gillmore 23 °C	OR 23 °C
AH2	++	0
MP4	0	0
LG30	0	–
LG26	–	–

Table 29 Effect of CHA on working times of the four cements (Gillmore with OR at 23 °C for comparison purposes)

++ extends to a greater degree, - reduces, 0 no change

5.2.3.3 Setting times – Oscillating rheometer

The setting times at the two temperatures 23 °C and 37 °C are shown in Table 30 and summarised in Table 31.

The cements can be separated into three groups. The first group consisting of AH2 and LG26 cements showed an increase in setting times at both temperatures with an increase in CHA content. The second group consisting of LG30 showed a slight increase in setting times at 37 °C and an indeterminate change at 23 °C with an increase in CHA content. The third group, consisting of MP4 cement, showed a decrease in setting times at both temperatures with the addition of CHA. Although the trend for LG30 at 23 °C is increasing, in

comparison with the others, there is little change and the direction is not clear. This is summarised in Table 31.

	Setting times at 23 °C / min		Setting times at 37 °C / min	
	0 %	10.1 %	0 %	10.1 %
AH2	16.15	25.0 (11.3 %)	8.5	14.5 (11.3 %)
MP4	43.0	16.7	17.7	12.1
LG30	47.5	44.0	14.5	19.0
LG26	27.5	33.9 (4.5 %)	18.7	20.3 (4.5 %)

Table 30 Setting times for selected concentrations of CHA (OR)

	23 °C	37 °C
AH2	++	++
MP4	– –	–
LG30	Not clear	+
LG26	++	++

Table 31 Effect of CHA on setting times of the four cements (based on linear regression lines) (OR)

+ extends, ++ extends to a greater degree, – reduces, – – reduces to a greater degree

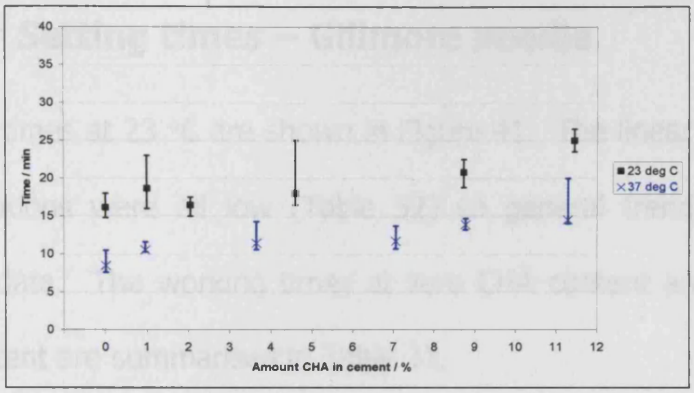

AH2

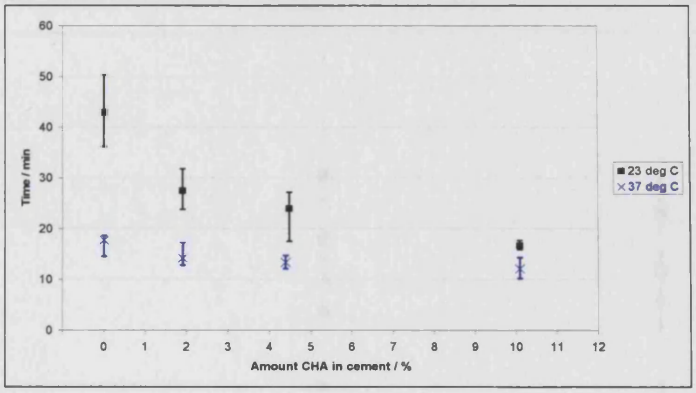

MP4

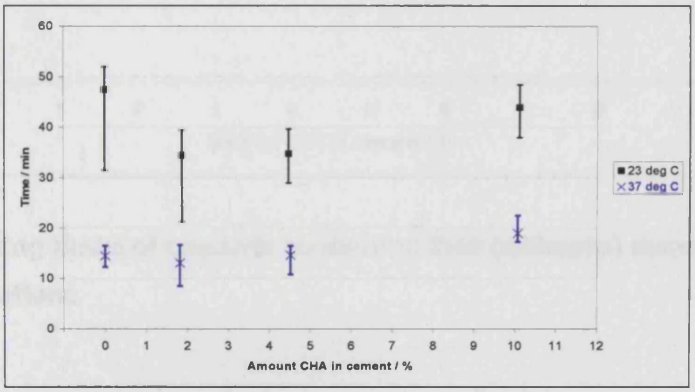

LG30

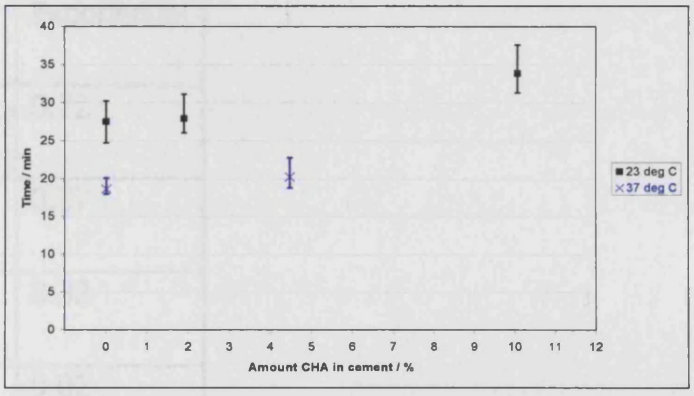

LG26

Figure 40 Setting times of cements containing CHA (OR). Medians (n=6), with 95% confidence limits

5.2.3.4 Setting times – Gillmore needle

The working times at 23 °C are shown in Figure 41. The linear and exponential curve correlations were all low (Table 32) so general trends were used to analyse the data. The working times at zero CHA content and the maximum included content are summarised in Table 33.

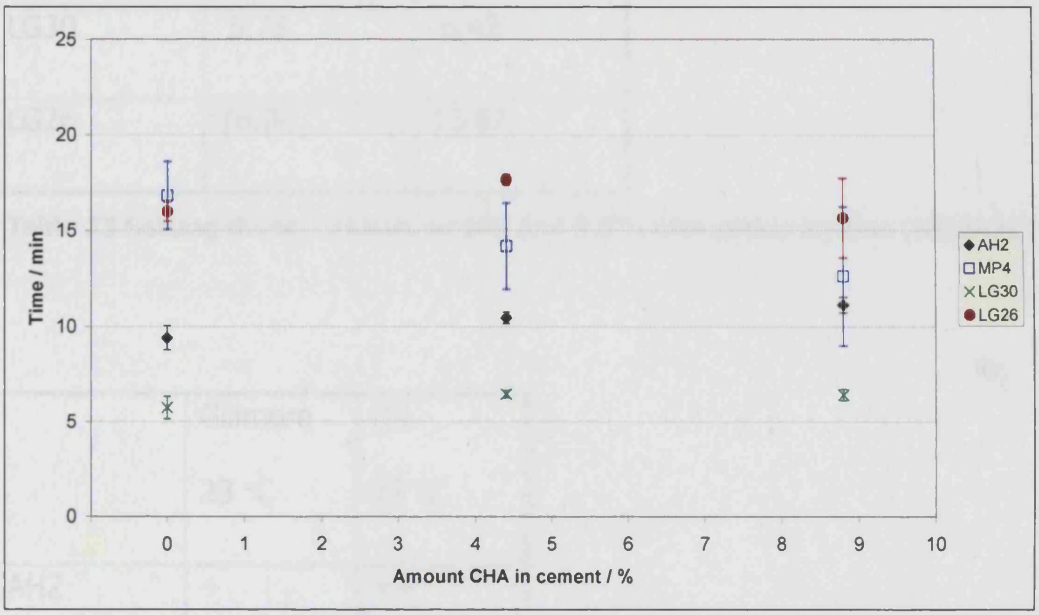

Figure 41 Setting times of cements containing CHA (Gillmore) means (n=3) with standard deviations

	Linear	Exponential
AH2	0.72	0.72
MP4	0.32	0.37
LG30	0.31	0.32
LG26	0.01	0.02

Table 32 Regression values for setting times of cements containing CHA (Gillmore)

	Setting times 23 deg C / min	
	0 %	8.8 %
AH2	9.42	11.13
MP4	16.85	12.63
LG30	5.75	6.42
LG26	16.00	15.67

Table 33 Setting times / minute at 0% and 8.8% CHA concentration (Gillmore)

	Gillmore 23 °C	OR 23 °C
AH2	+	++
MP4	–	– –
LG30	0	Not clear
LG26	0	++

Table 34 Effect of CHA on setting times of the four cements (Gillmore with OR at 23 °C for comparison purposes)
+ extends, ++ extends to a greater degree, – reduces, – – reduces to a greater degree, 0 no effect

The effect of AHCl on the setting times as measured by Gillmore needle showed a slight increase for AH2 cement, decrease for MP4 cement and no change for the other two cements.

5.2.4 Fourier transform infrared spectroscopy

Infrared studies were performed on the setting cements with the aim of providing additional information about the setting reaction. Infrared studies were also performed on various combinations of CHA/PAA, CHA/AH2, AHCl/PAA and AHCl/AH2 with the intention of providing information on interactions between the added species and components of the cement.

5.2.4.1 AH2 cement

Spectra were taken at regular intervals between 1800 cm^{-1} and 800 cm^{-1} of a cement made from AH2 glass, PAA and water. An example of these spectra at four different time intervals is shown in Figure 42.

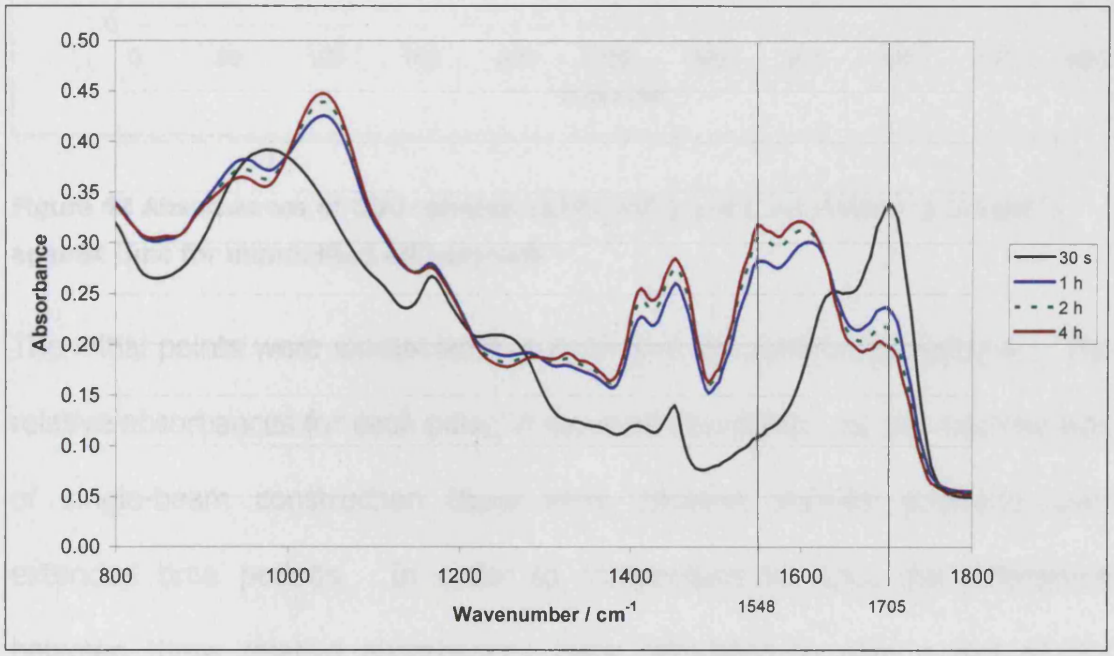

Figure 42 Absorbance spectra at selected time intervals of unmodified AH2 cement against wavenumber with salt (COO- stretch 1548 cm^{-1}) and acid (C=O stretch 1705 cm^{-1}) peaks marked

The absorbances at 1548 cm^{-1} for the salt formation (COO- stretch) and at 1705 cm^{-1} (C=O stretch) indicating the acid group degradation were then

plotted against time (Figure 43). The region below 1000 cm^{-1} is called the 'fingerprint' region and is difficult to resolve being due to vibrations of groups of bonds.

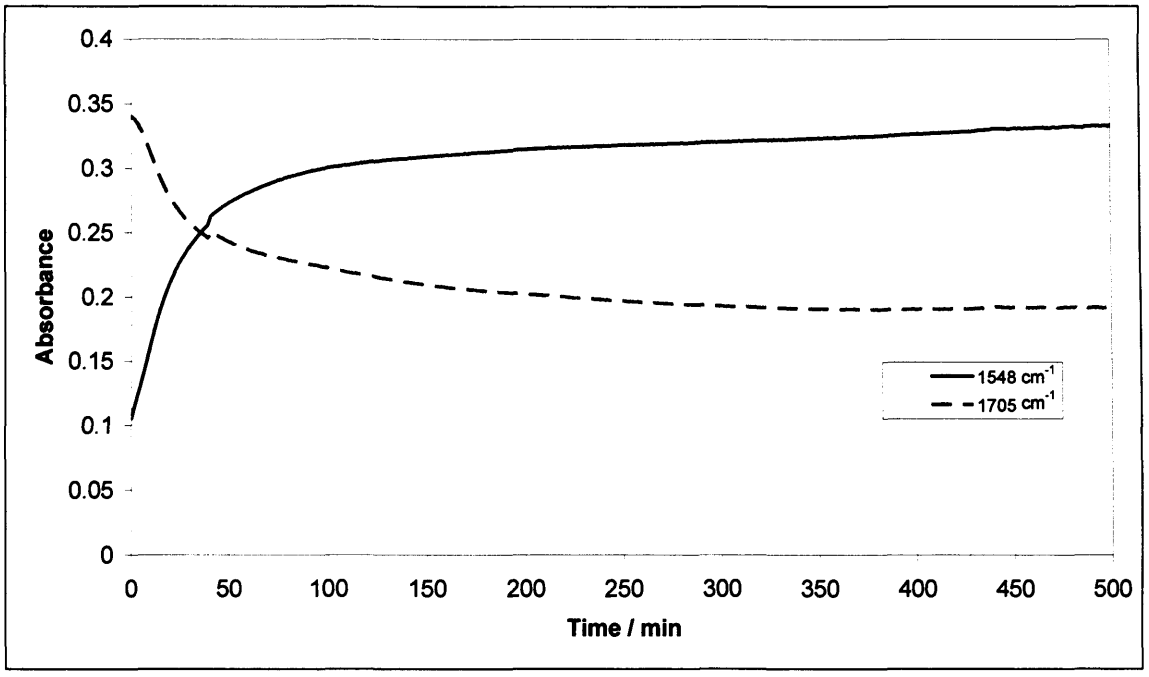

Figure 43 Absorbances of COO- stretch (1548 cm^{-1}) and C=O stretch (1705 cm^{-1}) against time for unmodified AH2 cement

The initial points were extrapolated to t_0 to give the absorbance value A_0. The relative absorbances for each point, $A-A_0$, were calculated. As the machine was of single-beam construction there were baseline stability problems over extended time periods. In order to compensate for this, the differences between these relative absorbances were calculated to give a plot of the relative acid neutralisation extent against time. The slope at any point is proportional to the rate of reaction at that time. The relative acid neutralisation extent versus time for AH2 cement is shown in Figure 44.

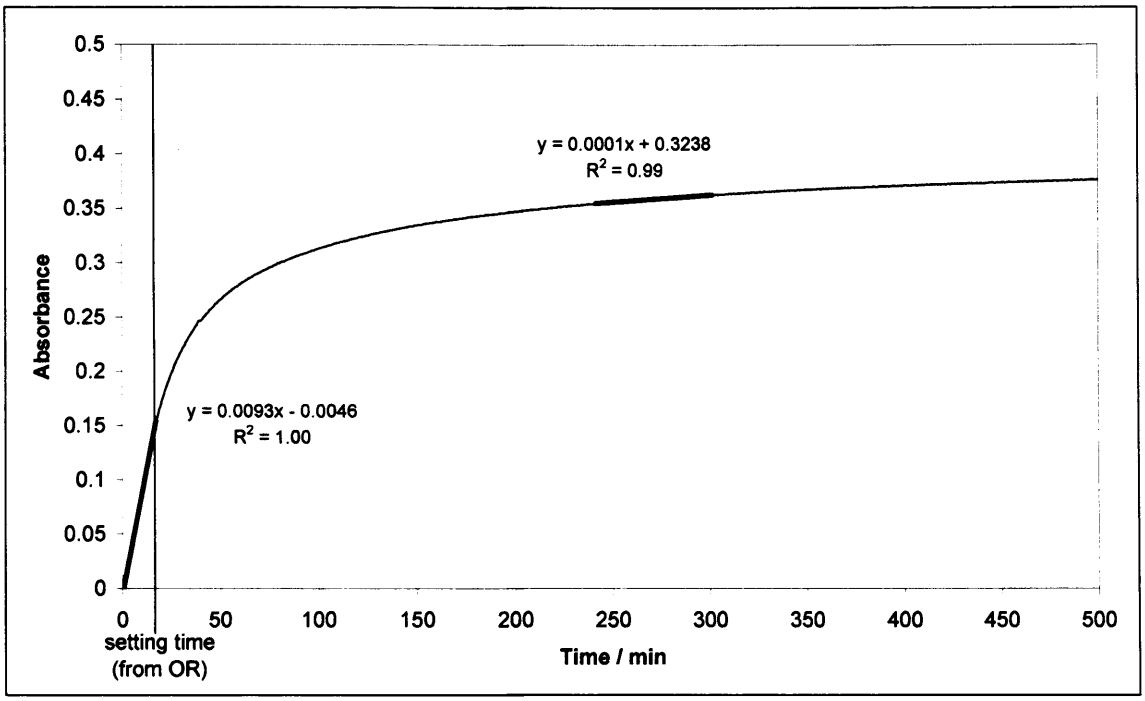

Figure 44 Relative acid neutralisation extent for the setting of AH2 cement

The slope of the initial part of the graph between 0 and 17 minutes was 0.0093 absorbance units per minute. This was reduced to 0.0001 absorbance units per minute between 240 and 300 minutes.

5.2.4.2 AH2 cement with AHCl

The experiment was repeated for an AH2 cement containing AHCl and examples of spectra at 4 time intervals is shown in Figure 45.

The acid peak at 1705 cm^{-1} is similar to that in Figure 42 for the unmodified AH2 cement but the area to the left shows interference from the included AHCl.

Absorbances at 1540 cm^{-1} (COO- stretch) and 1705 cm^{-1} (C=O stretch) were again plotted against time (Figure 46).

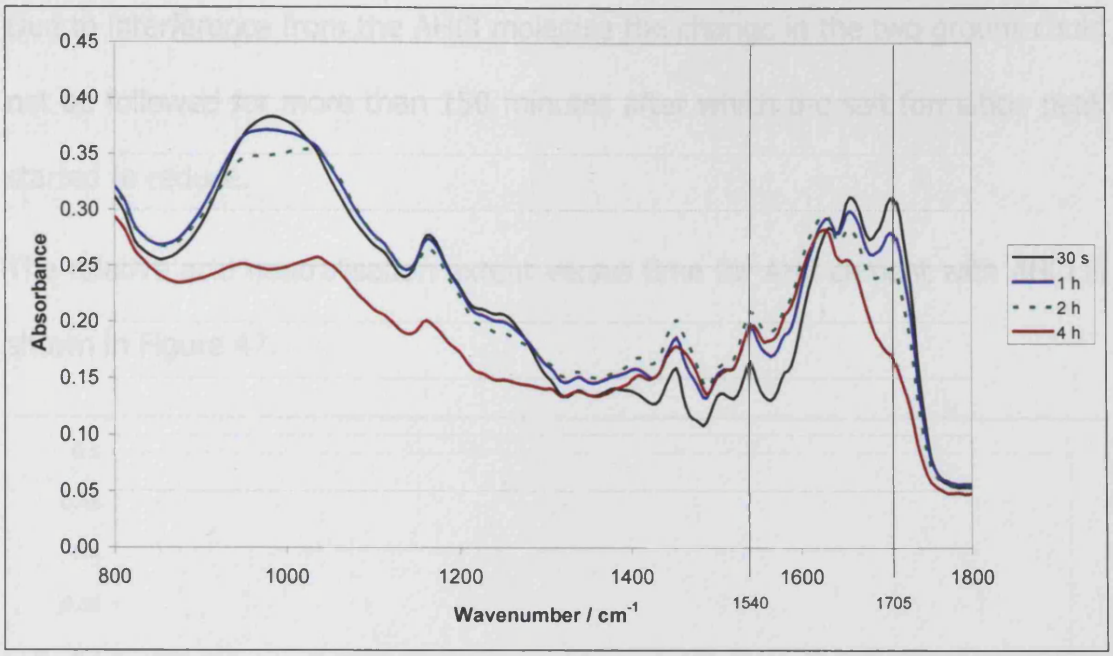

Figure 45 Absorbance spectra at selected time intervals of AH2 cement containing AHCl against wavenumber with salt (COO- stretch 1540 cm^{-1}) and acid peaks (C=O stretch 1705 cm^{-1}) marked

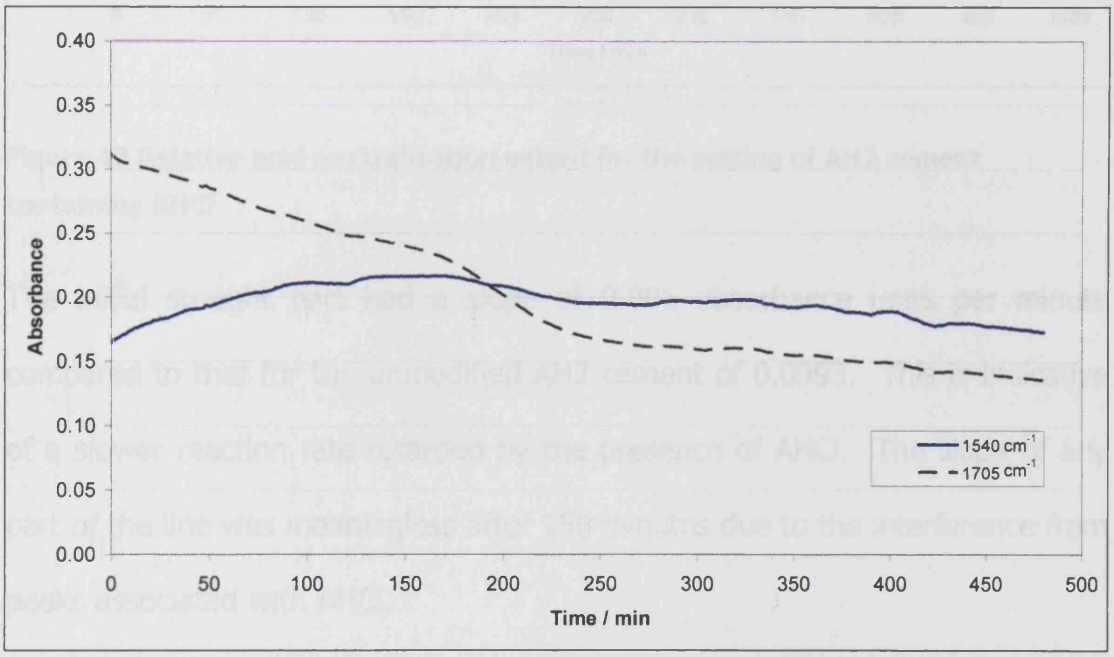

Figure 46 Absorbances of the COO- stretch (1540 cm^{-1}) indicating salt formation and the C =O stretch (1705 cm^{-1}) indicating acid degradation for the reaction between glass, PAA and AHCl.

Due to interference from the AHCl molecule the change in the two groups could not be followed for more than 150 minutes after which the salt formation peak started to reduce.

The relative acid neutralisation extent versus time for AH2 cement with AHCl is shown in Figure 47.

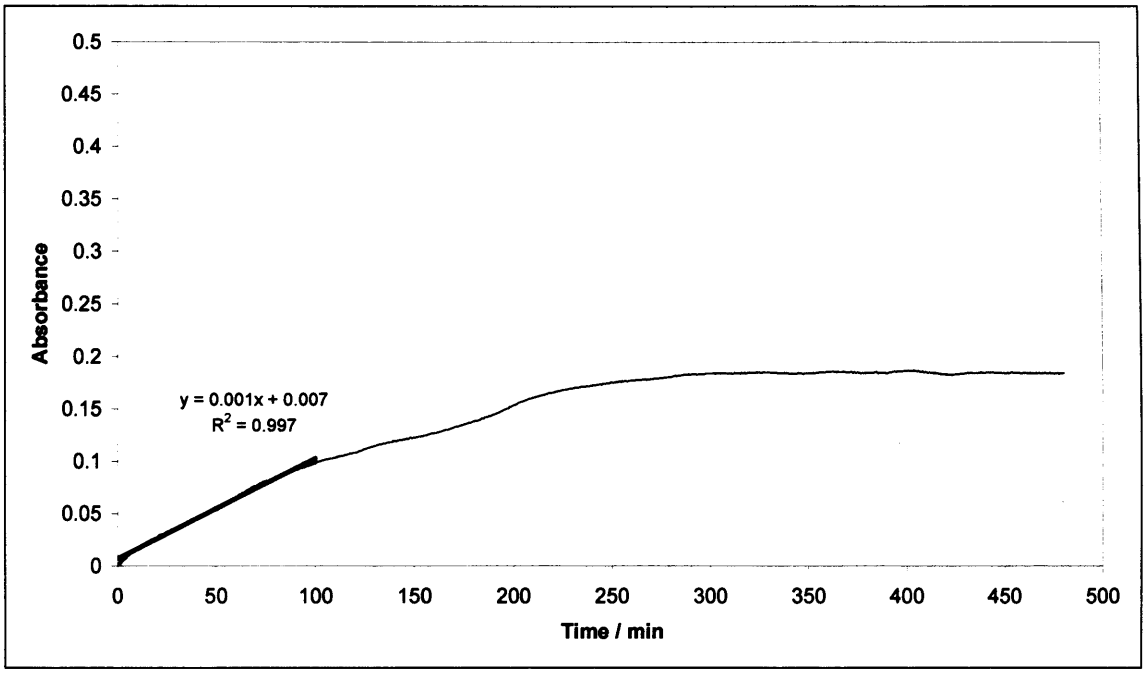

Figure 47 Relative acid neutralisation extent for the setting of AH2 cement containing AHCl

The initial straight part had a slope of 0.001 absorbance units per minute compared to that for the unmodified AH2 cement of 0.0093. This is indicative of a slower reaction rate retarded by the presence of AHCl. The slope of any part of the line was meaningless after 150 minutes due to the interference from peaks associated with AHCl.

5.2.4.3 AH2 cement with CHA

Spectra were taken at regular intervals between 1800 cm^{-1} and 800 cm^{-1} of a AH2 cement containing 8.8% CHA and examples of spectra at 4 time intervals is shown in Figure 48.

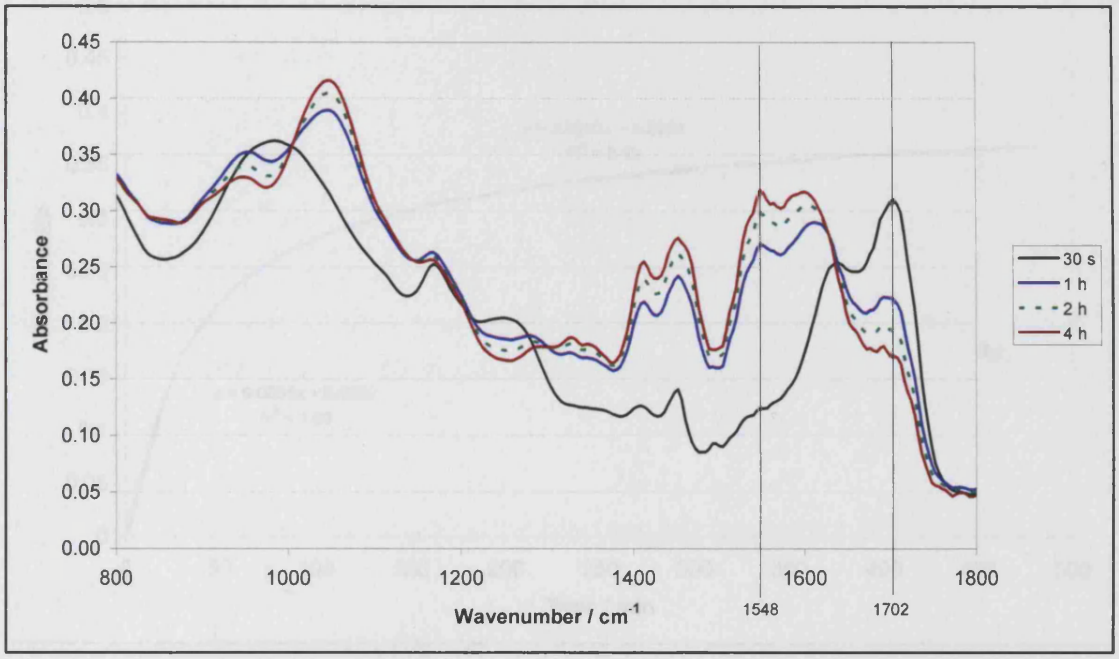

Figure 48 Absorbance spectra at selected time intervals of AH2 cement containing CHA against wavenumber with salt (COO- stretch 1548 cm^{-1}) and acid peaks (C=O stretch 1702 cm^{-1}) marked

The traces are almost identical to those obtained for unmodified AH2 cement (Figure 42).

The absorbances at 1548 cm^{-1} (COO^- stretch) and 1702 cm^{-1} (C=O stretch) were plotted against time and the initial points were extrapolated to t_0 to give the absorbance value A_0. The relative absorbances for each point, $A-A_0$, were calculated. The differences between these relative absorbances were calculated to give a plot of the relative acid neutralisation extent against time,

the slope at any point being proportional to the rate of reaction at that time. The relative acid neutralisation extents versus time for AH2 cement containing CHA is shown in Figure 49 and for comparison purposes, the same graph combined with the relative acid neutralisation extent for AH2 cement (from Figure 44) with added CHA is shown in Figure 50.

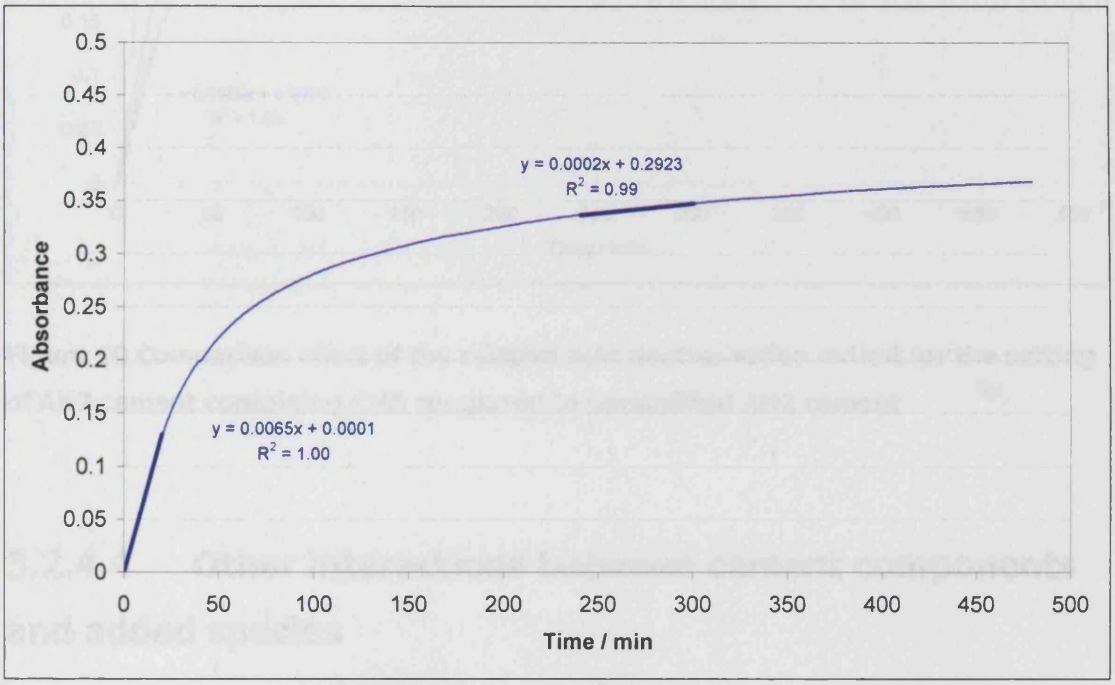

Figure 49 Relative acid neutralisation extent for the setting of AH2 cement containing CHA

The initial rate of reaction is slower for a cement containing CHA (slope = 0.0065 Abs min^{-1}) compared to a straight AH2 cement (slope = 0.0093 Abs min^{-1}). Between 4 and 5 h (240 – 300 minutes), the rate of reaction for the cement containing CHA had reduced (slope = 0.0002 Abs min^{-1}) and the rate of reaction of AH2 containing CHA had reduced even more (slope = 0.0001).

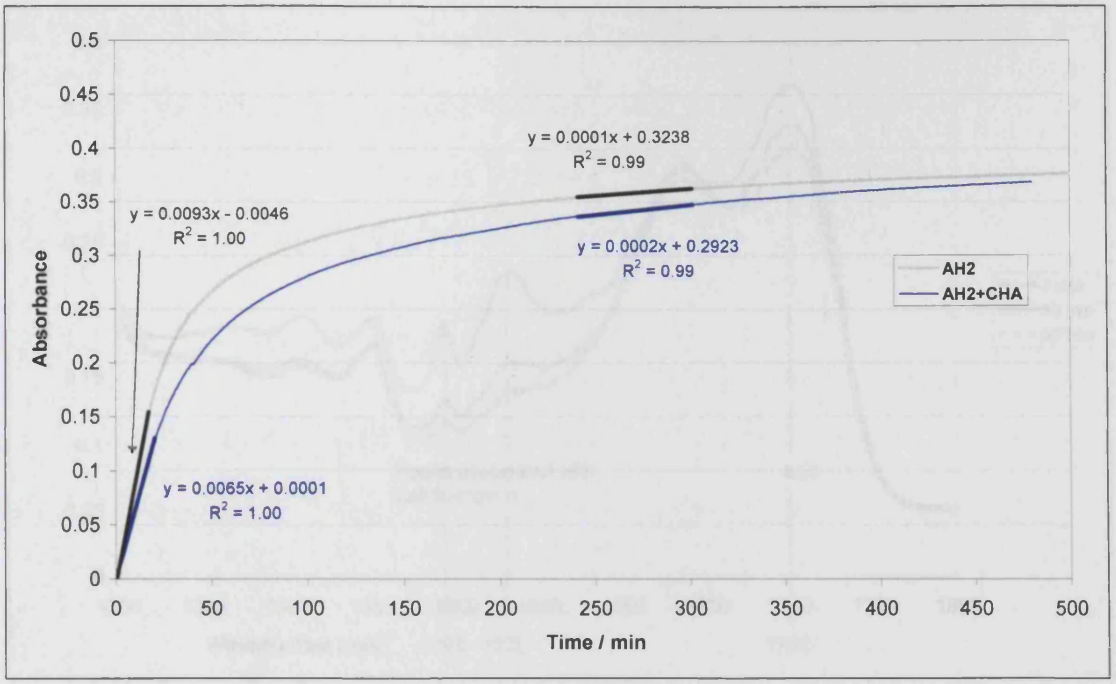

Figure 50 Comparison chart of the relative acid neutralisation extent for the setting of AH2 cement containing CHA compared to unmodified AH2 cement

5.2.4.4 Other interactions between cement components and added species

Spectra were run of various combinations of PAA, AH2 glass and added species to ascertain any interactions between them. Of the various combinations studied only the CHA/PAA showed an interaction. In contrast to this, there was no interaction between PAA and AHCl. Spectra were obtained for a mix of 0.38% PAA, 0.39% CHA and 0.32% water at various intervals up to 90 minutes, selected ones of which are shown in Figure 51.

The changes observed are very similar to those for the conventional GIC reaction (Figure 42) although the reaction was to a much lesser extent indicating much less interaction. The salt formation peaks are attributed to the

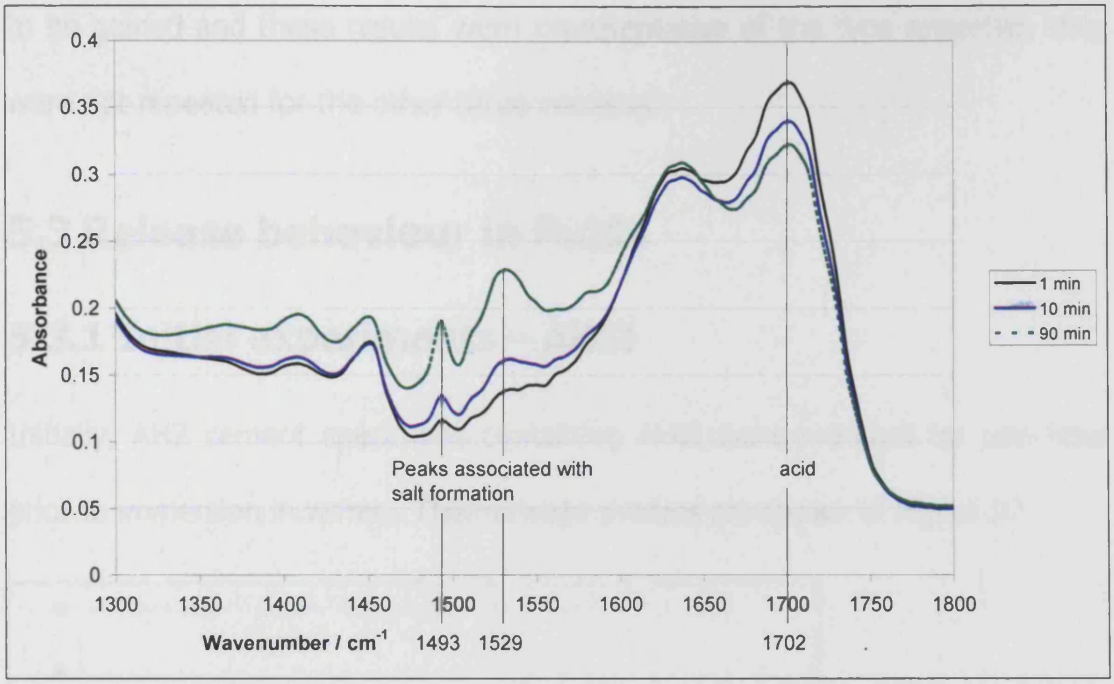

Figure 51 Absorbance spectra at selected time intervals of PAA, CHA & water mix against wavenumber with salt and acid peaks marked

formation of a polyacrylate salt based on chlorhexidine. Supplemental to this, a 1% aqueous solution of CHA was mixed with a 20% aqueous solution of PAA to rapidly form a flocculent precipitate.

5.2.4.5 Summary of FTIR spectroscopy

It is clear that the addition of AHCl retarded the initial setting reaction considerably as demonstrated by the smaller slope in the acid neutralisation graphs. The addition of CHA also reduced the rate of reaction but to a much lesser extent although the formation of CH polyacrylate was observed. The implication of this is that AHCl interfered hugely with the reaction but CHA doesn't seem to any great extent although in the spectrum of PAA, AHCl and water no reaction was observed. These experiments show similar results to those obtained from the working and setting times. As no real information was

to be gained and these results were representative of the type expected, they were not repeated for the other three cements.

5.3 Release behaviour in fluids

5.3.1 Initial experiments – AHCl

Initially, AH2 cement specimens containing AHCl were matured for one hour prior to immersion in water. Their release profiles are shown in Figure 52.

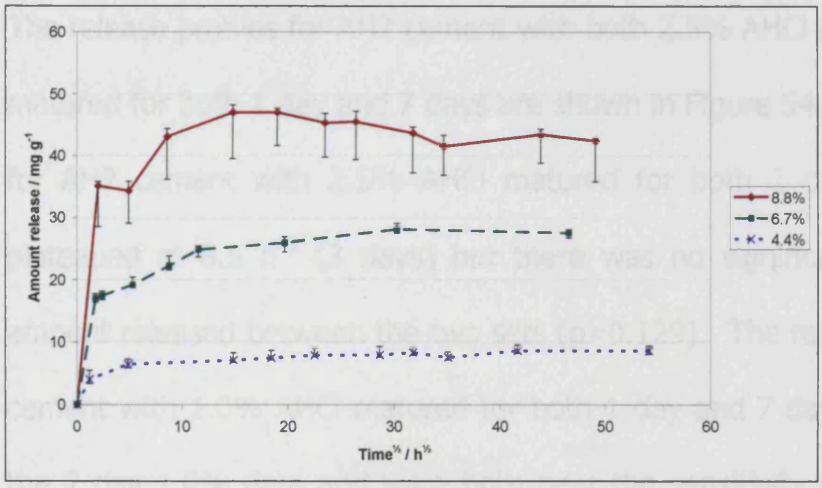

Figure 52 Cumulative AHCl release from 1 h maturation specimens / mg g^{-1} to $t_{1/2}$ = 60 $h^{1/2}$ (150 days), (n=6)

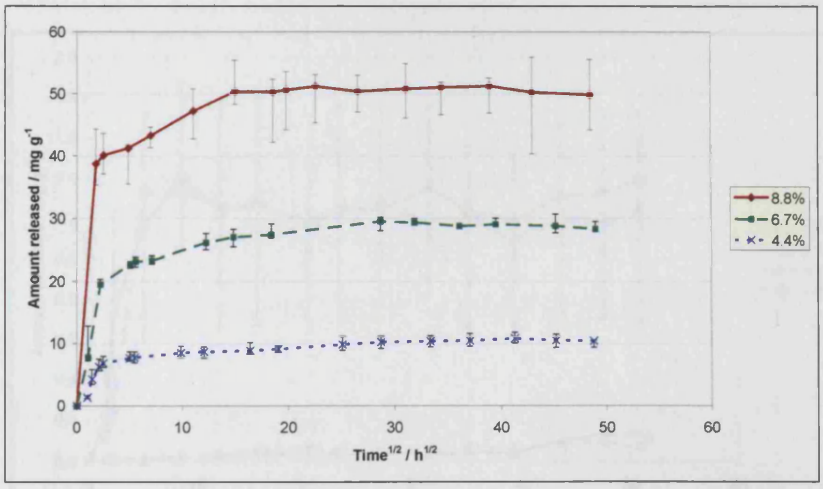

Figure 53 Cumulative AHCl release from 24 h maturation specimens / mg g^{-1} to $t_{1/2}$ = 60 $h^{1/2}$ (150 days), (n=6)

It was noticed during the preparation of these specimens that they appeared plastic in feel at the point of immersion in water and it was decided to mature all future AHCl containing specimens for 24 hours prior to immersion. For comparison purposes, three concentrations of AHCl in cement are shown in Figure 53. The release from specimens matured for 1 hour compared with those matured for 24 hours are very similar for all three levels of inclusion.

5.3.1.1 Further maturation time studies

The release profiles for AH2 cement with both 2.5% AHCl and 1.0% AHCl both matured for both 1 day and 7 days are shown in Figure 54. The release profiles for AH2 cement with 2.5% AHCl matured for both 1 day and 7 days both plateaued at 8.5 $h^{1/2}$ (3 days) but there was no significant difference in the amount released between the two sets (p=0.129). The release profiles for AH2 cement with 1.0% AHCl matured for both 1 day and 7 days differed little from the 7 day 1.0% data and were both near the sensitivity limit of the detection system used. Statistical analysis indicated that there was no significant difference between the two sets of data (p=0.293).

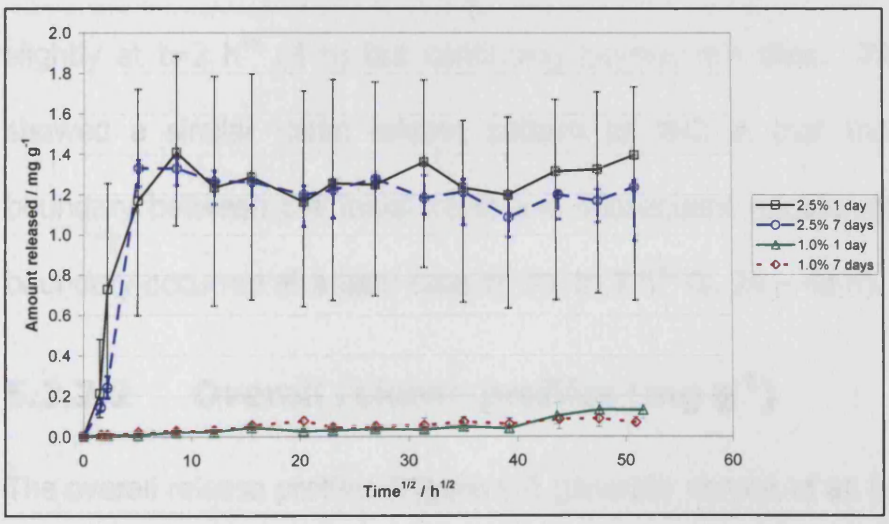

Figure 54 AHCl release from AH2 cement / mg g^{-1} (maturation time comparison)

5.3.2 Release (initial glass) – AHCl

All release studies were performed on the initial batches of glass. The early part of the release profiles expressed as mg AHCl released per g of cement with respect to time^{½} up to 10 h^{½} are set out in Figure 55. The release profiles expressed as mg AHCl release per g of cement with respect to time^{½} up to 60 h^{½} are set out in Figure 56, expressed as μg AHCl release per mm^2 surface area in Figure 57 and expressed as % AHCl release with respect to time^{½} in Figure 58. Initial plots with respect to time showed no linearity. Plot against time^{½} showed some amount of linearity.

5.3.2.1 Initial release profiles

In the initial release profiles (Figure 55), all graphs show a rapid initial release that decreases with increasing time. This release from AH2 cement and LG30 cement was more rapid initially than for the other two cements. The release rate was reduced markedly after 1½ to 2 h^{½} (2.3 – 4 h). The release from MP4 cement showed a gradual decrease in rate of release from time 0 slowing slightly at t=2 h^{½} (4 h) but continuing beyond this time. The LG26 cement showed a similar initial release pattern to AH2 in that there was a clear boundary between the initial burst and subsequent release rate although this boundary occurred at a later time of 4¾ to 7 h^{½} (c. 24 – 48 h).

5.3.2.2 Overall release profiles (mg g^{-1})

The overall release profiles (Figure 56) generally consist of an initial rapid wash-out to t ≈ 2.5 h^{½} (6 h) then a slower rate of release, which was in some cases

found to be linear. Finally release decreased to a point where there was a plateau (release had stopped). Although the plateau region that was observed in most of the release profiles is considered to indicate that all the material available for release had migrated out, it is possible that release was continuing at a very low rate beyond 60 $h^{1/2}$ (150 days) at a level difficult to detect. The two lower concentrations of AHCl in AH2 cement (Figure 55) showed the same release profiles as the higher concentrations. The LG26 cement had initial profiles very similar to AH2 but with lower release rates. Towards the end, the release from specimens with large amounts of included species had slowed and the release from the 4.4% AHCl content cement was still rising. The MP4 cement exhibited an initial rapid elution that fell off with time until a plateau region was reached. The lower the concentration of AHCl in the cement, the longer the delay before the release rate reached a maximum. The LG30 release profiles comprised generally of an initial rapid wash-out to $t \sim 2.0\ h^{1/2}$ (4 h). Thereafter, the three lines showed different characteristics. The 8.8% specimens exhibited a slight drop at $\approx 2\ h^{1/2}$ (4 h) then increased at a continuously reducing rate to the plateau.

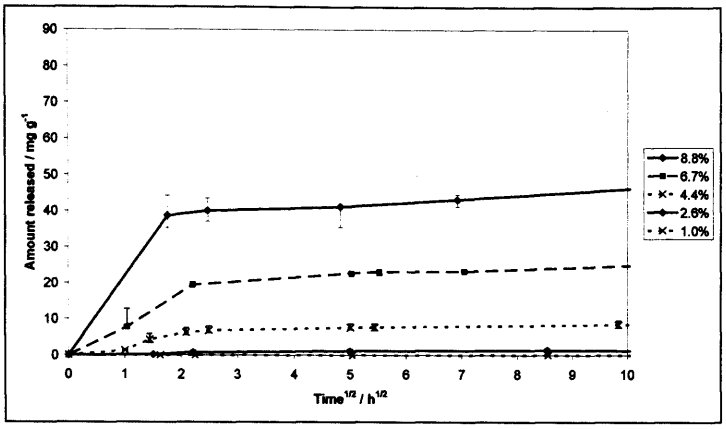

AH2

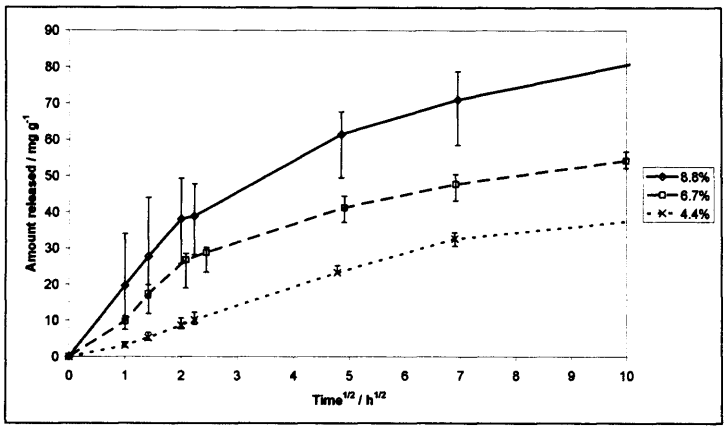

MP4

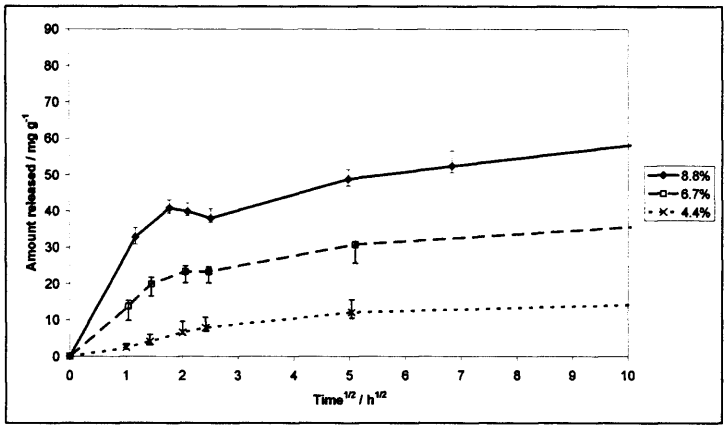

LG30

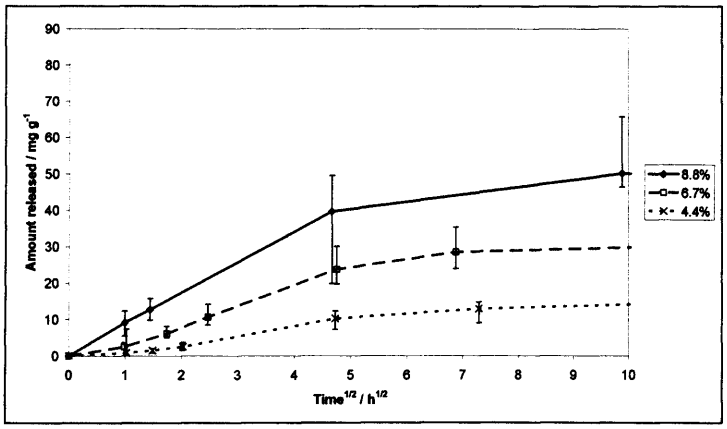

LG26

Figure 55 Initial part of cumulative AHCl release / mg g^{-1} to $t^{1/2}$ = 10 $h^{1/2}$, Medians (n=6), with 95% confidence limits

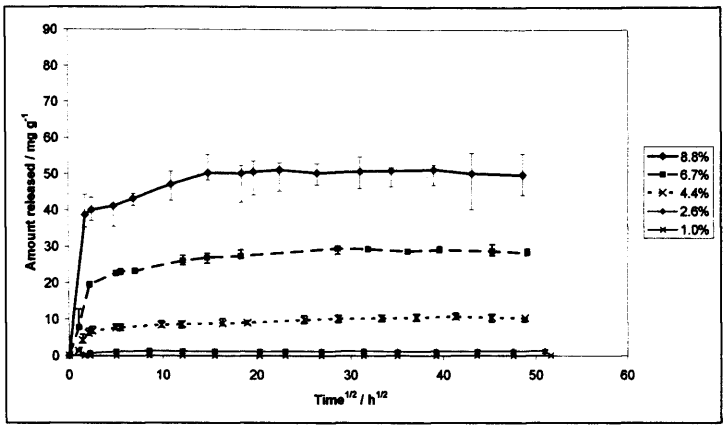

AH2

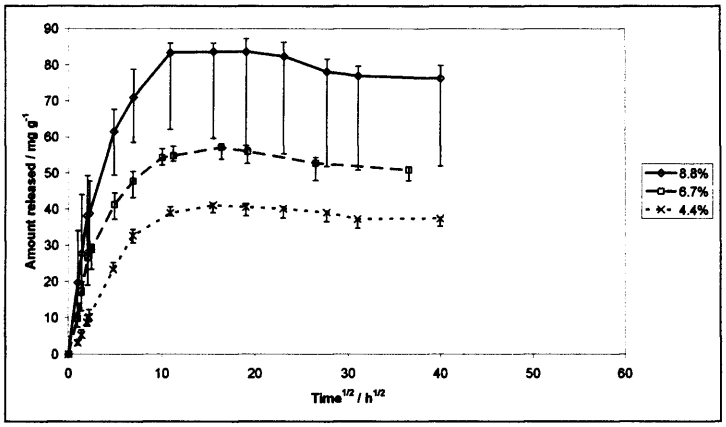

MP4

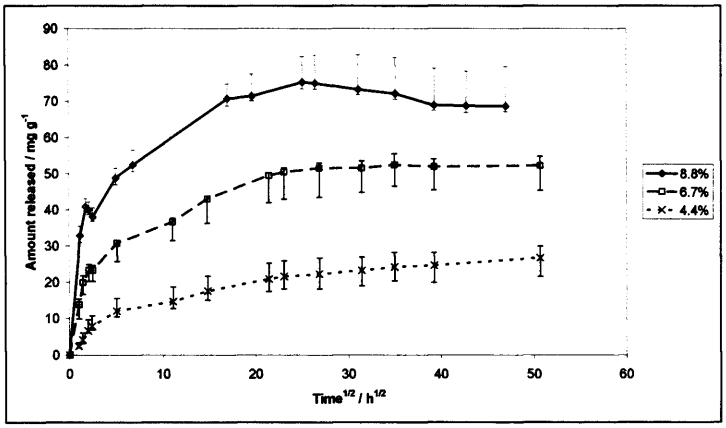

LG30

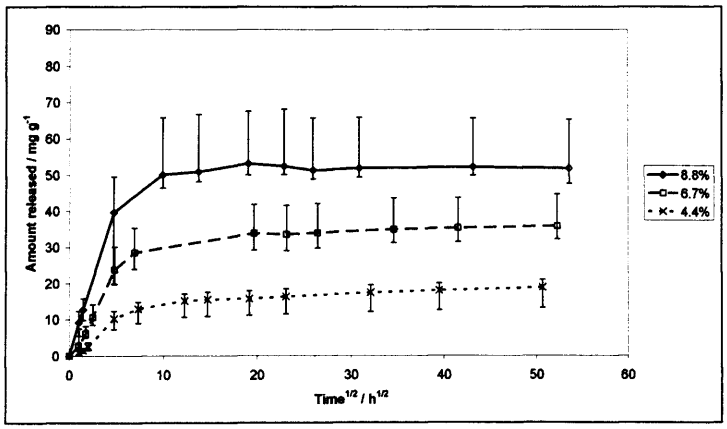

LG26

Figure 56 Cumulative AHCl release / mg g^{-1} to $t^{½}$ = 60 $h^{½}$ (150 days), Medians (n=6), with 95% confidence limits

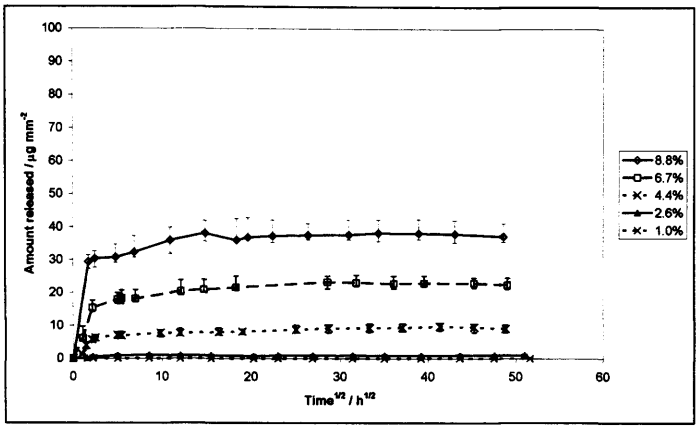

AH2

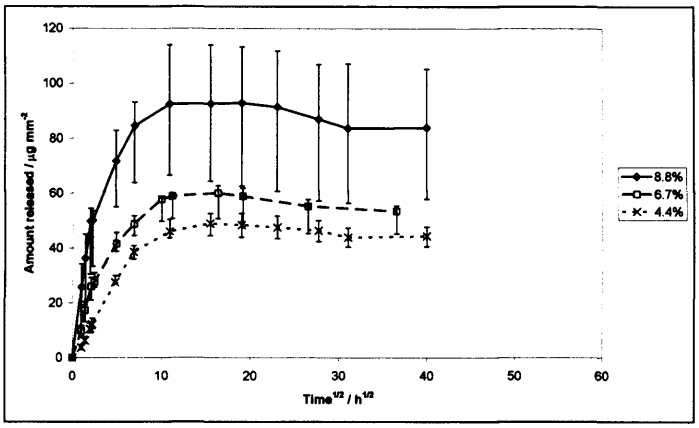

MP4

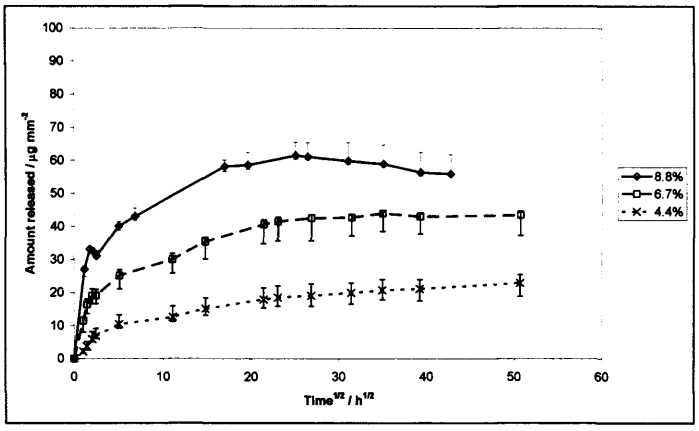

LG30

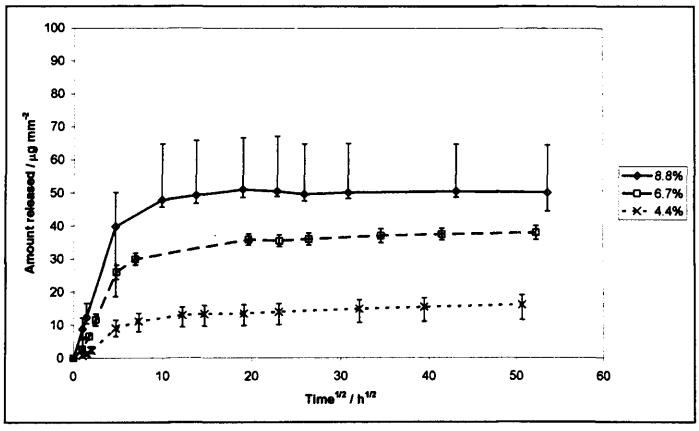

LG26

Figure 57 Cumulative AHCl release / µg mm^{-2} to t^{½} = 60 h^{½} (150 days), Medians (n=6), with 95% confidence limits

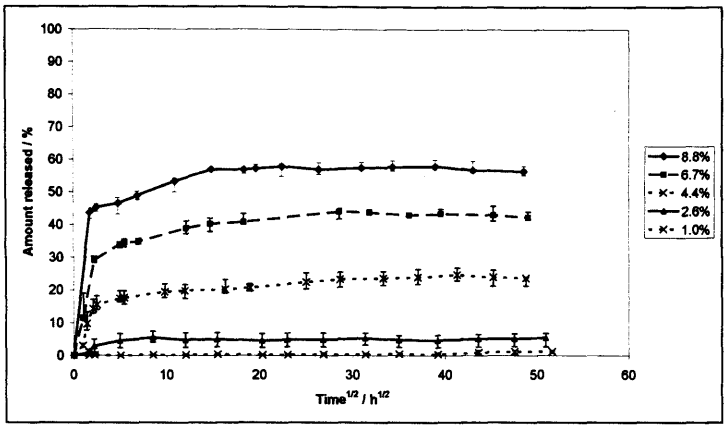

AH2

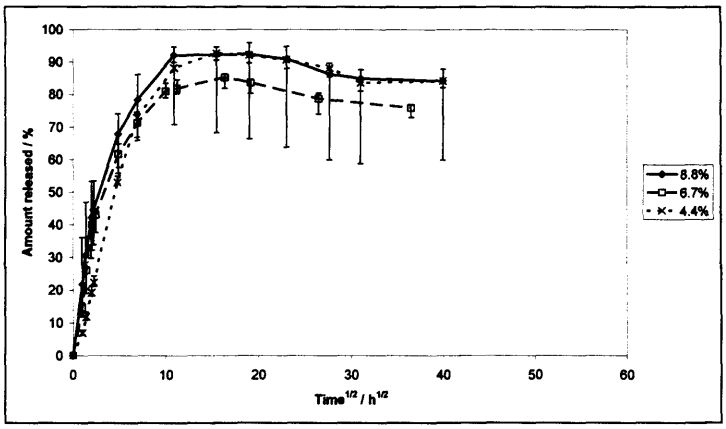

MP4

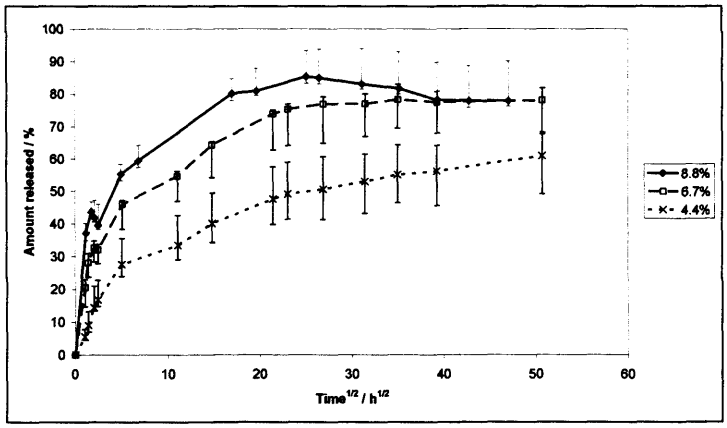

LG30

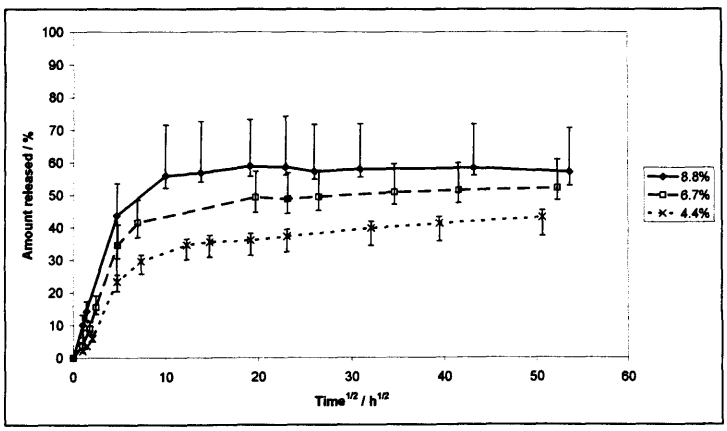

LG26

Figure 58 AHCl release / % to $t^{1/2}$ = 60 $h^{1/2}$ (150 days), Medians (n=6), with 95% confidence limits

The 6.7% AHCl content specimens exhibited a slight levelling off at the same time and increased at a reduced rate until reaching a plateau. The 4.4% specimens release profile showed a slower release rate without continuous reduction in release rate such that the AHCl release profile was still increasing slightly at the end of the experiment.

5.3.2.3 Release expressed as $\mu g\ mm^{-2}$

These release profiles are very similar to those expressed as mg g^{-1}. If the release was diffusion controlled throughout the whole of the experiment then surface area would have been important and the results expressed as release per surface area would have been appropriate. As this was not the case, there being hardly any linearity observed against $time^{1/2}$, release expressed as mg g^{-1} or % only were considered. Furthermore, the specimens were of all the same diameter and similar thickness and therefore of very similar surface areas.

5.3.2.4 Percentage release charts

The percentage release profiles (Figure 58) for AH2 and LG26 show that with increasing added concentrations of AHCl, increasing proportions of AHCl were released. The percentage release profiles for MP4 showed much less difference between amount incorporated and percentage released, there being very little difference between the three concentrations of AHCl. The percentage release profiles for LG30 show equal plateau release values for 8.8% and 6.7% AHCl.

The maximum release values for the four cements containing 8.8% AHCl were 56% from AH2, 57% from LG26, 78% from LG30 and 84% from MP4 cement.

The times taken to equilibrium are shown in Table 35 and Figure 59.

	[AHCl] in cement		
	4.4 %	6.7 %	8.8 %
	Time to plateau / $h^{1/2}$		
AH2	41	28	15
MP4	16	16	11
LG30	>51	35	25
LG26	>51	42	19

Table 35 Time to plateau (release stopped) / $h^{1/2}$ for AHCl doped cements

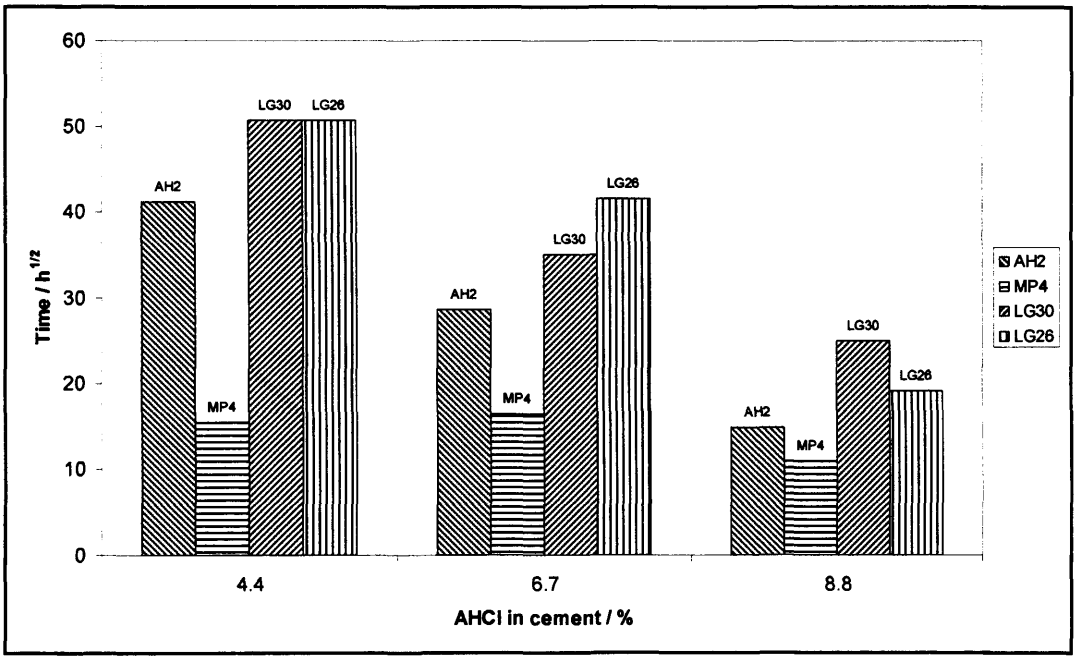

Figure 59 Bar chart showing time to plateau (where there is no further release) for AHCl doped cements at the three different doping levels

In general, the higher the content of AHCl in the cement, the quicker the release was completed. The exception was MP4 cement in which all three AHCl

content cements followed similar patterns. Comparing between cements, the ranking order for release rates was MP4 >> AH2 > LG30 ≈ LG26. This can clearly be seen in Figure 59.

The release values at the end of the experiments are shown in Table 36.

	[AHCl] in cement / %				
	1.0 %	2.6 %	4.4 %	6.7 %	8.8 %
	Release / %				
AH2	1.2	5.5	23.8	42.3	56.3
MP4	–	–	84.2	76.0	84.3
LG30	–	–	61.0	78.1	77.9
LG26	–	–	43.2	52.2	57.2

Table 36 Amount of AHCl released as a % of AHCl originally included after c. 40 $h^{1/2}$ (67 days)

Generally, the higher the initial AHCl content of the cement, the greater the final percentage of that released. Exceptionally, for MP4 cement containing AHCl, the percentage release of included material was similar for all amounts included. AH2 cement showed the most variation.

In order to explore the release mechanism in more detail, the linearity of the initial portion of each curve was assessed. This is presented in Table 37. With the few data points available linearity was only observed for AH2 cement with 8.8% and 6.7% additions of CHA.

	[AHCl] /% in cement		
	4.4 %	6.7 %	8.8 %
AH2	X	Yes	Yes
MP4	X	X	X
LG30	X	X	X
LG26	X	X	X

Table 37 Indication of which AHCl release curve contained a linear portion with respect to $t^{1/2}$

5.3.3 Release (initial and later glass) – CHA

The initial part of the release profiles expressed as milligram CHA released per gram of cement with respect to time are set out in Figure 60. The complete release profiles expressed as milligrams CHA release per gram of cement with respect to time are shown in Figure 61, expressed as μg CHA release per mm^2 surface area in Figure 62 and expressed as percentage CHA release with respect to time in Figure 64.

5.3.3.1 Initial release profiles

In the initial release profiles (Figure 60), all cements show a slight lead-in for c. 1 h followed by a rapid release that decreased with increasing time. The release rate reduced markedly for the AH2 cement between 1½ and 5 $h^{1/2}$. Comparing the later batches of MP4 and LG30 with the initial batches, the cements from the later batches exhibited initial slight retardation in release for up to 2 ½ $h^{1/2}$ followed by generally increased release rates. Overall the trends

were similar for both glasses. The release curves for the other cements consisted of a slower reduction in release with increasing time.

5.3.3.2 Overall release profiles

CHA release from MP4, LG30 and LG26 showed a rapid elution that levelled off to a plateau after a certain time (Figure 61). The times to plateau (point at which release has stopped) are shown in Table 38. The AH2 cement at some of the higher additions of CHA exhibited the same rapid elution followed by a linear section from 2 $h^{1/2}$ to 20 $h^{1/2}$. These linear regression curves are shown in Figure 63.

For the AH2 cements, the rate of release increased with the concentration of CHA included in the cement. The time taken to reach the plateau was found to be concentration dependent. In all cases, only a small amount of CHA was released. For the majority of concentrations of CHA in the AH2 cement there was no relationship between the amount of CHA included and the percentage released; all materials released between 3% and 5% of the incorporated CHA. The exception was the highest CHA content GIC (11.3%) in which a significantly greater proportion of CHA was released (~10%).

The general release pattern from cement made with initial MP4 was different from AH2 in that the initial elution was more rapid at the highest concentration of CHA but had no distinct linear portion, with the rate of elution decreasing from 5 $h^{1/2}$ (1 day) to a plateau region.

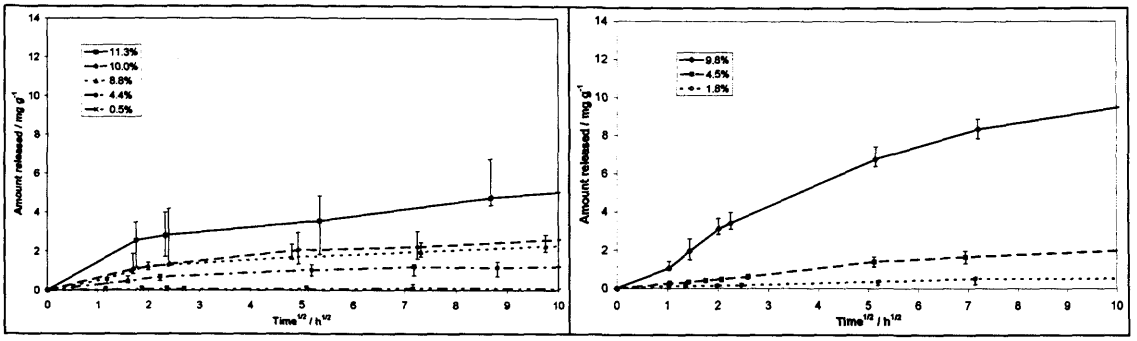

AH2 **LG26**

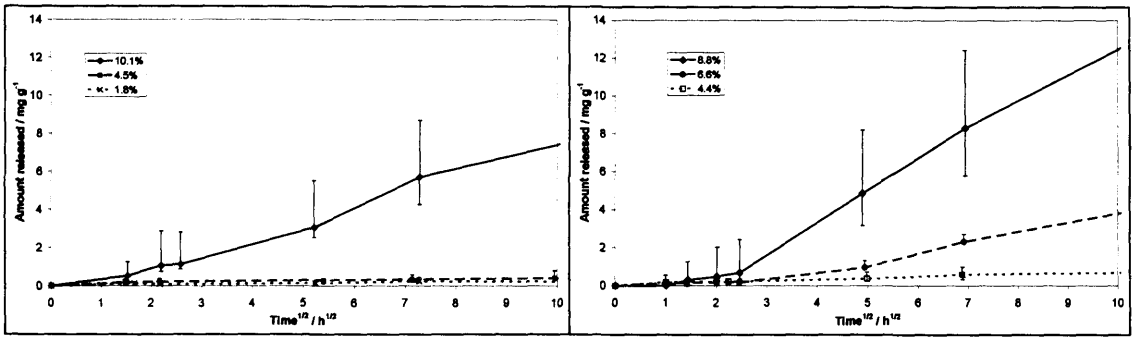

MP4 (initial) **MP4 (later)**

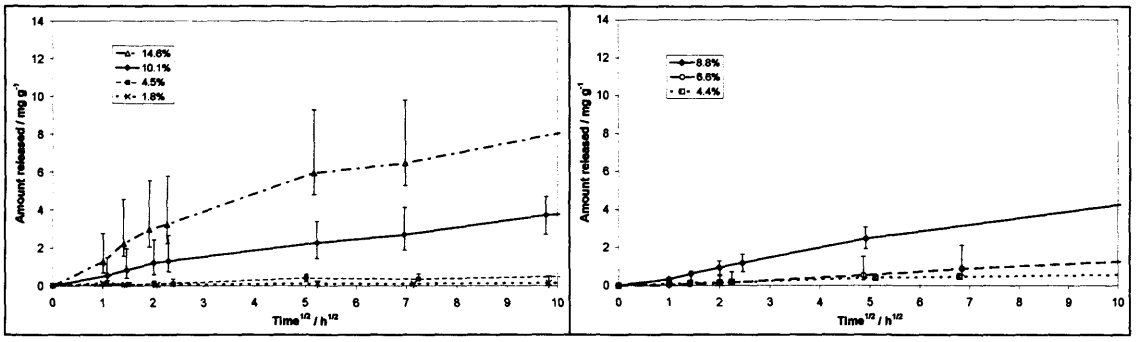

LG30 (initial) **LG30 (later)**

Figure 60 Initial part of CHA release / mg g^{-1} to $t^{½}$ = 10 $h^{½}$, Medians (n=6), with 95% confidence limits

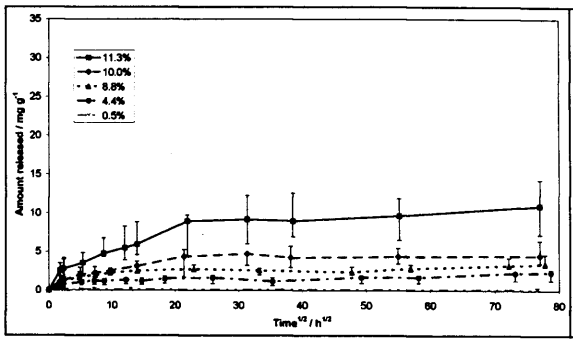

AH2

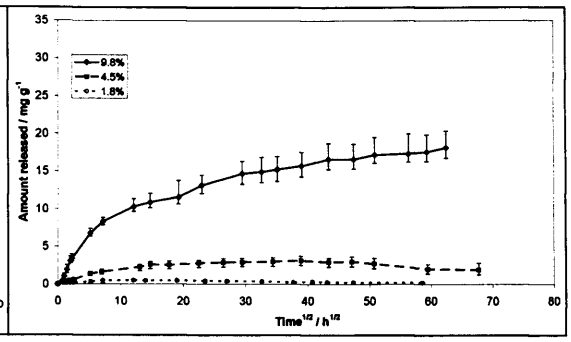

LG26

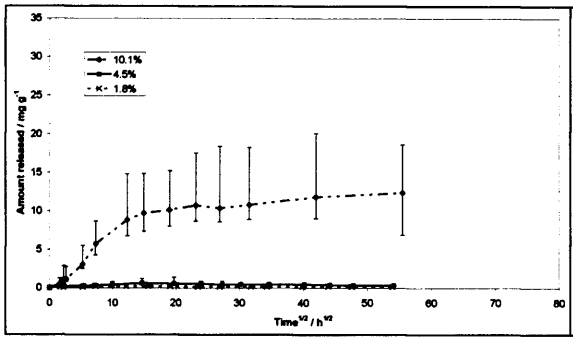

MP4 (initial)

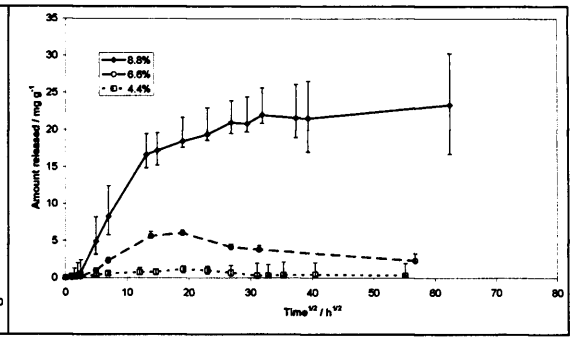

MP4 (later)

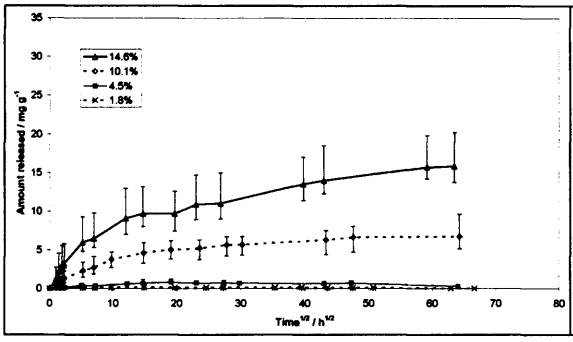

LG30 (initial)

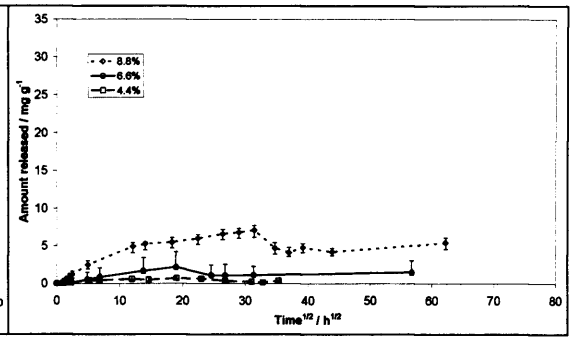

LG30 (later)

Figure 61 CHA release / mg g^{-1} to $t^{½}$ = 80 $h^{½}$ (270 days) Medians (n=6), with 95% confidence limits

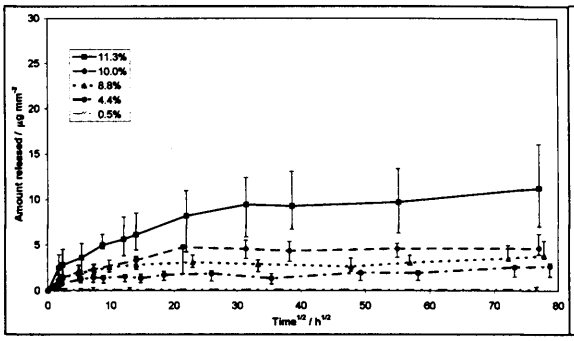

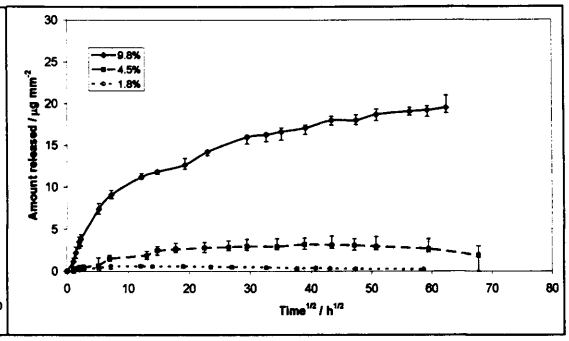

AH2 **LG26**

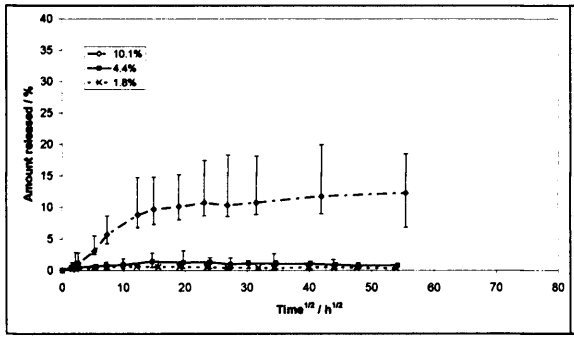

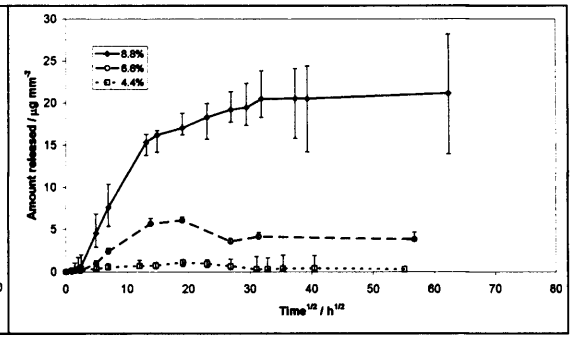

MP4 (initial) **MP4 (later)**

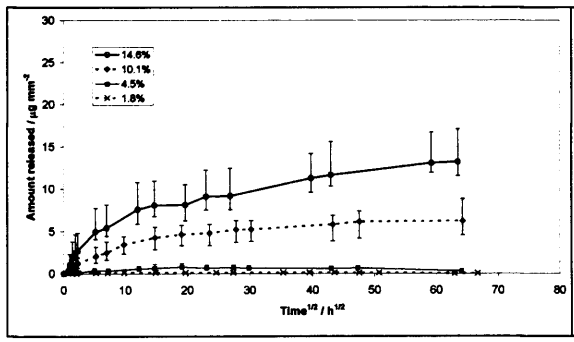

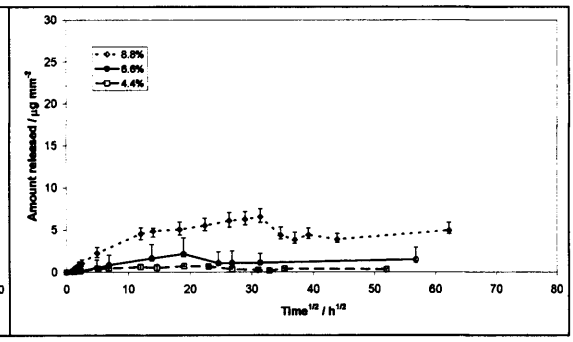

LG30 (initial) **LG30 (later)**

Figure 62 Cumulative CHA release / µg mm^{-2} to t^{½} = 80 h^{½} (270 days), Medians (n=6), with 95% confidence limits

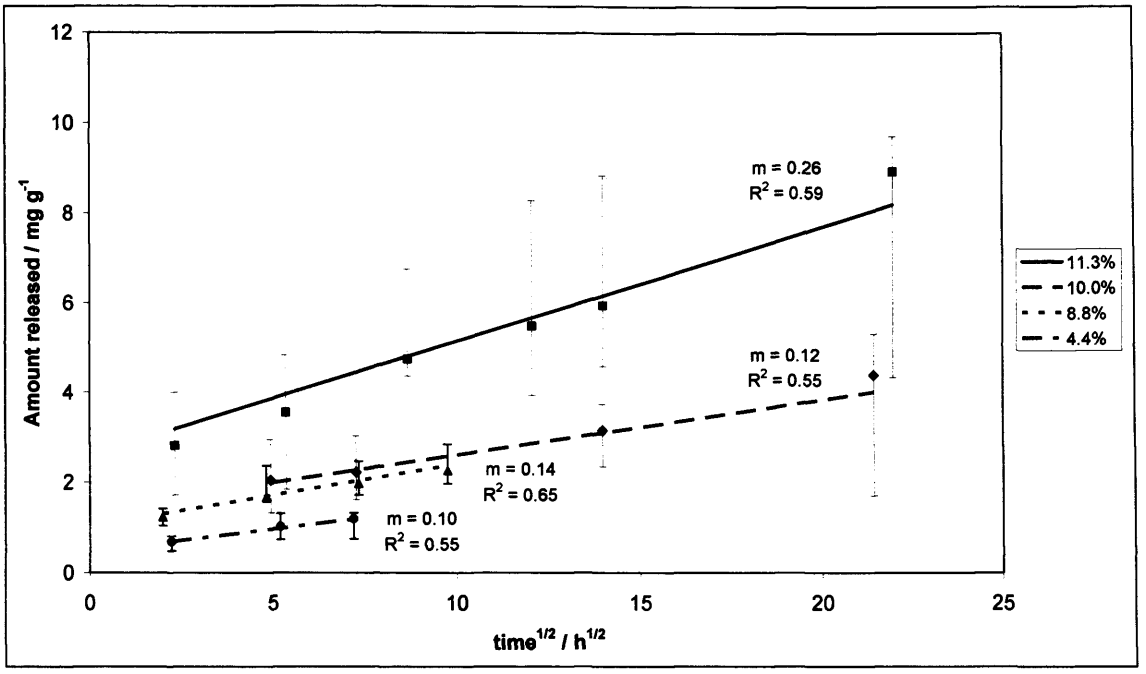

Figure 63 CHA release from AH2 cement / mg g^{-1} (linear portion only)

	[CHA] in cement			
	4.4 %	6.7 %	8.8 %	10.0 %
AH2	26	–	23	31
MP4 (initial)	19	–	–	26
MP4 (later)	33	27	37	>56
LG30 (initial)	23	–	–	>64
LG30 (later)	31	27	43	–
LG26	43	–	–	>63

Table 38 Time to plateau / $h^{½}$ for selected CHA doped glasses

The release profiles from cements made with the later batch of MP4 followed the same general shape as the cements made with the older glass with the exception of 8.8% CHA containing cement which had a more distinctly linear portion between 2.5 $h^{½}$ (6¼ h) and 13.1 $h^{½}$ (7 days). There then followed

another linear region of lower release rate from 13.1 $h^{1/2}$ (7 days) to 32 $h^{1/2}$ (42 days) at which point it levelled off. The release profile for the later MP4 cement containing 4.4% CHA followed a similar profile to the initial MP4 cement containing 4.4% CHA.

Comparing the initial and later batches of MP4, the later batch containing 4.4% CHA and 6.7% CHA followed the initial batch and gave release levels that would have been predicted from the initial results for the initial batch. The later batch containing 8.8% CHA gave a much higher release than that from the initial batch containing 10.1% CHA.

The general release pattern from the LG30 cement (initial glass) showed similar plateau values for comparable included CHA concentrations. The curves generally showed a continuous change in slope and hence rate of release from t_0 to the end of the experiment in a similar manner to MP4. There were no identifiably linear regions at the beginning as with AH2 and the relative release amounts showed a similar pattern to MP4 with very small amounts released up to 4.5% included CHA. However, a much higher proportion was released at 10% CHA. The highest concentration of included CHA (14.6%) showed the highest rate of release and the highest release.

The release profiles from the later batch of LG30 started off in a similar manner to the initial batch. The 4.4% and 6.6% curves gave release levels that would have been predicted from the initial results from the initial batch. The later batch containing 8.8% CHA gave a much higher release than expected in the same manner as the release of CHA from MP4.

The release profiles from the LG26 cement were similar to those of LG30 in that there were no identifiable linear sections at the beginning of the experiment although there was a slight initial delay in release. The 9.8% specimens had almost levelled off at t=56 $h^{1/2}$ (~ 131 days).

All cements, with varying degrees, showed little change in release profiles until a certain level of included CHA, at which point the release dramatically increased. This was particularly noticeable for AH2, MP4 (initial glass) and LG30 (initial glass). The data were also plotted against time, as with the AHCl release, to see if the release was zero-order but no linear portions were found indicating that the release was not zero-order.

5.3.3.3 Percentage release charts

The percentage release graphs (Figure 64) for LG26, LG30 (new and initial glass) and MP4 (later glass) show that with increasing added concentrations of CHA, increasing proportions of CHA are released. The percentage release profiles for MP4 (initial glass) show that at the two lowest concentrations of included CHA, the amount of included CHA gives the same proportion of release. Only at higher concentrations of included CHA does the proportion of release increase dramatically. The profiles for AH2 are similar to those for MP4 (initial glass) in that they show very little change in percentage CHA released for all concentrations below 10%. Only the 11.3% cement shows a much greater percentage release.

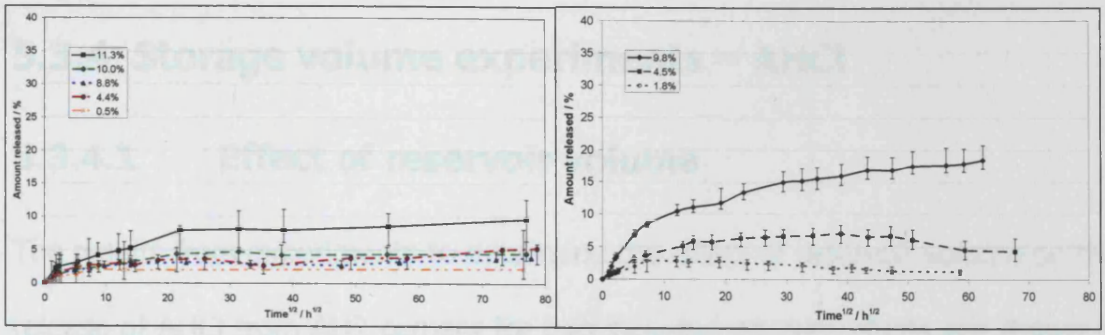

AH2 **LG26**

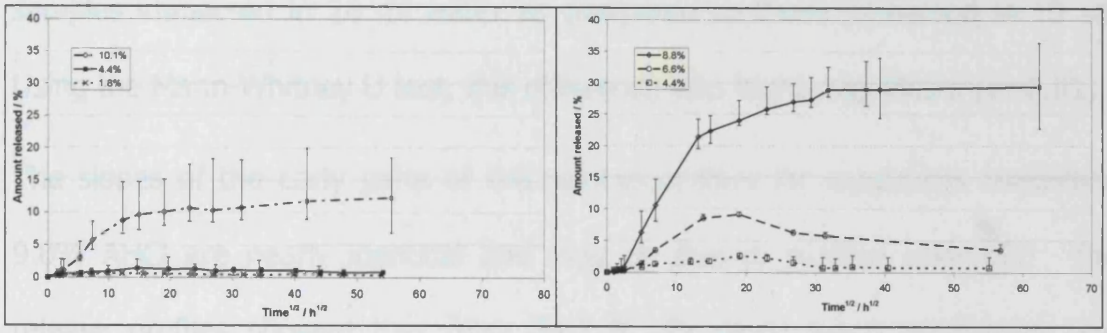

MP4 (initial) **MP4 (later)**

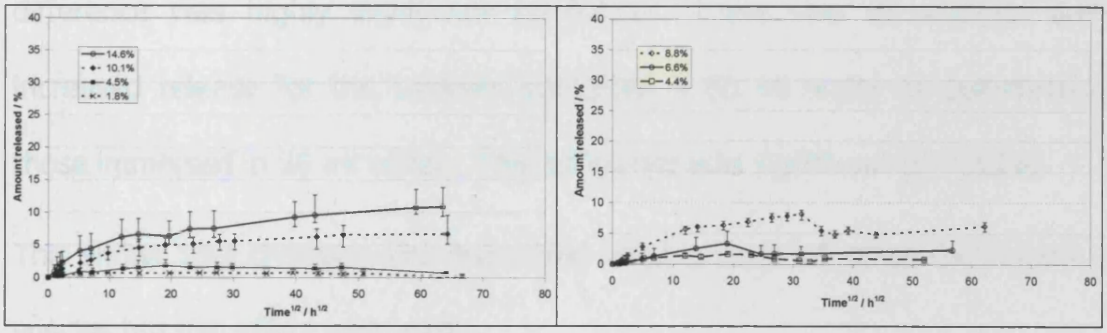

LG30 (initial) **LG30 (later)**

Figure 64 CHA release / % to $t^{1/2}$ = 80 $h^{1/2}$ (270 days), Medians (n=6), with 95% confidence limits

5.3.4 Storage volume experiments – AHCl

5.3.4.1 Effect of reservoir volume

The results from experiments to determine the effect of reservoir volume on the release of AHCl from AH2 cement for two included concentrations are shown in Figure 65. The release profiles showed that from t ~ 20 $h^{1/2}$ (17 days) when equilibrium was reached, there was an average 10.3% increased release for the samples immersed in 20 ml water as compared to those immersed in 10 ml. Using the Mann-Whitney U test, this difference was highly significant ($p<0.01$).

The slopes of the early parts of the release profiles for specimens containing 9.0% AHCl are nearly identical and may be due to surface wash-out. The release profiles showed that from 14.7 $h^{1/2}$ (9 days) when equilibrium was reached, there was an average 10.8% increased release for the samples immersed in 40 ml water as compared to those immersed in 20 ml water. This difference was highly significant ($p<0.01$). There was an average 6.0% increased release for the samples immersed n 60 ml water as compared to those immersed in 20 ml water. This difference was significant ($p=0.026$).

This shows that changing the immersion volume does influence the release of species but this effect was small.

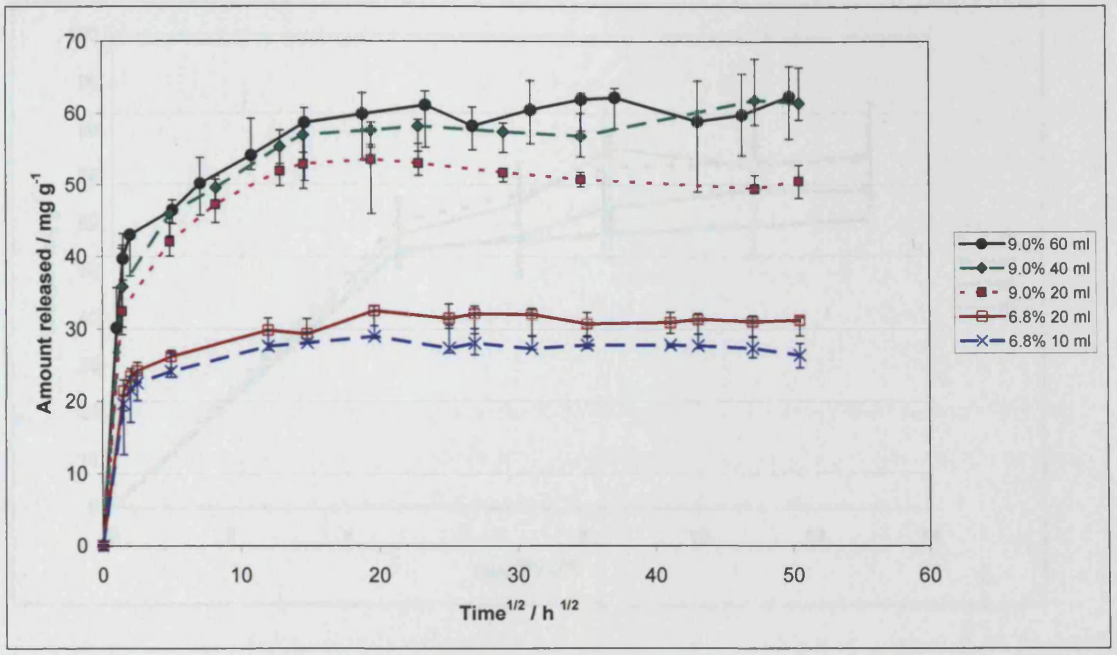

Figure 65 AHCl release from AH2 cement / mg g^{-1} (immersion volume comparison), Medians (n=6), with 95% confidence limits

5.3.4.2 Effect of reservoir volume and static volume vs changed volume

The effects of reservoir volume and comparison between static volume and changed volume on the release of AHCl from LG30 cement are shown in Figure 66. The release profiles were observed for seven days; this was not enough time to reach equilibrium but was enough to see the effect of immersion volume on AHCl release. From day 3 ($h^{½}$ = 8.5) the differences between the release profiles can more clearly be seen.

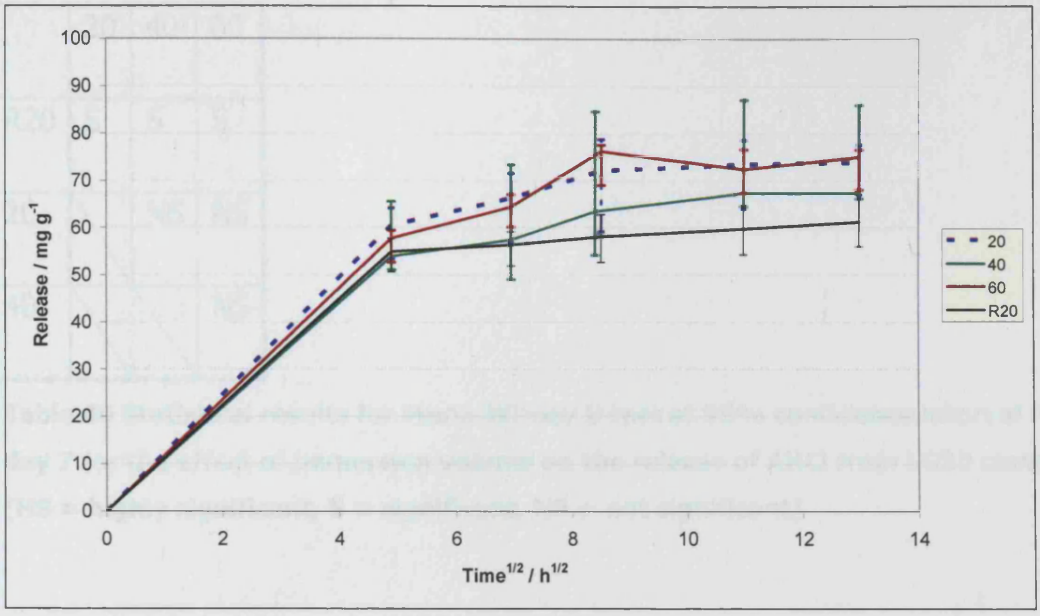

Figure 66 Effect of immersion volume and comparison between static volume and changed volume on AHCl release from LG30 cement containing 8.8% AHCl / mg g^{-1} Medians (n=6), with 95% confidence limits

5.3.4.2.1 Statistical analysis

There was no obvious difference between the four groups of specimens as the range of results overlapped considerably. The data for days 5 and 7, where the data is more clearly separated, were analysed using Mann-Witney U test and a 95% confidence interval. The results for this are shown in the following two tables.

	20	40	60
R20	S	S	S
20		NS	NS
40			NS

Table 39 Statistical results for Mann-Witney U test at 95% confidence interval for day 5 for the effect of immersion volume on the release of AHCl from LG30 cement (HS = highly significant, S = significant, NS = not significant)

	20	40	60
R20	S	S	S
20		NS	NS
40			NS

Table 40 Statistical results for Mann-Witney U test at 95% confidence interval for day 7 for the effect of immersion volume on the release of AHCl from LG30 cement (HS = highly significant, S = significant, NS = not significant)

At the two time intervals analysed the differences between group R20 and all other groups were highly significant. There was no other significant difference between any of the other groups.

5.3.5 Storage volume experiments – CHA

5.3.5.1 Limiting reservoir volume

A selection of specimens were removed from their immersion volumes and re-immersed in 10 ml fresh water and the amount of CHA released into the fresh water was measured after 7 days and 21 days. The results for this final experiment are shown in Table 41.

The release figures for both 7 days and 21 days are much reduced. This seems to indicate that nearly all release had occurred by the end of the previous experiments.

Glass	[CHA] / %	Release prior to re-immersion	Release 7 days	Release 21 days	Days after initial immersion
MP4	6.6	1.709	0.066	0.032	305
MP4	8.8	12.113	0.613	0.266	333
LG30	6.6	2.474	0.086	0.067	305
LG30	8.8	7.85	0.335	0.201	332

Table 41 Re-immersion release of CHA from selected specimens / mg g^{-1}

5.3.5.2 Effect of reservoir volume and static volume vs changed volume

The release profiles were observed for nine days; this was not enough time to reach equilibrium but was enough to see the effect of immersion volume on CHA release. From day 6 ($h^{1/2}$ = 12) the differences between the release profiles can clearly be seen.

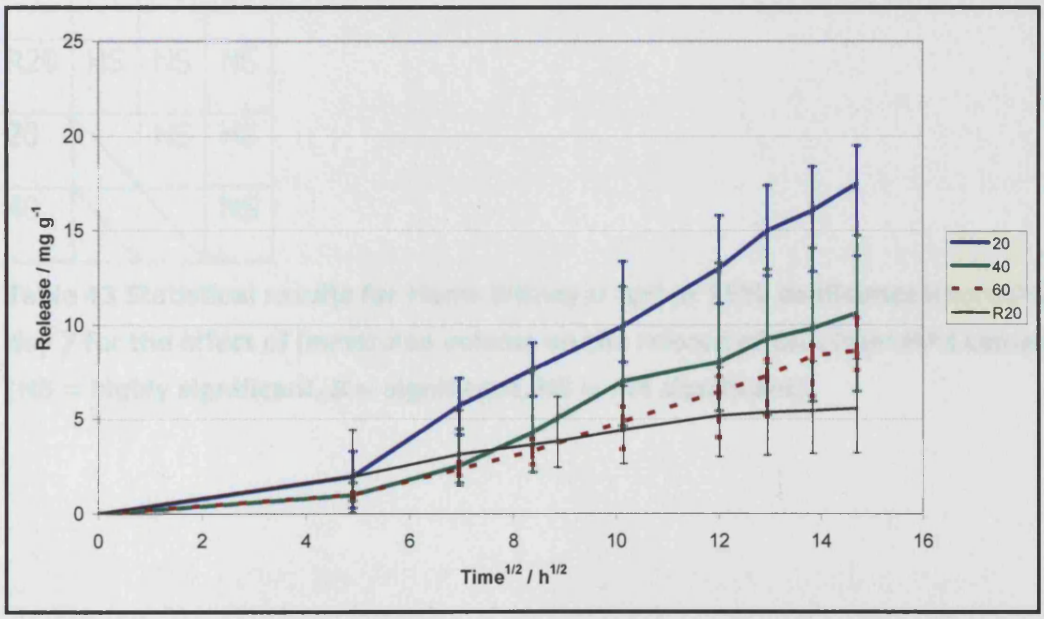

Figure 67 Effect of immersion volume and comparison between static volume and changed volume on CHA release from MP4 cement containing 8.8% AHCl / mg g^{-1} Medians (n=12), with 95% confidence limits

5.3.5.2.1 Statistical analysis

There were noticeable differences in release between the four groups of specimens. The data for days 6 to 9, where the data is more clearly separated, were analysed using Mann-Witney U test and a 95% confidence interval. The results for this are shown in the following four tables.

	20	40	60
R20	HS	NS	NS
20		HS	HS
40			NS

Table 42 Statistical results for Mann-Witney U test at 95% confidence interval for day 6 for the effect of immersion volume on the release of CHA from MP4 cement (HS = highly significant, S = significant, NS = not significant)

	20	40	60
R20	HS	NS	NS
20		HS	HS
40			NS

Table 43 Statistical results for Mann-Witney U test at 95% confidence interval for day 7 for the effect of immersion volume on the release of CHA from MP4 cement (HS = highly significant, S = significant, NS = not significant)

	20	40	60
R20	HS	NS	S
20		HS	HS
40			NS

Table 44 Statistical results for Mann-Witney U test at 95% confidence interval for day 8 for the effect of immersion volume on the release of CHA from MP4 cement (HS = highly significant, S = significant, NS = not significant)

	20	40	60
R20	HS	NS	HS
20		HS	HS
40			NS

Table 45 Statistical results for Mann-Witney U test at 95% confidence interval for day 9 for the effect of immersion volume on the release of CHA from MP4 cement (HS = highly significant, S = significant, NS = not significant)

At all time intervals analysed the differences between group 20 and all other groups were highly significant. At all time intervals the difference between group 40 and groups 60 and R20 were not significant. As time elapsed, the difference between R20, the group which showed the lowest release, and 60, the next lowest release, changed from not significant at day 6 to highly significant at day 9.

5.3.6 Ion release from LG30 cement containing CHA

The specimens from section 5.3.5.1 above were also used to determine ion release. Aliquots for ion release were taken immediately after those taken for

CHA release determination. The release profiles of Na^+ and Ca^{2+} were observed for nine days and are shown in Figure 68 and Figure 69 respectively. For ease of comparison, CHA release from the same specimens as shown in section 5.3.5.1 above, is shown in Figure 70.

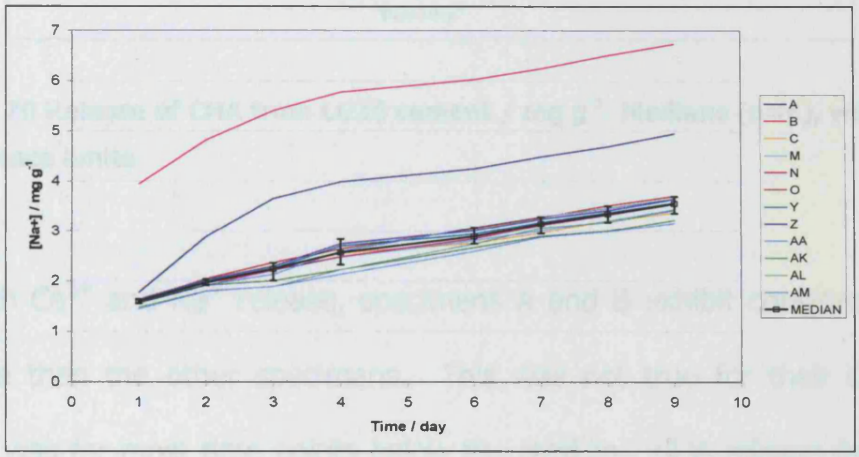

Figure 68 Release of Na^+ from LG30 cement / mg g^{-1}, Medians (n=12), with 95% confidence limits

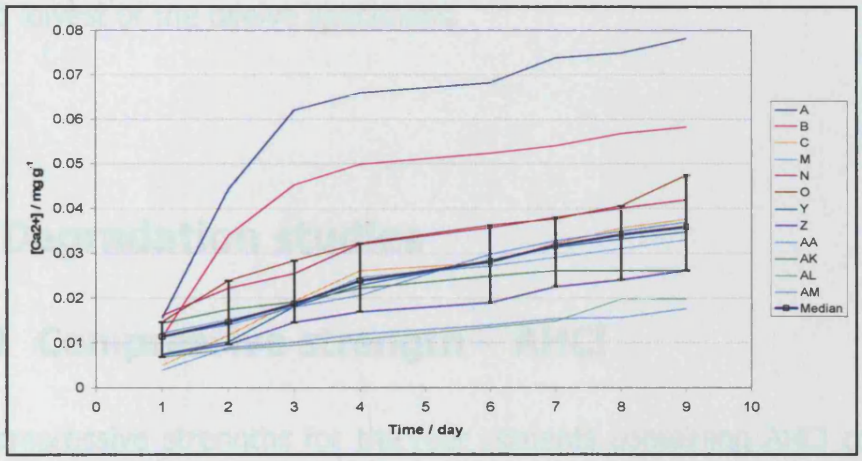

Figure 69 Release of Ca^{2+} from LG30 cement / mg g^{-1}, Medians (n=6), with 95% confidence limits

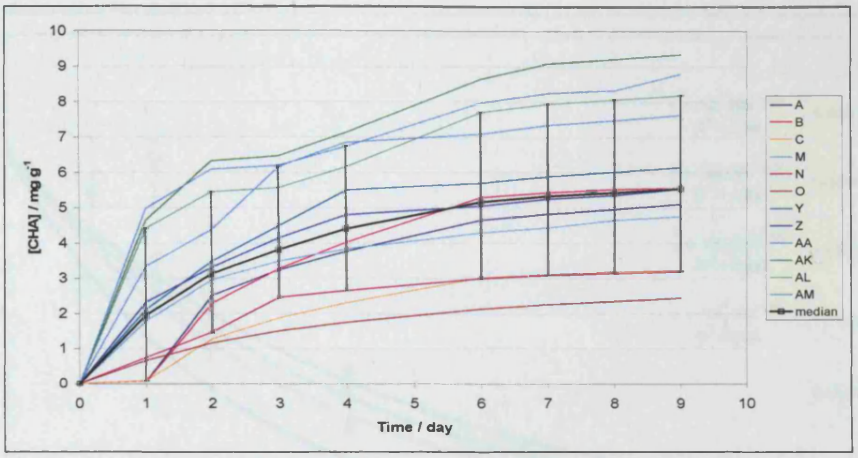

Figure 70 Release of CHA from LG30 cement / mg g^{-1}, Medians (n=6), with 95% confidence limits

In both Ca^{2+} and Na^{+} release, specimens A and B exhibit considerably higher release than the other specimens. This was not true for their CHA release which was for most time points below the median. CHA release from AM was for most time points the second highest release of the twelve specimens. This again was not true for the release of Ca^{2+} and Na^{+} where their release were second lowest of the twelve specimens.

5.4 Degradation studies

5.4.1 Compressive strength – AHCl

The compressive strengths for the four cements containing AHCl compared to an unmodified cement are shown in Figure 71. The addition of AHCl led to a decrease in compressive strength for all cements. The chosen regression line was exponential in each case and the R^2 values showed good correlation.

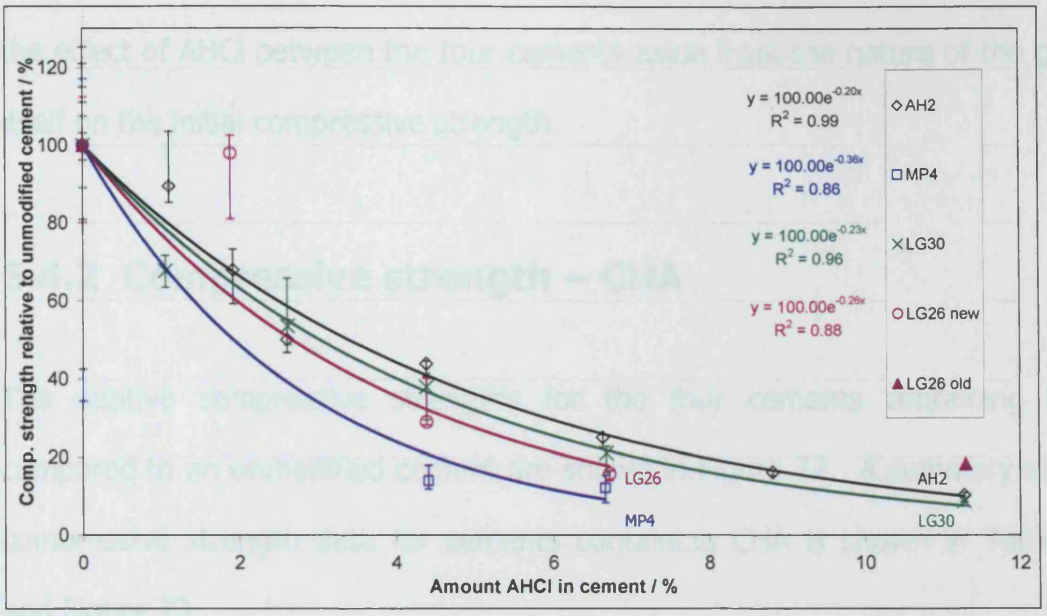

Figure 71 Compressive strengths of cements containing AHCl relative to unmodified cement (with initial batch LG26 put in for comparison purposes), Medians (n=6), with 95% confidence limits

A summary of the compressive strength data for cements containing AHCl is shown in Table 46.

Cement glass	Exponent / $\%^{-1}$	Compressive Strength at 0% AHCl / MPa	Compressive Strength at 6.7% AHCl / MPa
AH2	-0.20	220.9	55.5
MP4	-0.36	63.0	7.7
LG30	-0.23	65.2	13.8
LG26	-0.26	122.7	19.2

Table 46 Selected compressive strengths for cements containing AHCl

The exponent value is an indication of the slope and therefore the effect of the addition of AHCl on the cements. There was however, no great difference in

the effect of AHCl between the four cements aside from the nature of the glass itself on the initial compressive strength.

5.4.2 Compressive strength – CHA

The relative compressive strengths for the four cements containing CHA compared to an unmodified cement are shown in Figure 72. A summary of the compressive strength data for cements containing CHA is shown in Table 47 and Figure 73.

The addition of CHA led to a definite decrease in compressive strength for all cements except LG30 which showed very little change. The chosen regression line in each case was linear though the R^2 values were generally low indicating no linearity. The regression line for MP4 cement was formed from the first three points only as this gave a better fit than all four points and there appeared to be an indication that MP4 cement had reached a point at which increasing amounts of CHA produced little decrease in compressive strength. It is possible that if larger concentrations of CHA were added to the other cements, the same effect might be observed.

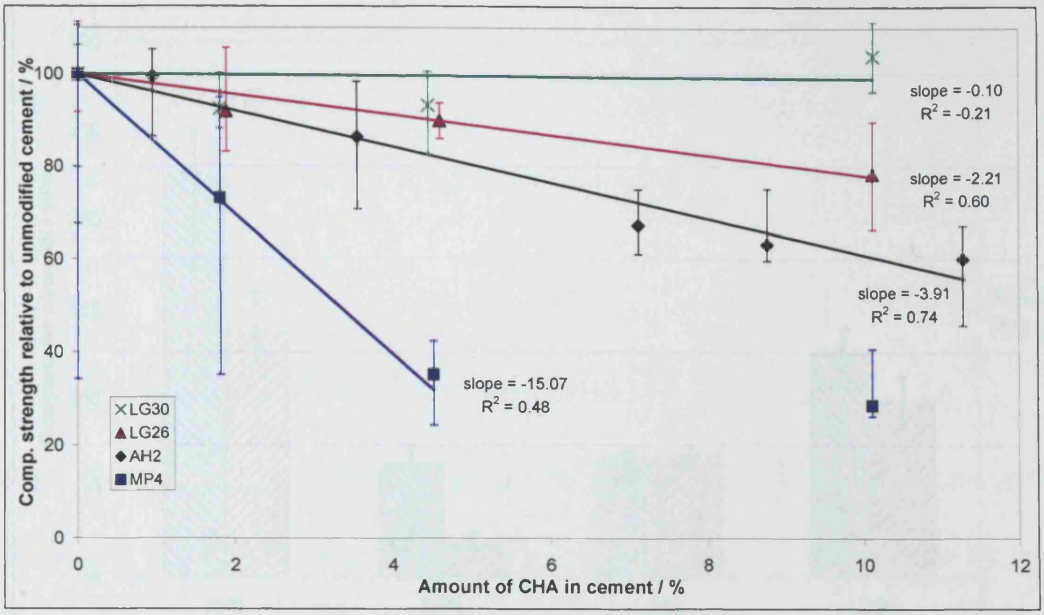

Figure 72 Compressive strengths of cements containing CHA relative to unmodified cement, Medians (n=6), with 95% confidence limits

Cement glass	Compressive Strength at 0% CHA / MPa	Compressive Strength at 10.1 % CHA / MPa	Slope / MPa $\%^{-1}$
AH2	220.9	138.3*	-3.9
MP4	63.0	18.1	-15.1#
LG30	67.1	69.2	-0.1
LG26	127.2	98.9	-2.2

Table 47 Selected compressive strengths for cements containing CHA

*** extrapolated**

 # based on first three points only

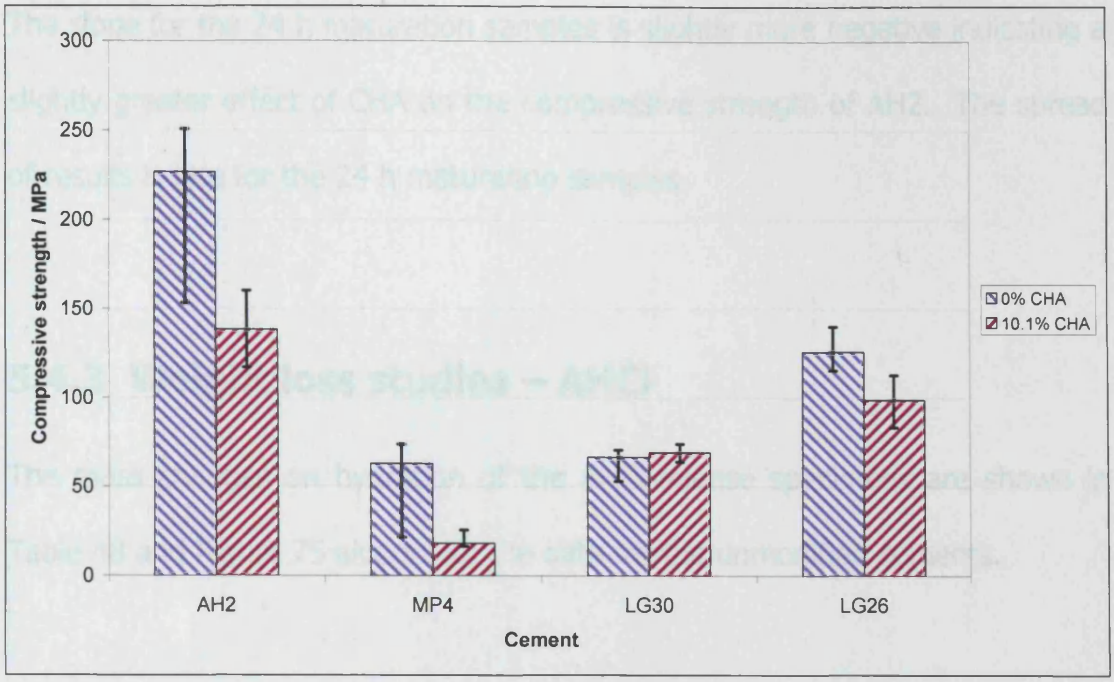

Figure 73 Compressive strengths of the four cements for unmodified cement and 10.1 % included CHA, Medians (n=6), with 95% confidence limits

To check the effect of maturity of cement on the compressive strengths of the cements, specimens of AH2 cement doped with CHA were made and matured for 24 h prior to immersion in water. This data is shown in Figure 74 along with the data for the specimens matured for 1 h.

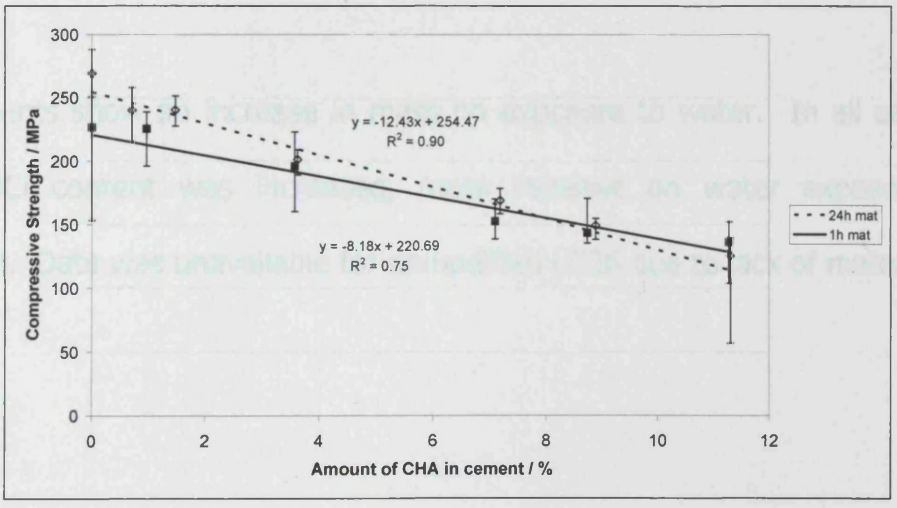

Figure 74 Comparison between compressive strengths of AH2 cement containing CHA at 1 h and 24 h maturation times

The slope for the 24 h maturation samples is slightly more negative indicating a slightly greater effect of CHA on the compressive strength of AH2. The spread of results is less for the 24 h maturation samples.

5.4.3 Weight loss studies – AHCl

The mass changes on hydration of the AHCl-release specimens are shown in Table 48 and Figure 75 along with the data for the unmodified cements.

[AHCl] / %	AH2	MP4	LG30	LG26
0	6.59	27.93	8.90	No data
4.4	4.95	25.58	6.39	33.63
6.7	3.15	17.92	6.39	7.01
8.8	1.83	15.20	5.84	6.18

Table 48 Mass change on hydration of GICs containing AHCl
n.b. all specimens matured for 24 hours

All cements show an increase in mass on exposure to water. In all cases, as the AHCl content was increased, mass increase on water exposure was reduced. Data was unavailable for unmodified LG26 due to lack of material.

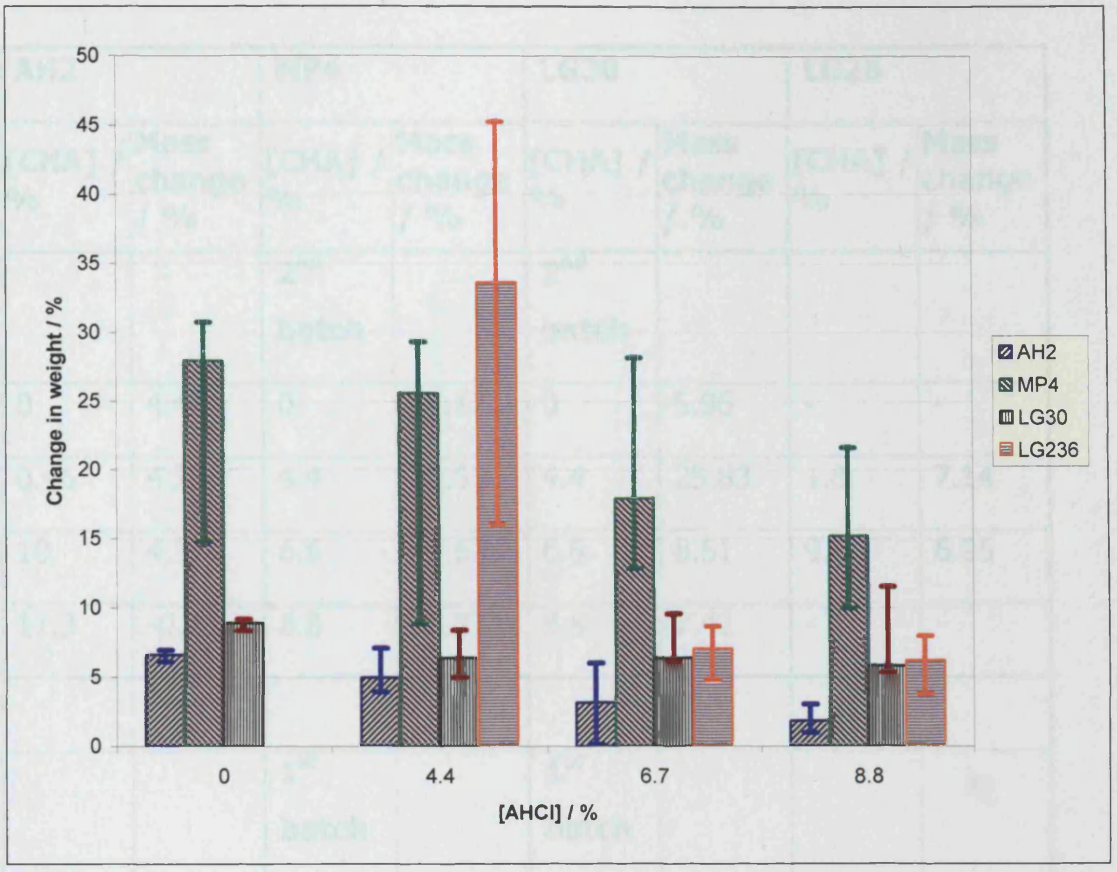

Figure 75 Mass change on hydration of GICs containing AHCl (medians with range of results)

5.4.4 Weight loss studies – CHA

The mass changes on hydration of the CHA – release specimens are shown in Table 49 and Figure 76 along with the data for the unmodified cements.

AH2		MP4		LG30		LG26	
[CHA] / %	Mass change / %	[CHA] / %	Mass change / %	[CHA] / %	Mass change / %	[CHA] / %	Mass change / %
		2nd batch		2nd batch			
0	4.42	0	35.17	0	5.96	-	-
0.46	4.77	4.4	29.53	4.4	25.83	1.8	7.14
10	4.37	6.6	29.63	6.6	8.51	9.8	6.95
11.3	-0.43	8.8	28.37	8.8	7.42	-	-
		1st batch		1st batch			
		1.8	17.70	4.5	7.49		
		4.4	13.05	10.1	5.89		
		10.1	-4.54	14.6	6.48		

Table 49 Mass change on hydration of GICs containing CHA
n.b. all specimens matured for 1 hour

Wit two exceptions, all cements show an increase in mass on exposure to water. The two exceptions are AH2 cement with 11.3% included CHA and MP4 cement (old batch) with 10.1% included CHA. In most cases as the CHA content was increased, mass increase on water exposure was reduced. Data was unavailable for unmodified LG26 and MP4 (old batch) due to lack of material.

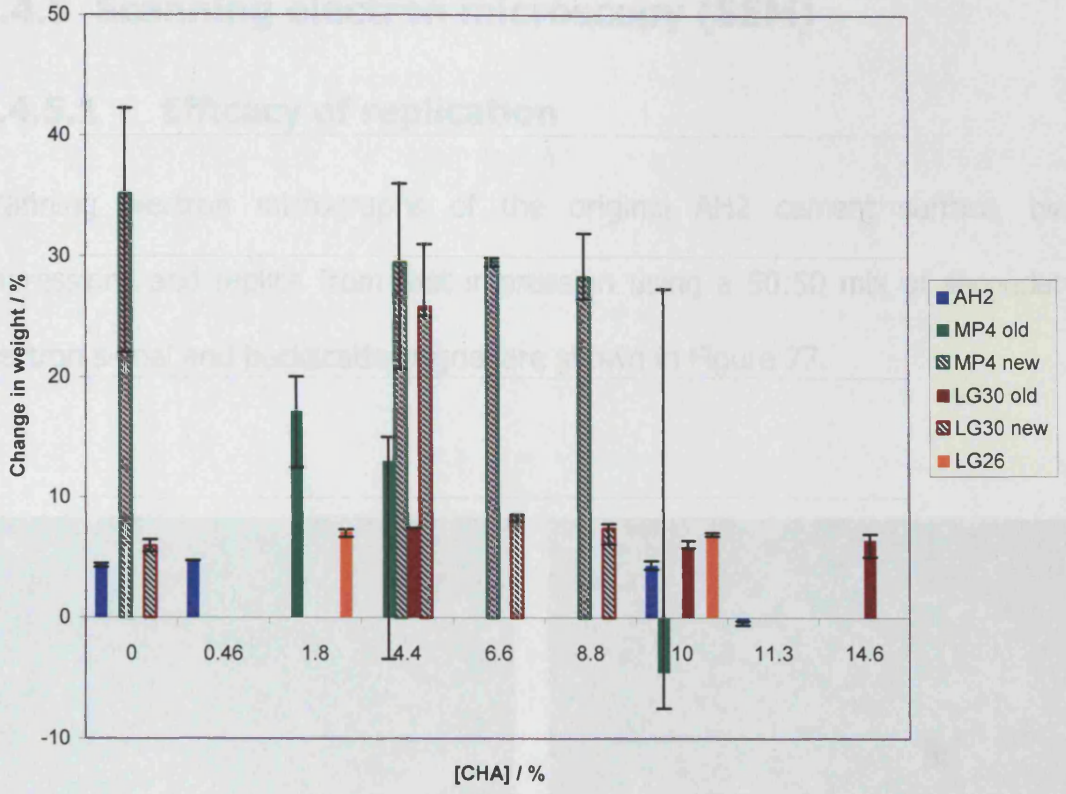

Figure 76 Mass change on hydration of GICs containing CHA (medians with range of results)

5.4.5 Scanning electron microscopy (SEM)

5.4.5.1 Efficacy of replication

Scanning electron micrographs of the original AH2 cement surface, two impressions and replica from first impression using a 50:50 mix of secondary electron signal and backscatter signal are shown in Figure 77.

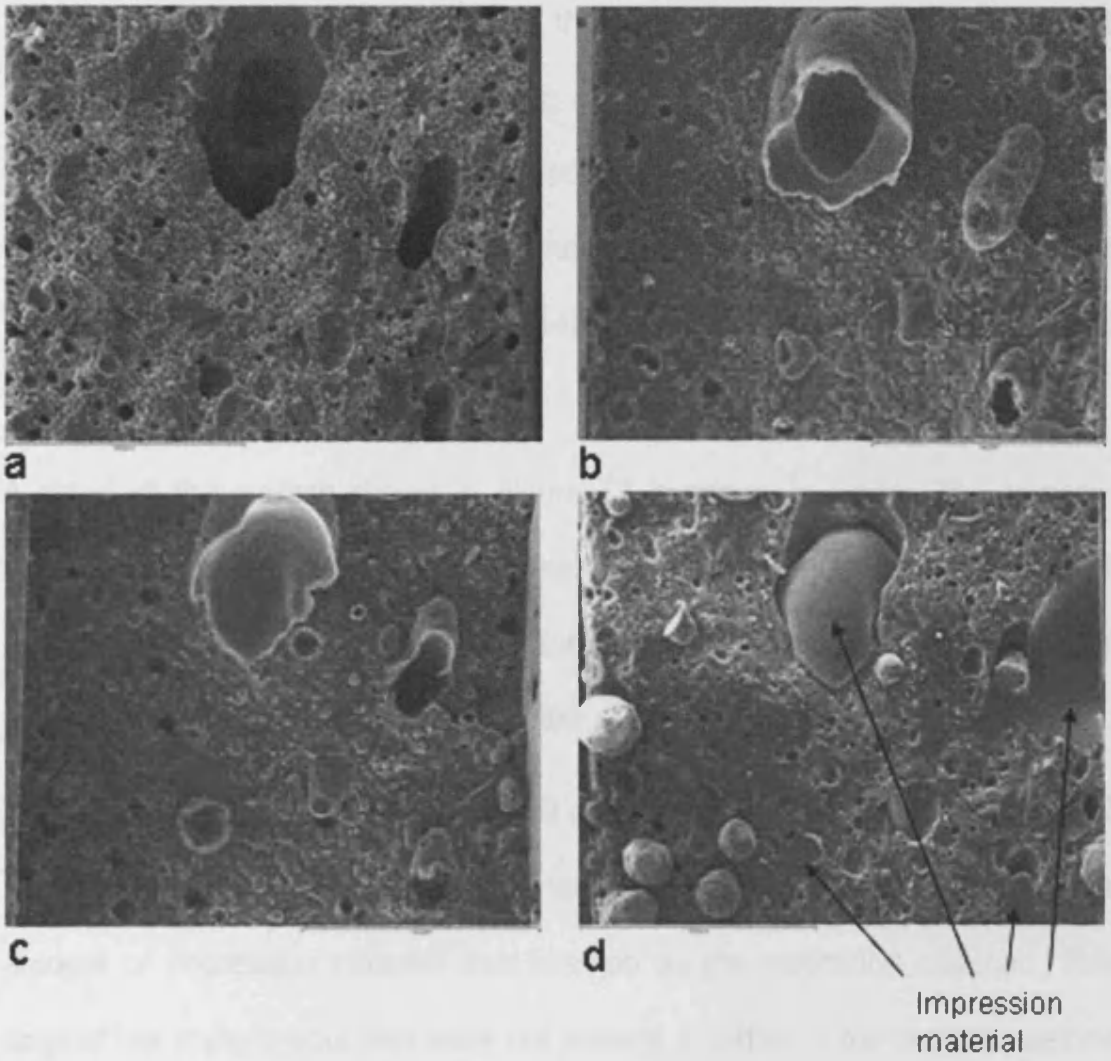

Figure 77 Scanning electron micrographs of AH2 cement. (a – original surface, b – scavenging impression, c – 2nd impression, d – replica) ×800 magnification, field of view 1120 μm

note: the two impressions have been flipped horizontally for comparison purposes

The replica reproduced the detail of the original well in places. These include the small holes, edges of the larger features, rough parts of the surface and the smoother parts. In Figure 77 (d) (replica) it appears that some of the impression material was retained by the replicating material. This was most noticeable in the two larger holes which had undercuts. Also in the same figure are inclusions 60 – 130 mm in diameter that are not on the original surface or impression. The manufacturers of the epoxy resin have confirmed that although the material is free from filler, it is produced in an atmosphere where there may be particles of talc or polyester beads of these approximate dimensions used as fillers for their other products. It was inferred from this that these were probably polyester particles and are therefore artefactual and should be ignored.

A detail of the surface shown in Figure 77 is shown in Figure 78. It again consists of scanning electron micrographs of part of the original AH2 cement surface, two impressions and replica from first impression using a 50:50 mix of secondary electron signal and backscatter signal.

The replica again reproduced the detail of the original well over the majority of the surface. The exception was the large hole to the right in which a large amount of impression material was retained by the replicating material. The original has some cracks that were not present in either of the two impressions or the replica. These were thought to be due to desiccation after the impressions were taken but prior to viewing with the electron microscope.

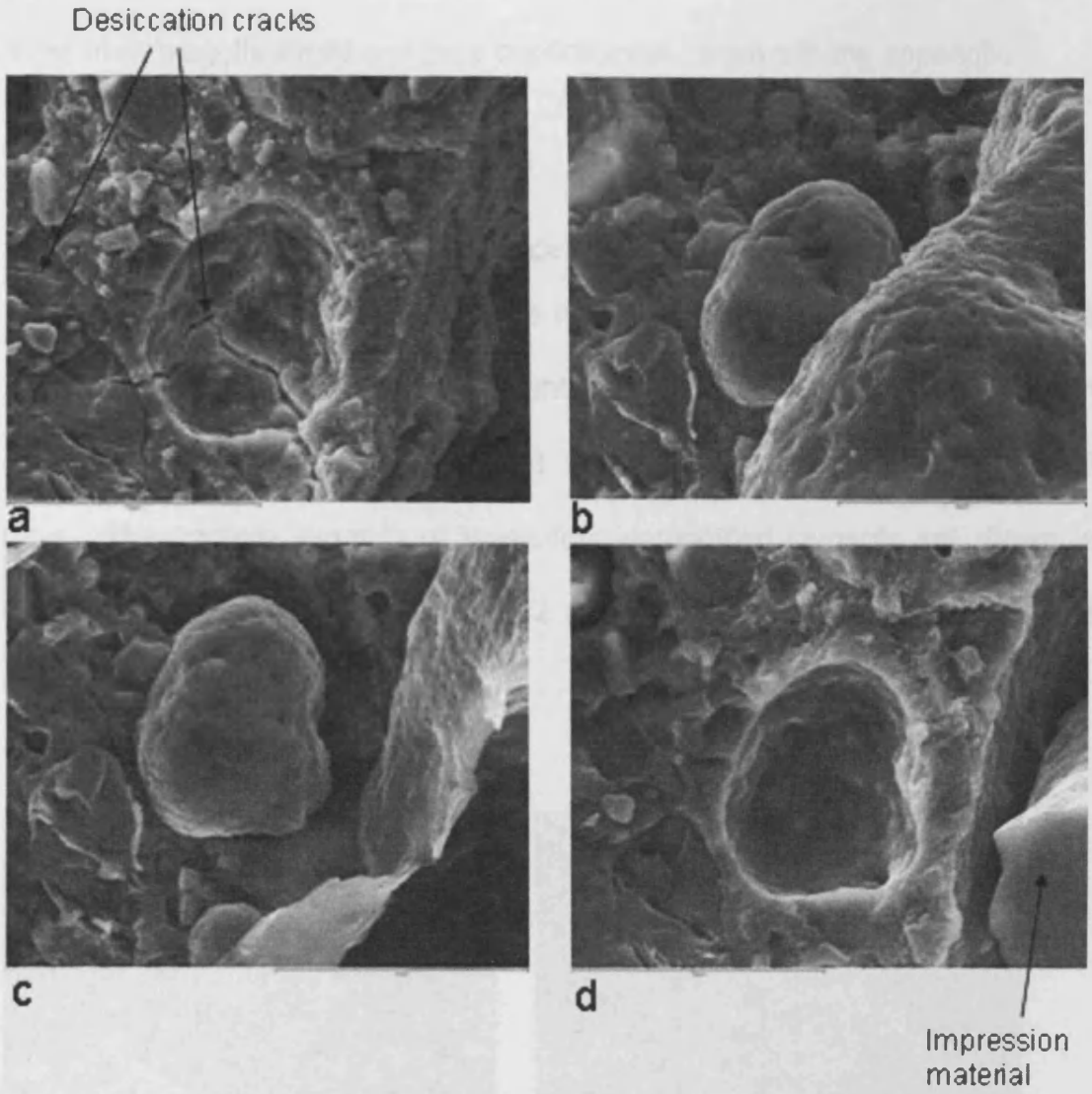

Figure 78 Scanning electron micrographs of AH2 cement. (a – original surface, b – first impression, c – 2nd impression, d – replica) ×800 magnification, field of view 144 μm

note: the two impressions have been flipped horizontally for comparison purposes

5.4.5.2 Surfaces and fracture surfaces

To investigate the effect of additives on the surface of the GICs and to investigate the possibility of crack and channel formation specimens were examined using the SEM. All the images of the four GICs, both surfaces and

cross-sectional fracture surfaces at three different levels of included species at three main magnifications and their duplicates are shown in the appendix.

5.4.5.2.1 Unmodified cements

5.4.5.2.1.1 Comparison Between cements

The differences between cements were most visible at x400 magnification. The surfaces of the four unmodified cements at x400 magnification are shown in Figure 79 before immersion, Figure 81 after 48 hours and Figure 83 after 35 days. The fracture surfaces of these four unmodified cements are shown in Figure 80 before immersion, Figure 82 after 48 hours and Figure 84 after 35 days.

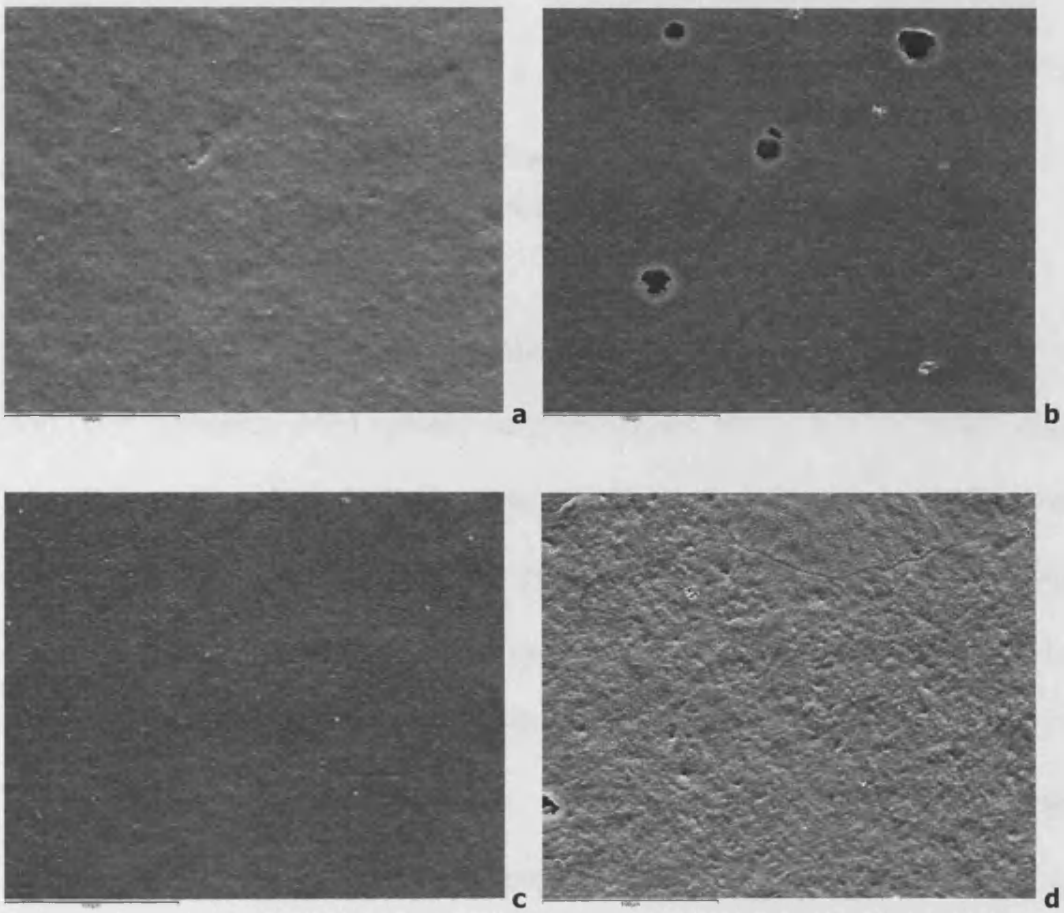

Figure 79 SEMs of surfaces of unmodified cement before immersion (a – AH2, b – MP4, c – LG30, d – LG26) ×400 magnification, field of view = 284

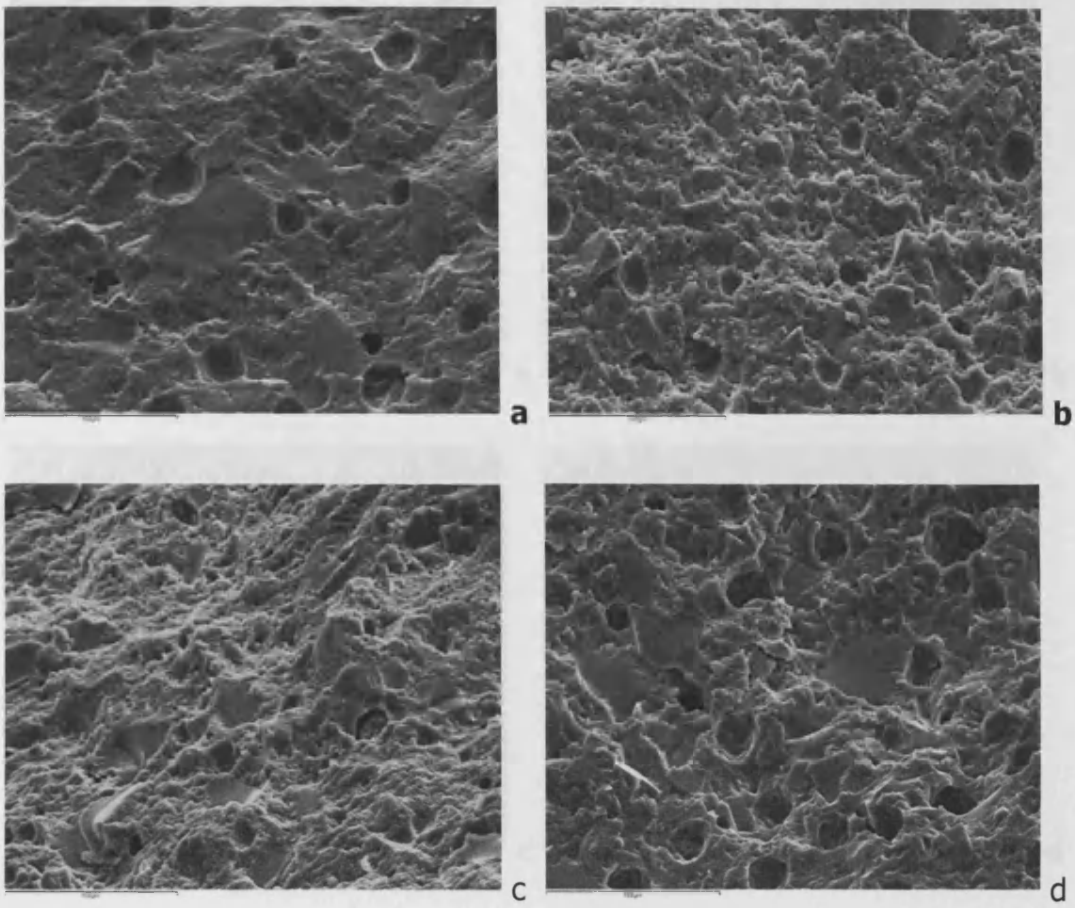

Figure 80 SEMs of fracture surfaces of unmodified cement before immersion (a – AH2, b – MP4, c – LG30, d – LG26) ×400 magnification, field of view = 284

Before immersion there appeared little difference between the surfaces of AH2 and LG30 cements. MP4 cement contained a few voids and LG26 was rougher than the others. The fracture surfaces all contained voids and AH2 cement appeared a little smoother than the others. After 48 hours immersion in water there was again little difference between the surfaces of AH2 and LG30 cements and LG26 was rougher. MP4 cement surface was disrupted and had more voids than the other cements. Again the fracture surfaces all contained voids. LG26 cement appeared slightly rougher and a few cracks were observed. MP4 cement exhibited more severe cracking and had the roughest surface.

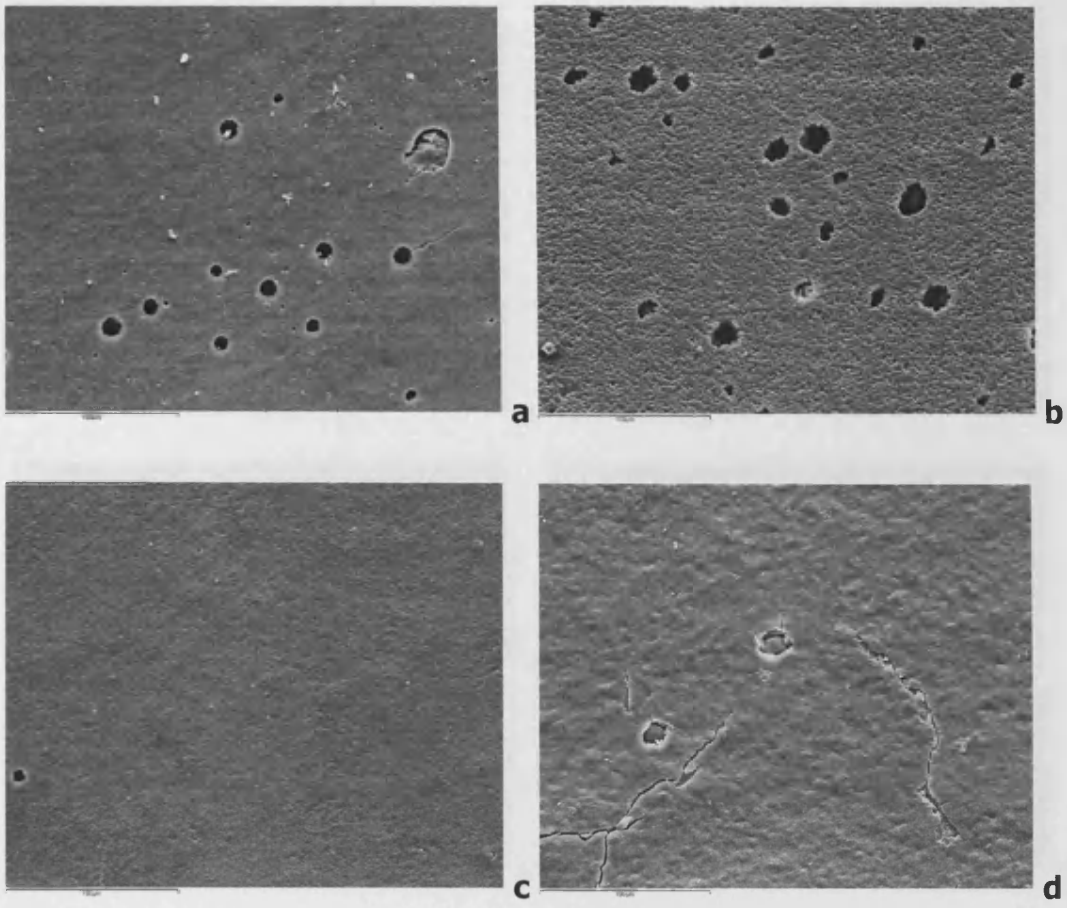

Figure 81 SEMs of surfaces unmodified cement after 48 hours immersion (a – AH2, b – MP4, c – LG30, d – LG26) ×400 magnification, field of view = 284

After 35 days immersion in water there was again little difference between the surfaces and fracture surfaces of AH2 and LG30 cements, LG26 cement was a little rougher and MP4 cement was considerably disrupted and had more voids than the other cements.

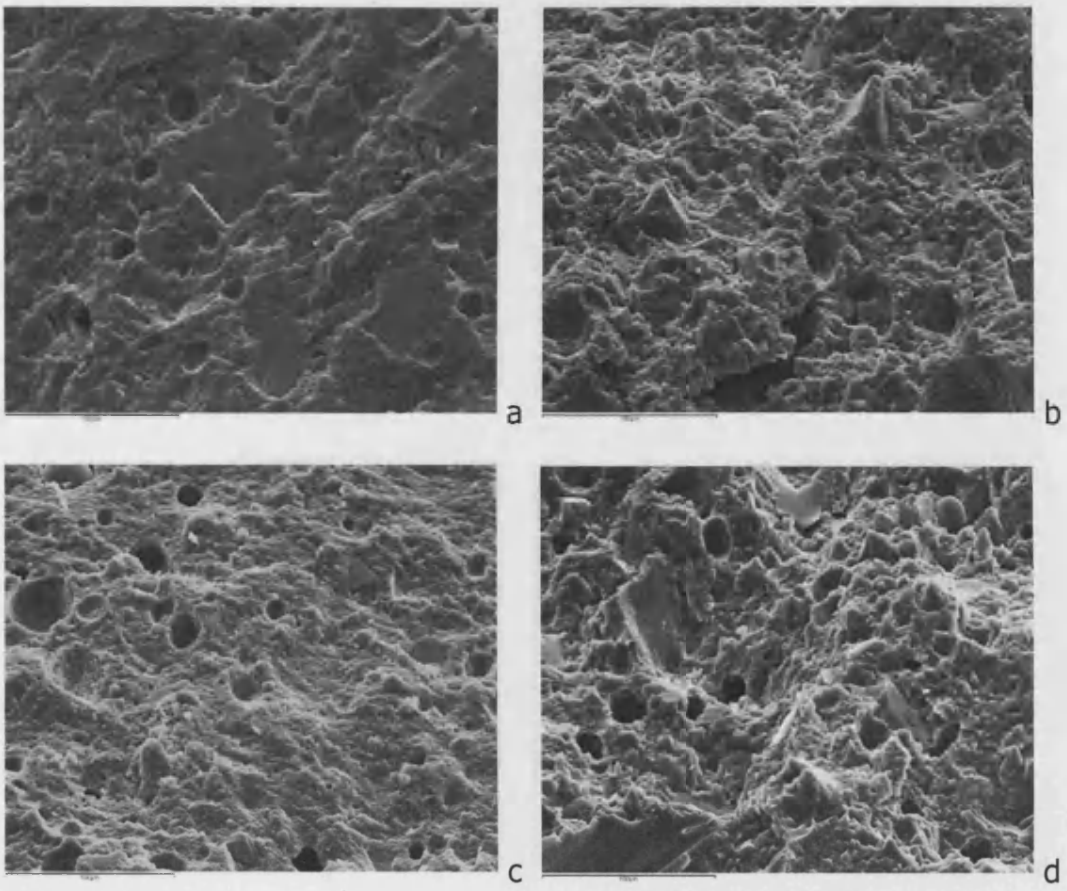

Figure 82 SEMs of fracture surfaces of unmodified cement after 48 hours immersion (a – AH2, b – MP4, c – LG30, d – LG26) ×400 magnification, field of view = 284

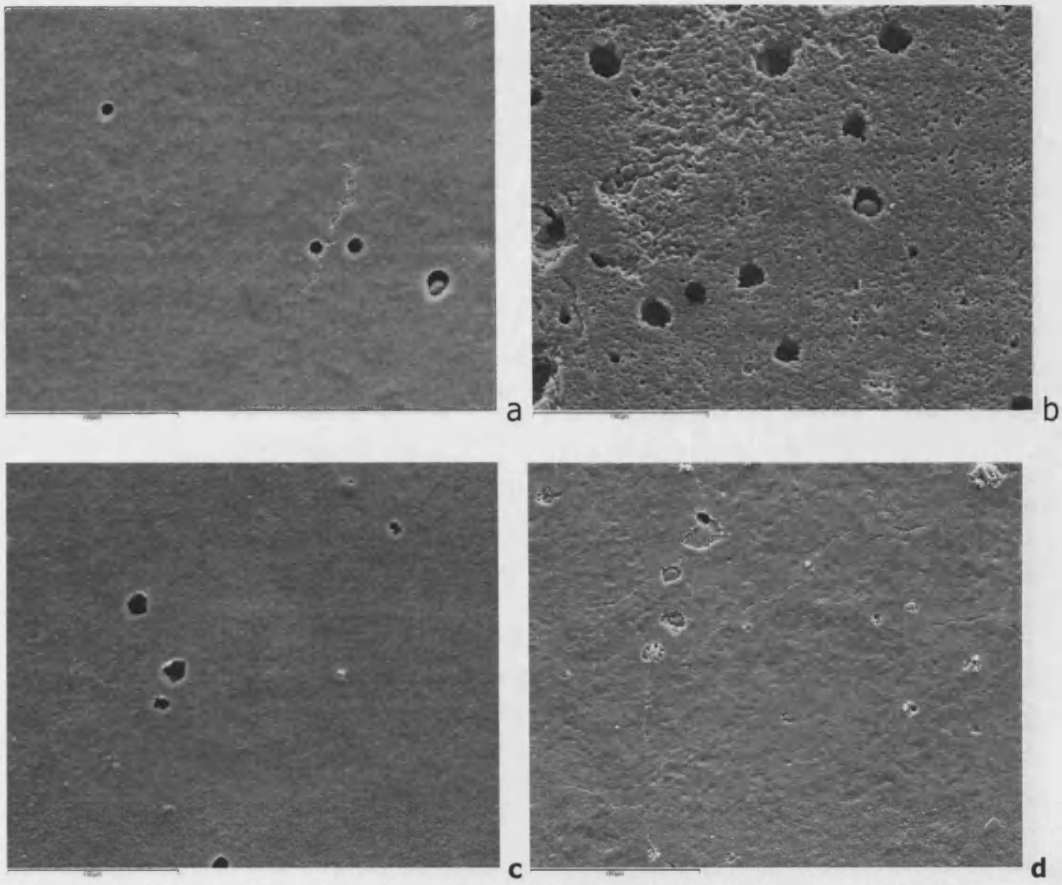

Figure 83 SEMs of surfaces of unmodified cement after 35 days immersion (a – AH2, b – MP4, c – LG30, d – LG26) ×400 magnification, field of view = 284

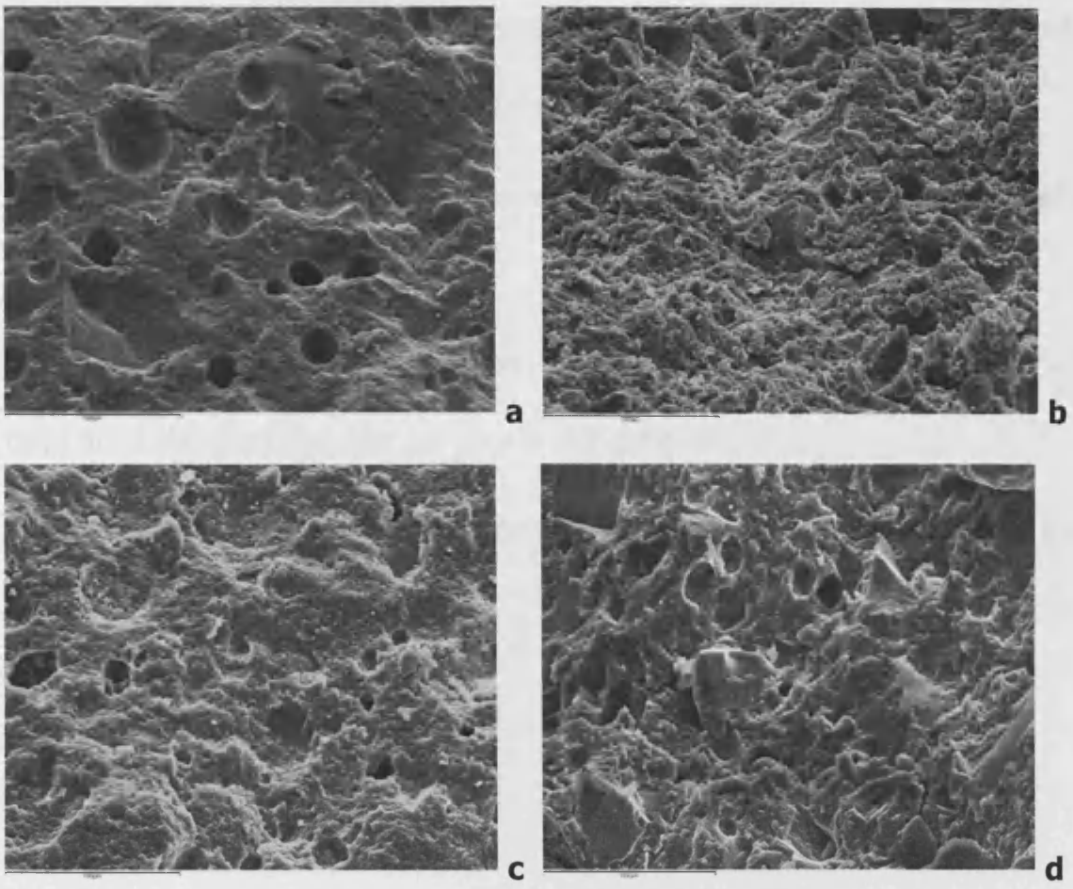

Figure 84 SEMs of fracture surfaces of unmodified cement after 35 days immersion (a – AH2, b – MP4, c – LG30, d – LG26) ×400 magnification, field of view = 284

5.4.5.2.1.2 Effect of hydration

The surfaces of unmodified AH2 cement before immersion, at 48 hours and 35 days at x1600 magnification are shown in Figure 85.

There appeared little or no change in the surfaces between these three stages of immersion.

The surfaces of unmodified MP4 cement before immersion, at 48 hours and 35 days at x1600 magnification are shown in Figure 86.

Substantial disruption of the surface can be observed after 48 hours immersion which increased after 35 days.

The surfaces of unmodified LG30 cement before immersion, at 48 hours and 35 days at x1600 magnification are shown in Figure 87.

A slight increase in pitting was observed at 48 hours immersion and a further increase after 35 days.

The surfaces of unmodified LG26 cement before immersion, at 48 hours and 35 days at x1600 magnification are shown in Figure 88.

There appeared little or no differences in the surfaces between these three stages of immersion.

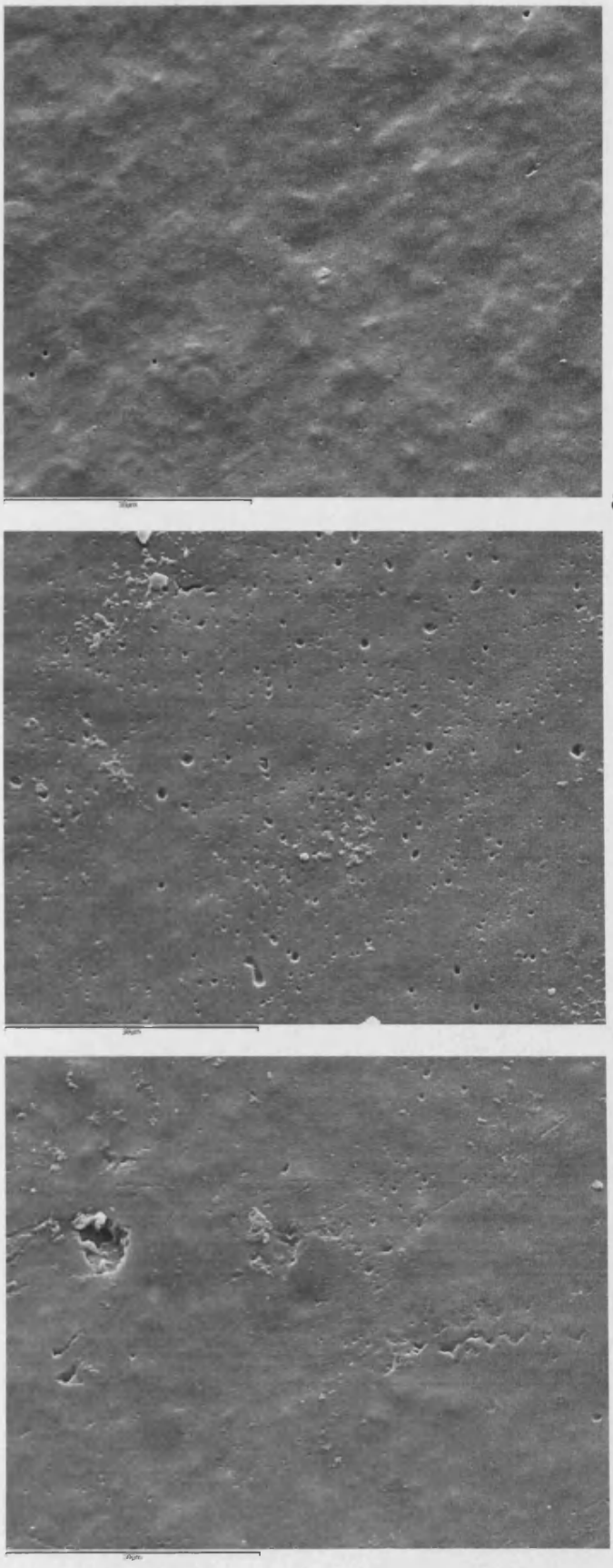

Figure 85 SEMs of unmodified AH2 cement (a – before immersion, b – after 48 hours, c – after 35 days) ×1600 magnification, field of view = 72 μm

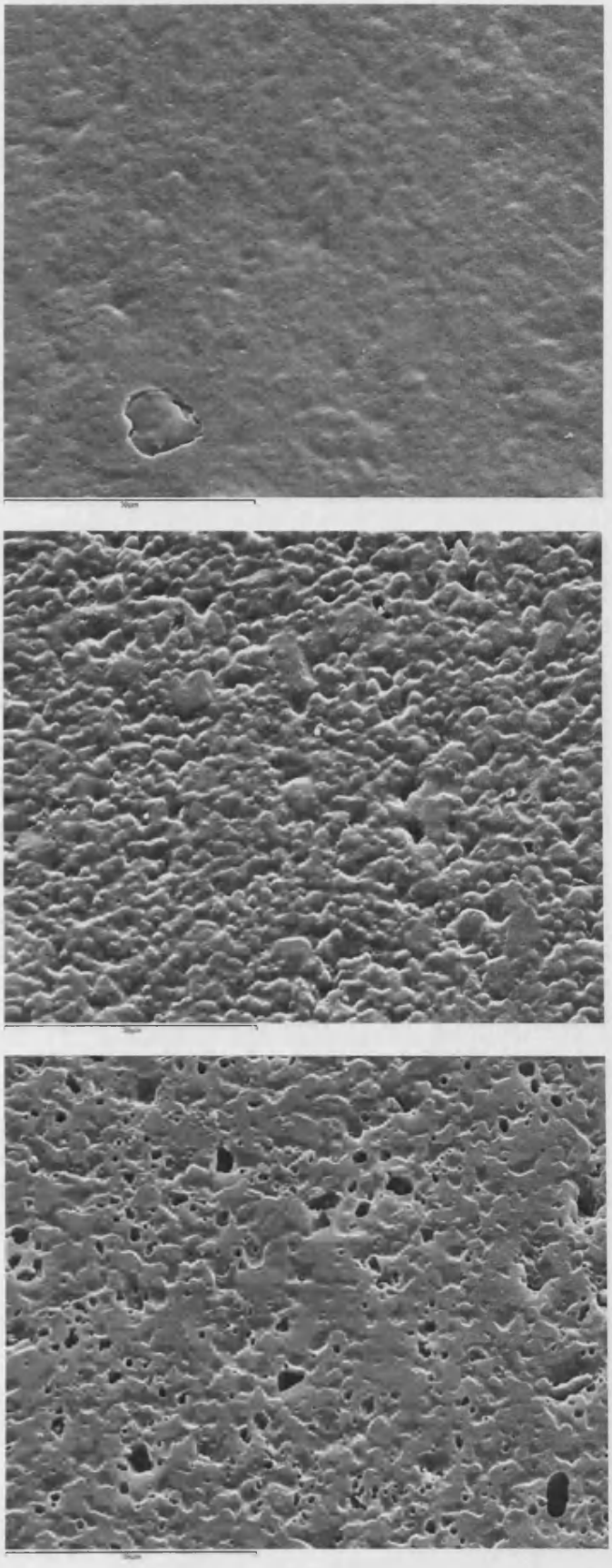

Figure 86 SEMs of unmodified MP4 cement (a – before immersion, b – after 48 hours, c – after 35 days) ×1600 magnification, field of view = 72 mm

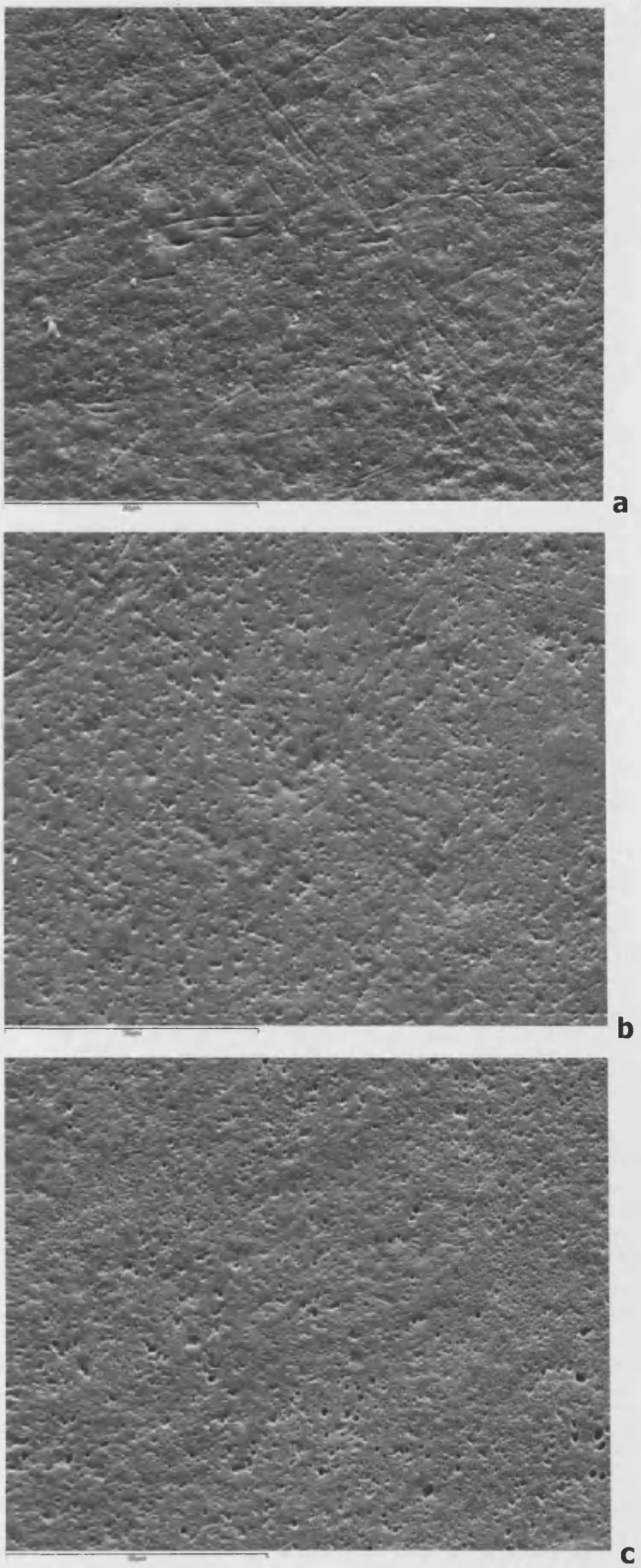

Figure 87 SEMs of unmodified LG30 cement (a – before immersion, b – after 48 hours, c – after 35 days) ×1600 magnification, field of view = 72 mm

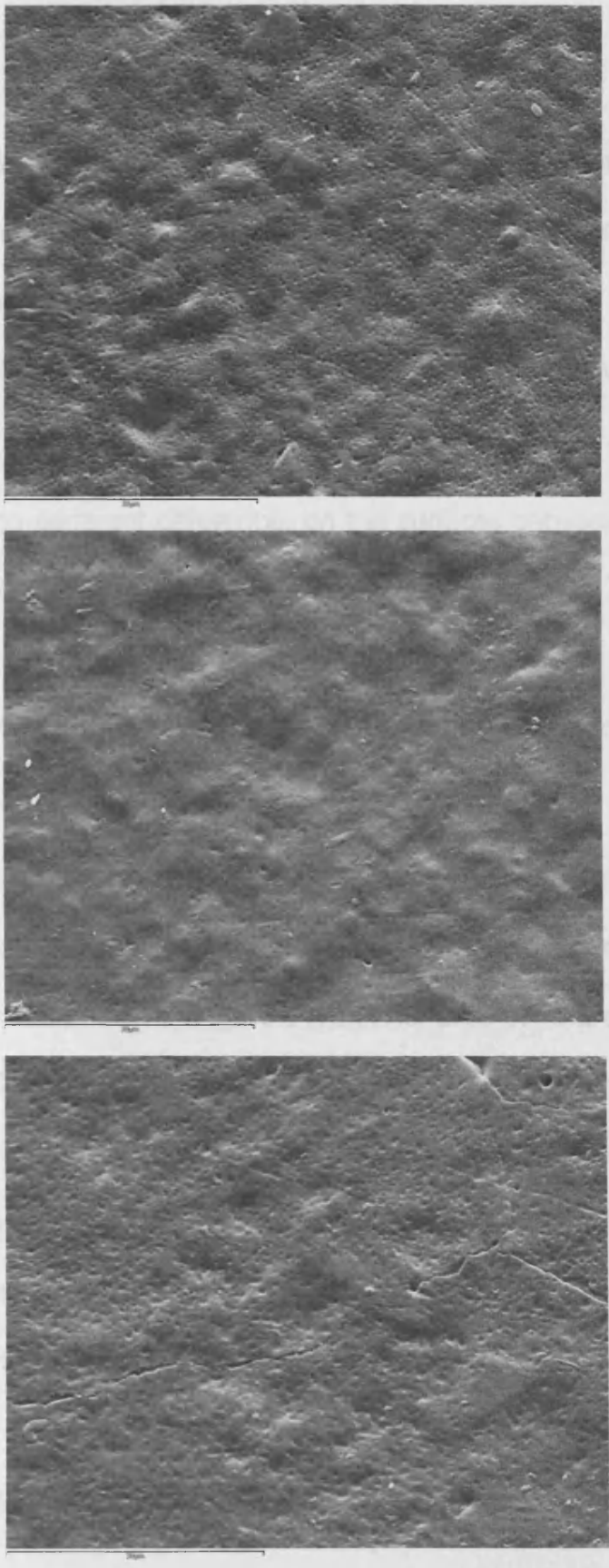

Figure 88 SEMs of unmodified LG26 cement (a – before immersion, b – after 48 hours, c – after 35 days) ×1600 magnification, field of view = 72 mm

5.4.5.2.2 Surfaces of modified cements

5.4.5.2.2.1 AH2

The surfaces of AH2 cement with 8.8% included CHA at time = 0 (pre-immersion), after 48 hours immersion and after 35 days immersion at x400 magnification are shown in Figure 89; and the surfaces of AH2 cement with 8.8% included CHA at time = 0 (pre-immersion), after 48 hours immersion and after 35 days immersion at x1600 magnification are shown in Figure 90.

There were no apparent differences on the surfaces between the AH2 cement with 8.8% included CHA at time = 0 (pre-immersion) and at 35 days as viewed at x400 and x1600 magnification. The cracks apparent on these surfaces as viewed at x400 and x1600 magnification were the same before immersion and after 35 days immersion.

The surfaces of AH2 cement with 4.4% included AHCl at time = 0 (pre-immersion), after 48 hours immersion and after 35 days immersion at x400 magnification are shown in Figure 91; the surfaces of AH2 cement with 4.4% included AHCl at time = 0 (pre-immersion), after 48 hours immersion and after 35 days immersion at x1600 magnification are shown in the Figure 92; the surfaces of AH2 cement with 8.8% included AHCl at time = 0 (pre-immersion), after 48 hours immersion and after 35 days immersion at x400 magnification are shown in Figure 93; and the surfaces of AH2 cement with 8.8% included AHCl at time = 0 (pre-immersion), after 48 hours immersion and after 35 days immersion at x1600 magnification are shown Figure 94.

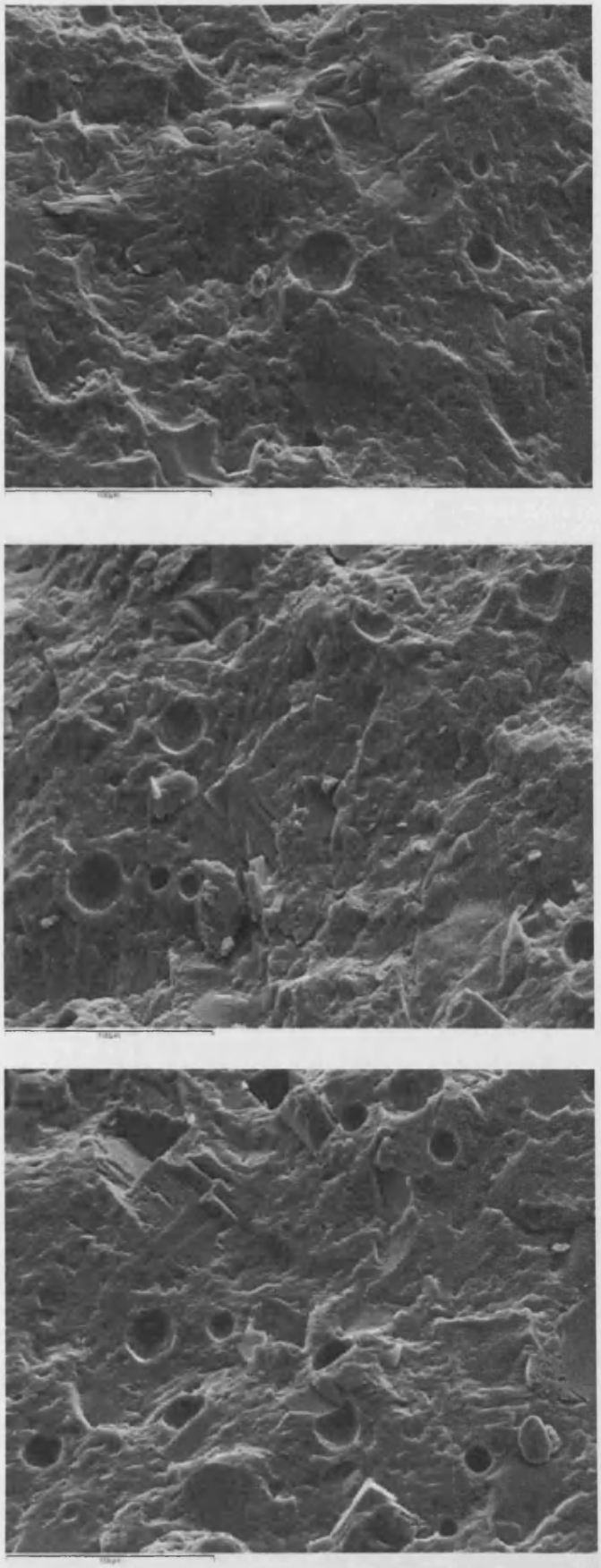

Figure 89 SEMs of AH2 cement containing 8.8% CHA (a - t=0, b - t=48 h, c - t=35 days) ×400 magnification, field of view = 284 μm

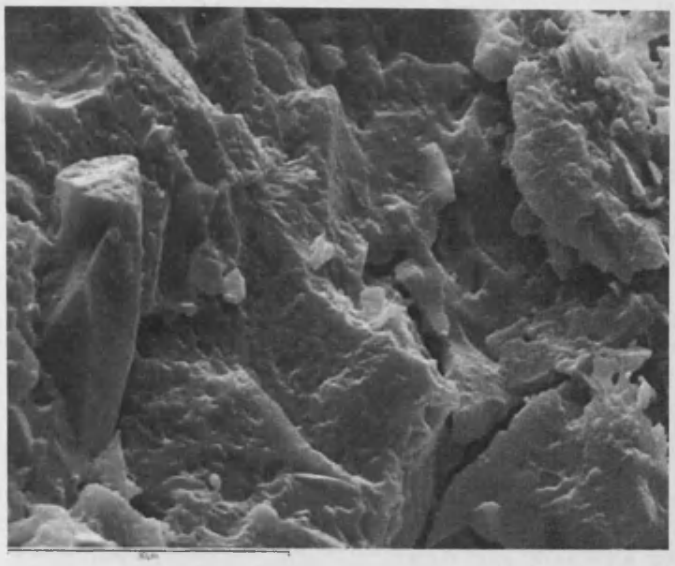

a

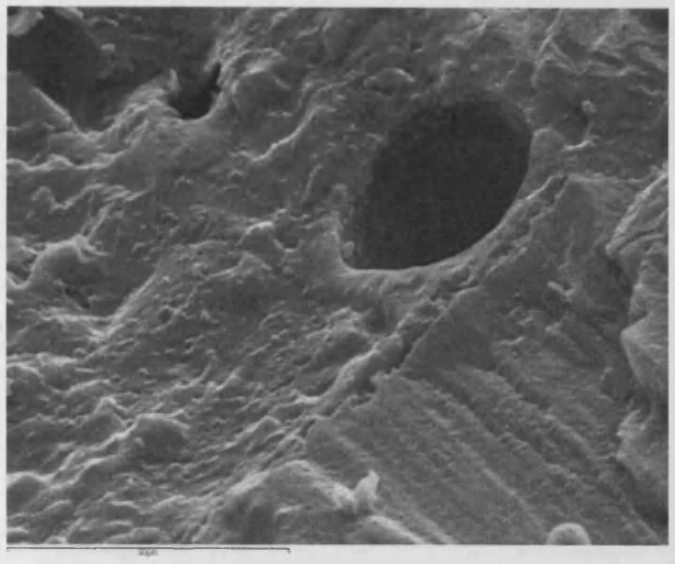

b

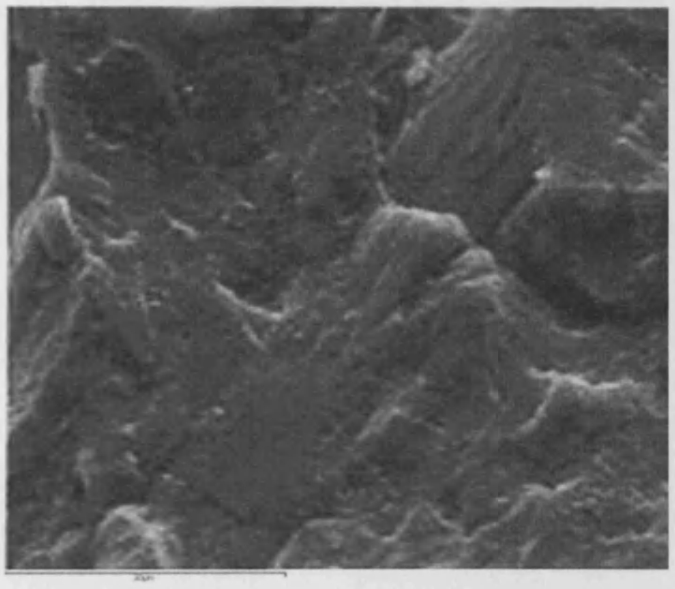

c

Figure 90 SEMs of AH2 cement containing 8.8% CHA (a - t=0, b - t=48 h, c - t=35 days) ×1600 magnification, field of view = 72 μm

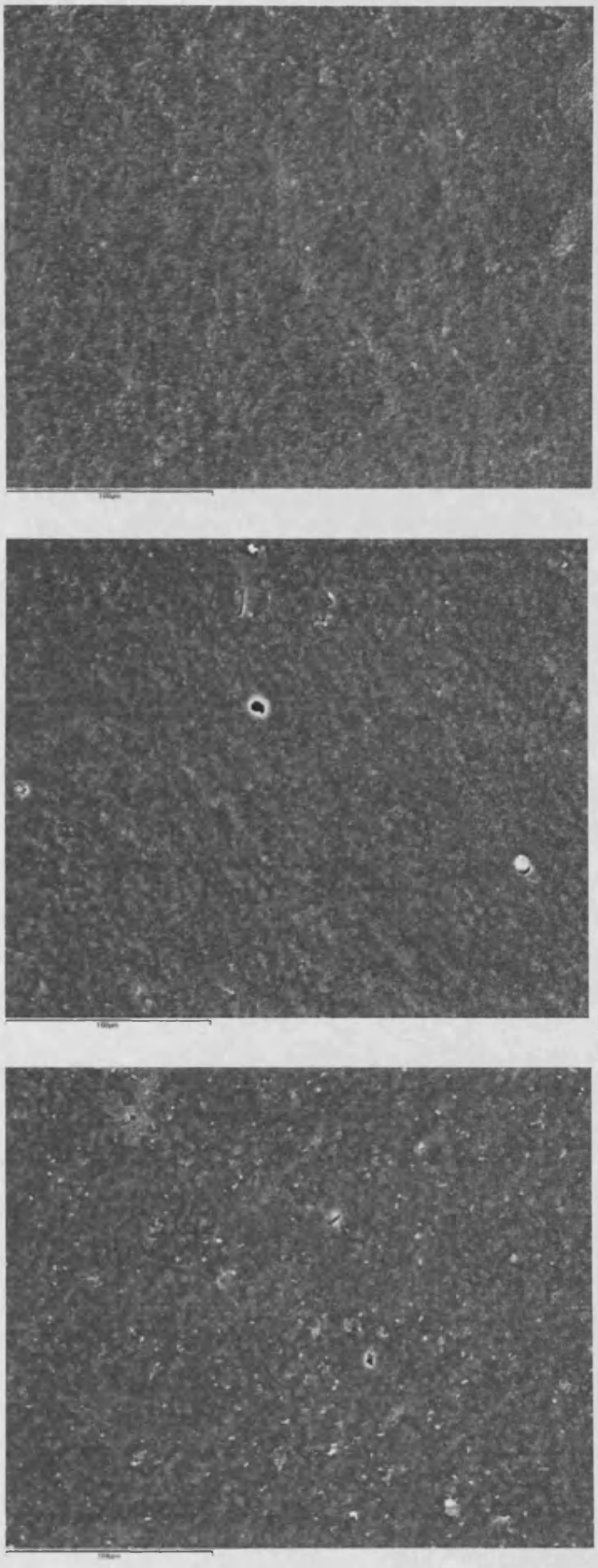

Figure 91 SEMs of AH2 cement containing 4.4% AHCl (a - t=0, b - t=48 h, c - t=35 days) ×400 magnification, field of view = 284 μm

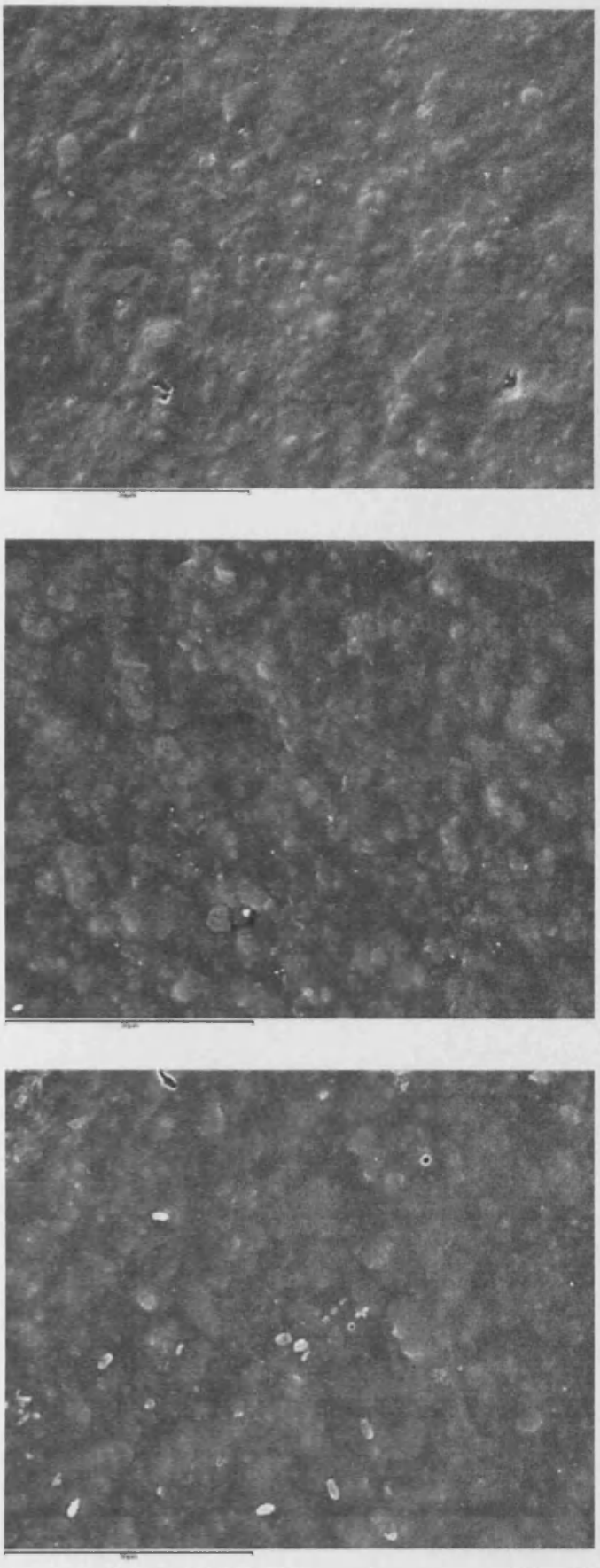

Figure 92 SEMs of AH2 cement containing 4.4% AHCl (a - t=0, b - t=48 h, c - t=35 days) ×1600 magnification, field of view = 72 μm

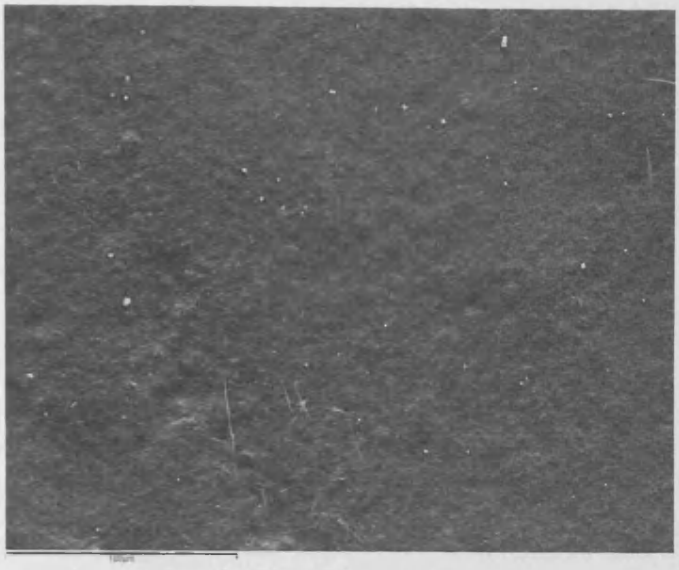

a

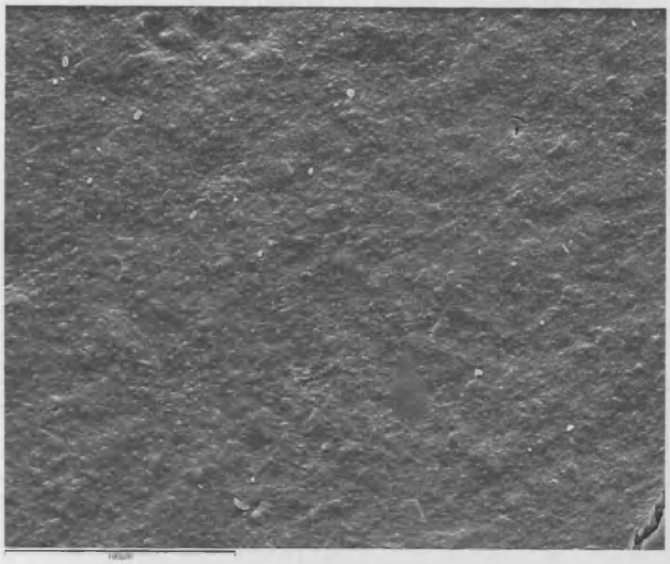

b

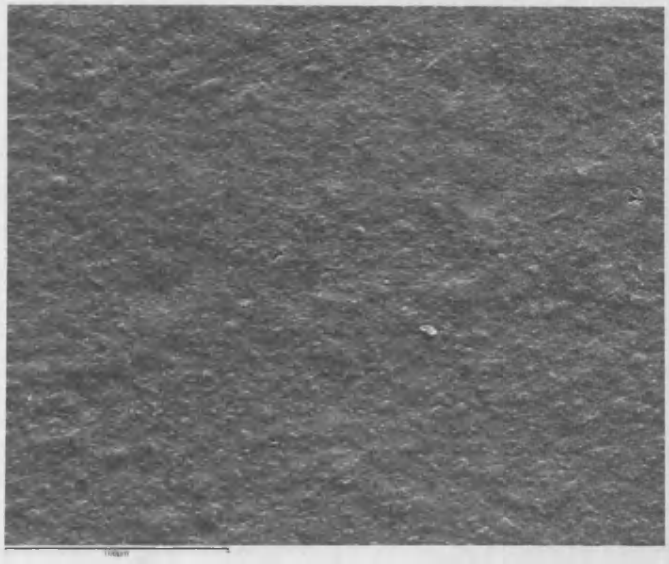

c

Figure 93 SEMs of AH2 cement containing 8.8% AHCl (a - t=0, b - t=48 h, c - t=35 days) ×400 magnification, field of view = 284 μm

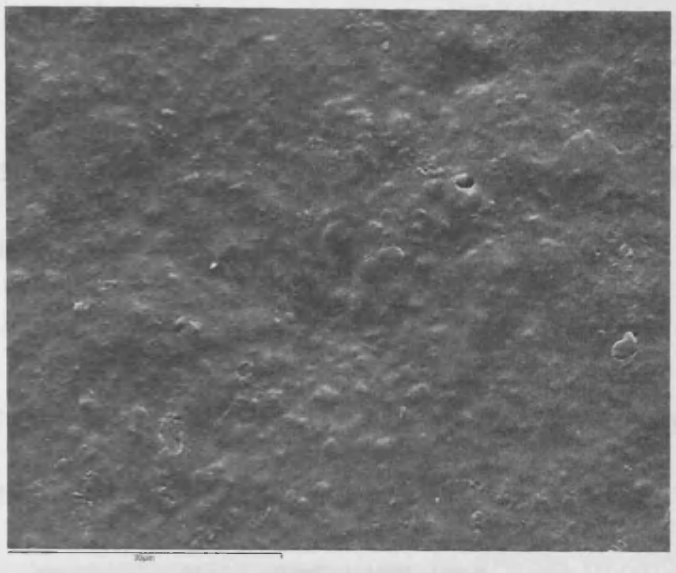

a

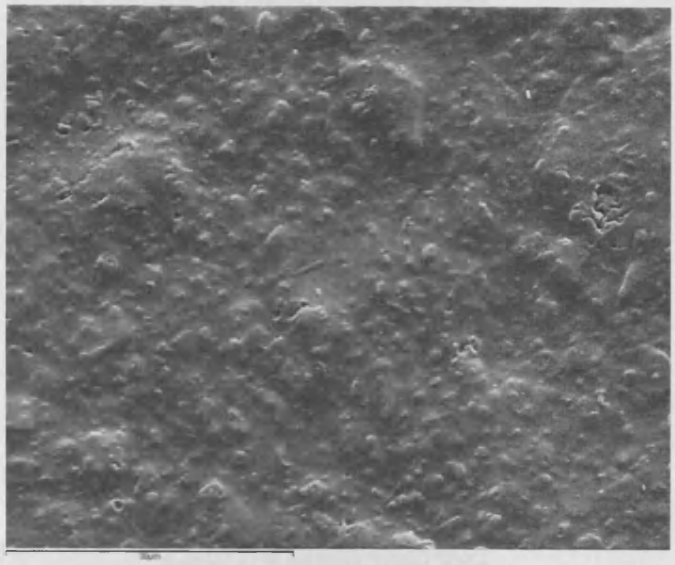

b

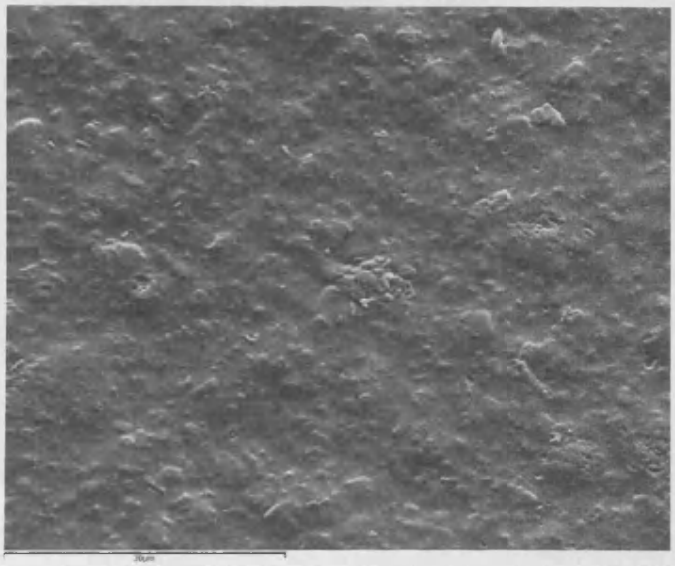

c

Figure 94 SEMs of AH2 cement containing 8.8% AHCl (a - t=0, b - t=48 h, c - t=35 days) ×1600 magnification, field of view = 72 μm

The specimens containing 8.8% AHCl that had been immersed for 35 days appeared rougher than those that were freshly prepared and those that had been immersed for 48 hours at both x400 magnification and at x1600 magnification.

5.4.5.2.2.2 MP4

The surfaces of MP4 cement with 8.8% included CHA at x100 magnification before immersion and after immersion for 35 days are shown in Figure 95.

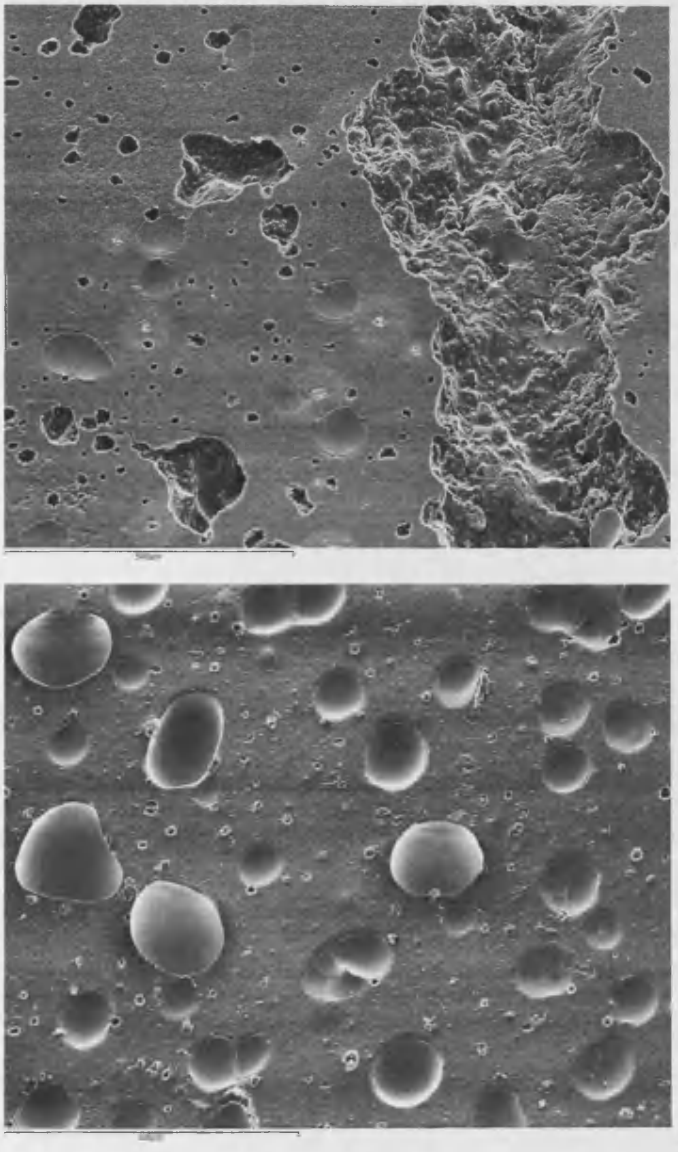

Figure 95 SEMs of MP4 cement containing 8.8% CHA (a – t=0, b – t=35 days) ×100 magnification, field of view = 1135 μm
note 'gully' to right hand side of 'a'

At x100 magnification specimen mixing problems are visible in the form of a 'gulley' to the right of the image and replication problems in the form of air blows. When viewed at x400 and x1600 magnification there were no apparent differences on the surfaces between the MP4 cement with 8.8% included CHA at time = 0 (pre-immersion) and at 35 days immersion.

The surfaces of MP4 cement with 8.8% included AHCl show no difference at x400 magnification before immersion and at 35 days immersion. The same surfaces at x1600 magnification are shown in Figure 96. The surfaces at pre-immersion and 48 hours immersion appeared similar. The surface of the MP4 cement immersed for 35 days appeared slightly disrupted compared to MP4 cement before immersion and after 48 hours immersion.

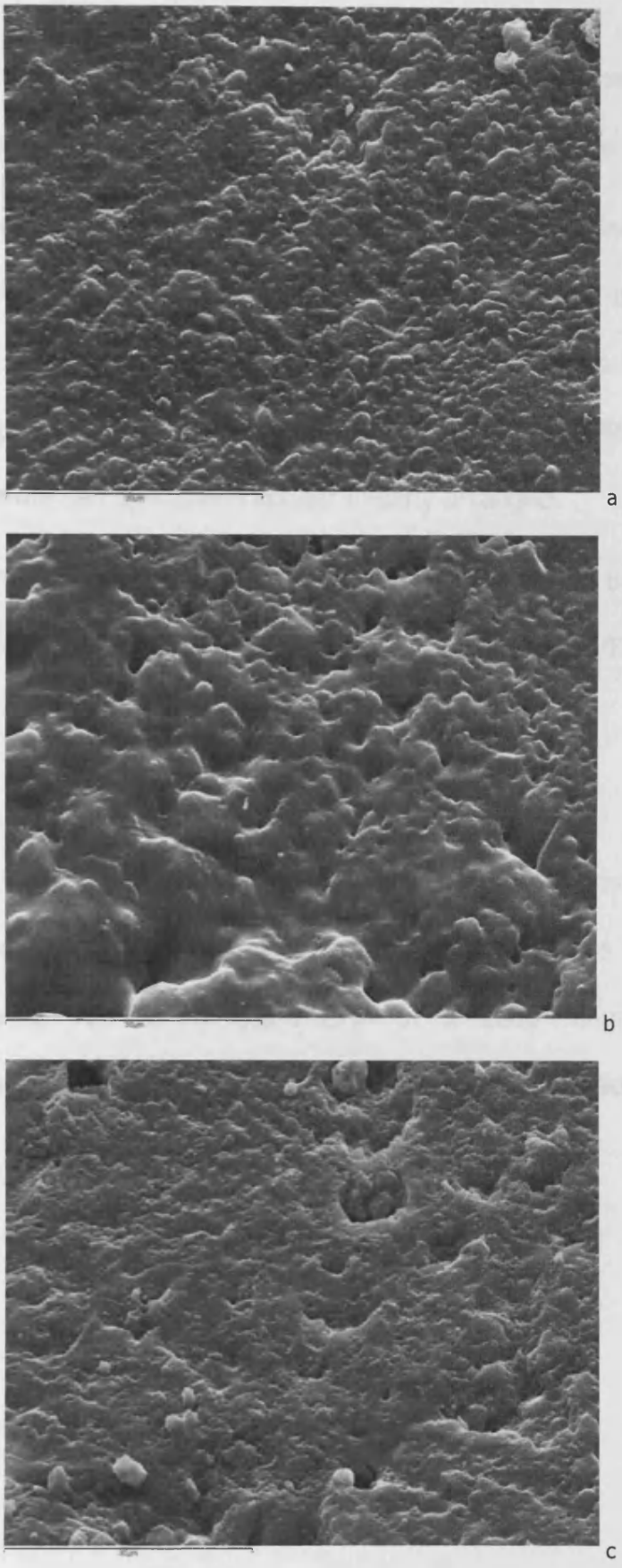

Figure 96 SEMs of MP4 cement containing 8.8% AHCl (a - t=0, b - t=48 h, c - t=35 days) ×1600 magnification, field of view = 72 μm

5.4.5.2.2.3 LG30

The surfaces of LG30 cement containing 8.8% CHA before immersion and after 35 days immersion at x1600 magnification are shown in Figure 97.

The un-immersed specimen appeared slightly rougher than the specimen immersed for 35 days. The specimens all had smooth and rough regions on them as can be seen for the two micrographs for specimens immersed for 48 hours. The pits visible at x1600 magnification on both the 48 hour immersed and 35 day immersed specimens appear linearly arranged.

There were no differences between LG30 cement containing 8.8% AHCl before immersion and after 35 days immersion at both x400 and x1600 magnification.

5.4.5.2.2.4 LG26

The surfaces of LG26 cement containing 8.8% CHA before immersion and after 35 days immersion at X400 magnification are shown in Figure 98. The surfaces of LG26 cement containing 8.8% CHA at x 1600 magnification before immersion, after 48 hours immersion and 35 days immersion are shown in Figure 99 .

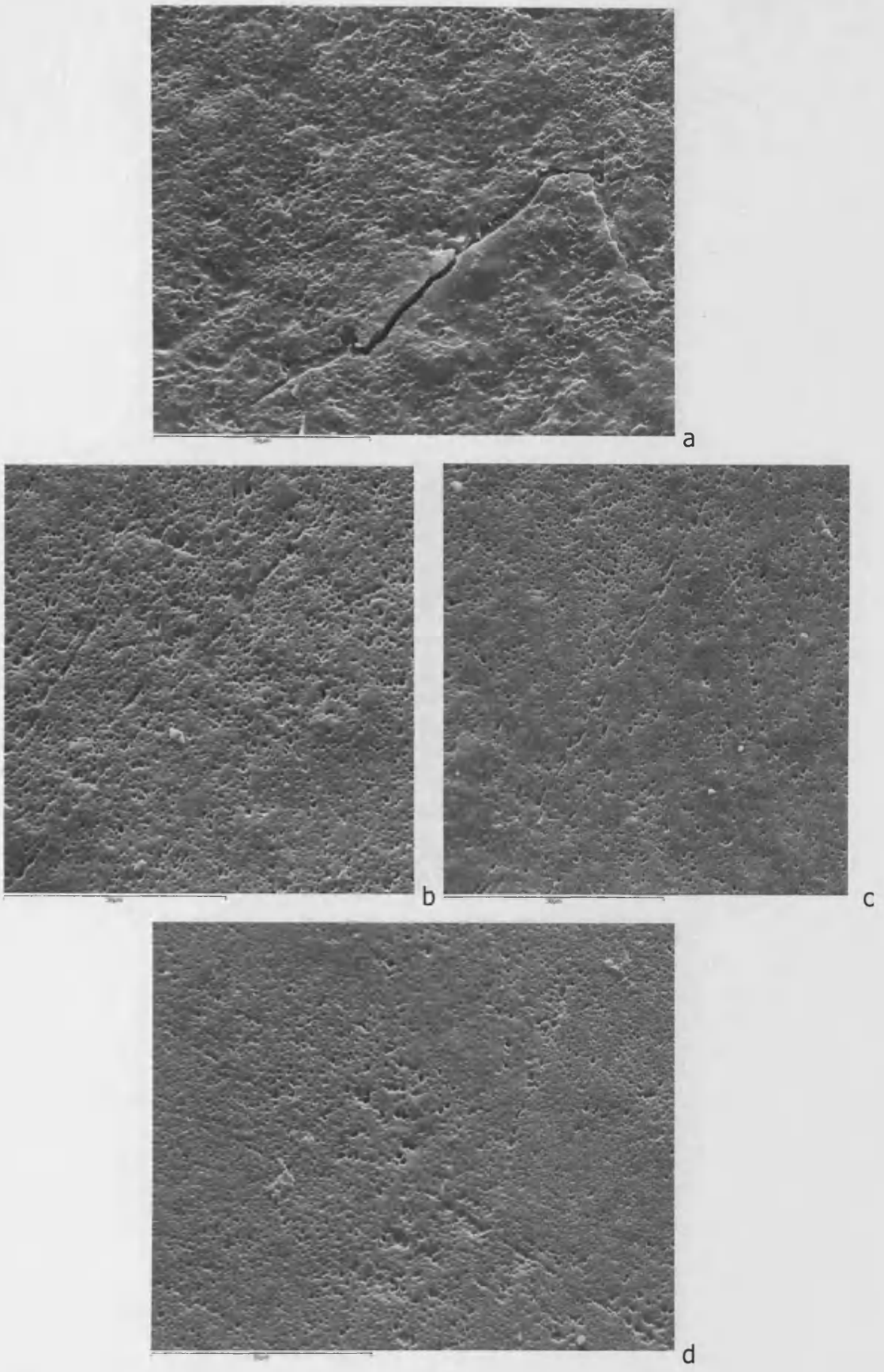

Figure 97 SEMs of LG30 cement containing 8.8% CHA (a – t=0, b,c – t=48 hours, d – t=35 days) ×1600 magnification, field of view = 72 μm

n.b. b and c are the same magnification but have been cropped

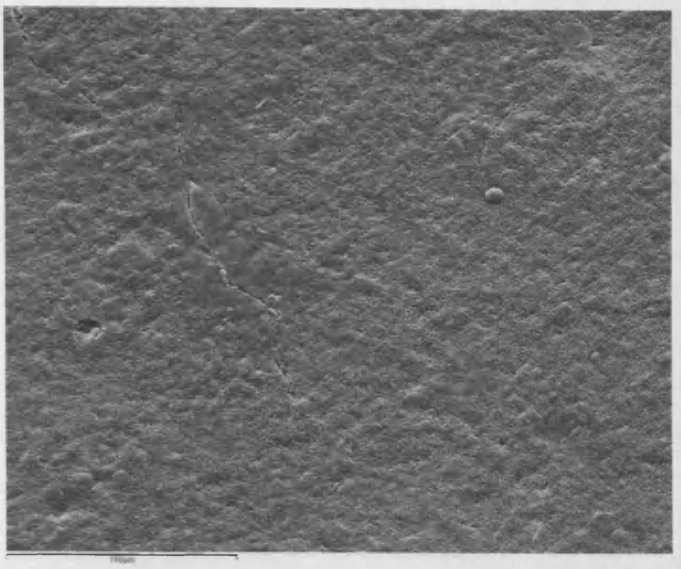

a

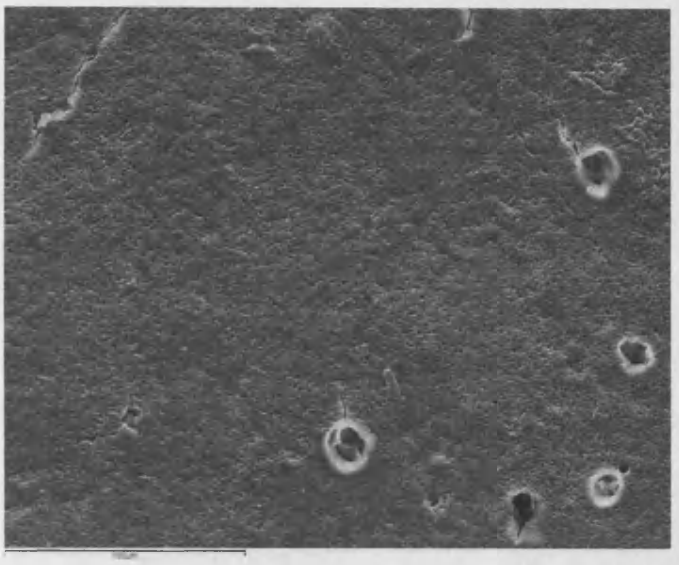

b

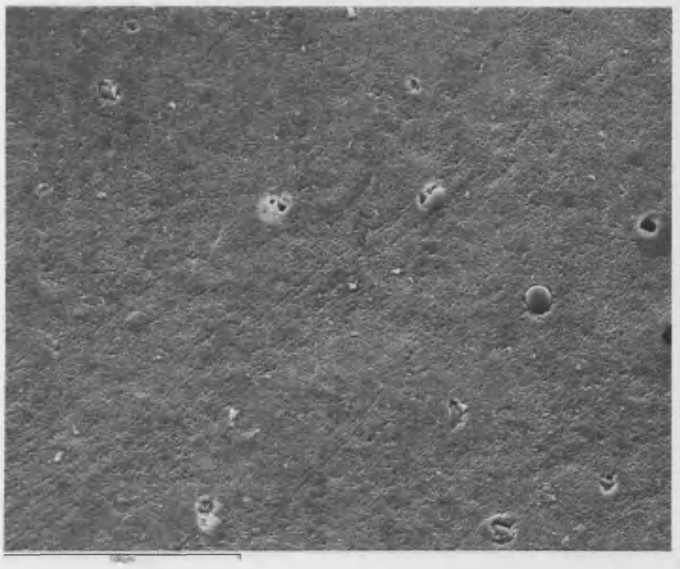

c

Figure 98 SEMs of LG26 cement containing 8.8% CHA (a – t=0, b – t=48 hours, c – t=35 days) ×400 magnification, field of view = 284 μm

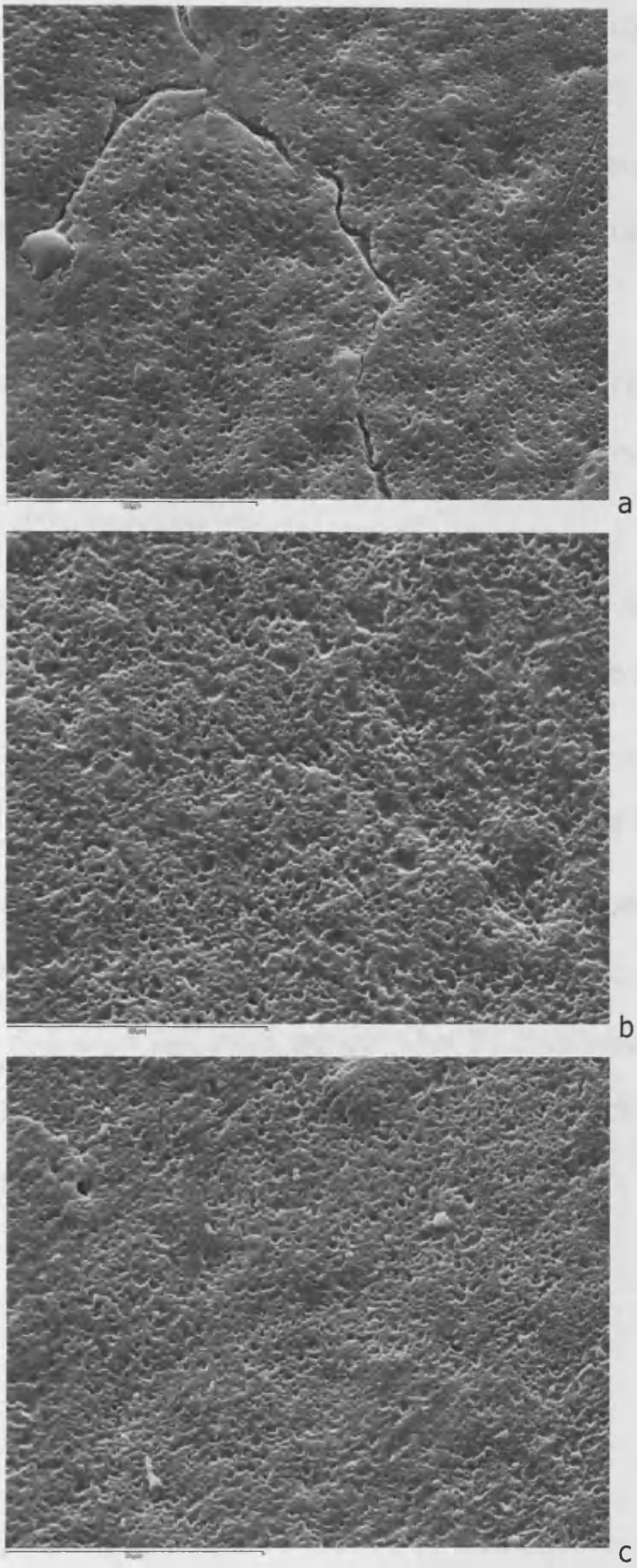

Figure 99 SEMs of LG26 cement containing 8.8% CHA (a - t=0, b - t=48 h, c - t=35 days) ×1600 magnification, field of view = 72 μm

There was no observable difference between the two sets of specimens at x400 magnification apart from shallow cracks that were observed in the unimmersed specimens. At x1600 magnification the pitting on the surface present in the unimmersed specimens became more prominent in the specimens immersed for 48 hours.

There were no differences observed in the surfaces of LG26 cement containing 8.8% AHCl before immersion, after 48 hours immersion and after 35 days immersion at x400 magnification.

The surfaces of LG26 cement containing 4.4% AHCl before immersion, at 48 hours and 35 days at x1600 magnification are shown in Figure 100.

The surfaces of LG26 cement containing 8.8% AHCl before immersion, at 48 hours and 35 days at x1600 magnification are shown in Figure 101.

For the cement containing 8.8% AHCl , at x1600 magnification there was a slight difference between the un-immersed cement and that immersed for 48 hours. This difference was more marked after 35 days where pitting of the surface was observed. There was no difference between differing immersions for LG6 cement containing 4.4% AHCl

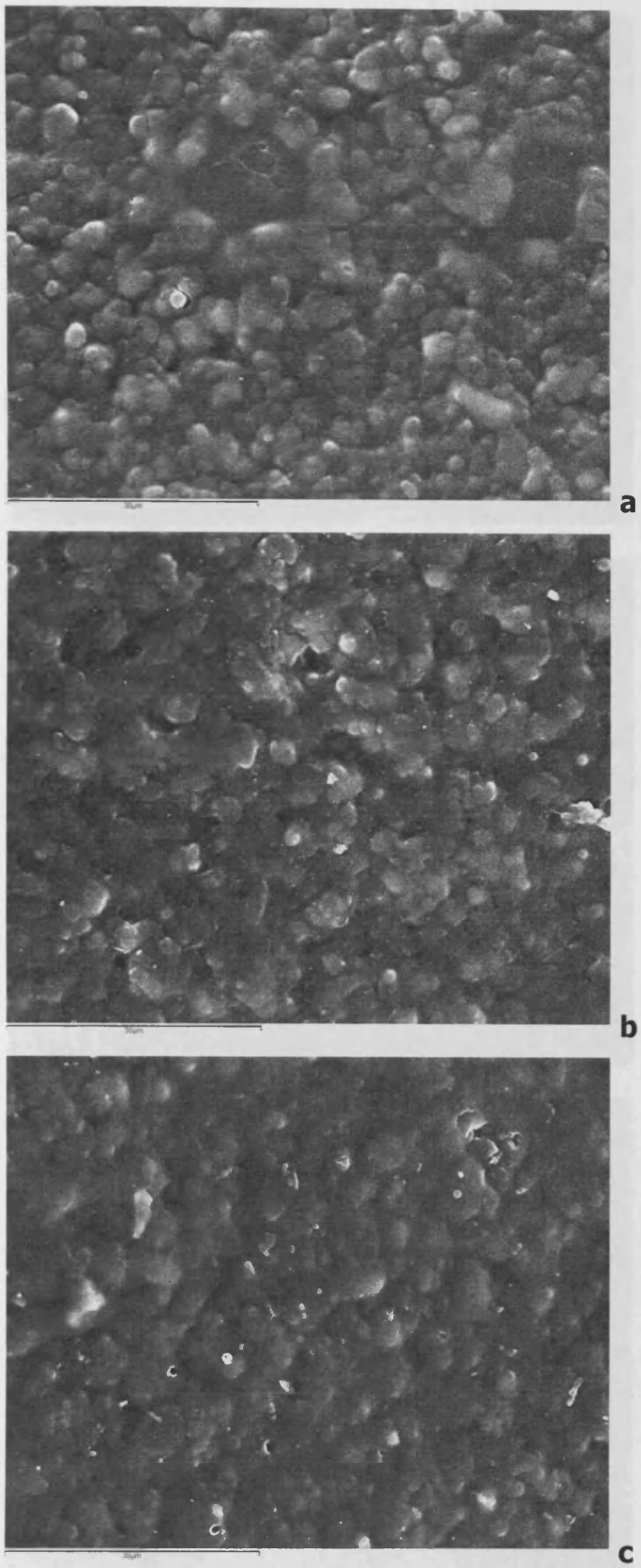

Figure 100 SEMs of LG26 cement containing 4.4% AHCl (a – t=0, b – t=48 h, c – t=35 days) ×1600 magnification, field of view = 72 μm

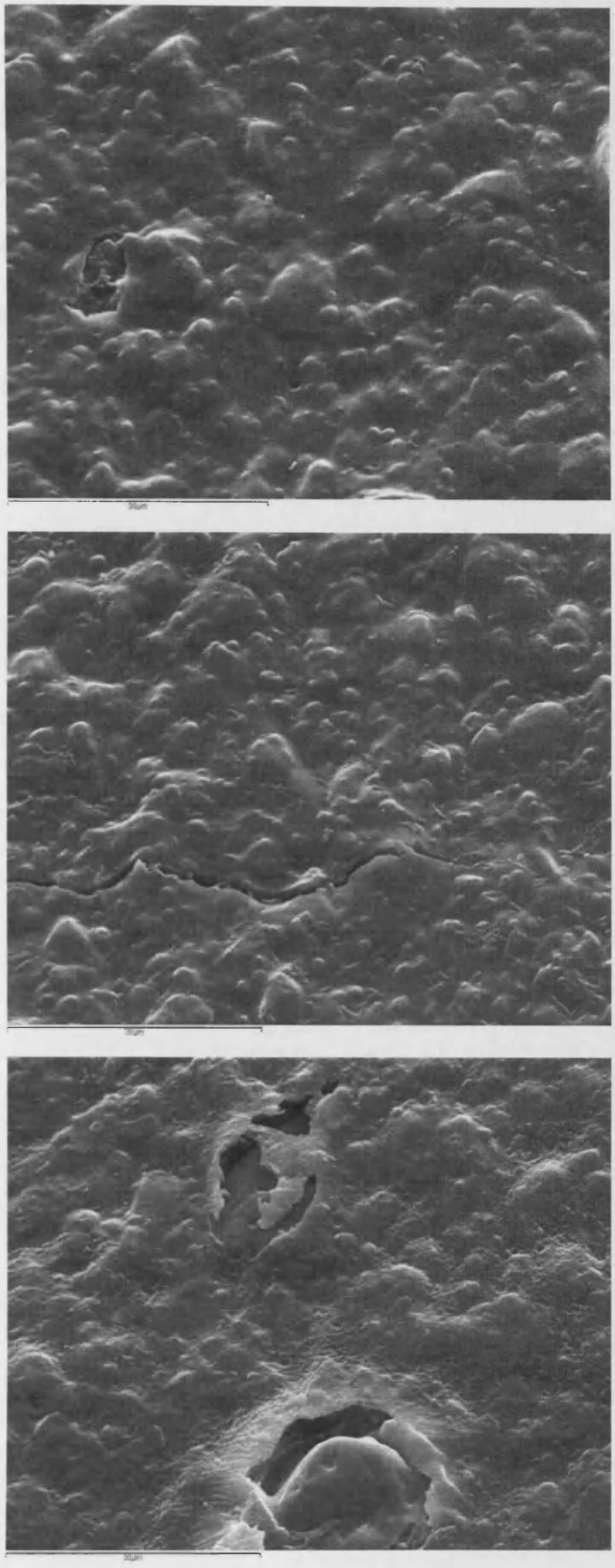

Figure 101 SEMs of LG26 cement containing 8.8% AHCl (a – t=0, b – t=48 h, c – t=35 days) ×1600 magnification, field of view = 72 μm

5.4.5.2.3 Cross-sections

There were no apparent differences for each GIC at each level of inclusion before immersion, after 48 hours immersion and 35 days immersion at both ×400 and ×1600 magnification. To illustrate this, the fracture surfaces of AH2 cement containing 8.8% AHCl before immersion, after 48 hours immersion and 35 days immersion at ×400 magnification and ×1600 magnification are shown in Figure 102 and Figure 103.

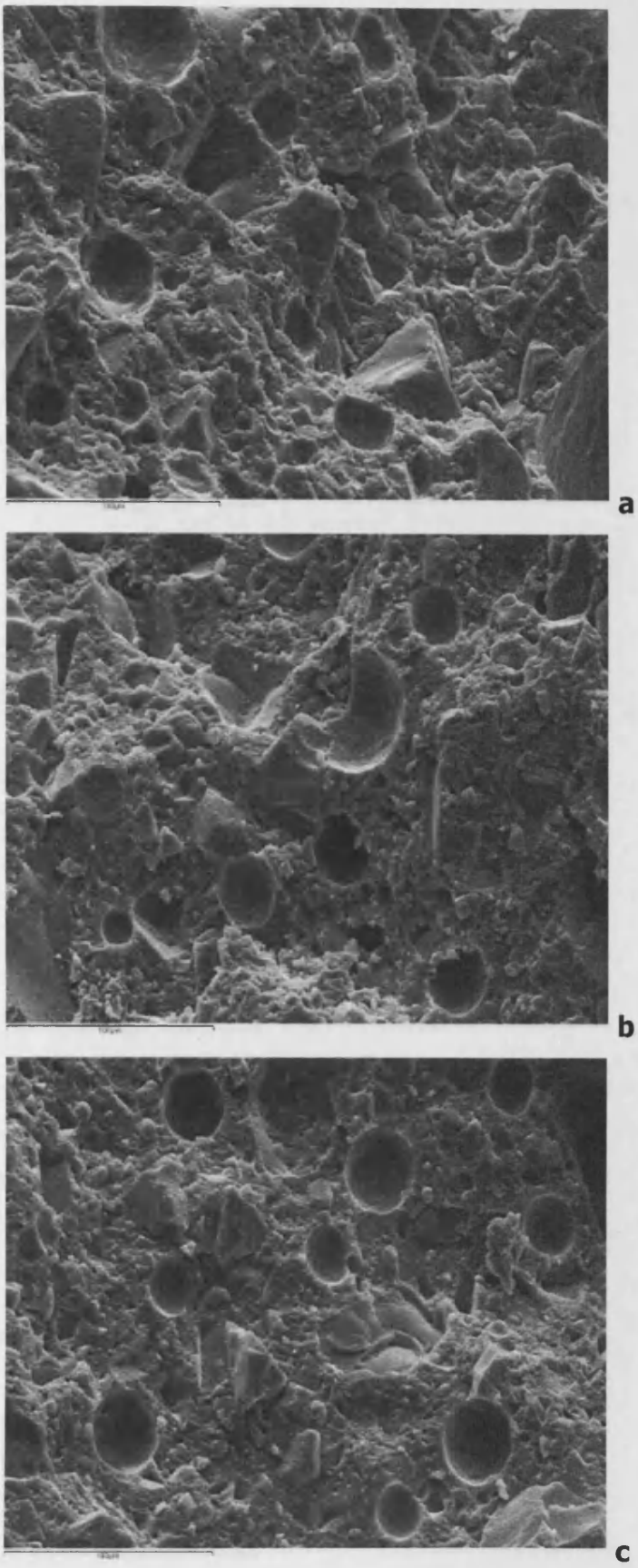

Figure 102 SEMs of AH2 cement fracture surfaces containing 8.8% AHCl (a – t=0, b – t=48 h, c – t=35 days) ×400 magnification, field of view = 284 μm

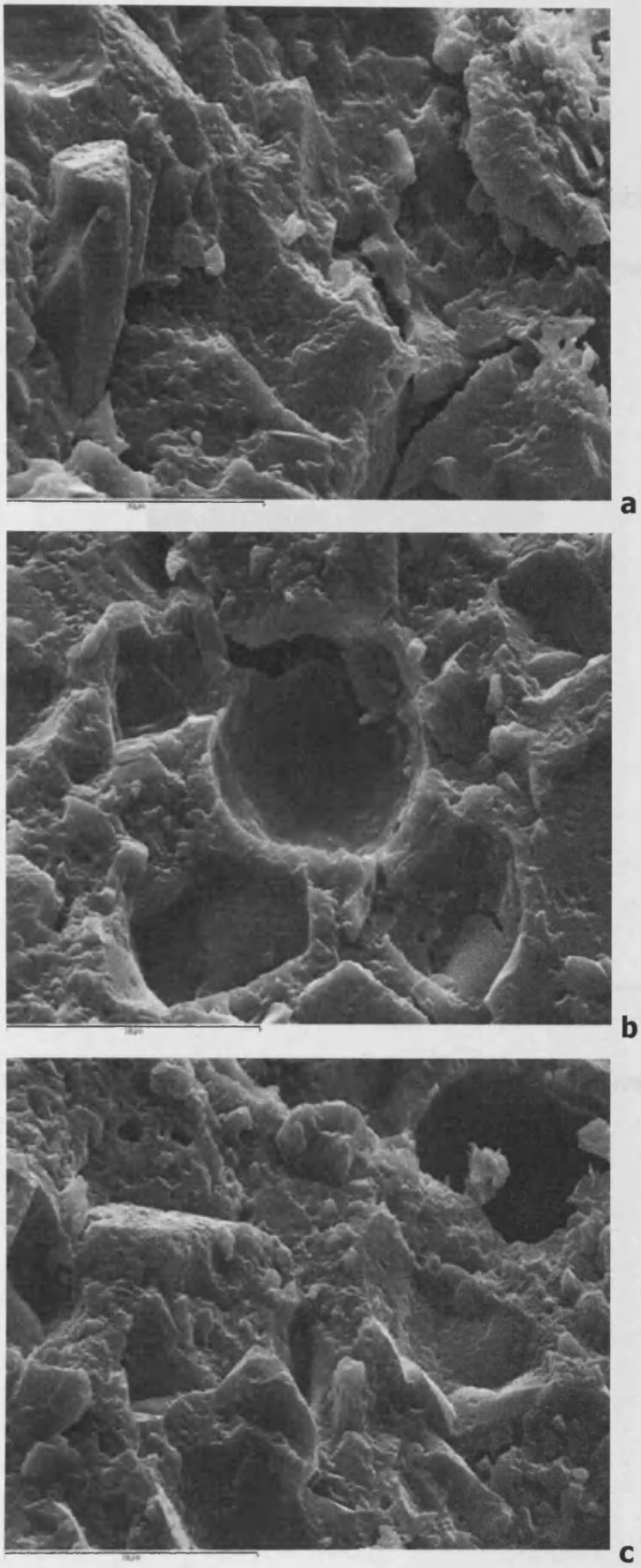

Figure 103 SEMs of AH2 cement fracture surfaces containing 8.8% AHCl (a – t=0, b – t=48 h, c – t=35 days) ×1600 magnification, field of view = 72 μm

5.4.5.3 Elemental analysis

5.4.5.3.1 Identification of peaks

The images of AHCl particles and CHA powder particles on black adhesive stubs together with the EDX spectra from typical particles are shown in Figures 47 and 48.

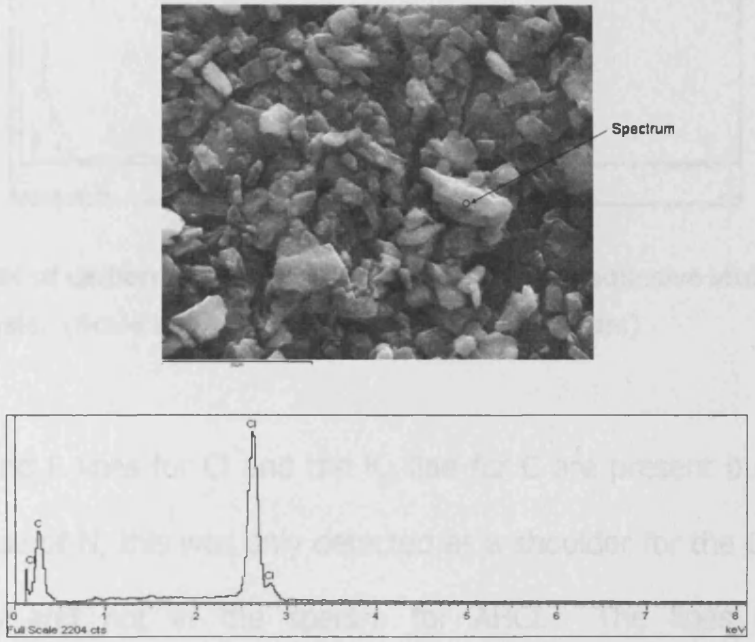

Figure 104 SEM of carbon coated AHCl particles on a black adhesive stub with spectral analysis. (Scale bar = 20 µm, field of view = 57 µm)

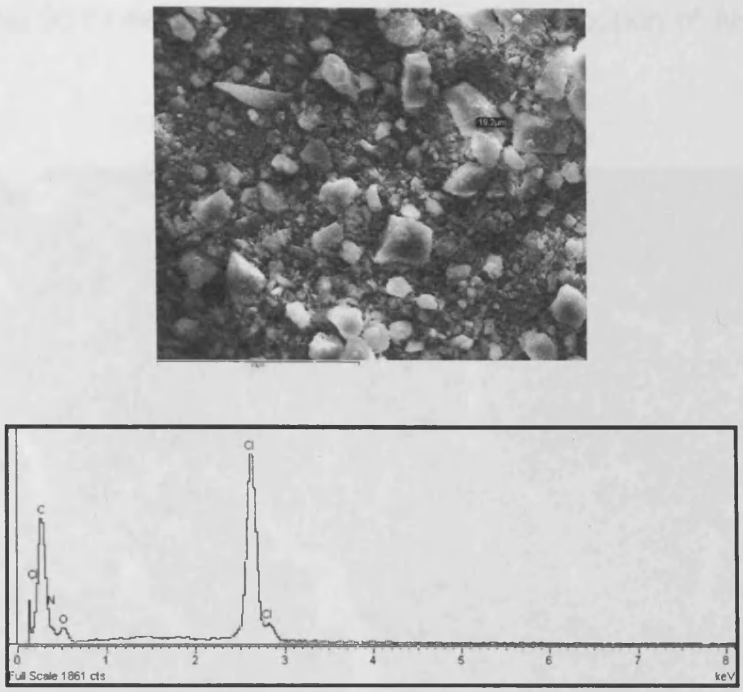

Figure 105 SEM of carbon coated CHA particles on a black adhesive stub with spectral analysis. (Scale bar = 90 µm, field of view = 260 µm)

The K_α, K_β and L lines for Cl and the K_α line for C are present but due to the weak response of N, this was only detected as a shoulder for the C peak in the CHA spectra and not in the spectra for AHCl. The lines for Cl were subsequently used for analysis.

The image of CHA particles on adhesive carbon stubs gave an indication of the particle distribution which is generally 10 – 20 microns. The image of AHCl particles on an adhesive carbon stub gave an indication that the particle size was generally 5 microns or less with an occasional 10 micron particle.

5.4.5.3.2 Surfaces

A magnification surface view of a newly prepared specimen containing 8.8% AHCl is shown in Figure 106 and an elemental analysis of the five spots is

shown in Table 50 to determine the evenness of distribution of AHCl within the set cement.

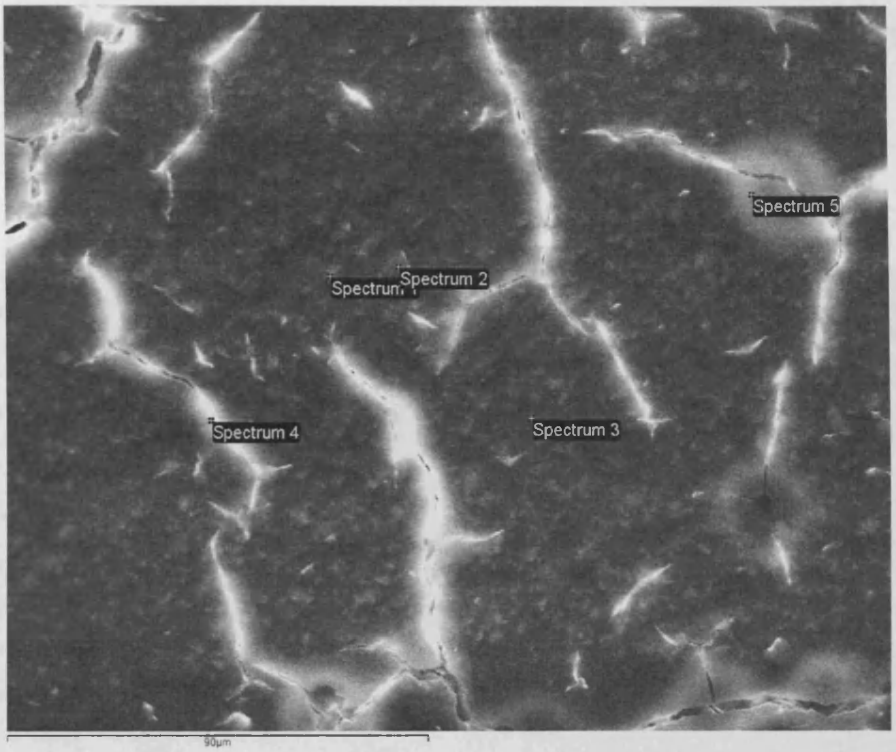

Figure 106 SEM of a carbon coated newly prepared AH2 cement containing 8.8% AHCl with the five spots marked where the spectra were taken from. (Scale bar = 90 µm, field of view = 190 µm)

	Site	O	F	Na	Al	Si	P	Cl	Ca	Total
Spectrum 1	Matrix	34.9	18.8	4.6	13.8	16.8	1.6	4.3	5.2	100.0
Spectrum 2	Matrix	29.7	12.2	2.7	14.3	15.9	1.5	12.0	11.6	99.9
Spectrum 3	Matrix	39.0	27.8	5.0	9.3	5.4	0.8	6.6	6.0	99.9
Spectrum 4	Crack	28.4	7.1	2.8	15.0	24.0	2.0	7.5	13.3	100.1
Spectrum 5	Hollow	46.3	-	2.4	12.0	18.1	1.8	11.0	8.5	100.1

Table 50 Elemental analysis of the five spots in Figure 106 / weight %

The above table shows that AHCl was not evenly distributed throughout the cement. There were, however, no regions in which AHCl alone was found.

5.4.5.3.3 Cross-sections

A cross-sectional low magnification view of an un-leached specimen containing 8.8% AHCl is shown in Figure 107 and an elemental analysis of the three marked areas in Table 51.

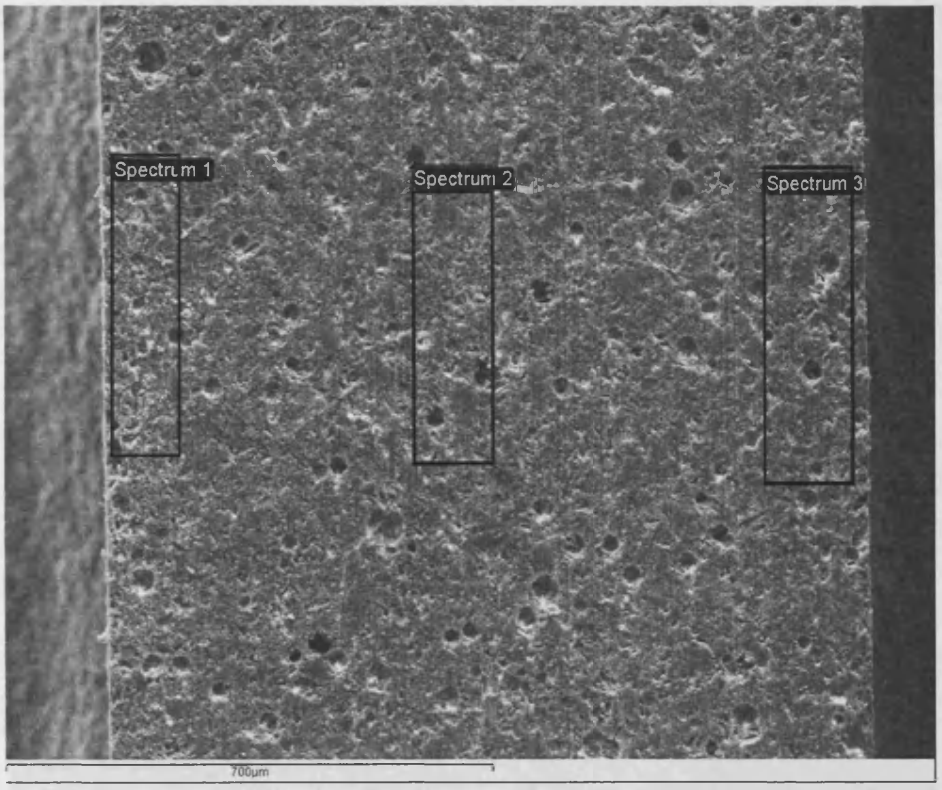

Figure 107 SEM of a carbon coated newly prepared AH2 cement containing 8.8% AHCl with the three areas shown where the spectra were taken from. (Scale bar = 700 µm, field of view = 1350 µm)

The spectra, in each case, were taken from the whole of each marked area.

As in the leached specimen, the usual cracks caused by drying under vacuum are present and air bubbles caused by mixing are also present. Unlike the leached specimen (Figure 108) there are no large cracks.

	Region	O	F	Na	Al	Si	P	Cl	Ca	Total
Spectrum 1	Edge	38.3	17.3	4.0	13.0	16.6	1.8	1.8	7.3	100.1
Spectrum 2	Centre	38.5	17.9	4.1	12.8	17.1	1.5	1.5	6.6	100.0
Spectrum 3	Edge	39.0	15.9	4.1	13.1	17.1	1.6	2.6	6.7	100.1

Table 51 Elemental analysis of the three marked regions in Figure 107 / weight %

Cl was detected in all three areas in the range 1.5 – 2.6 weight % showing fairly even distribution. There was no evidence of clumping in the cement.

A cross-sectional view of a leached specimen originally containing 8.8% AHCl is shown in Figure 108.

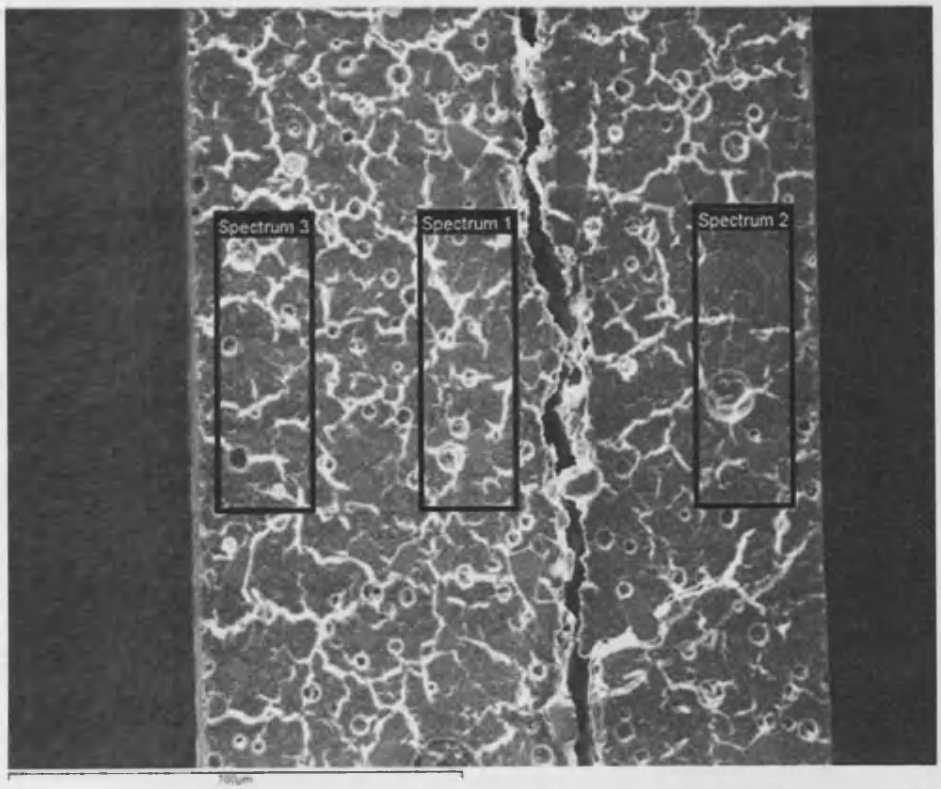

Figure 108 SEM of a carbon coated leached AH2 cement containing 8.8% AHCl with the three areas shown where the spectra were taken from. (Scale bar = 700 µm, field of view = 1430 µm)

The usual cracks caused by drying under vacuum are present and air bubbles caused by mixing are also present. The image shows a large crack through the centre of the specimen. The three rectangles are the areas from which the three spectra were taken, the results of which are in Table 52.

	O	F	Na	Al	Si	P	Ca	Total
Spectrum 1	44.0	15.1	2.1	12.8	17.5	1.7	6.8	100.0
Spectrum 2	44.6	14.2	2.6	13.1	18.2	1.5	5.8	100.0
Spectrum 3	44.7	13.1	2.3	13.1	18.9	1.5	6.5	100.1

Table 52 Elemental analysis of the marked regions in Figure 108 / weight %

The presence of Cl was not detected in any of the three areas examined. From the release data, 74% of the AHCl that was incorporated in the specimen had been released at the end of the release experiment meaning that 2.3% (w/w) of the specimen contained AHCl, of which a small amount (22.5%) was Cl (0.52% of specimen).

Spot readings were taken at ten different locations to determine the preferred binding sites of AHCl (Figure 109) and their elemental analysis is described in Table 53.

Of the two locations within the matrix, Cl was only detected in a small amount in location five.

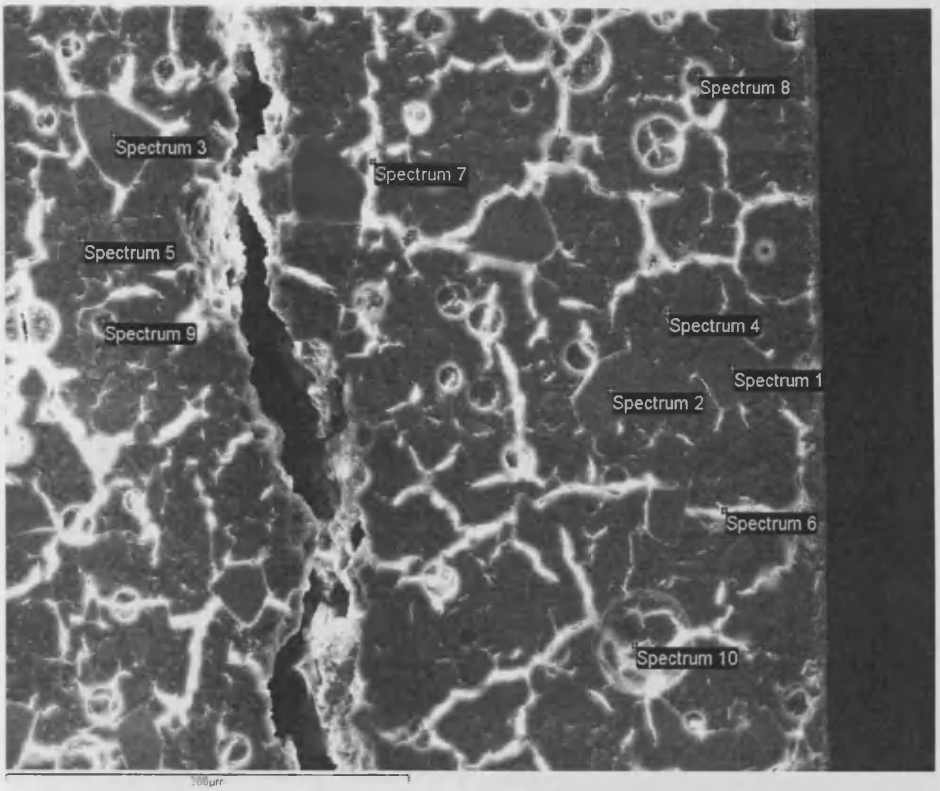

Figure 109 SEM of a carbon coated leached AH2 cement containing 8.8% AHCl with the ten spots shown where the spectra were taken from. (Scale bar = 300 µm, field of view = 690 µm)

	Site	O	F	Na	Al	Si	P	Cl	Ca	Total
Spectrum 1	Glass	36.1	21.0	4.5	14.1	16.7	1.4	-	6.3	100.1
Spectrum 2	Glass	36.6	19.8	4.5	14.5	17.1	1.3	-	6.3	100.1
Spectrum 3	Glass	36.2	20.9	4.7	13.9	16.5	1.3	-	6.5	100.0
Spectrum 4	Matrix	36.5	20.5	4.3	13.8	17.4	1.6	-	5.9	100.0
Spectrum 5	Matrix	45.3	10.8	-	11.8	22.5	1.6	0.1	8.0	100.1
Spectrum 6	Crack	45.1	9.9	1.2	10.9	26.3	1.7	-	4.9	100.0
Spectrum 7	Crack	41.5	13.3	-	16.6	15.0	2.3	-	11.3	100.0
Spectrum 8	Hole	46.5	-	-	5.2	7.5		-	40.8	100.0
Spectrum 9	Hole	-	-	-	14.8	21.6		-	63.7	100.1
Spectrum 10	Hole	41.5	9.6	-	12.4	20.7	2.4	-	13.4	100.0

Table 53 Elemental analysis of the ten spots in Figure 109 /weight %

Cross-sectional low magnification views of a newly prepared specimen containing 11.3% CHA followed by its elemental analysis and a leached specimen originally containing 11.3% CHA along with its elemental analysis are shown in the following two figures and associated tables below.

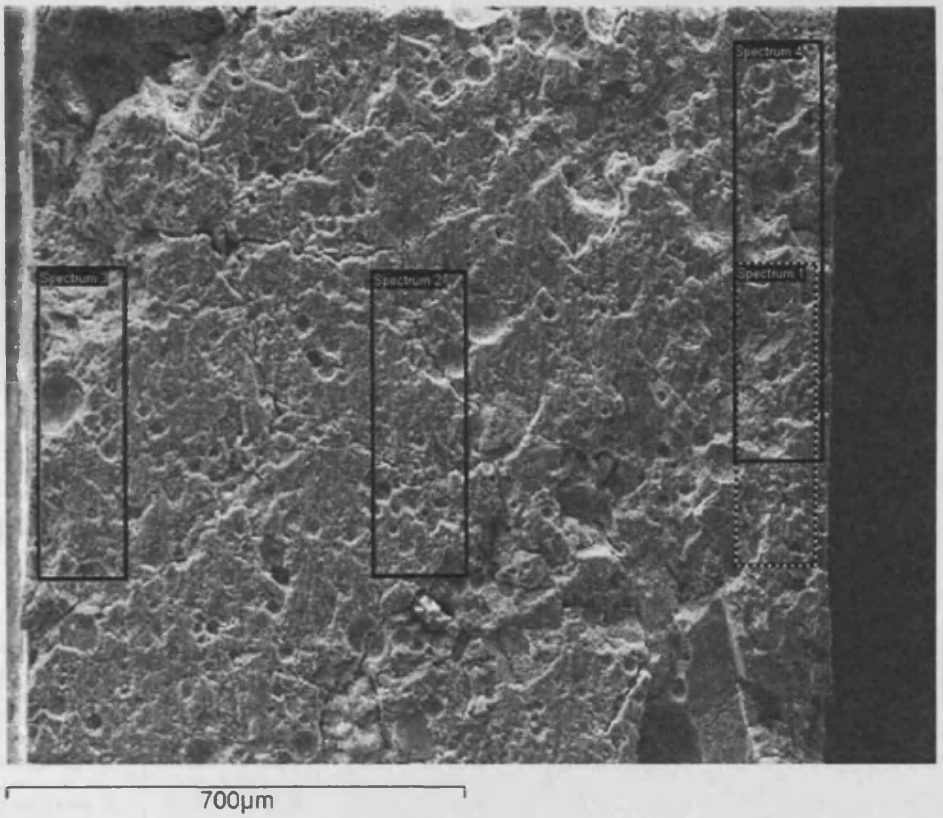

Figure 110 SEM of a carbon coated newly prepared AH2 cement containing 11.3% CHA. (Scale bar = 700 µm, field of view = 1410 µm)

Spectrum	O	F	Na	Al	Si	P	S	Cl	Ca	Total
Spectrum 1	40.0	16.7	3.7	11.8	14.9	1.2	0.7	4.2	6.8	100.0
Spectrum 2	40.4	18.8	4.4	12.3	15.4	1.4	-	1.2	6.3	100.2
Spectrum 3	41.5	16.0	4.6	12.6	15.9	1.4	-	2.2	5.8	100.0
Spectrum 4	42.5	16.7	4.4	11.5	13.7	1.3	-	4.1	5.9	100.1
Average	41.1	17.0	4.3	12.0	15.0	1.3	0.2	2.9	6.2	100.0

Table 54 Elemental analysis of the marked regions in Figure 110 / weight %

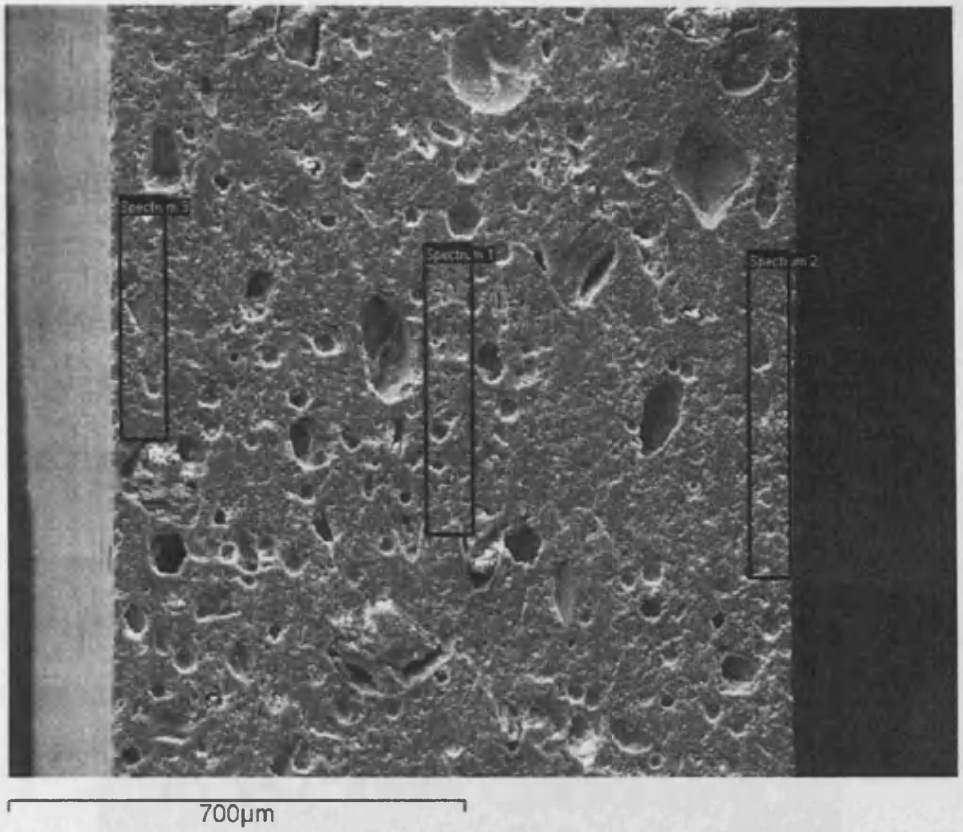

Figure 111 SEM of a carbon coated leached AH2 cement originally containing 11.3% CHA. (Scale bar = 700 µm, field of view = 1450 µm)

Spectrum	O	F	Na	Al	Si	P	Cl	Ca	Total
Spectrum 1	39.8	16.9	3.2	13.1	17.0	1.4	2.0	6.6	100
Spectrum 2	41.2	15.1	3.4	13.9	16.8	1.6	1.8	6.1	100
Spectrum 3	39.2	15.6	3.1	13.7	17.3	1.7	2.7	6.7	100
Average	40.1	15.9	3.2	13.6	17.0	1.6	2.2	6.5	100

Table 55 Elemental analysis of the marked regions in Figure 111/ weight %

The spectra for both leached and un-leached specimens were similar in that the Cl peaks varied in intensity through the specimen. This variation was probably due to particles of CHA embedded in the cement that remained undissolved (Figure 112) which may or may not have been included in the selected scan area. In Figure 111 there are many irregular shaped holes, different to the circular ones formed by air bubbles, that might have been where CHA particles

were embedded but that were plucked out during the grinding and polishing process. Spectra were taken of three areas of a leached specimen as shown in Figure 112 and the elemental breakdown is shown in Table 56. There was significant variability within the individual specimens at higher magnifications.

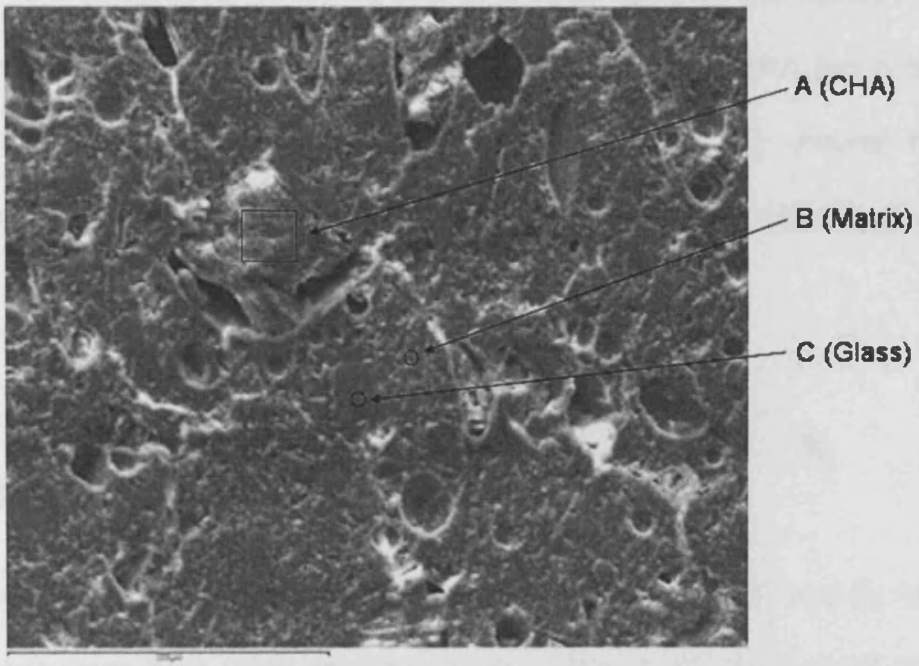

Figure 112 SEM of a leached AH2 cement originally containing 11.3% CHA. (Scale bar = 300 µm, field of view = 695 µm) The areas A, B and C were identified as being CHA, matrix and glass respectively.

	N	O	F	Na	Al	Si	P	Cl	Ca	Total
A CHA	31.9	33.1	-	-	-	-	-	35.0	-	100.0
B Matrix	-	41.3	17.0	2.5	12.3	17.9	1.6	1.4	6.1	100.1
C Glass	-	35.0	21.4	4.0	14.1	17.6	1.3	-	6.5	99.9

Table 56 Elemental analysis of areas identified as CHA, matrix and glass in Figure 112 / weight %

The elemental analysis of area A contained just N, O and Cl indicating the presence of CHA only. The elemental analysis of area B showed all the ions

expected in the glass plus Cl from the CHA. N was detected in area A although comparison with the spectra in Figure 105 shows it has a very weak response, even though it was present in larger amounts in the CHA molecule than Cl, the ratio of N:Cl being 5:1. Comparison of the relative responses of N and Cl between A and B showed that N in the matrix was possibly below the limit of detection of the instrument. This was therefore deemed to be the matrix with possibly smaller glass particles present. The nitrogen peak, which has a low response, was missing in the spectra. The glass particle (C) showed the presence of all the expected ions in a fluoro-alumino-silicate glass and no others.

5.4.6 XPS

The spectrum from the GIC sample showed major peaks due to C and O, with smaller contributions from other constituents, including Al, Si, Ca, P and F. The spectra from the CHA and AHCl powders also showed significant C1s and O1s. The main difference was the presence of strong N1s and Cl2p peaks due to the N and Cl atoms in the CHA molecule.

Changes in surface chemistry can be followed in most detail by recording narrow scan spectra for the main peaks.

5.4.6.1 C 1s

The C 1s region of the spectrum (Figure 113) shows a peak shape which is similar to that of poly(acrylic acid) (PAA) and which has been discussed in detail elsewhere (Jones *et al.*, 2003). The main peak (aligned at 285 eV binding

energy (BE)) is due primarily to electrons emitted from carbon atoms linked only to other carbon atoms and hydrogen. The smaller peak, at ~4 eV higher binding energy, arises from O-linked C atoms in the carboxyl and carboxylate groups of the unreacted and reacted poly(acrylic acid) respectively.

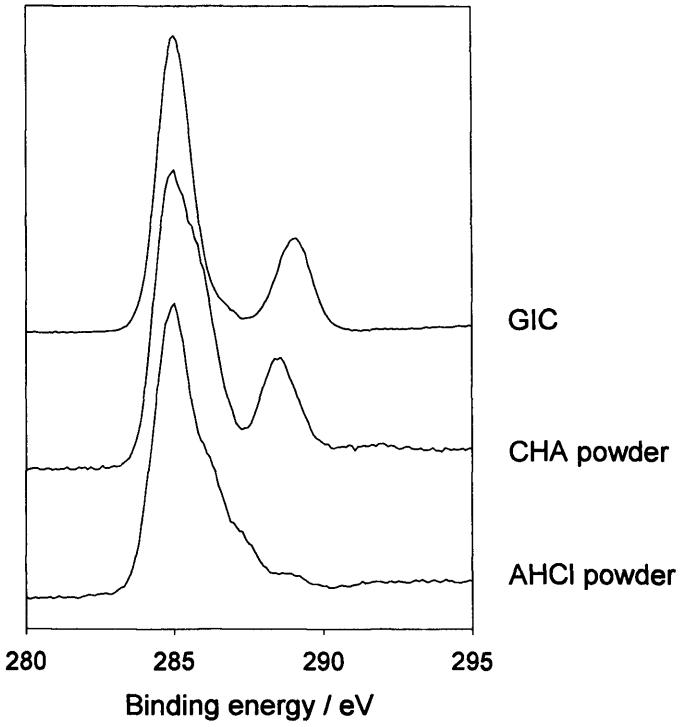

Figure 113 C1 s XPS spectra for GIC, CHA powder and AHCl powder

CHA has a similar spectrum to that of GIC. The high BE peak is probably due to C bonded to 2 N atoms, but there are C atoms in a range of different chemical environments, and they can't all be resolved. AHCl has 2 C atoms bonded to 2 N atoms, but they are C atoms in rings, which can push the BE down. The peak is broad and the individual C atoms cannot be resolved.

In summary, it is not straightforward to distinguish between GIC and CHA powder on the basis of the C 1s spectrum alone. The spectrum from the AHCl powder is readily distinguished from CHA, but a mixture of GIC/AHCl could not

be distinguished from a mixture of GIC/CHA. This can be seen later on in the doped samples.

5.4.6.2 N 1s

The N 1s region of the spectrum for AH2 cement, CHA powder and AHCl powder is shown in Figure 114.

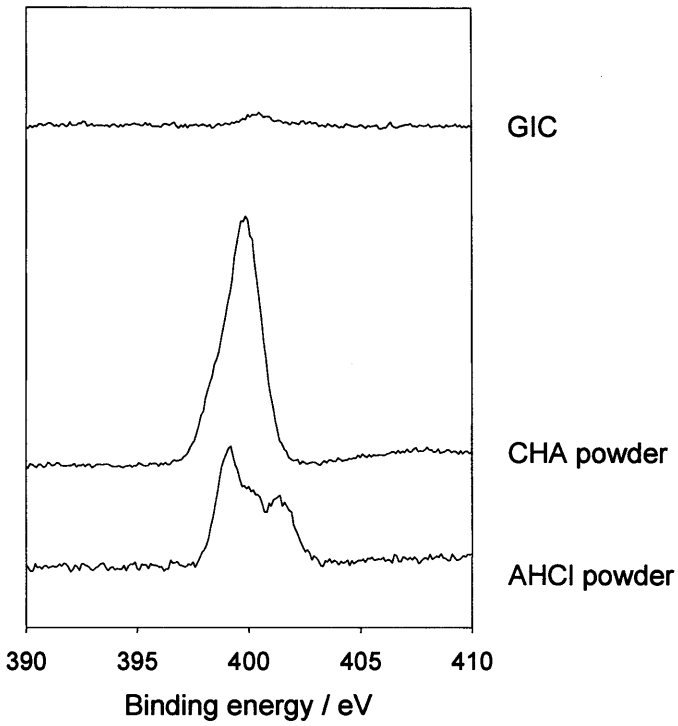

Figure 114 N1 s XPS spectra for GIC, CHA powder and AHCl powder (NB, the GIC and AHCl spectra have been expanded x2 on the y-scale relative to the CHA powder so that the peak shapes can be seen more clearly).

5.4.6.2.1 GIC

The GIC contains only a trace of nitrogen, probably due to contamination with protein-like species. The small peak at ~400 eV is at the binding energy typical

for N bonded to C / H. The two molecular species contain large amounts of N and are readily distinguished from each other.

5.4.6.2.2 CHA powder

This spectra contains at least 2 N components. Simple peak fitting locates these at ~400 eV and ~398.5 eV and indicates a ratio of 3.96:1 (High BE component to low BE component). This suggests that the high BE peak could be the N in the chain and the lower BE peak the N linked to the aromatic rings (would give a ratio of 4:1).

5.4.6.2.3 AHCl powder

This spectra contains at least 3 N components. Simple peak fitting indicates a ratio of (ratioed to lowest BE component) 2:1:3. This is unexpected as there are only 4 N atoms in an amprolium hydrochloride molecule. N^+ was attributed to the high BE component (~401.5 eV), the N linked only to C and H to the component at ~400 eV and the Ns in the ring to the low BE components (~399 eV), which would explain why this is the largest peak, even though the ratios are not quite as expected.

5.4.6.3 Cl 2p

The Cl 2p region of the spectrum for AH2 cement, CHA powder and AHCl powder is shown in Figure 115. GIC contains no Cl. CHA powder contains Cl primarily in the elemental oxidation state - i.e. bound covalently Cl 2p 3/2 EB ~200.5 eV. There appears to be a trace of Cl- at low binding energy (~197.9 eV).

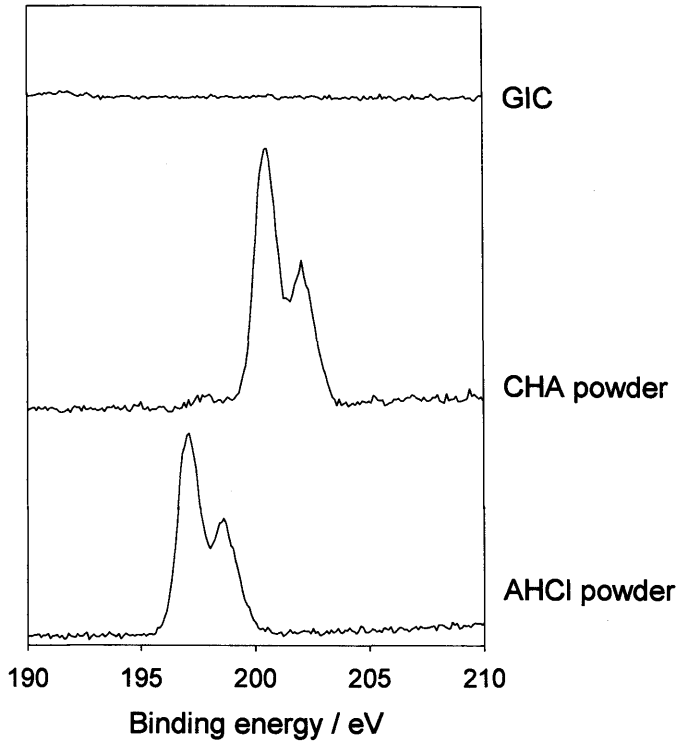

Figure 115 Cl 2p XPS spectra for GIC, CHA powder and AHCl powder

For AHCl, the appearance of the Cl 2p peaks at much lower BE is indicative of chloride ions Cl^- (Cl 2p 3/2 EB ~197.1 eV).

NB. All spectra are doublets (or multiples of doublets) due to spin orbit coupling (Spin orbit splitting ~1.6 eV).

5.4.6.4 CHA - doped, immersed and leached

The three regions of the spectrum for CHA powder, GIC containing CHA, GIC immersed in CHA solution and GIC containing CHA that had been leached are shown in Figure 116.

The C1s spectra show some peak shape differences, but even with complex curve fitting analysis, it is not likely that the contributions from the different components could be separated out.

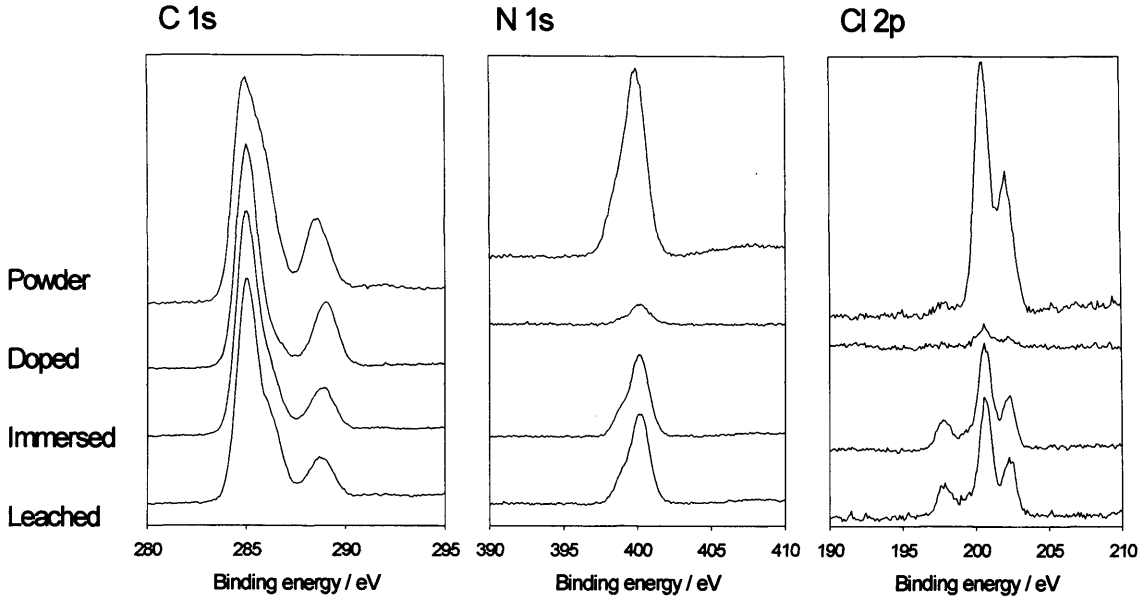

Figure 116 Comparison XPS spectra between CHA powder, GIC containing CHA, GIC immersed in CHA solution and GIC containing CHA that had been leached

For the powder, the N/C ratio was 0.44, the Cl/C ratio 0.07 and the N/Cl ratio 5.94, in reasonable agreement with the predicted values from the molecular structure of 0.39, 0.08 and 5.00.

For the doped GIC (11.0%), the peak shapes and positions are similar to those of the powder, but the intensities of the peaks are very much reduced, due largely to the presence of PAA. From the amount of CHA known to be included in the sample, the estimated N/C and Cl/C ratios, assuming homogeneous distribution, are 0.16 and 0.03 respectively, but the ratios measured using Casa processing software (Casa Software Ltd) were N/C=0.06, Cl/C=0.01 and N/Cl=6.79. This suggests the CHA may be obscured from detection – i.e. under a CHA-free layer, or with reduced CHA content at the surface.

The N1s and Cl2p peaks from the immersed sample are much stronger, with N/C=0.23 and Cl/C= 0.05 and N/Cl=5.20. The peak shapes are very similar to the powder, although there appears to be a greater contribution from chloride to low BE in the Cl2p spectrum, which suggests that there may be some decomposition of the molecule.

The leached sample is extremely similar, with N/C=0.25, Cl/C=0.05 and N/Cl=4.80.

5.4.6.5 AHCl - doped, immersed and leached

The three regions of the spectrum for AHCl powder, GIC containing AHCl, GIC immersed in AHCl solution and GIC containing AHCl that had been leached are shown in Figure 117.

For the powder, the N/C ratio was measured to be 0.15 and the Cl/C ratio 0.07, which are about half the values predicted from the molecular structure (N/C = 0.29 and Cl/C=0.14). The N/Cl ratio of 2.27 was found to be in reasonable agreement with the predicted value of 2.00.

The doped sample showed significant N and Cl peaks, with ratios not very dissimilar to the powder (N/C=0.12 Cl/C=0.04 N/Cl=2.88). The N peak was broadened and the individual components not resolvable. Similarly, the Cl peak has binding energies indicative of Cl^- but the peak was broadened indicating a number of different environments that the chloride ions are occupying.

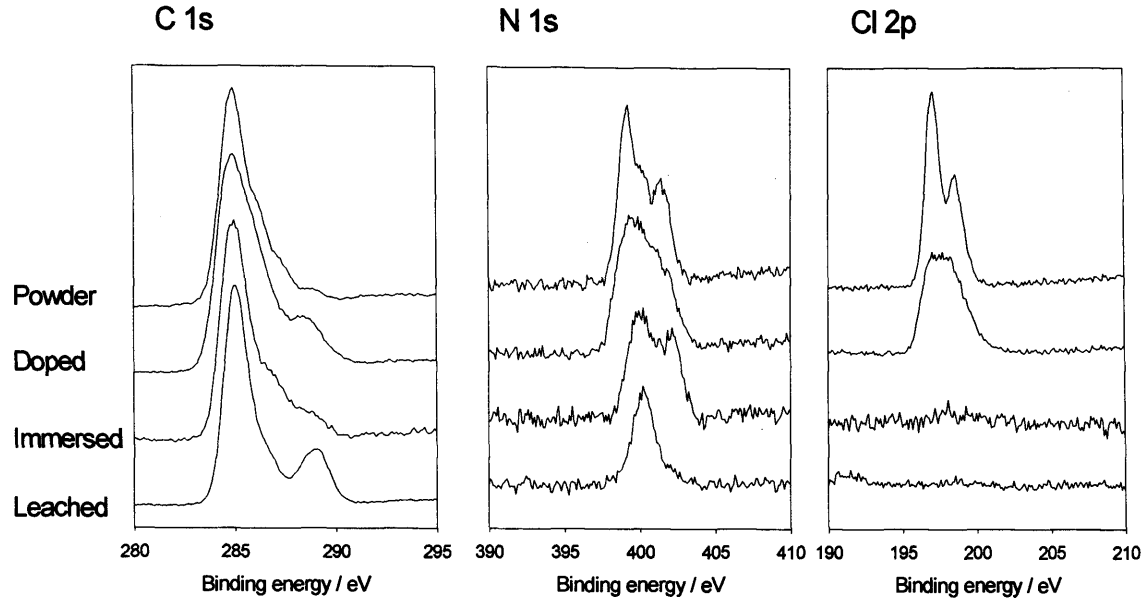

Figure 117 Comparison XPS spectra between AHCl powder, GIC containing AHCl, GIC immersed in AHCl solution and GIC containing AHCl that had been leached

The immersed sample looks much more similar to the AHCl powder, although there is now no chloride signal. The shape of the N1s peak is much more like that of the powder, suggesting that the molecule is not interacting in all the same ways as in the doped sample. The amount of nitrogen present at the surface relative to carbon is very similar to the doped sample (N/C=0.11).

5.5 Summary

5.5.1 Amprolium hydrochloride

Generally, the release profiles were similar for all four glasses with the exception of AH2 cement in which the percentage release was dependent on the percentage incorporated at the three concentrations of AHCl investigated. All three others appeared independent. The time to plateau (no further release) was markedly shorter for MP4 than for the other cements. In the case

of the setting times, MP4 again was different in that its presence reduced the setting time whereas for all other cements, the setting time was lengthened. Similarly, the working times for AH2 cement increased with increased AHCl concentration while that for MP4 cement decreased. The compressive strength data showed little difference between the four cements. Maturation time was not found to be a significant factor in the release of AHCl but immersion volume, to a small extent, was. It was also observed that the samples with high AHCl content were rubbery in feel on removal from the moulds.

5.5.2 Chlorhexidine acetate

Generally, the release profiles could be divided into two types. Type I (LG30 and LG26) in which larger amounts of added CHA gave increasing percentages of CHA release and type II (AH2 and MP4) in which increasing amounts at the low concentration end produced only small differences in CHA release. The percentage release from Type II increased significantly only when a certain threshold value of included CHA was reached.

In the case of the setting times, MP4 was different in that the presence of increasing amounts of CHA reduced the setting time whereas for all other cements, the setting time was lengthened to varying degrees. The working times were little affected by the addition of CHA with a slight decrease exhibited for LG30 and LG6 cements while the other two cements showed either no change or a slight increase.

5.6 Comparative Summary

A major part of this thesis is concerned with the difference in behaviour between the two active species CHA and AHCl in the inclusion within the various glass ionomer cements. A summary of the similarities and differences in the release profiles, working and setting times and compressive strengths is therefore given at this point in order to consolidate the data prior to the discussion section.

5.6.1 Comparative set

The results for the comparative set determination support the decision to mature GICs containing AHCl for a longer period than those containing CHA. The decision to use 24 hours and 1 hour respectively was due to the constraints of the working day. The exact maturation time for each cement type/included species/species concentration to bring all to the same degree of set would be various and would involve measuring each combination on the FTIR or Wallace micro-indentation tester.

5.6.2 Release of active species

A comparison between the maximum release values in percent against the percentage of added species to the four cements is shown in Figure 118. The most striking difference between the difference in release values between cements containing AHCl and cements containing CHA is that the bulk of AHCl

is released and the bulk of CHA is retained. This is generally more marked at higher concentrations of included species.

In the case of AH2, LG30 and LG26, the more AHCl that was included in the cement, the greater percentage released. In contrast, MP4 showed no general trend. In the case of CHA release from LG30 and LG26, the more CHA that was included in the cement, the higher percentage was released. AH2 and MP4 cements only exhibited a markedly higher percentage release at the highest concentration of CHA included.

Comparing the initial and later batches of LG30 and MP4, the later batch of MP4 gave greater percentage release at higher concentrations of included CHA but the LG30 showed no big difference between batches.

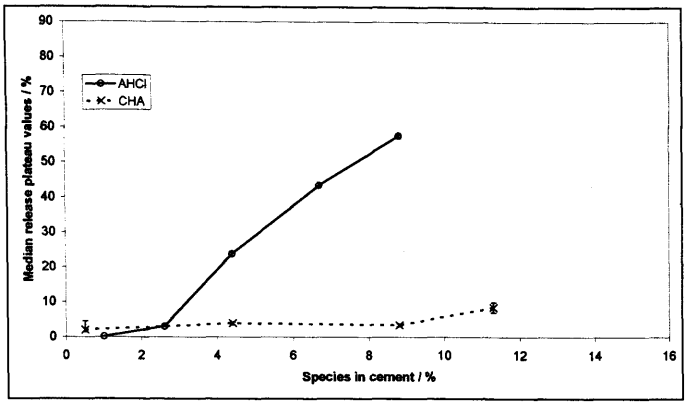

AH2

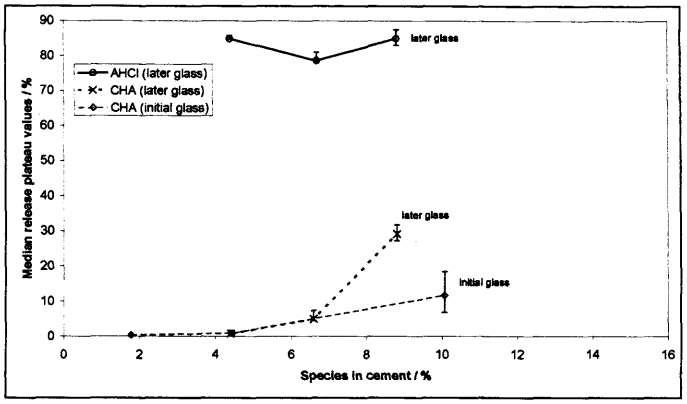

MP4

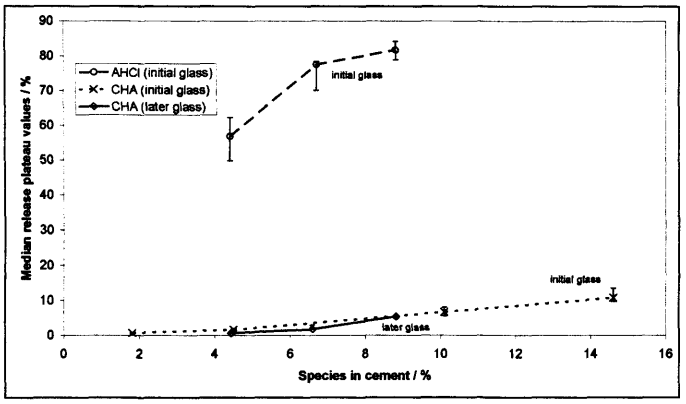

LG30

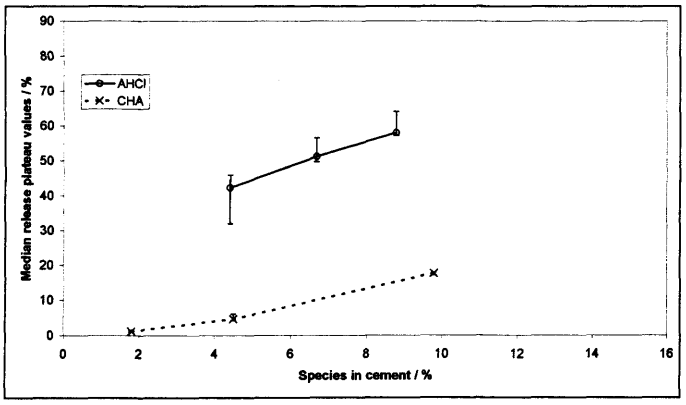

LG26

Figure 118 Comparison of AHCl and CHA total release values / % against percentage incorporation

5.6.3 Working, setting and compressive strength

The trends in working and setting times are tabulated in the three tables below.

	Working		Setting	
	AHCl	**CHA**	**AHCl**	**CHA**
AH2	++	0	++	++
MP4	– –	0	– –	– –
LG30	0	–	++	Not clear
LG26	0	–	+	++

Table 57 Working and setting times at 23 °C (OR)

	Working		Setting	
	AHCl	**CHA**	**AHCl**	**CHA**
AH2	++	++	++	+
MP4	–	0	– –	–
LG30	0	0	0	0
LG26	+	–	++	0

Table 58 Working and setting times at 23 °C (Gillmore)

	Working		Setting	
	AHCl	**CHA**	**AHCl**	**CHA**
AH2	++	0	++	++
MP4	–	0	–	–
LG30	0	0	++	+
LG26	0	–	++	++

Table 59 Working and setting times at 37 °C (OR)

Key: + slight increase, - slight decrease, ++ larger increase, -- larger decrease

In general, AHCl had a much greater effect on the working and setting times than CHA. AH2, LG30 and LG26 cements showed generally an increase in working and setting times, and MP4 cement showed a decrease in working and setting time with the addition of added species.

A summary table of the effect of species inclusion on compressive strength is shown in Table 60.

Cement glass	+ CHA (slope)	+ AHCl (exponent)
AH2	-3.9	-0.20
MP4	-15.1	-0.36
LG30	-0.1	-0.23
LG26	-2.2	-0.26

Table 60 Effect of species inclusion on compressive strengths

Various regressions were tried with both sets of graphs and the best fits were obtained by using linear fits for the CHA containing cements and exponential fits for the AHCl containing cements.

AHCl had a similar effect on all GICs studied in that they were all significantly reduced in strength. CHA however, reduced the compressive strengths of AH2, MP4 and LG26 cements to varying degrees and had no affect on the compressive strength of LG30 cement.

5.6.4 Scanning electron microscopy

Comparing the unmodified cements, AH2 and LG30 had the smoothest surfaces with LG26 being slightly rougher and MP4 being very much rougher. The more viscous a material, the more difficult it was to mix and hence the longer it took to mix adequately. This made it difficult to pack into the mould as it was already starting to set at this point. The material could therefore not flow against the surface of the glass slide as well.

The linear arrangement of pits on the surfaces were observed in unmodified cements as well as modified ones and are likely to be caused by scratches on the glass slides used in the moulds. Immersion in water affected the surface of MP4 cement noticeably, it becoming more pitted with time. The increase in pitting of LG30 cement indicated that it was slightly affected by immersion in water. The other two cements were not noticeably affected by immersion in water.

The surfaces of cements containing 8.8% CHA were rougher than those not containing any CHA. The immersion in water of AH2 and LG30 cement containing CHA had no affect on their respective surfaces at either rate of inclusion. MP4 cement with 8.8% included CHA was an especially stiff mix and did not pack into the mould properly. Many air blows were observed which may have either been in the original cement or have occurred during replication. LG26 cement containing 8.8% CHA exhibited more pitting after 48 hours; this was unchanged after 35 days.

The surfaces of cements containing 8.8% AHCl were also rougher than those not containing any AHCl. The surfaces of AH2, MP4 and LG26 cements

containing 8.8% AHCl were all slightly disrupted after 35 days. LG30 cement containing 8.8% AHCl appeared unaffected by immersion in water.

5.6.5 Elemental analysis

Elemental analysis showed fairly even distribution of AHCl within an unleached cement containing AHCl and slightly less even distribution on the surface. After leaching, cement containing AHCl showed no signs of AHCl even though 26% of the AHCl was still within the cement. CHA was found to be unevenly distributed within an unleached cement containing CHA. After leaching, CHA was still found in large amounts within the cement. Only 4.7% of the CHA in this specimen had been released. Discreet particles of CHA were found within the leached cement.

5.6.6 XPS

5.6.6.1 AHCl

The leached sample again shows no Cl2p peak, suggesting that all the chloride has been released into solution. The N1s peak is relatively sharp and is located at 400.2 eV, indicating that it is probably N bonded to C and H. It may actually be that all the AHCl has been released from the surface. Although the N present could be due to decomposed AHCl, it could also be due to contamination as the sample had been in the solution for a long time. Proteins could give a similar signal although the peak is quite large compared to e.g. the trace of contaminant N on the unmodified GIC surface (N/C=0.07).

5.6.6.2 CHA

The doped sample showed much smaller amounts of CHA than expected from the doping levels, possibly due to the fact that surfaces are often different from the bulk of the material. The leached sample showed that a significant amount of CHA was retained in the GIC. The immersed samples showed a significant amount of CHA present at the surface and were remarkably similar to leached samples.

6 Discussion

6.1 Critical evaluation of experimental techniques

6.1.1 Glass preparation

The variation in glass preparation was a result of limited amounts of glass which could be prepared initially by covered crucible firing. The cold top method used for the later batches of glass provides a more consistent formulation since the amount of fluoride lost from the surface of the melt is minimised as only the bottom 50% of the melt is used at each stage. Fresh ingredients are added at the top for further production. The limitation of this technique is that it is a bulk manufacturing process and is less appropriate for small experimental batches. This study only used this method latterly since the glasses produced initially were experimental formulations and crucible fired. Subsequently the materials became available in commercial quantities and the top melt method was used.

6.1.2 The glasses used in the study

Glasses were chosen of differing compositions, some of which would be cement forming agents. They formed a series from MP4 which contains the fewest components, namely Al, Si, Ca, O and Na to AH2 which contains additionally P and F. As this study involves incorporating additional ionic species into the cement system and in order to gain an understanding of the possible interactions between the ionic species, in the following discussion, the glass with the fewest components is considered first. The effect of adding active species to the material was pursued to determine how much of the added

species was released and the consequence of its addition on the physical properties of the cement. A study of the effect of additives on cements made with different glasses will give an indication of the influence of the various glass constituents on the cement formation and its subsequent behaviour.

In the present study tartaric acid was excluded from the mix because this would add further ionic species to an already ion-rich system for which it would be difficult to relate the interactions that were occurring. It would also alter the profile of the set. Since it is normally added to increase the working time and sharpen the setting time this would mask possible effects that the added species in this study may have on cement formulation. To clarify the ion complement of the glasses, a modified version of Table 3 from Chapter 4 section 4.1.1 is reproduced below.

	Na	F	P	Al, Si, Ca, O
MP4	X	-	-	X
LG30	-	-	X	X
LG26	-	X	X	X
AH2	X	X	X	X

Table 61 Ions present in the glasses

The P/L ratio was 7:1 and glass : PAA ratio 4 : 1 in all cases with the exception of the initial batch of LG26 which had to be modified as at this ratio it set before being able to be introduced to the mould. The glass/PAA ratio was 2 :

0.67, and the powder/water ratio was 5.733 : 1. The consequences of reducing the P/L ratio of the LG26 cement would be to weaken the cement and alter the setting rate (Crisp *et al.*, 1976b). This initial batch was used for making all the release and compressive strength specimens whilst the final batch was used for the working and setting times.

6.1.3 Characterisation of the glasses – XRF

The final composition of the glass after firing needed verifying by XRF. X-ray fluorescence spectrometry is a relatively quick and effective way to measure major oxide and trace element abundances in powdered whole rock samples. The main principle behind XRF spectrometry is that X-rays of characteristic wavelength (and energy) are emitted from a sample when the sample is ionised by a stream of X-rays; this process is known as X-ray fluorescence. Most elements between atomic number 11 and 92 (e.g. Na to U) are routinely measured. There are two main sample preparation methods used for analysis: light elements and major oxides are very susceptible to mineralogical (matrix) effects and must be fused into a glass disk; heavier elements are more straight-forward and samples can be pressed into pellets.

The advantages of XRF are relatively simple, cheap and quick analyses, accurate for a large range of elements, minimal sample preparation needed and few consumables needed. Its main disadvantages are that it is unsuitable for analysis of very light elements and the fused bead preparation is time consuming and requires a certain amount of practice. With the setup used for this study, powdered samples in a helium atmosphere containing mylar

windows, the element with the lowest atomic weight that could be detected was Na, hence the absence of data for F. Also, the standardless method used, only determines concentration to within an accuracy of ±10%.

6.1.4 Characterisation of the glasses – particle size

There was a need to assess particle size and determine that the glass had comparable distribution. The particle size of the glass powders used is important because the setting reaction mechanism of a GIC involves ion release from the glass surface. These ions are involved in cross-linking the PAA. Since the reaction is a surface reaction, the surface area exposed to attack will determine the rate of reaction. Similar particle size and distribution for all glasses are important in order to ensure that direct comparisons can be made. While an exact match would be difficult, it was important to ensure that the distribution and range of particle size fell within a relatively narrow range. It has been shown however, that small variation in particle size and distribution has only a limited effect on the setting reaction of a GIC (Kaplan *et al.*, 2004).

One of the commonest methods is sedimentation. This provides a relatively accurate measure of size distribution but requires that the glass is thrown into a column of water. The larger / heavier particles will sink faster and over time various fractions of glass of different size may be obtained. These are then sieved to obtain an accurate measure of particle size. This is however quite time consuming and the particle size range is determined by the frequency of fractionation. Alternatively dry sieving of the glass may be carried out giving an approximation of particle distribution. This however is quite crude in that long

thin particles can go through a finer sieve than would be expected given their overall size.

The Malvern particle size analyser provides a quick way of obtaining a particle size distribution. The results may vary depending on the stirrer speed, intensity of the ultrasonic probe and the speed at which the suspension is pumped past the cell. To avoid the instrument setup influencing the results, these settings were kept constant for all experiments. The detection method assumes spherical particles. As glass particles are not spherical the resulting particle distributions obtained are not necessarily an absolute value. However, as the glass particles for all the glasses are of the same general shape, the technique was considered suitable for this comparative study.

Most of the glasses had similar particle size distributions with the exception of LG26 (initial) which had a generally smaller particle size distribution and MP4 (initial) which had a generally larger particle size distribution. It might be expected that this effectively would result in the glass with the smaller particle size (0.12 – 102 μm) with the greater surface area per mass of cement having a greater reactivity and shorter working and setting times. In fact, there was little difference between batches of different glasses and the relative distribution in the materials was considered appropriate for this study. This tends to confirm the results of Kaplan *et al.* Kaplan *et al.*, 2004).

6.1.5 Choice of Species

The two species that were added to the glass-ionomer mixes are reiterated in Table 62.

	Chlorhexidine di-acetate	Amprolium hydrochloride
	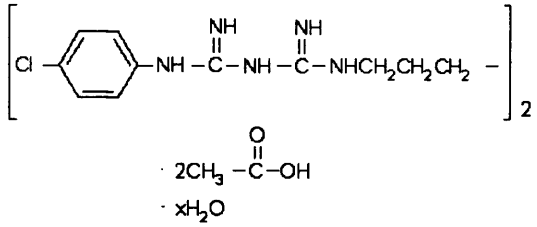	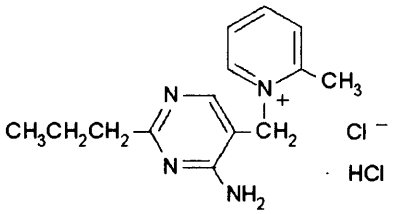

Table 62 Added species

The species differ in some important ways: The species differ in some important ways:

- **Solubility**. The solubility of CHA is 1.9% (w/v) in water and that of AHCl is 33% (w/v) in water at 23 °C.
- **Size**. The CHA molecule is approximately twice the size of the AHCl molecule; their molecular weights being 626 and 315 respectively.
- **Shape**. The CHA molecule consists of a chain 16 units long (C and N) terminated at both ends by a chlorinated benzene ring whilst the AHCl molecule consists of two close aromatic groups with a much shorter chain on the end of one of the groups.
- **Functional groups**. The CHA molecule had acetate and AHCl molecule, chloride and hydrochloride. In the cement forming process the added species was likely to have an effect. It could either have acted as an inert filler that interrupted the cement formation but did not interact

chemically with the system or it could itself have taken part in the cement reaction, thus binding into the matrix.

There are many possible interactions between molecules and ions in a normal GIC system, and the totality of these is still not understood. The addition of another species will further complicate matters.

Of interest are the physical size and ionic charge of the ions present and the physical size and heats of formation of the possible molecules that might be formed. Heats of formation and ionic radii of some of these possible species are outlined in Appendix II, Table 64.

Some of the possible compounds formed in the cement are shown in Table 63.

Cations present	**Anions present**	**Possible compounds**
Na^+	F^-	NaF
Al^{3+}	Cl^-	NaCl
Ca^{2+}	CH_3COO^-	$NaCH_3COO$
		AlF_3
		$AlCl_3$
		$Al(CH_3COO)_3$*
		CaF_3
		$CaCl_3$
		$Ca(CH_3COO)_2$

Table 63 Possible interactions between CHA and other species in AH2 cement

*** There are many variations on this basic formula (Kubicki *et al.*, 1996).**

e.g. MP4 cement contains Al, Si, Ca, O & Na. If Cl^- in the form of amprolium hydrochloride was added to MP4 cement, the ion complement would more closely resemble AH2 without P. This may give an indication of the behaviour of P in AH2 cement. If halide in the form of Cl^- is added to AH2 cement, the total halide ion concentration will be altered possibly altering release. If acetate in the form of chlorhexidine acetate is added to both LG30 and LG26 cement, then possibly Al and Ca acetates will be formed. If however, acetate is added to AH2 and MP4 cement, additionally Na acetate may be formed. Comparison of these two groups may give an indication of the effect of acetate on the cements.

6.1.6 Incorporation of added species

The method of incorporating the added species was to blend the glass, PAA and either CHA or AHCl together as a powder and then tumble them for a fixed period of time in an attempt to give an even distribution within the mix. There was no method readily available to measure the degree of success of mixing. Each batch was used to make three mixes and from each mix two specimens were produced. Inhomogeneity is likely to be reduced during mixing of the cement. It was likely that uneven distribution remained as there were some varying release results from specimens made from the same mix.

Although CHA is a common antibacterial, its exact form in solution is unknown. Recent unpublished work (Braden, 2004) involving the measurement of osmotic pressure of CHA (aq) has indicated that CHA exists as four ionic species although what precisely these are has not as yet been elucidated.

AHCl has been used in the veterinary industry for as long as CHA. It has a structure similar to that of thiamine (Shin and Oh, 1993) and research to date has been concerned with its antibacterial effects.

6.1.7 Effect of CHA on cements

When approximately equal amounts of CHA and PAA are mixed together in water a white precipitate is formed (Leung, 2003). FTIR data from the present study shows that CHA reacts to a small extent with PAA to form a compound which is likely to be some form of polyacrylate salt.

According to Fukazawa *et al.* in 1990 immersion of a set cement in organic acid solutions apparently results in an erosion of the glass ionomer merely as a result of a disruption of the polyalkenoate cement matrix, the formation of which depends upon the diffusion of the eluted species. More recently however, it has been suggested that the glass as well as the polyacrylate matrix is attacked (De Moor and Verbeeck, 1998b). The composition of the glass may also alter resistance to acid attack, it being known that AH2 is more susceptible to acid attack (Billington *et al.*, 2000). It is possible that on introducing CHA to PAA in an aqueous environment some ionic exchange may occur resulting in the formation of acetic acid. It has been shown by Wasson and Nicholson in 1991 that a weak cement can be formed from acetic acid and an ionomer glass. They found however, evidence for aluminium acetate formation but not calcium acetate. (It is known that GIC glass with acetic acid will form various salts. This varies with glass composition therefore addition of acetate may affect the cement structure.)

6.1.8 Hardness

The Wallace micro hardness indenter is a speedy and effective method for measuring the hardness of a specimen. The hardness is measured by lowering an indenter slowly onto the surface and measuring the width of the indent. This is then converted to a hardness value. The method used in this study measured the depth of penetration from which the hardness was determined. Small depths were measured, ≈ 20 μm in some cases. It was essential that the specimen had a flat base so that it did not move when the weight was applied and that the indenting machine was free from vibrations. The initial null setting was technique sensitive and required care to ensure that undue force was not applied to the machine when the null lever was pressed. This was found to be the area most likely to produce errors. The shape of the diamond was important for roughness calculations which were based on the geometry of the pyramid. Indenters may be damaged by rough handling and were visually inspected periodically.

6.1.9 Working and setting

Working time is the point at which the material can no longer be manipulated without influencing the bonds already formed in the material. The disadvantage of the oscillating rheometer in measuring working and setting time is that the material is continuously being subjected to shear forces which may disrupt the bonds formed in the material. To reduce this effect, the angle of movement of the oscillating plate is kept low. The limiting factor here is that if the movement is too small, the signal becomes so small that it may be

masked by electrical and mechanical noise from the amplification and from the contact between the eccentric cam and the arm respectively. Setting time is the time at which the material is set enough to be used for the purpose it was made for but does not necessarily indicate the completion of the chemical reaction. The latter may be measured by IR spectroscopy.

The working and setting times measured with the oscillating rheometer had a high degree of scatter. Other workers have also observed high scatter (Griffin and Hill, 1999) particularly with experimental materials. They attributed it to variation in blending technique of the components, small variation in temperature of the test laboratory and variations in glass particle size. This study was executed by an operator who had very substantial experience of handling this type of material so variation in mixing technique was not considered to be a major contribution to specimen variation. One option would have been to double the number of specimens from 6 to 12 hence reducing the error bars from ranking positions 1 and 6 to ranking position 3 and 10 thus eliminating two outliers from each extreme. There was no indication as to whether this might have been enough and may have lead to even greater number of specimens having to be tested. The oscillating rheometer can produce reliable results with glass-ionomer cements (Khouw-Liu *et al.*, 1999; Fleming *et al.*, 2003). Most workers, however, do not show the results graphically.

The main cause of inaccuracy of the working time as measured on the oscillating rheometer for the materials used in this study was the fact that the cement had started to become more viscous before it was placed on the platen and it was difficult to determine the early change in viscosity as the placing of

the cement on the platen disturbed the rheometer and took two cycles to stabilise. There was potential inaccuracy in the measurement of setting time due to variation in the spring constant (Cook and Brockhurst, 1980). Over time, this changes as the springs are continually stretched and relaxed. As the material is constantly being sheared during setting, there is a possibility of breaking newly formed bonds and therefore giving what appears to be an extended set. The OR can give additional data other than working or setting time. It does provide an indication of setting characteristics of a material as it measures the amplitude of the oscillation continuously throughout the experiment. It could be used to give an indication of the rate of setting by measuring the rate of change of amplitude from wide to narrow.

The Gillmore needle has been discussed in section 2.12.1.1, its main disadvantages being that unlike the oscillating rheometer, it cannot easily be used to determine setting characteristics other than working time and setting time, and a certain amount of operator skill is required for reproducible results.

6.1.10 Spectroscopy

The two methods for measuring the chemical changes involved in a reaction are Raman and infrared (IR) spectroscopy. Raman spectroscopy shows only weak peaks for the acid and the various acrylate groups (Na, Ca, Al) involved in the GIC reaction (Young *et al.*, 2000). This weak signal is compounded by a noisy background caused by high fluorescence and so Raman spectroscopy is not ideal for the task despite the fact that Raman is more effective in the presence of water. Infrared spectroscopy has proven to be suitable and has been used

successfully (Crisp *et al.*, 1974). More recently, this technique has been improved by modern instrumentation with Fourier transform infrared (FTIR) which has a greater peak resolution and a more rapid scan rate (Nicholson *et al.*, 1988; Young, 2002).

6.1.10.1 Fourier transform infra-red spectroscopy (FTIR)

The FTIR is an established technique for identifying the chemical groups in a material. In complex materials the identification of peaks is difficult as they are usually broad and often overlap. They may also interfere with one another causing peak shift; presence of chemical species adjacent to the species of interest can cause a shift in the wavenumber of the peak. More recently the use of reflectance mode has permitted investigation of solid materials.

It scans are run as a function of time, the results may be used to follow the changes in chemical groups as a reaction progresses providing the functional groups involved in the reaction have been identified. It was possible to follow the progress of the glass-ionomer reaction, more specifically the polyacrylate formation, in the unmodified cement and with the cement containing CHA. A problem arose when AHCl was incorporated in cement as its presence masked the salt-formation peak at 1548 cm^{-1} (COO- stretch) after approximately 100 minutes.

In a dual-beam machine the reaction could be followed by observing the reduction in the acid peak at 1702 cm^{-1}, any fluctuations in the baseline being compensated for by the reference beam. In the single beam instrument used, these fluctuations were compensated for by measuring both the increase in the

salt peak and reduction in the acid peak. By subtracting the absorbance of the acid peak from that of the salt peak baseline drift was eliminated. A major disadvantage of using FTIR for this study was that in a GIC with added CHA, the polyacrylate peak is indistinguishable from the acetate peak as they are both represented by COO^-.

A further practical consideration is that as the cement sets it may pull away from the diamond surface used in reflectance mode thus increasing signal to noise ratio. This can be alleviated to some extent by prevention of specimen dehydration.

6.1.11 High performance liquid chromatography (HPLC)

There are two methods of measuring the release of species from a material: UV spectroscopy and HPLC. UV spectroscopy was considered first but was found not to be sensitive enough for the detection of the amounts of species that were released. The alternative technique of HPLC was then used as it was found to show much greater sensitivity.

The reproducibility of the injection volume was improved by the introduction of an autosampler that reduced human error in injecting. Human error was not concerned with the actual injection into the rheodyne injector as a larger volume than was necessary to fill the loop was injected, the excess going to waste. The variability was in the manual movement of the rheodyne injector from the 'load' position to 'inject' position; a swifter injection leads to a sharper peak.

A well maintained HPLC pumping system will give a pulse-free flow through the system. The pumping system was microprocessor controlled (Z80, ZiLOG, San Jose, California, USA) and continuously monitored the back pressure to keep the flow rate constant. This was therefore not considered a source of error.

The reverse-phase columns chosen for AHCl and CHA determination were similar to previous workers' successful experimentation. (Tan *et al.*, 1996 and Izumoto *et al.*, 1997). The column is in a perpetual state of change necessitating daily calibration. It changes in response to the chemical nature of the mobile phase flowing through it, its temperature, the flow rate and also the species continually adsorbed onto and desorbed off of it. Columns therefore have a finite lifespan. As they degrade with time the backpressure usually increases and peak retention times shift as active sites become 'used up'. There is a further problem with CHA in that it can become irreversibly bound to a column if the right mobile phase conditions are not observed (Ha and Cheung, 1996). The experimenter observed this when trying to reduce the amount of the aqueous part of the mobile phase in order to save time. The aqueous component was more time consuming to make as two components had to be weighed and the pH adjusted. The aqueous/non-aqueous ratio was changed from 60:40 to 40:60 to this end. Over the course of two months the amount of CHA detected declined until none was detected using the HPLC system. After weeks of troubleshooting it was ascertained that the CHA was irreversibly absorbed onto the column necessitating discarding the column.

One of the limiting factors of the software was the peak area determination. The CHA peak had a long tail making it less easy to determine its end, thus the presence of a peak modifer (SDS) in the mobile phase helped to reduce this

tailing but also increased the retention time thus necessitating the making-up of more mobile phase.

6.1.12 Compressive strength

The compressive strength test is a widely accepted test for mechanical strength and the specimens are easy to produce. An alternative test, the biaxial flexural (shell), is more discriminating of differences between materials (Williams *et al.*, 1998). The edge effects are minimised as the specimen sits on an annulus with th periphery of the sample outside the test area. Imperfections on the surface were eliminated by grinding specimens on 1000 grit SiC paper and testing between damp Whatmann No. 1 filter paper.

6.1.13 SEM

Scanning electron microscopy is a well-known technique for observing surfaces at the microscopic level. An electron beam is directed at the surface of a specimen. On interacting with the surface some electrons bounce off and are referred to as 'reflected or back-scatter electrons'. Their intensity is related to the atomic weight of the atoms on the surface and is a qualitative indication of atomic weight. Others displace electrons that are emitted at a shallower angle and are called 'secondary electrons'. These give topographical information of the subject. X-rays are also emitted that give quantitative information on the elemental composition of the specimen. The depth of penetration of the beam is dependant on the accelerating voltage of the instrument and intensity of the beam. This is of significance when the term 'surface' is used to describe the

image observed as in theory a surface has no thickness whereas in reality it has some depth. The main disadvantage of SEM analysis is that specimens have to be viewed under high vacuum. In order to achieve this high vacuum, specimens have to be desiccated. This process of desiccation and subsequent vacuuming causes stresses in the cement resulting in the formation of cracks. These cracks cannot easily be differentiated from cracks present in the surface prior to processing. The alternative is to make replicas of the material and observe these replicas. A one-step process using silicone impression material provides the simplest process although the silicone forms a negative of the surface and interpretation of this requires care to avoid misinterpreting the surface. Silicone impression material melts around 80 deg C. An electron beam may cause heating of the surface and the higher the magnification, the smaller the area on what the beam is concentrated. There is a consequently higher temperature of the area being viewed. Silicone impression material is therefore unsuitable for viewing at high magnification as the sample may be damaged. To circumvent this problem, a two-stage process was used in which a slow-setting epoxy resin was poured onto the silicone impression and a positive replica made. Epoxy resin is more stable under an electron beam. Even with this material there was potential for specimen damage during focussing and the procedure was carried out in the shortest time possible. The stated resolution of Cambridge Stereoscan 90Bis 25 nm when operating at peak performance. The factors which would influence the resolution are focal length beam current and specimen composition.

6.1.14 X-ray photoelectron spectroscopy (XPS)

The main feature of XPS is its surface sensitivity, down to a few nanometres. As it is a surface technique, it is easy for contamination to dominate, and it is also possible that the sample surface is considerably different to that of the bulk material. XPS as a technique has many limitations; it's only sensitive down to around 1 % so is not good at trace material analysis. Ultra-high-vacuum conditions are required so specimens have to be dried in the same manner as those for the SEM. Insulating samples are problematic, and require special techniques to analyse accurately. The X-ray beam can cause damage to sensitive materials and there can be some heating of the sample, which may also cause artefacts.

6.2 Discussion of results

6.2.1 XRF

The main differences between the glasses and the reason they were chosen was because of the presence or absence of Na, F and P. Both LG30 and LG26 had no Na added in the original mixture but small amounts, 0.7 mol % and 0.5 mol % respectively were detected in the final glass composition. This is not entirely unexpected as Na is a common element that often exists in trace form in many compounds. P, which has been linked to the rate of setting reaction (Wilson *et al.*, 1980; Griffin and Hill, 2000a), was confirmed in the three cements that contained it in the original compositions and not in MP4 that did not have it in its original composition. The XRD technique used could not

detect F which unfortunately is the most volatile, and hence most likely to vary, of the components. Although this was one of the components that was important in the choice of glasses, the original pre-firing data had to be accepted. It was likely, however, that F would still be present in the post-firing compositions of AH2 and LG26 glasses although in possibly smaller amounts. The small amount of Sr in LG26 may have been present as a contaminant in CaF^2 or CaO, it belonging to the same chemical group as Ca. As stated above, these glasses were chosen for their presence of absence of certain components. The XRD data confirmed the choice of glasses with the slight reservation about the final F content of AH2 and LG26.

6.2.2 Particle size

The particle size data showed generally that the glasses had similar distributions. The differences for the initial batches of LG26 and MP4, although noticeable, may not have been of significance as during the production cycle of a glass, it is acid treated to adjust its setting time. The method of measuring particle size was quick and easy and with a competent operator could be reliable at giving relative particle distribution measurements.

It has been shown however, that small variation in particle size and distribution has only a limited effect on the setting reaction of a GIC (Kaplan *et al.*, 2004).

6.2.3 XPS

The broadening of N1 s and Cl 2p peaks suggests that AHCl interacts strongly with GIC components on inclusion by mixing or that N and Cl atoms are in many different chemical bonding environments. It is also possible that the molecule may decompose when in water for long periods. The lack of a chloride signal in the immersed sample suggests that only the organic part of the molecule has bound to the GIC. After the doped sample has been immersion for long periods, AHCl appears to be completely lost from the surface. This supports the release data where AH2 cement doped with AHCl released approximately 60% of the AHCl. The lack of Cl s signal in the immersed sample and the shape of the N1 s peak suggesting that the molecule is not interacting in the same way as in the doped sample indicated that it is adsorbed in a single conformation / adsorption site on the surface and is not in many different chemical environments like the doped sample.

The XPS data for CHA shows that CHA is not homogeneously distributed throughout the cement but that the molecule is somewhat obscured from detection at the surface, perhaps with a layer of low or negligible CHA content. In composites, it is quite normal for the surface layer to be resin-rich. It is possible that this phenomenon is occurring here as well. There appears to be a loss of Cl from the surface of the leached sample which may be due to decomposition in the X-ray beam or partial decomposition of the CHA molecule by reaction with the cement components. Spectra from the leached samples indicate that a considerable amount of CHA remains in the specimen after immersion in water. N1 s and Cl 2p peaks for the leached specimen were more intense than for the doped specimen indicating that the release is not simply a

surface wash-off effect. One explanation for the increase in CHA signal would be degradation or dissolution of CHA-depleted surface layer. This supports the elemental analysis data suggesting that CHA is present in the cement as encapsulated powder particles. An alternative explanation is that CHA in solution may be re-adsorbed onto the specimen surface from the leaching solution. This explanation is attractive, since the spectra from the specimen immersed in CHA solution are similar to those from the leached sample. It should be borne in mind, however, that the solution surrounding the leached sample contained a significantly lower concentration of CHA than the solution used for the immersion experiment (0.01% compared to 2%). The possible re-adsorption of CHA to the surface is supported by an anomaly in the release data where some of the cumulative release plots show a slight dip at about five hours. Perhaps at this time, the GIC has reached a stage of maturation that allows binding to certain sites (the setting reaction takes ~24 h).

6.2.4 Release

The purpose of the study was to determine the effects of the addition of different species to a complex cement system to ascertain whether the structure of the inclusion would have effect on both the chemical and mechanical cement structure and also on the release characteristics of the cement so formed. It is well established that the conventional cements will release ions which are present in the components and pass into the matrix such as fluoride (Wilson *et al.*, 1985; Forsten, 1990; Williams *et al.*, 2002) and also Al (Andersson and Dahl, 1994).

The factors which may influence this phenomenon would be:-

- The composition of the glass as this contains components which influence the setting reaction (De Maeyer *et al.*, 1998; De Maeyer *et al.*, 2002; De Maeyer and Verbeeck, 2001).
- The acid species available for cement formation. It is known that cements may be formed with polyacid as well as lactic and acetic acid (Wasson and Nicholson, 1993b; Shahid *et al.*, 2007).
- The nature of the included species, which includes:
    - Reaction with the cement forming components.
    - Provision of additional ions of a chemically similar nature to those already present which might influence the release and also behaviour of the set cement.

6.2.5 Amprolium hydrochloride

6.2.5.1 Release

The release of AHCl was high for all cements, the bulk being released for all cements at the highest level of inclusion of AHCl (8.8%). The release was also rapid for all cements. In general similar % release occurs regardless of the amount included with the exception of AH2 cement. All AHCl that can be released is released within 5 days with the exception of LG30 where the release reaches a plateau at 10 days. There is no evidence for diffusion in the release profiles with the exception of AH2 cement with 8.8% and 6.7% AHCl that show some a slight pattern of diffusion in the early stage. The release, as expressed

as mg g^{-1}, μg mm^{-2} or %, all show that AH2 had the lowest maximum release and MP4 the highest in the following ascending order:

AH2 < LG26 < LG30 < MP4.

The factors affecting the release are:

1. Diffusion either through the cement matrix or through cracks and fissures
2. Setting and maturation of the cement
3. Inclusion
    a. Behaviour within the cement
    b. Behaviour in the solution

The bulk of the AHCl was released from the cement. AHCl dissolves fast compared to PAA and during the initial mixing of the cement it is likely that all the AHCl dissolved. After immersion of the cement in water, water will diffuse into the cement, allowing AHCl to diffuse out either through the matrix or via channels. Elemental analysis by SEM (Figure 107) showed that AHCl was evenly distributed throughout the set cement. AHCl will therefore potentially exist in ionic form within the matrix and be capable of passage out to the exterior.

XPS data showed that the Cl part of AHCl was completely lost from the surface of a doped AH2 sample although the release from this sample was only 53% indicating that the remaining 47% was within the sample. This suggests that the dissolution of AHCl from the surface of the matrix into the surrounding water was a faster than migration of the AHCl from the bulk of the cement to

the surface or that the main part of the molecule was still bound in the cement. The N1 s peak indicates that N is bonded more simply than for the unleached sample. The N present may be due to decomposed AHCl or it might be a contaminant, protein giving a similar signal. XPS data should be treated with caution as a cement immersed in AHCl solution did not have a chloride signal, suggesting that only the organic part of the molecule was bound to the cement.

AHCl existing within the matrix is likely to diffuse out into the surrounding water. This diffusion is dependent on the concentration of AHCl in water compared to that at the surface of the specimen and the volume of the water into which it is immersed. The maximum recorded concentration of AHCl in the surrounding solution was 1316 ppm which is 0.33 % of a saturated solution of AHCl (400,000 ppm) so it was unlikely that the volume of water in which the specimen was immersed was of significance in prevent passage of the material to the exterior. Experiments to investigate the effect of the reservoir volume and changing the water periodically showed no significant difference between the release of AHCl into 20, 40 or 60 ml. It did show, however, that release into 20 ml of water that was changed daily was slightly less than release into the three static volumes. Although this difference was significant, it was small and the wide scatter suggests that experimental variation might be the cause of this difference.

6.2.5.2 Scanning electron microscopy of the surface and the internal structure

The surfaces of cements containing 8.8% AHCl were rougher than those not containing AHCl. The fluidity and ease of mixing of cements containing AHCl

would have been expected to have produced a smoother surface if smoothness was related solely to degree of mixing of the ingredients and it is likely that what was observed related to surface disruption and wash out as has been seen with immature cements in conventional GICs. This tends to be supported by the SEM images that show considerable surface disruption of MP4 cement on water immersion and the release results showing that MP4 exhibited the highest release of AHCl. The surfaces of all cements containing 8.8% AHCl except LG30 showed slight disruption after immersion for 35 days. It is likely that after the bulk of included species had been released then the cement would have a more porous structure. In the case of MP4 cement, the plateau release value for 8.8% included AHCl showed 92% of the total inclusion was released. Since this was equivalent to nearly 10% (8.4%) of the total mass of the specimen, disruption of the sample surface was observed and expected. The fracture surfaces do not show evidence of cracks and fissures forming. All show a similar appearance and these are also similar to the CHA samples.

Despite this observed disruption to the surface of some cements, weight loss studies gave no indication of mass loss. It appears that water uptake masked any weight loss that might have occurred.

6.2.5.3 Compressive strength

The compressive strength results show that all cements are affected to the same degree by the addition of AHCl. Considering the possible different chemistries of the different cements, this would indicate that AHCl is not chemically involved in the cement forming process but behaves in the same

manner as fluoride where large amounts added cause reduction in strength of the cement. MP4 and LG30 cement exhibit the most AHCl release; they also are the two glasses that do not contain fluoride. It has been reported (Akselsen *et al.*, 1987) that total disintegration of GIC occurs when immersed in 2% NaF solution. It has been found (Billington *et al.*, 2000) that fluoride addition to a fluoride-free glass ionomer cement (LG30) renders it vulnerable to surface disruption by NaF solution.

The high release of AHCl from the GICs suggests that most of the AHCl exists as ionic species within the matrix. The near identical compressive strength data suggests that deterioration in mechanical properties is glass independent. Other workers have found an inverse relationship between fluoride release and compressive strength (Xu and Burgess, 2003), i.e. materials with high fluoride release had lower mechanical properties. As the current work also shows that as more AHCl is added to cement, the more is released, this seems to suggest that Cl^- from AHCl interacts in the same way as F^-.

6.2.5.4 Working and setting

The working times as measured by Gilmore needle and OR are in close agreement. The working times of LG30 and LG26 cement are very little affected by the addition of AHCl whilst the working time of MP4 cement is reduced and AH2 cement extended.

The setting times of AH2, MP4 and LG26 cements as measured by Gilmore needle and OR are also in close agreement. The setting times of AH2 cement

and LG26 cement were extended considerably whilst that of MP4 reduced. The setting time of LG30 cement as measured by OR was extended considerably by the addition of AHCl and not affected as measured by Gilmore needle. The results for both working and setting times indicate that the setting reactions of AH2, LG30 and LG26 cements were disrupted and that of MP4 cement accelerated. If fluoride were to have some accelerating affect on the setting reaction then it is possible that the presence of a similar Cl^- ion might also accelerate the setting. This would not explain what happens to LG30 cement where the presence of Cl^- disrupts setting. The unidentified peaks of the FTIR spectra for the setting of AH2 cement with AHCl suggests that there are other reactions occurring within the setting cement. This is supported by the XPS data for the AH2 sample containing AHCl which shows N in many different chemical environments suggesting either strong interaction with the cement or that the molecule may have decomposed.

6.2.5.5 Cement dependence

As explained above, the maximum amount of release occurred in the following ascending order:

AH2 < LG26 < LG30 < MP4.

There appears to be an inverse relationship between this and the amount of indigenous specie present in the cements:

MP4 (Na) = LG30 (P) < LG26 (F P) < AH2 (Na F P)

Interestingly, as we progress along this series, the % released became less dependent on the amount included.

6.2.6 Chlorhexidine acetate

6.2.6.1 Release

The release of CHA was low from all cements formed from the different glass formulations. In all cases a substantial amount of the included species was retained within the cement even after 150 days; the amount retained did however vary with glass composition. At low levels of species inclusion, the release was very low. In fact, below additions of 4.4% there appeared to be little or no release species detected from differing glasses.

Although at low inclusion of species the release was very low, there was a point at which the release increased markedly. This can be seen in Figure 118. This is to some extent dependent on the cement in question, this effect being most marked in those cements using MP4 glass and least evident in cements formed from LG26 glass. The ranking for this effect was:-

MP4 > AH2 > LG30 > LG26.

The release pattern which was observed appeared to vary with respect to time. Although there were some parts of the release profiles, especially with AH2 and MP4, which were linear with respect to the square root of time suggesting a Fickean diffusion process this was not true for the complete duration of the experiment with any of the different cements. After a period of time the

release stopped for most cements. The time at which this occurred for each cement variant was:

AH2 – 10 days, MP4 initial batch – 11 days, MP4 final batch – 19 days, LG30 final batch – 19 days. (The exceptions were LG30 initial batch and LG26 where release was still continuing at the end of the experiment.)

This type of release profile has previously been reported for zinc polycarboxylate cement (Billington *et al.*, 2001).

The CHA has the potential to react with PAA and it has demonstrated that a precipitate is formed when CHA solution is mixed with PAA (Leung, 2003). This has been confirmed by the author. If the surfaces of the CHA particles are attacked by the PAA then it seems likely that there will be a reaction between the acid and the CHA binding the particle into the conventional matrix. This would in turn lead to release of a small volume of actetate ions into the matrix. The low pH of the mixed cement initially would encourage this dissolution process. There is evidence that there are spare/unused PAA–COOH groups residing in the cement which are not neutralised during the initial reaction (Young *et al.*, 2000) and these may be available to create a surface reaction on the CHA particle. This would possibly account for the insubstantial release at low concentrations of included CHA. Once these spare COOH groups had been used up then CHA release would proceed. Again this tends to support the findings here that above a certain concentration the release becomes much greater.

The total release varies from cement and this may be influenced by ions which have gone into solution during the process described above. Some acetate ions

will be release and these are likely to react with anions released from the glass. Calcium and sodium acetate are highly soluble while aluminium acetate is only sparingly soluble. The small amount of acetate release may weaken the cement slightly. The degree to which this may occur is likely to be determined by the glass composition. The effect is most marked in the current study with MP4 where the glass has a very simple formulation, without fluoride or phosphorous being present. Shahid *et al* have shown that cement matrices are not formed when acetic acid is used with MP4 but do slowly form with LG30 which contains P but readily form with AH2 containing F and P. This suggests that any disruption of a cement matrix in any way with a glass with no F and P present will lead to a weakened cement.

In any release process there are a number of factors which will influence the amount and release of any included species. These include:-

- The relative solubility of the species in the immersing fluid. This will influence the release which can occur.
- The rate of setting and maturation of the cement: an immature cement will be prone to matrix degradation. Disruption will occur, leading to more rapid loss of any included species particularly if the exposure to the storage medium occurs before the cement is mature. This has been shown for conventional GIC cements (Andersson and Dahl, 1994; Causton, 1981).
- Structure of the set cement: whether this remains intact or whether cracks and fissures develop as a result of breakdown due to stresses set up within the material. This has been reported for some resin materials

(Parker and Braden, 1989). The effect, however, is determined by the level of fluid uptake and the elastic modulus of the material (Riggs *et al.*, 2001).

6.2.6.2 Solubility

The relatively low solubility of CHA will certainly limit the rate of release but if concentration gradient is established between the outer surface of the specimen and the immersing medium and the specimen it would be reasonable to assume that a normal diffusion process would continue slowly with respect to time. In all cases although release does occur this appears to have ceased by day 38 in the majority of cements. The only exception appears to be the cements formed with the initial batch of LG30 and LG26 where very slow release still appears to be occurring.

6.2.6.3 Setting

If cement formation was taking place, even with a surface reaction of CHA with PAA to form a matrix type, one would expect that the working and setting times would be relatively similar. It is interesting to note that with both the oscillating rheometer and Gillmore needle methods of assessment, all cements set in a relatively similar time.

The working times for three of the cements as measured by Gillmore needle were not much affected by the inclusion of CHA with the exception of AH2, the working time of which was extended considerably. The working time of three cements as measured on the oscillating rheometer at 37 °C were not much affected by the inclusion of CHA. The exception was LG26 cement where the working time was reduced slightly. At 23 °C LG26 and LG30 cements showed a

slight reduction in working time. The setting times for AH2 cement as measured by Gillmore needle was slightly extended by the inclusion of CHA and that of MP4 cement slightly reduced. The other two cements were not much affected. The setting times of AH2 and LG26 cements as measured on the oscillating rheometer at 23 °C and at 37 °C were extended considerably. That of MP4 cement was reduced considerably at 23 °C and reduced slightly at 37 °C. The setting time of LG30 cement was unclear at 23 °C and extended slightly at 37 °C. This gives the following general conclusion. Addition of CHA to the cements disrupted their setting in the following order of increasing effect:

MP4 < LG30 < LG26 < AH2

This is a very similar trend to that of the effect of AHCl on the working and setting times. In general, it can be said that the effect on MP4 cement was different to the effect on the other cements.

6.2.6.4 Compressive Strength

It might be expected that there would be a reduction in compressive strength as the CHA would either form inert inclusions or partly contribute to the matrix formation which might in itself be weaker. The initial cement did show some reduction in strength, the most marked being with the MP4 glass where the compressive strength was reduced from 63.0 MPa for the unmodified cement to 18.1 MPa for the cement containing 10.1 % CHA. This may be influenced by the absence of F and P. The addition of CHA affected the compressive strengths of the cements in the following increasing order:

LG30 (P) > LG26 (F P) < AH2 (Na F P) < MP4 (Na)

This is very different of AHCl where the effect on the compressive strengths of the cements was almost equal.

It is difficult to see any obvious trends in this series other than the fact that the two cements most affected, MP4 and AH2, both contain Na. There is a potential for Na to form acetate. All cements have the potential for forming acetates with Al and Ca; MP4 and AH2 also have the ability to form acetate with Na. The difference for Na is that it is monovalent and Na acetate is therefore unlikely to form a matrix.

6.2.6.5 Continued release

Since the glass ionomer cements are water based cements and there is evidence of transfer of ions, it should be assumed that inclusions may go into solution and migrate out from the structure.

In a resin system the theory for passage of material to the surface is that there is an initial diffusion process of water into the material and any soluble impurities (included species) will dissolve in the water establishing a concentration gradient across the specimen. It is thought that during the dissolution process the internal pressure at the site of the inclusion increases to a point at which either the surrounding material stress relieves or the material will crack creating channels through which solution may migrate. Materials with low elastic moduli such as THFMA (Riggs *et al.*, 1999; Patel *et al.*, 1999) will stress relieve but those stiffer material will crack and craze. Cracking and crazing would be much more likely to occur in glass ionomer cement which is brittle by nature.

It seems likely that a concentration gradient will be established in water based cement but the initial presence of water may alter the effect. Theoretically ions can migrate relatively freely through GIC matrices when in ionic form. To determine what influences this process, evidence was collected of the internal structure of the cements at the varying time intervals after the cement had set and the evidence of any changes in physical properties over time.

6.2.6.6 Scanning electron microscopy of the surface and the internal structure

Immersion in water showed significant surface disruption of the MP4 cement. The LG26 cement showed this to a lesser extent. This correlated with the greatest release of CHA, the highest being from MP4 cement with only a slightly lower release from the LG26 cement. This is significant in that Shahid et al indicated that surface breakdown occurred with MP4/acetic acid cements. The release profiles show that after 48 hours MP4 cement containing 8.8 % CHA had released 10.6 % of a possible 29 % CHA. This suggests that the release was primarily from a surface washout and degradation of the material. The micrographs showed that MP4 cement was rougher than the other cements and it was observed during specimen preparation that the mix was stiff and difficult to pack into the mould. Micrographs also showed that water immersion of the unmodified MP4 cement appeared to cause disruption to the cement surface indicating possible breakdown of the cement or weaker matrix formation which may be associated with absence of P and F in the matrix.

On viewing the fracture surface of these specimens there was no evidence of increase in the fissures and cracks with time. Specimens evaluated at all time

intervals and at all concentrations of inclusion appear similar to one another. If release was related solely to the formation of cracks and channels, the effect of the increasing release might be an increase in the crack propagation and the cements made from MP4 and AH2 glasses would show a greater number of cracks and channels than the other cements. In fact it was difficult to observe any channels in any of the cements. It must however be born in mind that glass ionomer cements are porous structures and the air incorporation during mixing means that the structure may be honeycombed. Polishing the specimen surface might have assisted in determining what cracks were present but this process may also introduce smearing.

Elemental analysis by SEM (Figure 112) showed discrete particles of CHA existing within the set cement and indicated that CHA was present in solid form within the cement. The existence of discrete particles of CHA on the surface would perhaps explain the high scatter for the release results; specimens exhibiting higher release having more particles on the surface. This is a more likely explanation than poor blending of cement ingredients that was not indicated by the ion release results.

The existence of these discrete particles suggests that CHA or its components therefore appear to exist in three forms:

- Discrete undissolved particles within the matrix
- In ionic form within the matrix
- Probably as ions within the water in the cement

The presence of partly undissolved CHA particles in the cements is likely to have some effect on the mechanical properties since although there may be some interaction with the surface between the matrix and the filler it resides as an inert filler which is likely to weaken the structure. The greater the amount of inclusion, the greater the effect will be. This generally appears to be the case. The compressive strength of AH2 cement was reduced from 221 MPa for the unmodified cement to 149 MPa for the cement containing 8.8 % CHA. Most affected was MP4 cement where the compressive strength was reduced from 63.0 MPa for the unmodified cement to 18.1 MPa for the cement containing 10.1 % CHA. The effect was least marked with LG30, the ranking order for effect being:-

LG30 < LG26 < AH2 < MP4.

Around the particle of CHA within the cements it is to be expected that the following might occur:-

- Surface dissolution of the particle until the concentration in the surrounding medium is at equilibrium with the solubility of CHA.
- Slow diffusion of these ionic species into the surrounding area with the water in the cement acting as a carrier vehicle.
- Potentially a surface exchange between the immersing water and the specimen which would continues until the media were at equilibrium. (i.e. Diffusion from the cement matrix into the surrounding water)

The area in the vicinity of a discrete CHA particle would become saturated at low concentration thus delaying any further release by dissolution into this area until ions had diffused from this immediate vicinity via the water within the specimen. This diffusion would depend on the matrix characteristics of porosity and tortuosity and the solubility and diffusivity of CHA. Passage from the cement matrix into the surrounding water is dependent on concentration of CHA in water. This is related to the relative solubility of the CHA and the volume of the water into which it dissolves. The maximum recorded concentration of CHA in the surrounding solution was 300 ppm which is 1.5 % of a saturated solution of CHA (19000 ppm) so it was unlikely that the volume of water in which the specimen was immersed was of significance. Thus, if CHA was available at the surface it would be expected to migrate from a higher to lower concentration. This implies that after a certain time (150 days) in the experiment when release has stopped, the surface of the specimen and the immersing solution are at equilibrium.

An addition experiment on the effect of limiting reservoir volume (section 5.3.5.1) in which very little additional CHA was released after re-immersing selected specimens in fresh water supports this to some extent though it is possible that at that stage of release, release was occurring at a much reduced rate.

Additional experiments to investigate the effect of the reservoir volume and changing the water periodically to maintain a very low concentration of CHA in the immersing liquid showed that as this volume was increased, the release decreased. Release into a reservoir that changed daily appeared to be less than into a static volume. There was a however, wide scatter of results and it

is possible that there is no difference in release behaviour between these volumes. There is therefore no evidence that the volume of 20 ml influenced the amount of CHA released. The dissolved CHA within the matrix is likely to be the part most easily released as it has already gone through the dissolution stage and only needs to diffuse out to the surrounding water. As this is the most easily released CHA, it is likely that it is released first and is the major cause of the first part of the release profiles. The release from AH2 cement and MP4 cement show some linearity at the beginning of the release profiles. Both these cements contain Na as one of their glass components.

7 Conclusions

- The inclusion of either CHA or AHCL in all experimental cements leads to release of the included species with respect to time.
- The effect on the physical properties was dependent on included species and composition of glass used in cement.
- Addition of AHCl:-
- Most of the additions were released before release stopped. Percentage release was independent of the amount added with the exception of AH2 cement. All release appeared to be finished by 5 days with the exception of LG30 cement which completed in about 10 days. The total amount released appeared to be related to the presence or absence of F in the cement with the presence of F inhibiting release. The working and setting times were extended for all cements except MP4 which showed a reduction on addition of AHCl. The addition of AHCl decreases the compressive strength in proportion to what is added. This is independent of the glass in the cement.
- Addition of CHA:-

  Only a proportion of the additions was release before release stopped. At low inclusion levels the level of release was very small. Increasing inclusion level above 8.8 % led to a much larger release. All release appeared to be finished by day 38 with exception of LG26 and the initial batch of LG30. The total amount released was related to the glass

formulation used in the cement. The working and setting time were generally unaffected by low levels of inclusion but addition of CHA to AH2 cement extended working time. Setting times were extended for all cements except MP4 that showed a marked reduction. The compressive strengths of all cements except LG30 were reduced by varying degrees, MP4 being the worst affected. LG30 showed no overall effect.

As these two additives behave very differently it is very important, if using these materials as a vehicle for delivery of physiologically active materials, that it should be realised that this may have quite different effects on cements depending on the chemical structure of the species that are added.

Unlike release from a polymeric material, in which there is no chemical interaction between the species being released and the polymer carrier, the release from a GIC seems to involve chemical interactions.

Glass composition and specifically the lack of P in MP4 seems to be the governing factor, although exactly what interactions occur is not clear.

8 Further work

1 A more detailed analysis of all possible species released along with that of acetate and chloride would lead to a greater understanding of the interactions between acetate and polyacid and Al, Ca and Na; and between chloride and Al, Ca and Na. This might include larger molecules containing fluoride. A study of their relative diffusion coefficients would possibly give an understanding of the rates of release of the various salts formed. Acetate and chloride could be determined by ion exchange HPLC (Natishan and Sajonz, 2001) and standard ion chromatography could be used to determine Al, Ca and Na. NMR spectroscopy might shed some light on acetate binding to Al, Ca or Na (Matsuya *et al.*, 1996).

2 The use of environmental SEM with the newly available technique of low vacuum (to eliminate artefacts) together with nano-indentation measurements to determine the changes within the cement structure and the mechanical properties of the set cement. Compressive strength data for samples pre-immersion, after 48 hours and 35 days would be useful for comparison with existing SEM data on surface disruption.

3 Further work should involve incorporating CHA into GIC as above while carrying out time dependent elemental analysis by SEM to test the hypothesis that there are agglomerates of CHA on or below the surface of the specimens that exhibit greater release. The specimens would be viewed as a function of time to monitor any dissolution of the CHA and to determine possible species at the surface and surrounding the agglomerates.

4 Further work should attempt to quantify if release rate, surface roughness, and hence surface area, are linked. This would be effectively carried out using laser profilometry.

5 A more detailed study of the various reactions which may take place should be carried out using FTIR/Raman spectroscopy. Despite the problems of overlapping peaks, differentiation of the various salts with respect to time during the setting process may provide greater understanding of the many interactions which are proceeding. The use of experimental materials with controlled variation of the composition of the ingredients should be considered. Raman spectroscopy could give an overall picture of the interactions taking place, it being particularly good at differentiating between the various metal polyacrylate groups (Young *et al.*, 2000).

FINIS

References

1. Akselsen, J. P., Afseth, J., and Rolla, Gunnar. In vitro damage to glass-ionomer cements by fluoride ion. Caries Research 21, 188. 1987.

2. Andersson,OH and Dahl,JE (1994). Aluminium release from glass-ionomer cements during early water exposure in-vitro. *Biomaterials* 15(11):882-888.

3. ASTM Annual Book of Standards. ASTM Annual Book of Standards. Cement; Lime; Gypsum. 04.01. 1999. West Conshohocken, PA, American Society for Testing and Materials.

4. Athanassopoulou,F, Karagouni,E, Dotsika,E, Ragias,V, Tavla,J, Christofilloyanis,P *et al.* (2004). Efficacy and toxicity of orally administrated anti-coccidial drugs for innovative treatments of Myxobolus sp infection in Puntazzo puntazzo. *Diseases of Aquatic Organisms* 62(3):217-226.

5. Balazs,AC, Calef,DF, Deutch,JM, Siegel,RA, and Langer,R (1985). The role of polymer matrix structure and interparticle interactions in diffusion-limited drug release. *Biophysical Journal* 47:97-104.

6. Barry,TI, Clinton,DJ, and Wilson,AD (1979). The structure of a glass-ionomer cement and its relationship to the setting process. *J Dent Res* 58:1072-1079.

7. Beeuwkes,H and Devries,HR (1956). Chlorhexidine in Urology. *Lancet* 271(Nov):913-914.

8. Billington,RW, Hadley,PC, Towler,MR, Pearson,GJ, and Williams,JA (2000). Effects of adding sodium and fluoride ions to glass ionomer on its interactions with sodium fluoride solution. *Biomaterials* 21(4):377-383.

9. Billington,RW, Hadley,PC, Williams,JA, and Pearson,GJ (2001). Kinetics of fluoride release from zinc oxide-based cements. *Biomaterials* 22:2507-2513.

10. Billington,RW, Williams,JA, Dorban,A, and Pearson,GJ (2004). Glass ionomer cement: evidence pointing to fluorine release in the form of monofluorophosphate in addition to fluoride ion. *Biomaterials* 25(17):3399-3402.

11. Billington, R. W., Williams, J. A., and Strang, R. Effect of 'neutral' sodium fluoride on glass-ionomers in vitro. Journal of Dental Research 66, 844. 1987.

12. Bovis,SC, Harrington,E, and Wilson,HJ (1971). Setting characteristics of composite filling materials. *BDJ* 131(8):352-356.

13. Braden, Mike. Private Communication. 2004.

14. British Pharmacopoeia (2007)., p. 469.

15. Brook,IM and van-Noort,R (1985). Drug release from acrylic polymers via channels and cracks: In vitro studies with hydrocortisone. *Biomaterials* 6:281-285.

16. Brune,D and Smith,D (1982). Microstructure and strength properties of silicate and glass-ionomer cements. *Acta Odontol Scand* 40:389-396.

17. BS EN 196-3. BS EN 196-3:2005 Methods of testing cement - Part 3: determination of setting times and soundness. 9-11. 2005.

18. Causton,BE (1981). The physico-mechanical consequences exposing glass ionomer cements to water during setting. *Biomaterials* 2(2):112-115.

19. Clarke's analysis of drugs and poisons (2004). Clarke's analysis of drugs and poisons. 3rd ed. Pharmaceutical press.

20. Cook,WD (1983a). Degradative analysis of glass ionomer polyelectrolyte cements. *J Biomed Mater Res* 17:1015-1027.

21. Cook,WD (1983b). Dental polyelectrolyte cements: II: Effect of powder/liquid ratio on their rheology. *Biomaterials* 4(1):21-24.

22. Cook,WD and Brockhurst,P (1980). The oscillating rheometer-what does it measure? *J Dent Res* 59:795-799.

23. Coombs,D (1998). The Use of DIamond as an ATR Material. *Int J Vibr Spect* 2:3-4.

24. Cowsar,DR, Tarwater,OR, and Tanquary,AC (1976). Controlled release of fluoride from hydrogels for dental applications. *Am Chem Soc Symph* 31:180-197.

25. Crisp,S, Kent,BE, Lewis,BG, Ferner,AJ, and Wilson,AD (1980). Glass ionomer cement formulations. II. The synthesis of novel polycarboxylic acids. *J Dent Res* 59:1055-1063.

26. Crisp,S, Lewis,BG, and Wilson,AD (1976a). Characterisation of glass-ionomer cements. 1. Long-term hardness and compressive and compressive strength. *J Dent* 4:162-166.

27. Crisp,S, Lewis,BG, and Wilson,AD (1976b). Characterisation of glass-ionomer cements. 2. Effect of the powder : liquid ratio on the physical properties. *J Dent* 4(6):287-290.

28. Crisp,S, Lewis,BG, and Wilson,AD (1977). Characterisation of glass-ionomer cements. 3. Effect of polyacid concentration on the physical properties. *J Dent* 5(1):51-56.

29. Crisp,S, Pringuer,MA, Wardleworth,D, and Wilson,AD (1974). Reactions in Glass Ionomer Cements: II. An Infrared Spectroscopic Study. *J Dent Res* 53:1414-1419.

30. Crisp,S and Wilson,AD (1974). Reactions in Glass Ionomer Cements: III. The Precipitation Reaction. *J Dent Res* Nov-Dec:1420-1424.

31. Crisp,S and Wilson,AD (1976). Reactions in Glass Ionomer Cements: V. Effect of Incorporating Tartaric Acid in the Cement Liquid. *J Dent Res* 55:1023-1031.

32. Cuckler,AC, Garzillo,M, Malanga,C, and Mcmanus,EC (1960). Amprolium .1. Efficacy for Coccidia in Chickens. *Poult Sci* 39(5):1241.

33. Culbertson,BM (2001). Glass-ionomer dental restoratives. *Prog Polym Sci* 26:577-604.

34. Davies,EH, Sefton,J, and Wilson,AD (1993). Preliminary study of factors affecting the fluoride release from glass-ionomer cements. *Biomaterials* 14(8):636-639.

35. De Barra,E and Hill,RG (2000). Influence of glass composition on the properties of glass polyalkenoate cements. Part III: influence of fluorite content. *Biomaterials* 21(6):563-569.

36. De Maeyer,EA, Verbeeck,RMH, and Vercuysse,CWJ (2002). Infrared Spectrometric Study of Acid-degradable Glasses . *J Dent Res* 81(8):552-555.

37. De Maeyer,EAP and Verbeeck,RMH (2001). X-ray diffraction study of acid-degradable glasses. *J Dent Res* 80(8):1764-1767.

38. De Maeyer,EAP, Verbeeck,RMH, and Vercruysse,CWJ (1998). Reactivity of fluoride-containing calcium aluminosilicate glasses used in dental glass-ionomer cements. *J Dent Res* 77(12):2005-2011.

39. De Moor,RJG and Verbeeck,RMH (1998a). Changes in surface hardness of conventional restorative glass ionomer cements. *Biomaterials* 19(24):2269-2275.

40. De Moor,RJG and Verbeeck,RMH (1998b). Effect of acetic acid on the fluoride release profiles of restorative glass ionomer cements. *Dent Mater* 14:261-268.

41. Deininger,G and Halasz,I (1971). Control of flow rate in high pressure liquid chromatography. *Journal of Chromatography* 60:65-73.

42. Demoor,RJG, Verbeeck,RMH, and DeMaeyer,EAP (1996). Fluoride release profiles of restorative glass ionomer formulations. *Dent Mater* 12(2):88-95.

43. Devlin,AJ, Hatton,PV, and Brook,IM (1998). Dependence of in vitro biocompatibility of ionomeric cements on ion release. *J Mater Sci Mater in Med* 9(12):737-741.

44. Edelman,E, Kost,J, Bobeck,H, and Langer,R (1985). Regulation of drug release from polymer matrices by oscillating magnetic fields. *J Biomed Mater Res* 19:67-83.

45. Ellis,J, Anstice,HM, and Wilson,AD (1991). The glass polyphosphonate cement: a novel glass ionomer cement based on poly(vinyl phosphonic acid). *Clin Mater* 7:341-346.

46. Fleming,GJP, Farooq,AA, and Barralet,JE (2003). Influence of powder/liquid mixing ratio on the performance of a restorative glass-ionomer dental cement. *Biomaterials* 24:4173-4179.

47. Forss,H, Seppa,L, and Lappalainen,R (1991). In vitro abrasion resisitance and hardness of glass-ionomer cements. *Dent Mater* 7:36-39.

48. Forsten,L (1976). Fluoride release from a fluoride-containing amalgam and two luting cements. *J Dent Res* 84:348-350.

49. Forsten,L (1990). Short- and long-term fluoride release from glass-ionomers and other fluoride-containing filling materials in vitro. *Scand J Dent Res* 98:179-185.

50. Fukazawa,M, Matsuya,S, and Yamane,M (1990). The mechanism for erosion of glass-ionomer cements in organic-acid buffer solutions. *J Dent Res* 69(5):1175-1179.

51. Gemalmaz,D, Yoruc,B, Ozcan,M, and Alkumru,HN (1998). Effect of early water contact on solubility of glass ionomer luting cements. *J Prosthet Dent* 80(4):474-478.

52. Griffin,SG and Hill,RG (1999). Influence of glass composition on the properties of glass polyalkenoate cements. Part I: influence of aluminium to silicon ratio. *Biomaterials* 20(17):1579-1586.

53. Griffin,SG and Hill,RG (2000a). Influence of glass composition on the properties of glass polyalkenoate cements. Part II: influence of phosphate content. *Biomaterials* 21(4):399-403.

54. Griffin,SG and Hill,RG (2000b). Influence of glass composition on the properties of glass polyalkenoate cements. Part IV: influence of fluorine content. *Biomaterials* 21(7):693-698.

55. Guggenberger,R, May,R, and Stefan,KP (1998). New trends in glass-ionomer chemistry. *Biomaterials* 19:479-483.

56. Gurny,R, Doelker,E, and Peppas,NA (1982). Modelling of sustained release of water-soluble drugs from porous, hydrophobic polymers. *Biomaterials* 3(1):27-32.

57. Ha,Y and Cheung,AP (1996). New stability-indicating high performance liquid chromatography assay and proposed hydrolytic pathways of chlorhexidine. *J Pharm Biomed Anal* 14:1327-1334.

58. Hadley,PC, Billington,RW, and Pearson,GJ (1999). Effect of monovalent ions in glass ionomer on their uptake and re-release. *Biomaterials* 20:891-897.

59. Hamilton,RJ and Sewell,PA (1982). Equipment. In: Introduction to high performance liquid chromatography. London: Chapman and Hall.

60. Hatton,PV and Brook,IM (1992). Characterization of the ultrastructure of glass-ionomer (poly-alkenoate) cement. *BDJ* 173(8):275-277.

61. Hill,G and Holman,J (1989). Aluminium. In: Chemistry in Context. Thomas Nelson ans Sons Ltd, pp. 254-262.

62. Hill,RG, Debarra,E, Griffin,SG, Henn,G, Devlin,J, Hatton,PV *et al.* (1995). Fluoride Release from Glass Polyalkenoate (Ionomer) Cements. *Key Eng Mater* 99-100:315-321.

63. Hill,RG and Wilson,AD (1988a). A Rheological Study of the Role of Additives on the Setting of Glass-ionomer Cements. *J Dent Res* 67(12):1446-1450.

64. Hill,RG and Wilson,AD (1988b). Some structural aspects of glasses used in ionomer cements. *Glass Technology* 29:150-158.

65. Hoszek,A and Ericson,D (1990). transient reduction of mutans streptococci on tooth surfaces using a chlorhexidine-containing glass ionomer cement varnish. *Swed Dent J* 23:97-105.

66. Hurrell-Gillingham,K, Reaney,IM, and Hatton,PV (2003). In vitro biocompatibility of a novel Fe(2)O(3)-containing glass-ionomer bone cement. *J Dent Res* 82:501.

67. ISO 9917. ISO 9917 Dental water-based cements. 5. 1991.

68. Izumoto,S, Machida,Y, Nishi,H, Nakamura,K, Nakai,H, and Sato,T (1997). Chromatography of crotanin and its application to the determination of active ingredients in ointments. *J Pharm Biomed Anal* 15:1457-1466.

69. Jacobsen,PH (1976). Working Time of Polymeric Restorative Materials. *J Dent Res* 55(2):244-251.

70. Jedrychowski,JR, Caputo,AA, and Kerper,S (1983). Antibacterial and mechanical properties of restorative materials combined with chlorhexidines. *J Oral Rehab* 10(5):373-381.

71. Jones,FH, Hutton,BM, Hadley,PC, Eccles,AJ, Steele,TA, Billington,RW *et al.* (2003). Fluoride uptake by glass ionomer cements: a surface analysis approach. *Biomaterials* 24:107-119.

72. Kamitakahara,M, Kim,HM, Miyaji,F, Kokubo,T, and Nakamura,T (2000). Preparation of Al-free glass-ionomer cement. *J Ceram Soc Jpn* 108(12):1117-1118.

73. Kaplan,AE, Williams,JA, Billington,RW, Braden,M, and Pearson,GJ (2004). Effect of variation in particle size on biaxial flexural strength of two conventional glass-ionomer cements. *J Oral Rehab* 31(4):373-378.

74. Karagouni,E, Athanassopoulou,F, Lytra,A, Komis,C, and Dotsika,E (2005). Antiparasitic and immunomodulatory effect of innovative treatments against Myxobolus sp infection in Diplodus puntazzo. *Veterinary Parasitology* 134(3-4):215-228.

75. Kaye,GWC, Laby,TH (1995). Tables of physical and chemical constants. 16 ed.

76. Kent,BE, Lewis,BG, and Wilson,AD (1979). Glass-ionomer cement formulations. 1: The preparation of novel fluoroaluminosilicate glasses high in fluorine. *J Dent Res* 58:1607-1619.

77. Kent,BE and Wilson,AD (1973). The properties of a glass ionomer cement. *BDJ* 135:322-326.

78. Kerby,RE and Bleiholder,RF (1991). Physical-Properties of Stainless-Steel and Silver-Reinforced Glass-Ionomer Cements. *J Dent Res* 70(10):1358-1361.

79. Khouw-Liu,VHW, Anstice,HM, and Pearson,GJ (1999). An in vitro investigation of a poly (vinyl phosphonic acid) based cement with four conventional glass-ionomer cements Part 2: maturation in relation to surface hardness. *J Dent* 27(5):359-365.

80. Krishnan,VK and Sreekumar,J (1996). Effect of polyacid on the properties of polyalkenoate cements. *Curr Sci* 70(8):730-733.

81. Kubicki,JD, Blake,GA, and Apitz,SE (1996). Molecular orbital models of aqueous aluminum-acetate complexes. *Geochimica et Cosmochimica Acta* 60(24):4897-4911.

82. Kuhn,AT and Wilson,AD (1985). The dissolution mechanisms of silicate and glass-ionomer dental cements. *Biomaterials* 6(6):378-382.

83. Kuhn, A. T., Winter, G. B., and Davies, E. M. Dissolution and fluoride release from silicate and glass-ionomer cement. Journal of Dental Research 6, 555. 1982.

84. Lacefield,WR, Reindl,MC, and Retief,DH (1985). Tensile bond strength of a glass-ionomer cement. *J Prosthet Dent* 53(2):194-198.

85. Langer,R (1982). Controlled Release of Macromolecules. *Chemtech* 12(2):98-105.

86. Langer,R, Siegel,R, Brown,L, Leong,K, Kost,J, and Edelman,E (1986). Controlled Release - 3 Mechanisms. *Chemtech* 16(2):108-110.

87. Langer,RS (1983). Science and Technology. In: Biocompatible polymers. Technomic publishing, pp. 585-596.

88. Langer,RS, Hsieh,DST, Peil, Bawa, and Rhine,WD (1981). Polymers for the controlled release of macromolecules : kinetics, applications and external control. *Americal Institute of Chemical Engineering* 77:10.

89. Leung, D. Private communication. 2003.

90. Loew,FM and Dunlop,RH (1972). Induction of Thiamine Inadequacy and Polioencephalomalacia in Adult Sheep with Amprolium. *American Journal of Veterinary Research* 33(11):2195-&.

91. Majors,RE (1980). Recent advances in HPLC packings and columns. *Journal of Chromatographic Science* 18:488-511.

92. Matsuya,S, Maeda,T, and Ohta,M (1996). IR and NMR analysis of hardening and maturation of glass ionomer cement. *J Dent Res* 75:1920-1927.

93. McLean,JW and Gasser,O (1985). Glass cermet cements. *Quintessence Int.*

94. McLean,JW and Wilson,AD (1977). The clinical development of the glass-ionomer cements. II. Some clinical applications. *Aust Dent J* 22(2):120-127.

95. Meryon,SD and Smith,AJ (1984). A comparison of fluoride release from three glass ionomer cements and a polycarboxylate cement. *Int Endod J* 17:16-24.

96. Meyer,VR (1988). Reverse-phase chromatography. In: Practical high-performance liquid chromatography. London: John Wiley and Sons Ltd.

97. Mojon,P, Kaltio,R, Feduik,D, Hawbolt,EB, and MacEntee,MI (1996). Short-term contamination of luting cements by water and saliva. *Dent Mater* 12(2):83-87.

98. Muller,J, Geyer,G, and Helms,J (1994). Good Audiological Results by Reconstruction of Defects of the Incudo-Stapedial Joint in the Middle-Ear by Reconstructing the Ossicles in Their Normal Position. *Laryngo-Rhino-Otologie* 73(3):160-163.

99. Nakajima,N, Watkins,JH, Arita,K, Hanoaka,K, and Okabe,T (1996). Mechanical properties of glass ionomers under static and dynamic loading. *Dent Mater* 12:30-37.

100. Natishan,TK and Sajonz,P (2001). Acetate and chloride determination by ion exchange HPLC with indirect photometric detection and its application to a beta-methylcarbapenem antibiotic. *Journal of Liquid Chromatography & Related Technologies* 24(17):2583-2599.

101. Ngo, H., Marino, V., and Mount, Graham J. Calcium, strontium, aluminium, sodium and fluoride release from four glass ionomer cements. Journal of Dental Research 77, 75. 1998.

102. Nicholson,JW and Wilson,AD (1987). Thermal-Behavior of Films of Partially Neutralized Poly(Acrylic Acid) .1. Influence of Metal-Ions. *Brit Polym J* 19(1):67-72.

103. Nicholson,JW (1998). Chemistry of glass-ionomer cements: a review. *Biomaterials* 19:485-494.

104. Nicholson,JW, Brookman,PJ, Lacy,OM, and Wilson,AD (1988). Fourier Transform Infrared Spectroscopic Study of the Role of Tartaric Acid in Glass-ionomer Dental Cements. *J Dent Res* 67(12):1451-1454.

105. Nicholson,JW, Hawkins,SJ, and Wasson,EA (1992). A study of the structure of zinc polycarboxylate dental cements. *J Mater Sci Mater in Med* in press.

106. Otsuka,M, Matsuda,Y, Kokubo,T, Yoshihara,S, Nakamura,T, and Yamamuro,T (1995). Drug release from a novel self-setting bioactive glass bone cement containing cephalexin and its phsiochemical properties. *J Biomed Mater Res* 29(1):33-38.

107. Palmer,G, Anstice,HM, and Pearson,GJ (1999). The effect of curing regime on the release of hydroxethyl methacrylate (HEMA) from resin-modified glass-ionomer cements. *J Clin Dent* 27:303-311.

108. Parker,S and Braden,M (1989). Water-absorption of methacrylate soft lining materials. *Biomaterials* 10(2):91-95.

109. Patel,MP, Swai,H, Davy,KWM, and Braden,M (1999). Water sorption behaviour of polymeric systems based on tetrahydrofurfuryl methacrylate. *J Mater Sci Mater in Med* 10(3):147-151.

110. Pearson, G. J. Private communication. 2005.

111. Pearson,GJ and Atkinson,AS (1991). Long-term flexural strength of glass-ionomer cements. *Biomaterials* 12:658-660.

112. Prosser,HJ, Powis,DR, Brant,P, and Wilson,AD (1984). Characterization of glass-ionomer cements. 7. The physical properties of current materials. *J Dent* 12:231-240.

113. Prosser,HJ, Powis,DR, and Wilson,AD (1986a). Glass-ionomer cements of improved flexural strength. *J Dent Res* 65:146-148.

114. Prosser,HJ, Richards,CP, and Wilson,AD (1982). NMR spectroscopy of dental materials, II. The role of tartaric acid in glass-ionomer dental cements. *J Biomed Mater Res* 16:431-435.

115. Prosser,HJ, Wilson,AD, Groffman,DM, Brookman,PJ, Allen,WM, Gleed,PT *et al.* (1986b). The development of acid-base reaction cements as formulations for the controlled release of trace elements. *Biomaterials* 7(2):109-112.

116. Rafferty,A, Hill,R, and Wood,D (2000). Amorphous phase separation of ionomer glasses. *J Mater Sci* 35(15):3863-3869.

117. Rhine,WD, Hsieh,DST, and Langer,R (1980). Polymers for Sustained Macromolecule Release - Procedures to Fabricate Reproducible Delivery Systems and Control Release Kinetics. *Journal of Pharmaceutical Sciences* 69(3):265-270.

118. Ribeiro,J and Ericson,D (1991). In vitro antibacterial effect of chorhexidene added to glass-ionomer cements. *Scand J Dent Res*(99):533-540.

119. Riggs,PD, Braden,M, Tilbrook,DA, Swai,H, Clarke,RL, and Patel,MP (1999). The water uptake of poly(tetrahydrofurfurylmethacrylate). *Biomaterials* 20(5):435-441.

120. Riggs,PD, Kinchesh,P, Braden,M, and Patel,MP (2001). Nuclear magnetic imaging of an osmotic water uptake and delivery process. *Biomaterials* 22(5):419-427.

121. Saito,S (1978). Characteristics of glass ionomer cements and its clinical application. I. Relations between hardening reactions and water. *Int Dent J*:1-16.

122. Saltzman,WM (2001). Drug Delivery. 1 ed. New York: Oxford University Press.

123. Sanders,BJ, Gregory,RL, Moore,BK, and Avery,DR (2002). Antibacterial and physical properties of resin modified glass-ionomer combined with chlorhexidine. *J Oral Rehab* 29:553-558.

124. Sanders, B. J., Moore, B. K., Gregory, R. L., and Avery, D. R. Effects of chlorhexidine on glass ionomer. Journal of Dental Research 76, 2491. 1997.

125. Scheerer,EW, Swartz,ML, Norman,RD, and Phillips,RW (1964). Residual Monomer of Restorative Resins. *J Dent Res* 43(5P1):672-&.

126. Schmitt W, Purrmann R, Jochum P, and Gasser, O. US patent 4,376,835 - Calcium depleted aluminium fluorosilicate glass powder for use in dental or bone cements. [US patent 4,376,835]. 1983. ESPE Fabrik Pharazeutischer Preparate GmbH.

127. Shahid,S, Billington,RW, and Pearson,GJ (2007). The role of glass composition in the behaviour of glass acetic acid and glass lactic acid cements. *J Mater Sci Mater in Med* in press.

128. Shin,WC and Oh,DG (1993). Structure of amprolium hydrochloride. *Acta Crystallographica Section C-Crystal structure communications* 49(2):282-285.

129. Shirley,DA (1972). High resolution X-ray photoemission spectrum of the valence bands of gold. *Phys Rev B* 5:4709-4714.

130. Sinha,PK and Krishnasamy,V (1996). Fixation of caesium, strontium and thorium ions in commercial synthetic zeolite matrices by thermal treatment. *J Nucl Sci Technol* 33(4):333-340.

131. Skoog,DA, Leary,JJ (1992). Principles of Instrumental Analysis. 4 ed. Harcourt Brace.

132. Smith,DC (1968). A new dental cement. *BDJ* 124(9):381-384.

133. Smith,DC (1998). Development of glass-ionomer cement systems. *Biomaterials* 19(6):467-478.

134. Snyder,LR, Stadalius,MA, and Quarry,MA (1983). *Analytical Chemistry* 55:1412-1430.

135. Tan,HSI, Ramachandran,P, and Cacini,W (1996). High performance liquid chromatographic assay of amprolium and ethopabate in chicken feed using solid-phase extraction. *J Pharm Biomed Anal* 15(2):259-265.

136. Thevadass,KP, Pearson,GJ, Anstice,HM, and Davies,EH (1996). Method for enhancing the fluoride release of a glass-ionomer cement. *Biomaterials* 17(4):425-429.

137. US patent 4019920. US patent 4019920 Gypsum set accelerator. 1977.

138. Wagner,CD, Davis,LE, Zeller, Taylor,JA, and Raymond,RM (1981). *Surf Interf Anal* 3:211.

139. Walls,AWG, McCabe,JF, and Murray,JJ (1988). Factors influencing the setting reaction of glass polyalkenoate (ionomer) cements. *J Clin Dent* 16:32-35.

140. Wasson,EA and Nicholson,JW (1990). A study of the relationship between setting chemistry and properties of modified glass-poly(alkenoate) cements. *Brit Polym J* 23:179-183.

141. Wasson,EA and Nicholson,JW (1991a). Studies on the setting chemistry of glass-ionomer cements. *Clin Mater* 7:289-293.

142. Wasson,EA and Nicholson,JW (1993b). New aspects of the setting of glass-ionomer cements. *J Dent Res* 72(2):481-483.

143. Waters,DN and Henty,MS (1977). Raman-Spectra of Aqueous-Solutions of Hydrolyzed Aluminum(Iii) Salts. *J Chem Soc [Dalton]*(3):243-245.

144. Wernery,U, Haydn-Evans,J, and Kinne,J (1998). Amprolium-induced cerebrocortical necrosis (CCN) in dromedary racing camels. *Journal of Veterinary Medicine Series B-Infectious Diseases and Veterinary Public Health* 45(6):335-343.

145. West,C (1977). Handbook of chemistry and physics. 58 ed. CRC Press.

146. White,AF, Bullen,TD, Vivit,DV, Schulz,MS, and Clow,DW (1999). The role of disseminated calcite in the chemical weathering of granitoid rocks. *Geochimica et Cosmochimica Acta* 63(13-14):1939-1953.

147. Williams,JA and Billington,RW (1991). Changes in compressive strength of glass ionomer restorative materials with respect to time periods of 24 h to 4 months. *J Oral Rehab* 18(2):163-168.

148. Williams,JA, Billington,RW, and Pearson,GJ (1992a). The comparative strengths of commercial glass-ionomer cements with and without metal additions. *BDJ* 172:279-282.

149. Williams,JA, Billington,RW, and Pearson,GJ (1992b). The effect of maturation on in-vitro erosion of glass ionomer and other dental cements. *BDJ* 173:340-342.

150. Williams,JA, Billington,RW, and Pearson,GJ (1997). Silver and fluoride ion release from metal-reinforced glass- ionomer filing materials. *J Oral Rehab* 24(5):369-375.

151. Williams,JA, Billington,RW, and Pearson,GJ (1998). Effect of moisture protective coatings on the strength of a modern metal-reinforced glass-ionomer cement. *J Oral Rehab* 25(7):535-540.

152. Williams,JA, Billington,RW, and Pearson,GJ (1999). Comparison of ion release from a glass ionomer cement as a function of the method of incorporation of added ions. *Biomaterials* 20(6):589-594.

153. Williams,JA, Billington,RW, and Pearson,GJ (2001). Potassium ion release from a glass ionomer cement matrix. *Biomaterials* 22(6):547-554.

154. Williams,JA, Billington,RW, and Pearson,GJ (2002). The glass ionomer cement: the sources of soluble fluoride. *Biomaterials* 23(10):2191-2200.

155. Williams,JA, Briggs,E, Billington,RW, and Pearson,GJ (2003). The effects of adding fluoride compounds to a fluoride-free glass ionomer cement on subsequent fluoride and sodium release. *Biomaterials* 24(7):1301-1308.

156. Wilson,AD (1968). Dental Silicate Cements .7. Alternative Liquid Cement Formers. *J Dent Res* 47(6):1133-1136.

157. Wilson,AD (1978). The chemistry of dental cements. *Chem Soc Rev* 7:265-296.

158. Wilson, A. D. and Crisp, S. US patent 4209434 - Dental cement containing poly(carboxylic acid), chelating agent and glass cement powder. 1980.

159. Wilson,AD, Crisp,S, and Paddon,JM (1981). The hydration of a glass-ionomer (ASPA) cement. *Brit Polym J* 13:66-70.

160. Wilson,AD, Crisp,S, Prosser,HJ, Lewis,BG, and Merson,SA (1980). Aluminosilicate glass for polyelectrolyte cements. *Ind Eng Chem Prod Res* 19:263-270.

161. Wilson,AD, Groffman,DM, and Kuhn,AT (1985). The release of fluoride and other chemical species from a glass-ionomer cement. *Biomaterials* 6:431-433.

162. Wilson,AD and Kent,BE (1972). A New Translucent Cement for Dentistry, The Glass Ionomer Cement. *BDJ* 132:133-135.

163. Wilson,AD and McLean,JW (1988). Glass composition. In: Glass-ionomer cement. New York: Quintessence Publishing Co. Inc.

164. Wilson,AD, Paddon,JM, and Crisp,S (1979). The hydration of dental cements. *J Dent Res* 58:1065-1071.

165. Wilson,HJ (1964). A method of assessing the setting characteristics of impression materials. *BDJ* 117:536-540.

166. Wise,DL (2000). Handbook of Pharmaceutical Controlled Release Technology. Marcel Dekker, Inc.

167. Wittwer,C, Downes,S, Devlin,AJ, Hatton,PV, and Brook,IM (1994). Release of serum proteins and dye from glass-ionomer (polyalkenoate) and acrylic cements: a pilot study. *J Mater Sci Med* 5:711-714.

168. Wolcott,RB, Paffenbarger,GC, and Schoonover,IC (1951). Direct Resinous Filling Materials - Temperature Rise During Polymerization. *Journal of the American Dental Association* 42(3):253-263.

169. Xu,XM and Burgess,JO (2003). Compressive strength, fluoride release and recharge of fluoride-releasing materials. *Biomaterials* 24(14):2451-2461.

170. Young,AM (2002). FTIR investigation of polymerisation and polyacid neutralisation kinetics in resin-modified glass-ionomer dental cements. *Biomaterials* 23:3289-3295.

171. Young,AM, Sherpa,A, Pearson,GJ, Schottlander,B, and Waters,DN (2000). Use of Raman spectroscopy in the characterisation of the acid-base reaction in glass-ionomer cements. *Biomaterials* 21:1971-1979.

Appendix I Conference abstracts and publications

BSDR Leeds, 1999

Study of chlorhexidine acetate release from glass-ionomer-cement using HPLC.
G PALMER*, G J PEARSON (Department of Biomaterials, Eastman Dental Institute, London, UK)

Glass-ionomer-cements (GIC) can potentially be used as slow release agents, as has been shown with previous studies with Fluoride. Previous work on HEMA release from RMGICs showed that free HEMA was released within four hours. This study investigated the use of a GIC containing vacuum dried PAA as a release agent for Chlorhexidine acetate (CHA) and HEMA using high-performance liquid chromatography (HPLC). Different dosages (0.5%, 1.0%, 1.4%, 1.9%, 5.0%) of CHA were added to the powder component of the mixture. The mixed material was allowed to set for 60 minutes and then placed in water and measurements taken until equilibrium was reached. HPLC was carried out with CHA as external standard on a C_{18} column with methanol-water 40:60 containing octane sulphonic acid, triethylamine and acetic acid as mobile phase. Eluate was monitored at 270 nm.
All free CHA was released within 48 hours, however this was less than 3% of the total mass incorporated in the specimens. An increased percentage of CHA incorporated into the powder, gave an increased release into the surrounding water. The bulk of the CHA appears to remain bound in the cement.

BSDR Lancaster, 2000

Study of amprolium hydrochloride release from glass-ionomer-cement using HPLC.
G PALMER*, G J PEARSON (Departments of Biomaterials, Eastman Dental Institute and SBRLMDS QMW, London, UK)

Glass-ionomer-cements (GIC) can potentially be used as slow release agents. This has been shown by inclusion of extrinsic and intrinsic fluoride ions. Initial studies on the release of unpolymerised HEMA from resin modified GIC showed release within 4 hours. Inclusion of chlorhexidine acetate in a conventional GIC showed that free CHA was released within 48 hrs. This study investigated the use of a GIC containing a glass and vacuum dried PAA to which was added Amprolium Hydrochloride (AmpHCl). Different dosages of AmpHCl were added as a % of the powder. This was mixed with water at a P/L ratio of 7:1 by weight. The mixed material was placed in a split mould at 37°C and allowed to set for 60 minutes.The specimens were placed in water and measurements taken of the AmpHCl concentration in the immersing solution until equilibrium was reached. HPLC was carried out on each solution with AmpHCl as external standard on a C_8 column with methanol-water 40:60 containing octane sulphonic acid, triethylamine and acetic acid as mobile phase. Eluate was monitored at 274 nm.
AmpHCl was released for up to 400 hours, however this was less than 50% of the total mass incorporated in the specimens. An increased percentage of AmpHCl incorporated into the powder, gave an increased release into the surrounding water. Substantial amounts of AmpHCl appear to remain bound in the cement.

2nd European conference on glass ionomers, Warwick 2004

Study of chlorhexidine acetate release from four glass-ionomer-cements using HPLC.

G PALMER*, F JONES, G J PEARSON[1] (Departments of Biomaterials, Eastman Dental Institute and SBRLMDS QMW[1], London, UK)

Glass-ionomer-cements (GIC) can potentially be used as slow release agents. This has been shown by inclusion of extrinsic and intrinsic fluoride ions. Initial studies on the release of unpolymerised HEMA from resin modified GIC showed release within 4 hours. This study investigated the use of a GIC containing one of four glasses, AH2, MP4, LG30, LG26 (each differing by the type of ions present) and vacuum dried PAA, as a release agent for Chlorhexidine acetate (CHA). Different dosages of CHA were added as a % of the powder. This was mixed with water at a P/L ratio of 7:1 by weight with the exception of LG26 glass cement for which the ratio was 5.73:1 by weight. The mixed material was placed in a split mould at 37°C and allowed to set for 60 minutes. The specimens were placed in water and measurements taken of the CHA concentration in the immersing solution until equilibrium was reached. HPLC was carried out on each solution with CHA as external standard on a C_8 column with 2-PA:water 40:60 containing NaH_2PO_4 adjusted to pH 3.0 with phosphoric acid as mobile phase. Eluate was monitored at 270 nm.

CHA was released in some cases for up to 150 days, however this was less than 30% of the total mass incorporated in the specimens. An increased percentage of CHA incorporated into the powder, gave an increased release into the surrounding water. Substantial amounts of CHA appear to remain bound in all cements.

Publications

Palmer, G., Jones, F. H., Billington, R. W., & Pearson, G. J. 2004, "Chlorhexidine release from an experimental glass ionomer cement", *Biomaterials*, vol. 25, pp. 5423-5431.

Available online at www.sciencedirect.com
SCIENCE DIRECT®
Biomaterials 25 (2004) 5423–5431
Biomaterials
www.elsevier.com/locate/biomaterials

Chlorhexidine release from an experimental glass ionomer cement

G. Palmer[a,*], F.H. Jones[a], R.W. Billington[b], G.J. Pearson[b]

doi:10.1016/j.biomaterials.2003.12.051

Appendix II – Physical data

Ion	Ionic radius / Å	
Na^+	0.97	
Ca^{2+}	0.99	
Al^{3+}	0.51	
Molecule	Enthalpy of formation ΔH^0_f / kJ mol^{-1}	Solubility / g 100 ml^{-1} (° C)
AlF_3	-1510	0.559 (25)
AlF_3 $3½H_2O$	-2297	Insoluble
CaF_2	-1228.0	0.0017 (26)
NaF	-569	4.22 (18)
$AlCl_3$	-704	69.9 (15)
$CaCl_2$	-795	74.5 (20)
NaCl	-411.2	35.7 (0), 39.2 (100)
$Al(CH_3COO)_3$	-	Almost insoluble (20)†
$Ca(CH_3COO)_2$	-	34.7 (20)
$NaCH_3COO$	-	46.4 (20)

Table 64 Physical data of ionic species and selected molecules in a GIC (West, 1977; Kaye and Laby, 1995)

† Merck safety data sheet